MICRO-RNA REGULATION OF HEPATIC DRUG METABOLISM: AGE-RELATED CHANGES IN MICRO-RNA EXPRESSION AND GENETIC VARIANTS IN MICRO-RNA TARGET SITES

Kimberly Sherrelle Burgess

Submitted to the faculty of the University Graduate School
in partial fulfillment of the requirements
for the degree
Doctor of Philosophy
in the Department of Pharmacology & Toxicology,
Indiana University

December 2017

Accepted by the Graduate Faculty, of Indiana University, in partial fulfillment of the requirements for the degree of Doctor of Philosophy.

Doctoral Committee

Todd C. Skaar, Ph.D., Chair

Gustavo Arrizabalaga, Ph.D.

Theodore Cummins, Ph.D.

Zeruesenay Desta, Ph.D.

August 31, 2017

Richard Nass, Ph.D.

Jian-Tian Zhang, Ph.D.

DEDICATION

For Mom and Christopher

ACKNOWLEDGEMENTS

First and foremost, I would like to thank God.

To Brian, for all of his support over the years as a friend and now husband. For walking me to and from lab at night when the lab was located in Wishard and for taking off work to attend my seminars.

I would like to thank my mother and brother, who have supported me unconditionally throughout my graduate education. I am also grateful to my other family members who have supported me along the way.

To my grandma, who would not let me drive home from Indiana alone so she purchased my plane ticket for Christmas one year.

I would like to express my sincerest gratitude to my advisor, Dr. Todd Skaar, for the continuous support throughout my PhD. For his patience, understanding, motivation, and immense knowledge. For allowing me to take extra courses, study abroad in Sweden, and for opening up the lab to my little sister and NOBCChE high school students for hands-on experiments. I could not have imagined having a better advisor and mentor for my PhD study.

To past, current labmates and close collaborators, Anu, Santosh, Eric, Michael, Joseph, Marelize, Tom, and Katie for help conducting various experiments, scientific input, as well as social endeavors.

To Dr. Zeruesenay Desta and his lab members and collaborators, Jessica, Ingrid, Brandon, and Nancy, for providing me with access to his laboratory, clinical samples, and all their assistance. Without their support, it would not have been possible to conduct this research.

To collaborators, Dr. Yunlong Liu and his lab members for assistance with all the bioinformatics and statistical analyses work, Dr. Andrea Gaedigk, Dr. Roger Gaedigk, and

Dr. Robin Pearce for access to human liver samples and data which helped make my research project a success.

Thanks to Dr. Richard Nass for reviewing my F31 grant which allowed for it to get accepted on the first submission.

My sincerest thanks go to my thesis committee: Dr. Richard Nass, Dr. Desta, Dr. Theodore Cummins, Dr. JT Zhang, and Dr. Arrizabalaga for their insightful comments and encouragement.

Special thanks to the Clinical Pharmacology Division and the late, Dr. David Flockhart for their love and support over the years. This was such an awesome environment to work in that I decided to stay a few more years as a post-doctoral fellow.

Thanks to the Pharmacology & Toxicology Department and the IBMG program former and current faculty, staff, fellows, and students. I don't want to list all the names individually from fear of skipping someone. You know who you are!

To all my friends, Indy family, and Mount Zion Baptist Church family who have supported me in every other aspect of my life: thank you.

Thanks for all your support and encouragement over the years!

Kimberly Sherrelle Burgess

MICRO-RNA REGULATION OF HEPATIC DRUG METABOLISM: AGE-RELATED CHANGES IN MICRO-RNA EXPRESSION AND GENETIC VARIANTS IN MICRO-RNA TARGET SITES

Developmental changes in the liver significantly impact drug disposition. Due to the emergence of microRNAs as important regulators of drug disposition, we hypothesize that age-dependent change in microRNA expression and genetic variants in microRNA target sites contribute to variability in drug disposition. In human liver tissues, expression of 533 microRNAs and over 14,000 genes were measured. In all, 114 microRNAs were upregulated and 72 downregulated from fetal to pediatric, and 2 and 3, respectively, from pediatric to adult. Among these microRNAs, 99 microRNA-mRNA interactions were predicted or have previously been validated to target drug disposition genes and over 1,000 significant negative correlations were observed between miRNA-mRNA pairs. We validated these interactions using various cell culture models. Genetic variants in the promoter and coding regions of drug disposition genes have also been shown to alter enzyme expression and/or activity. However, these variants do not account for all variability in enzyme activity. Emerging evidence has shown that variants in the 3'UTR may explain variable drug response by altering microRNA regulation. Five 3'UTR variants were associated with significantly altered CYP2B6 activity in healthy human volunteers. The rs70950385 (AG>CA) variant was associated with decreased CYP2B6 activity among normal metabolizers. *In vitro* luciferase assays confirmed that the CA allele altered miR-1275 targeting of *CYP2B6* mRNA. Due to the large number of 3'UTR variants predicted to alter microRNA regulation, a high-throughput method, PASSPORT-seq, was developed to test over 100 3'UTR variants simultaneously in different cell lines. Thirty-eight variants

resulted in FDR-significant altered expression between wild-type and variant sequences. Our data suggest a mechanism for the marked changes in hepatic gene expression between the fetal and pediatric developmental periods, support a role for these age-dependent microRNAs in regulating drug disposition, and provide strong evidence that 3'UTR variants are also an important source of variability in drug disposition.

Todd C. Skaar, Ph.D., Chair

TABLE OF CONTENTS

LIST OF TABLES

LIST OF FIGURES

LIST OF ABBREVIATIONS

3’	3 prime
5’	5 prime
ABC	adenosine triphosphate-binding cassette
ADME	absorption, distribution, metabolism, excretion
Ago2	argonaute 2
AUC_{0-48}	area under curve 0-48 hours
bp	base pair
BUP	bupropion
CAR	constitutive androstane receptor
cDNA	complementary DNA
C_{max}	maximum concentration
CNS	central nervous system
C_T	threshold cycle
CYP	cytochrome P450
DPYD	dihydropyrimidine dehydrogenase
EFV	efavirenz
FC	fold-change
FDR	false discovery rate
GST	glutathione S-transferase
HLM	human liver microsomes
HNF4A	hepatocyte nuclear factor 4 alpha
HPLC	high pressure liquid chromatography
Hsa	*Homo sapiens*
LD	linkage disequilibrium
let	lethal

mRNA	messenger RNA
miR	microRNA
miRNA	microRNA
NAT	N-acetyltransferase
NR1I	nuclear receptor subfamily 1
nt	nucleotide
OH	hydroxy
PASSPORT	Parallel ASSessment of POlymorphisms in miRna Target sites
PCA	principal components analysis
PCR	polymerase chain reaction
PXR	pregnane X-receptor
RISC	RNA-induced silencing complex
RNA	ribonucleic acid
RPKM	reads per kilobases per million
RQI	RNA quality index
seq	sequencing
SLC	solute carriers
SLCO	solute carrier organic anion
SNP	single nucleotide polymorphism
SULT	sulfotransferases
TALE-TF	transcription factor like effector-transcription factor
TPMT	thiopurine S-methyltransferase
UGT	uridine 5’-diphospho-glucuronosyltransferases
UTR	untranslated region
Var	variant
WT	wild-type

INTRODUCTION

Introduction to pharmacogenes

Pharmacogenes are genes that encode for proteins responsible in the absorption, distribution, metabolism, and excretion of drugs. These include phase I and II enzymes responsible for biotransformation of drugs in order to make them more hydrophilic and easily eliminated, transporters that allow drugs to move across various membranes, and upstream transcription factors that regulate the expression of the previously mentioned proteins. Together, these pharmacogenes play a critical role in drug pharmacokinetics and impact the safety and efficacy of drug treatments.

The most well-studied Phase I enzymes include members of the cytochrome P450 (CYP) superfamily. The CYPs are a superfamily of heme-thiolate monooxygenase enzymes involved in oxidative metabolism that are essential for the production of cholesterol, steroids, prostacyclins and thromboxane A_2, as well as metabolism of exogenous drugs and carcinogens (Slaughter and Edwards, 1995). These CYPs were named due to being bound to membranes within a cell (cyto), containing a heme pigment (chrome and P) which absorbs light at a wavelength of (450) nm in its reduced state when complexed with carbon monoxide (Klingenberg, 1958; Lu and Coon, 1968; Omura and Sato, 1964a, b). In humans, there are 57 functional CYPs and 18 families (Guengerich, 2008; Nelson et al., 2004). These CYPs are expressed in the endoplasmic reticulum of different tissues such as the liver, small intestines, lungs, placenta, and kidneys (Nelson et al., 2004; Slaughter and Edwards, 1995).

Of these CYPs, members of families 1-3 are responsible for metabolism of 70-80% of clinically used drugs and are less conserved across species (Bertz and Granneman, 1997; Evans and Relling, 1999). These CYPs determine the rate of biotransformation of a parent

drug into an active/inactive metabolite which affect drug concentrations in the body and subsequent effects. In the case of CYP2D6, it is responsible for the biotransformation of codeine to morphine, a more pharmacologically active analgesic used to alleviate pain (Caraco et al., 1999). Members of these CYP families are also associated with the metabolism of endogenous substrates such as testosterone and cortisol by CYP3A and endocannabinoids by CYP2D6 (Kim et al., 2017; Snider et al., 2008; Uehara et al., 2017). Members of the remaining CYP families (4, 5, 7, 8, 11, 17, 19, 20, 21, 24, 26, 27, 39, 46 and 51) are more closely associated with metabolism of endogenous substrates and conserved across other species (Ingelman-Sundberg and Rodriguez-Antona, 2005). For example, CYP19A1 is an aromatase responsible for the biosynthesis of estrogens (Czajka-Oraniec and Simpson, 2010).

Phase II enzymes are responsible for conjugation reactions to serve as a detoxification step in drug metabolism. These are mostly transferases such as uridine 5'-diphospho-glucuronosyltransferase (UGTs), sulfotransferases (SULTs), N-acetyltransferases (NATs), glutathione S-transferases (GSTs) and methyltransferases such as thiopurine S-methyl transferase (TPMT). UGTs are of the most clinically-important Phase II enzymes and are responsible for transferring a glucuronide from glucuronic acid to its substrate, a process called glucuronidation. This results in the glucuronidated product being eliminated in the bile or urine as it becomes more hydrophilic and unable to be reabsorbed. UGTs are responsible for glucuronidation of over 40% of clinically-used drugs, and in combination with CYPs, they metabolize over 90% of drugs (Evans and Relling, 1999; Rowland et al., 2013). After codeine is metabolized to morphine, morphine is then glucuronidated by UGT2B7. The morphine-6-glururonide is 100 times more potent as an opioid receptor agonist than morphine (Paul et al., 1989).

In humans, there are five UGT families consisting of 22 proteins. As the liver is the main organ for detoxification, UGTs are expressed more abundantly in the liver, but are also expressed in other organs such as the intestines and kidneys (Rowland et al., 2013). Phase II enzymes are responsible in the elimination of many endogenous substrates as well. SULTs are known to metabolize estrogens whereas UGTs eliminate endogenous compounds such as bilirubin, steroids, and fat soluble vitamins (Liu et al., 2017; Miners and Mackenzie, 1991). Specifically, UGT1A1 is responsible for the conjugation of bilirubin, a by-product of red blood cell catabolism. Measurement of conjugated and unconjugated bilirubin levels in the blood is a classic test used to measure liver function, as increased levels of unconjugated bilirubin is associated with reduced liver function (Clarke et al., 1997).

Another group of pharmacogenes include transporters, which facilitate the movement of compounds across biological membranes. Among these transported compounds include both exogenous and endogenous compounds. Common “drug” transporters include members of the ATP-binding cassette (ABC) and solute carrier (SLC) superfamilies. Due to substrate redundancy of transporters, studying the effects of a single transporter on a specific drug can be difficult (Hillgren et al., 2013). As such, ABCB1 has been shown to export many drugs, steroids, lipids, and bilirubin and is ubiquitously expressed, but mainly located in the intestine, brain, liver and kidney. SLC22A1 is mainly expressed in the liver and a few known substrates include metformin, acyclovir, monoamine neurotransmitters and choline (Liang et al., 2015).

Lastly, upstream transcription factors have been shown to regulate drug metabolism and disposition through regulating the expression of Phase I and II enzymes and transporters. Many of these transcription factors have been labelled as orphan transcription factors, as

endogenous ligands remain to be elucidated. Studies have identified endogenous ligands in one species, but findings did not hold true for the mammalian version of the gene (Moore et al., 2000). In the case of hepatic nuclear factor 4α (HNF4A), an essential fatty acid, linoleic acid, has been identified as an endogenous ligand for both mice and mammalian-expressed HNF4A (Yuan et al., 2009). HNF4A is a highly conserved nuclear receptor, known as a "master" regulator of liver-specific gene expression. HNF4A was first identified in the rat liver where it was found to be bound to the apolipoprotein C-III gene and was identified as the gene mutated in an inheritable form of non-insulin-dependent diabetes called maturity onset diabetes of the young so it was thought to be associated with carbohydrate and lipid metabolism (Ellard and Colclough, 2006; Sladek et al., 1990). This nuclear receptor has been shown to be highly expressed in the liver, kidney, and intestines, where most drug metabolism occurs and known to regulate the expression of many Phase I and II enzymes (Aueviriyavit et al., 2007; Goodwin et al., 2002; Jover et al., 2009; Tirona et al., 2003). Furthermore, HNF4A binds DNA as a homodimer and has been shown to be required for other nuclear receptors, such as PXR and CAR, to induce expression (Tirona et al., 2003).

The pregnane X-receptor (PXR) and constitutive androstane receptor (CAR) are main members of the nuclear receptor (NR1I) family that have been shown to regulate transcription of many pharmacogenes and are mainly expressed in the liver and intestines. In general, ligand binding results in PXR and CAR forming heterodimers with retinoid X receptor in order to be translocated into the nucleus and bind to response elements in the promoter region of target genes (Baes et al., 1994; Wang et al., 2015). Many exogenous ligands have been identified for these nuclear receptors, but no obvious common structural features have been deciphered (Waxman, 1999). PXR and CAR also overlap in ligand binding and DNA binding regions so they have been shown to co-regulate many

genes; however, PXR is a well-known CYP3A inducer and CAR as a CYP2B inducer (Wang et al., 2003; Wei et al., 2002). In the case of many CYPs, their expression levels increase with drug exposure and return to normal levels after exposure is gone. This response is thought to be an adaptive response established to protect against foreign compounds. In the case of polypharmacy, this can pose a problem in drug response. Especially when commonly used drugs such as rifampicin (antibiotic), troglitazone (diabetes drug) and dexamethasone (anti-inflammatory) have been identified as PXR ligands. So induction of CYP3A4 mediated by PXR will increase the rate of biotransformation of CYP3A4 substrates (Lehmann et al., 1998; Li et al., 1995). This can have serious consequences in drug treatment as CYP3A4 is responsible for the biotransformation of 50-60% of clinically-used drugs.

Developmental changes in pharmacogenes

Developmental changes in drug disposition create the need for age-appropriate pharmacotherapy (Hines, 2008, 2013; Kearns et al., 2003; Van Driest and McGregor, 2013). Although there have been many approaches for estimating pediatric drug dosing (e.g. extrapolation from adult data), these approaches are not adequate for many children (Sage et al., 2014). Developmental changes in drug response are difficult to predict at the individual patient level, in part due to our poor understanding of the mechanisms that regulate these developmental changes. Consequently, the high off-label use of drugs in this pediatric population is associated with an increased number of adverse events (Cuzzolin et al., 2006). Although more clinical studies are now being conducted in pediatric populations as a result of the Pediatric Exclusivity and the Best Pharmaceuticals for Children Acts, a fundamental understanding of the ontogeny of pharmacogenes is still needed to develop more accurate dosing guidelines for both the clinical trials and clinical care in the young.

The majority of drug disposition genes, those involved in drug distribution and elimination, are known to change during early and late developmental stages in humans; however, little is understood about the mechanisms that control these changes. The most well characterized age-associated drug disposition genes involve expression of drug metabolizing enzymes in the liver (Blake et al., 2005; Blake et al., 2007; de Wildt et al., 1999; Hines, 2007). These include the phase I and II enzymes that are responsible for the modification and elimination of many drugs. The most notable of the phase I enzymes are the CYPs and many developmental changes have been observed in their expression patterns (Blake et al., 2005; Blake et al., 2007; de Wildt et al., 1999; Hines, 2007). For example, the predominant *CYP* gene expressed in fetal liver, *CYP3A7*, peaks shortly after birth and becomes undetectable in most children and adults. In contrast, *CYP1A1*, *2C9*, *2C19*, *2D6*, and *2E1* are undetectable or expressed extremely low in the fetus, but are expressed at high levels after birth (Lacroix et al., 1997; Sonnier and Cresteil, 1998; Treluyer et al., 1997; Treluyer et al., 1991; Vieira et al., 1996). A well-documented example of phase II enzyme ontogeny is the delayed onset of a member of the *UGT2B* family responsible for “gray baby” syndrome in neonates as an adverse event of chloramphenicol therapy (McCarver and Hines, 2002). There is also data indicating that *UGT1A6* and *UGT1A9* function increases in older children and adults compared to younger children (Miller et al., 1976). Recently, developmental patterns of drug transporter expression indicates that hepatic *MDR1* (*ABCB1*), *MRP* (*ABCC2*), *OATP1B1* (*SLCO1B1*) and *OATP1B1* (*SLCO1B3*) expression is also increased in adults compared to fetal and neonates (Mooij et al., 2014).

Mechanisms of developmental changes in pharmacogenes

Many developmental changes in pharmacogenes have been identified, but a fundamental understanding of mechanisms that facilitate these changes are necessary for safer and more effective drug therapy. Emerging evidence has shown that epigenetic regulation may explain some of the observed developmental changes in pharmacogenes (Fisel et al., 2016; Kacevska et al., 2012). Epigenetics refers to heritable changes in gene expression without altering the DNA sequence. Such modifications include DNA/histone methylation and non-coding RNAs such as miRNAs (Goldberg et al., 2007). These epigenetic modifications may fluctuate over time and in response to various stimuli, which may explain some of the unknown reasons for developmental changes in pharmacogenes (Holliday, 2006; Jones and Baylin, 2007). Epigenetic regulation of pharmacogenes, pharmacoepigenetics, may not only explain variability in drug response, it can also affect the metabolism of endogenous substrates and lead to the progression of various diseases.

Pharmacogepigenetics and its implications in the ontogeny of drug disposition genes are limited. Many studies focused on DNA methylation of pharmacogenes have been associated with their gene expression in different cancers (Belanger et al., 2010; Okino et al., 2006; Olsson et al., 2007). However, hyper-methylation has been shown to contribute to the lack of CYP3A4 expression in the fetal liver, whereas after birth, the methylation patterns are altered to increase expression (Kacevska et al., 2012). In HepG2 liver cells, treatment with 5-aza-2'-deoxycytidine, a DNA methyltransferase inhibitor, resulted in upregulation of *CYP3A7* mRNA expression suggesting that DNA methylation may explain this CYPs expression in the fetal liver and downregulation in pediatric and adults (Dannenberg and Edenberg, 2006).

MicroRNAs, the main focal point of this project, are another source of epigenetic modification that may contribute to variability in gene expression of pharmacogenes. These miRNAs are small noncoding RNAs, approximately 17 to 22 nucleotides in length that bind to mRNAs and regulate their translation and stability. These miRNAs have previously been shown to negatively regulate the expression of pharmacogenes such as *CYP1B1* and miR-27b, *UGT1A1* and miR-491-3p, and *HNF4A* and miR-34a-5p (Dluzen et al., 2014; Ramamoorthy et al., 2012; Tsuchiya et al., 2006). A single miRNA can also regulate the expression of many protein coding genes. This promiscuity can make it difficult to understand miRNA-mediated regulatory networks. In order to understand how miRNAs can alter pharmacogene expression to contribute to ontogenesis and inter-individual variability in gene expression, much is needed to be studied regarding the regulation of miRNAs themselves.

Aging has been associated with alterations in the hepatic expression of several miRNAs in rats (Mimura et al., 2014), which may be true for humans as well. These age-dependent changes in hepatic miRNAs may contribute to known age-related changes in pharmacogene expression and activity. MicroRNAs have been implicated in many biological processes and hepatic miRNA expression has also been shown to be altered under a variety of conditions. Hepatic diseases, such as liver cancer, cirrhosis, and hepatitis C infection, are associated with altered miRNA expression (Gupta et al., 2014; Liang et al., 2013; Tao et al., 2013). We have previously shown that rifampin, a known inducer of drug metabolism genes (Anderson et al., 2013; Rae et al., 2001), alters miRNA expression patterns in primary human hepatocytes (Ramamoorthy et al., 2013). Altered hepatic miRNA expression patterns may contribute to rifampin-mediated drug interactions. Understanding these changes in miRNA expression may prove miRNAs to be useful as biomarkers for drug response, disease progression and diagnoses.

Discovery of miRNAs, biogenesis and mechanisms of action

The first miRNA, *lin-4*, was discovered in 1993 by Victor Ambros in *C. elegans*. It was shown to negatively regulate levels of LIN-14 protein involved in postembryonic development in *C. elegans* (Lee et al., 1993). These miRNAs are endogenous to humans and known to be transcribed by RNA polymerase II/III into primary miRNA, cleaved by the Drosha-DGCR8 microprocessor complex to precursor miRNA, and exported into the cytoplasm by Exportin-5-Ran-GTP as shown in Figure 1. Next, they are cleaved into microRNA duplexes by Dicer-TRBP where one strand is loaded into the RNA-induced silencing complex (RISC) to guide the complex to its target. The other strand is degraded (Winter et al., 2009).

The majority of miRNAs bind imperfect complimentary sequences in the 3'UTRs of target mRNAs (Liu, 2008; Olsen and Ambros, 1999; Selbach et al., 2008; Xie et al., 2008). In addition, a minority of miRNAs target other regions of the mRNA such as the 5'UTR and coding regions to repress translation, and in some cases, have even increased gene expression (Duursma et al., 2008; Orom et al., 2008; Place et al., 2008). The 3'UTR 'seed sequence' located at the 5' end from bases 2-8 is a critical feature required for miRNA binding to its target mRNA (Lambert et al., 2011). This 'seed sequence' binding is critical for many miRNA-mRNA prediction databases such as TargetScan (Agarwal et al., 2015), which includes the identification of several classes of target sites. Listed in order of effectiveness are the 8mer site (perfect complimentary binding at positions 2-8 with an A at the first position), 7mer-m8 site (perfect complimentary binding at positions 2-8), 7mer-A1 site (positions 2-7 with an A at the first position), 6mer (positions 2-7) and offset-6mer (position 3-8) (Brennecke et al., 2005; Friedman et al., 2009; Krek et al., 2005; Lewis et al., 2005). The adenosine located on the mRNA sequence, opposite of position one on

the miRNA has been shown to improve miRNA binding due to recognition within a binding pocket of the Argonaute protein (Schirle et al., 2014).

While the biogenesis and post-transcriptional activity of miRNAs has been extensively studied, much remains to be elucidated about the regulation of these miRNAs. Studies regarding miRNA stability, expression in various tissues, and transport between tissues are only a few of the questions that need to be answered to enable a better understanding of how miRNAs function. Such regulatory networks of miRNAs remain to be fully elucidated. As miRNAs are transcribed from DNA, they are also subject to epigenetic factors such as DNA methylation. Changes in miRNA expression levels have been observed when cells were treated with histone deacetylase inhibitors (Scott et al., 2006). Methylation patterns in the promoter region of miRNAs have also been observed in various diseases. For example, let-7a-3 was found to be hypo-methylated in some lung cancers, but hyper-methylated in normal human tissues (Brueckner et al., 2007). To further complicate miRNA regulation, miRNAs can target DNA and histone methylation genes (Li et al., 2009). As these regulatory networks of miRNAs become uncovered, better understanding of miRNA regulation of pharmacogenes and miRNAs as diagnostic markers will follow.

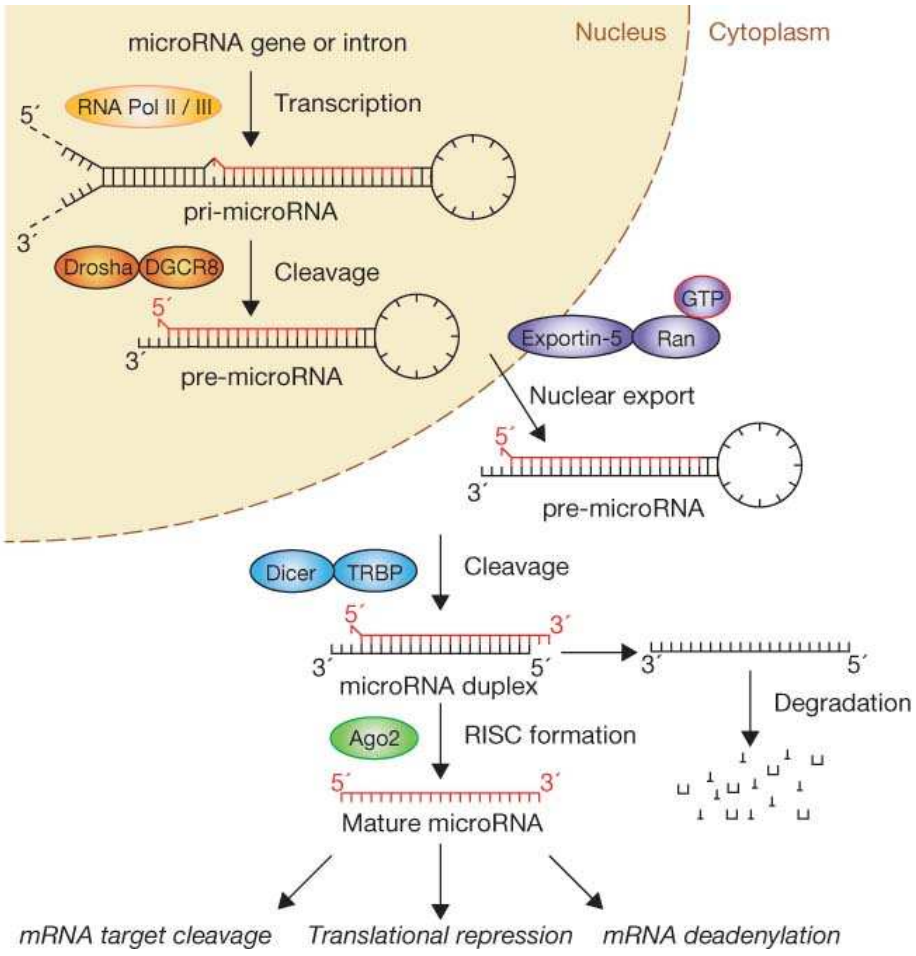

Figure 1: The canonical pathway of microRNA processing

The miRNA processing pathway has long been viewed as linear and universal to all mammalian miRNAs. This canonical maturation includes the production of the primary miRNA transcript (pri-miRNA) by RNA polymerase II or III and cleavage of the pri-miRNA by the microprocessor complex Drosha-DGCR8 (Pasha) in the nucleus. The resulting precursor hairpin, the pre-miRNA, is exported from the nucleus by Exportin-5-Ran-GTP. In the cytoplasm, the RNAse Dicer complex with the double-stranded RNA-binding protein TRBP cleaves the pre-miRNA hairpin to its mature length. The functional strand of the mature miRNA (red) is loaded together with Argonaute (Ago2) proteins into the RNA-induced silencing complex (RISC), where it guides RISC to silence target mRNAs through mRNA cleavage, translational repression, or deadenylation, whereas the passenger strand (black) is degraded. [figure reproduced and modified from Winter et al., 2009]

Genetic variants in miRNA target sites

Pharmacogenetics, a term coined by Friedrich Vogel in the 1950s, is defined as the use of a persons' genomic information to guide medical management (Vogel, 1959). This area of research has focused on identifying the genetic foundations of diseases, how genes and the environment interact to cause disease, and using genetics to facilitate effective drug treatment among individuals. The clinical implementation of pharmacogenetics has grown rapidly as the FDA has revised drug labels to include pertinent pharmacogenetic information (Frueh et al., 2008; Lesko and Zineh, 2010). The incorporation of genetic testing at various medical institutions is also becoming more routine in order to facilitate the individualization of healthcare.

As discussed previously, codeine is bioactivated to morphine, by CYP2D6. Approximately 5-10% of individuals carry two nonfunctional *CYP2D6* alleles, such as *CYP2D6*4* characterized by a single nucleotide change from G to A (Crews et al., 2012). The variant A allele disrupts proper formation of CYP2D6 mRNA resulting in a nonfunctional protein. As a consequence, these individuals are unable to produce morphine to achieve its analgesic effects, so a different drug therapy is required (Desmeules et al., 1991). Variations also impact the metabolism of endogenous substrates, such as the *UGT1A1*28* allele and altered bilirubin conjugation. The *UGT1A1*28* allele has been identified as the causal genetic variant of Gilbert's syndrome, a form of unconjugated hyperbilirubinemia, and is characterized by seven TA repeats in the promoter region versus the wild-type allele having six repeats (Bosma et al., 1995). This additional TA repeat results in the reduced transcription of *UGT1A1* by decreasing the binding affinity of the TATA-binding protein to the promoter *(Hsieh et al., 2007)*. This interaction is also important as atazanavir, an antiretroviral protease inhibitor, inhibits UGT1A1. The resultant hyperbilirubinemia, which

can lead to jaundice, can cause patients to discontinue treatment, in which patients with already reduced functioning UGT1A1 are at an increased risk for (Gammal et al., 2016).

In an effort to summarize information on pharmacogenetics, organizations have curated these data into website such as PharmGKB (https://www.pharmgkb.org/), PharmaADME "Core ADME Gene List" (http://www.pharmaadme.org/), and The Human CYP Allele Nomenclature Database (http://www.cypalleles.ki.se/). However, much of the information regarding the use of genetic variants to predict an individual's response to a drug focuses on variations in the promoter and coding regions of genes. As there are over 2500 miRNAs identified to date (miRBase Registry version 20), miRNAs have been shown to regulate many genes, including pharmacogenes (Jin et al., 2016; Li et al., 2016; Pan et al., 2009; Ramamoorthy et al., 2012; Shi et al., 2007; Takagi et al., 2008; To et al., 2008). Emerging evidence has shown that genetic variations in the 3'UTR may contribute to variability in drug response by altering miRNA regulation as well (Ramamoorthy et al., 2012; Swart and Dandara, 2014). Variants within the seed sequence of miRNA target sites may abolish miRNA target sites, as well as create new miRNA target sites (Bhattacharya et al., 2014). These genetic variations in miRNA binding sites of pharmacogenes may explain some of the inter-subject variability in pharmacokinetics and drug response. One particular example that we highlight in this study involves genetic variant effects on miRNA regulation of *CYP2B6*. Various miRNAs have been predicted and experimentally validated to alter expression and activity of *CYP2B6* (Burgess et al., 2015; Jin et al., 2016; Rieger et al., 2015).

CYP2B6 is a highly polymorphic cytochrome P450. Of these variants, the *CYP2B6*6* (516G>T, Q172H and 785A>G, K262R) and *CYP2B6*18* (983T>C, I328T) haplotypes, have been shown to be the most clinically important by causing a reduction in protein

expression and activity (Desta et al., 2007; Hofmann et al., 2008; Klein et al., 2005). The *CYP2B6*6* haplotype results in a splice variant that lacks exons 4 to 6, and has been associated with altered elimination and response of many clinically-relevant drugs, such as efavirenz, bupropion, methadone, and cyclophosphamide (Desta et al., 2007; Eap et al., 2007; Hofmann et al., 2008; Nakajima et al., 2007); however, these and other frequently studied genetic variants do not account for all inter-variability observed for drugs undergoing CYP2B6 metabolism.

Efavirenz, a non-nucleoside reverse transcriptase inhibitor, is prescribed as part of the World Health Organization recommended first-line combination antiretroviral therapy to treat HIV type 1 infection (Organization, 2016). However, efavirenz has been associated with central nervous system adverse events such as hallucinations and insomnia and with treatment failure in some patients (Adkins and Noble, 1998). Higher efavirenz plasma concentrations have also been associated with increased likelihood of adverse CNS effects, whereas lower levels more likely result in treatment failure (Marzolini et al., 2001). Efavirenz has also been shown to have wide variability in plasma concentrations among patients, some of which has been accounted for by genetic polymorphisms in *CYP2B6*, the enzyme primarily responsible for efavirenz biotransformation. Variability in CYP2B6-mediated biotransformation has been observed for other CYP2B6 substrates after the more well-studied polymorphisms have been accounted for, such as the variability in methadone metabolism and clearance (Kharasch et al., 2015). As some drugs have narrow therapeutic windows, better understanding of the inter-individual variability in drug concentrations and response will facilitate better treatment regimens to reduce treatment failure and adverse events in individuals that differ from what is considered standard.

Summary and research aims

The main objective of this proposal is to evaluate developmentally-regulated miRNA regulation of drug disposition genes. My central hypothesis is that hepatic miRNAs post-transcriptionally regulate expression of drug metabolizing genes and their upstream regulatory genes, and that genetic variants in the miRNA target sites within these genes alter the ability of miRNAs to regulate targeted mRNAs. Studies outlined in this dissertation test this hypothesis through the following specific aims:

Specific Aim 1. Identify hepatic miRNAs that have age-related expression patterns.

Specific Aim 2. Determine the ability of developmentally-regulated miRNAs to post-transcriptionally modify the expression of drug metabolism genes.

Specific Aim 3. Identify and functionally validate polymorphisms in predicted miRNA target sites and evaluate their association with clinical drug metabolism.

To test this hypothesis, we measured and analyzed miRNA and mRNA expression in human liver tissues from subjects in three different age groups (fetal, pediatric, and adult). We then validated *in silico* miRNA-mRNA predictions using *in vitro* cell culture models. Next, we identified genetic variants in the 3'UTR of *CYP2B6* of healthy volunteers that were administered efavirenz. Genetic variants that were associated with CYP2B6 activity were further characterized with *in vitro* functional assays to assess their impact on miRNA regulation of *CYP2B6* expression. Due to the large number of genetic variants, a high-throughput method was developed to test hundreds of 3'UTR variants simultaneously in multiple cell lines.

CHAPTER 1

Age-related changes in microRNA expression and pharmacogenes in human liver

Introduction

The expression of hepatic drug disposition genes undergo large changes during liver development; however, the mechanisms behind these changes remain unknown. Emerging evidence implicate miRNAs in regulation of drug disposition genes. In this study, we hypothesize that miRNA expression in human liver tissue changes with age and that this variable expression contributes to the developmental changes in drug metabolism and disposition genes. To test this hypothesis, we measured and analyzed miRNA and mRNA expression in human liver tissues from subjects in three different age groups: fetal, pediatric, and adult. Our results suggest that miRNAs are likely to regulate these genes directly or indirectly through upstream regulatory genes (Burgess et al., 2015).

Materials and Methods

Tissue samples, RNA preparation and cDNA

Human liver tissue specimens were obtained from the NIH-supported tissue programs: the Liver Tissue Cell Distribution System (LTCDS) (n=22), the Minnesota and Pittsburg collection centers (n=35) and the Laboratory of Developmental Biology at the University of Washington (Seattle, WA; n=30). Three liver tissue samples were provided by XenoTech, LLC (Lenexa, KS). Liver tissues were stored at -80ºC. This study was approved by the Indiana University Institutional Review Board.

Total RNA was extracted from 90 human liver samples (fetal, pediatric, and adult; n=30 each). Estimated fetal ages ranged from 15-24 weeks (average=18.8 weeks), pediatric ages from 1-17 years (average=8.6 years), and adult ages 28-80 years (average=54.5 years). This cohort consisted of tissue specimen from 43 male and 35 female donors (the

sex of the remaining samples was unknown). Of the 90 tissue samples, 16, 10, 1 and 63 samples were from Caucasian, African-American, Hispanic or donors of unknown ethnicity, respectively.

Total RNA, including small RNAs, was extracted with the Qiagen miRNeasy Mini Kit (Valencia, CA). Briefly, approximately 30 mg frozen liver tissue was excised and homogenized for 30 sec with a PRO 200 rotary homogenizer (PRO Scientific, Oxford, CT) in QIAzol Lysis Reagent. Subsequently, chloroform was added, mixed, centrifuged, and the aqueous phase transferred to a new tube and mixed with 100% ethanol. The sample was applied onto an RNeasy Mini spin column and washed as recommended by the protocol. To avoid any DNA contamination, an on-column DNase digest was performed using Qiagen RNase-Free DNAse Set (Valencia, CA). After 2 additional washes of the column, RNA was eluted twice with 30 µL of RNase-free water. RNA quality (RQI; RNA quality index) was determined on an Experion StdSens RNA chip (Bio-Rad, Hercules, CA) and concentration measured with a NanoDrop 1000 instrument (Thermo Scientific, Wilmington, DE). The RQI values of the RNA preparations ranged between 7.0 and 9.9. Seventy-six RNA samples had RQI values above 8.1. RNA preparations were stored at -80ºC until analysis.

cDNA for the miRNA panel was made with Megaplex Primer Pools A and B and individual miRNAs tested using TaqMan MicroRNA Assays (hsa-miR-431, hsa-miR-668, hsa-let-7b) with the supporting TaqMan MicroRNA Reverse Transcription Kit (Applied Biosystems, Foster City, CA). cDNA was made according to manufacturer's protocol using the Applied Biosystems GeneAmp PCR System 9700 (Foster City, CA).

miRNA expression profiling

Expression of 754 microRNAs was measured using TaqMan OpenArray Human miRNA Panel using the NT Cycler (Applied Biosystems, Foster City, CA). The threshold cycles were set manually based on visual inspection of real-time amplification curves of each miRNA.

Bioinformatics analysis of the miRNA expression data

The miRNA expression data was quantile normalized using the threshold cycle values of miRNA data obtained from the TaqMan OpenArray. Differential expression of the miRNAs was determined by *p*-value comparisons between the 60 fetal and pediatric samples and between the 59 pediatric and adult samples (one outlying adult sample was removed from statistical analyses). They were corrected for by false discovery rate (FDR) using the Benjamini Hochberg equation (Benjamini et al., 2001). The top absorption, distribution, metabolism, excretion (ADME) genes (http://www.pharmaadme.org/joomla/) that were predicted to be targeted by the differentially expressed miRNAs in this study were determined using Ingenuity Pathway Analysis (Qiagen, Valencia, CA). The IPA program extracts predicted and experimentally validated miRNA targets from TargetScan, miRecords, TarBase, and text mining through Ingenuity Expert Findings and Ingenuity Expert Assisted Findings.

Measurement of mRNA expression in human liver samples

RNA-seq was performed as previously described (Ramamoorthy et al., 2012). Standard methods were used for RNA-sequencing library construction, EXBead preparation, and Next-Generation sequencing, based on the protocol provided for the Life Technologies SOLiD4 system. Briefly, 2 µg of total RNA per sample of only 30 of the 90 total samples

(fetal, pediatric, and adult; n=10) were used for library preparation. The ribosomal RNA was depleted using RiboMinus Eukaryote Kit for RNA-Seq (Invitrogen, Carlsbad, CA).

Bioinformatics analysis of RNA-seq data

RNA-seq data analysis included the following steps: quality assessment, sequence alignment, and gene expression analysis.

Data processing and quality assessment

We used SOLiD Instrument Control Software and SOLiD Experiment Tracking System software for the read quality recalibration. Each sequence read was scanned for low-quality regions, and if a 5-base sliding window had an average quality score less than 20, the read was truncated at that position. Any reads less than 35 bases were discarded. Our experience suggested that this strategy effectively eliminated low-quality reads while high-quality regions were retained (Breese and Liu, 2013; Juan et al., 2013; Todd et al., 2013).

Sequence alignment

The BFAST (http://bfast.sourceforge.net) (Homer et al., 2009) was used as the primary alignment algorithm because it has high sensitivity for aligning reads on loci containing small insertions and deletions compared to the reference genome (hg19). NGSUtils (http://ngsutils.org/) (Breese and Liu, 2013), a TopHat-like strategy (Trapnell et al., 2009), was employed to align the sequencing reads that crossed splicing junctions. After aligning the sequence reads to a filtering index including repeats, ribosomal RNAs, and other sequences that were not of interest, a sequence alignment was conducted for three levels: genome, known junctions (University of California Santa Cruz Genome Browser), and novel junctions (based on the enriched regions identified in the genomic alignment). We

restricted our analysis to the uniquely aligned sequences with no more than two mismatches.

RNA-Seq differential expression analysis

Differentially expressed genes were identified using edgeR (Robinson et al., 2010), a Bioconductor package for differential expression analysis of digital gene expression data, based on a negative binomial distribution. To ensure reliable gene expression measurements, genes with less than 1 read per million mappable reads were removed. A *p*-value was calculated both for differential expression of the drug disposition genes between the 20 fetal and pediatric samples and between the 20 pediatric and adult samples analyzed for RNA-seq. Benjamini-Hochberg's algorithm was used to control the FDR (Benjamini et al., 2001).

Inverse correlations

A linear regression model considering developmental periods as a cofactor was used to identify inverse correlations between the expression levels of the developmentally changing miRNAs and the drug disposition mRNA expression levels. The resultant *p*-values were FDR corrected using Benjamini-Hochberg (Benjamini et al., 2001).

Results

miRNA expression changes with developmental periods

To determine miRNA expression patterns across the fetal, pediatric (0-18 years old), and adult (over 18 years old) developmental periods, we detected the expression of 533 miRNAs in 90 liver samples using a predesigned, commercially-available TaqMan OpenArray MicroRNA panel for humans. The estimated fetal ages ranged from 15-24 weeks, pediatric from 1-17 years (average=8.6 years), and adults 28-80 years (average=54.5). These liver samples consisted of 43 male and 35 female donors (the sex of the remaining samples was unknown) and 16, 10, 1 and 63 samples were from Caucasian, African-American, Hispanic or unknown ethnicity, respectively. We also measured three of these miRNAs, each in a unique set of 20 samples using single TaqMan assays to validate patterns in the Open Array platform (Figure 2). miRNAs that did not generate threshold cycle values in at least 6 samples in a given developmental period were excluded from analysis unless that miRNA was not expressed in the group at all. Only miRNAs that were statistically significant after false discovery rate (FDR) correction are discussed. FDR was used to adjust for multiple comparisons as the expression of over 500 miRNAs were measured which could lead to increased Type I error (false positives). It is of note that, FDR is a less stringent correction method than the Bonferroni correction, which is designed to eliminate the probability of even one Type I error at the risk of increasing the Type II error. Since our next steps are to validate these changes in miRNA expression and determine their targets, the FDR correction method was appropriate.

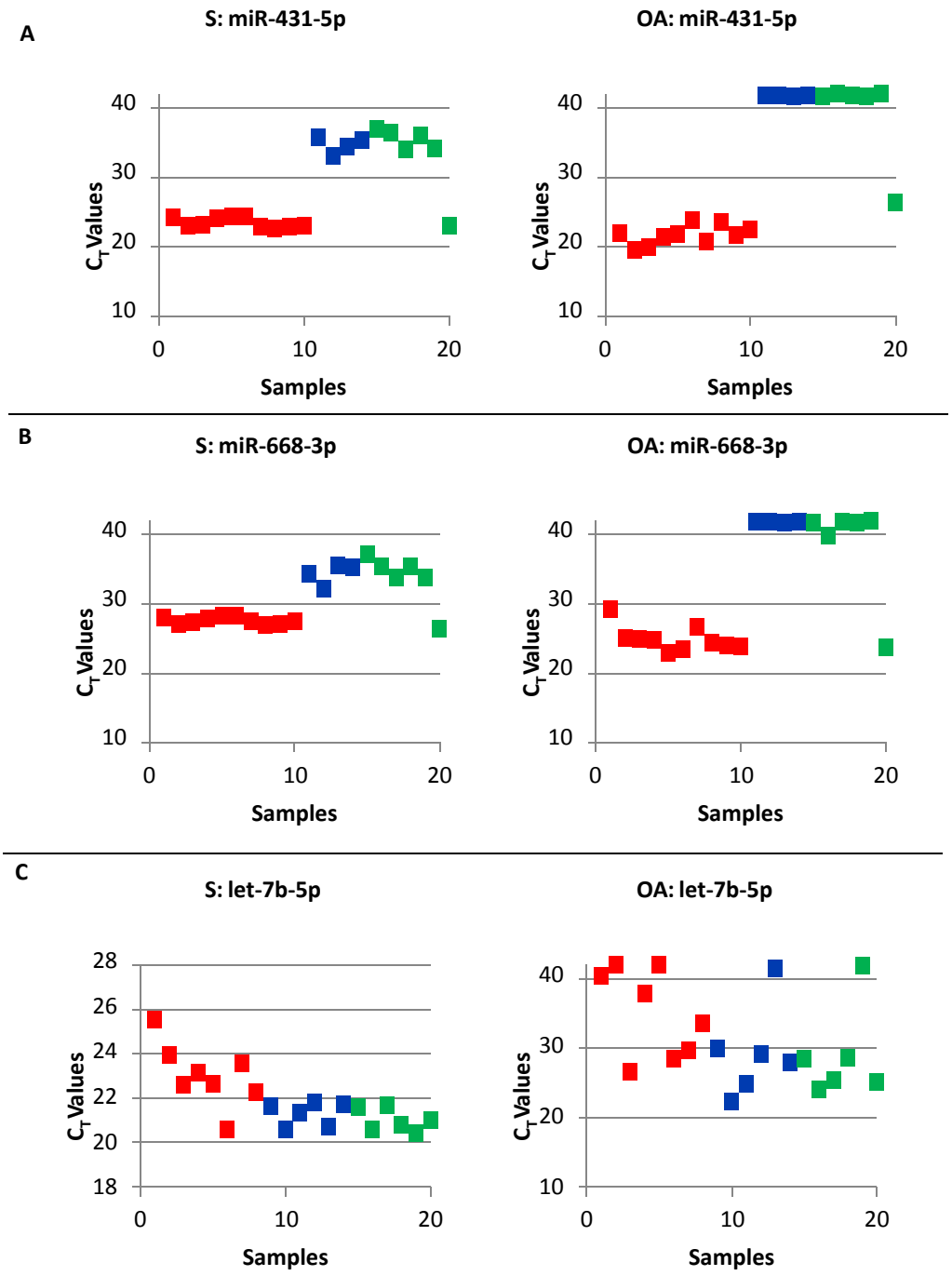

Figure 2: Quantification of selected miRNAs by TaqMan OpenArrays and by individual TaqMan assays

Comparison of miRNA expression among 20 randomly selected human liver samples between TaqMan OpenArray (OA) and individual TaqMan assays (S). Fetal (Red), Pediatric (Blue), Adult (Green).

Next, we created a Principal Components Analysis (PCA), a tool that is often used to visualize the distance and relatedness between populations. As shown in the PCA, the expression profiles for the fetal group are distinctly separated from the pediatric and adult groups (Figure 3). Hierarchical clustering, using Spearman Rank Dissimilarity, was implemented to depict the grouping of both samples and miRNAs (Figure 4) and reveal 71% dissimilarity between the fetal group and the pediatric/adult groups. Although not as dramatic, there are notable dissimilarities among the pediatric and adult groups as well. There are also clusters of miRNAs that are significantly upregulated and downregulated together among the developmental groups. We primarily focus on the top 45 developmentally-regulated miRNAs between the groups (first 20 in each category of Table 2 and all in Table 3) in the results and discussion. To enable comparisons with previously published literature, the alternative nomenclature for select miRNAs are provided (Table 1). The -5p and -3p refers to the mature products produced by either the 5' or 3' arm of the hairpin precursor (i.e. miR-625-5p and miR-625-3p). The # or * refers to the strand of the miRNA considered nonfunctional or expressed at lower concentrations. However, it has been shown that that the miR* sequences can be functional and may be dependent on tissue type and other factors (Czech and Hannon, 2011; Griffiths-Jones et al., 2011; Yang et al., 2011).

During the transition from the fetal to the pediatric period, 114 miRNAs were upregulated and 72 miRNAs were downregulated (Table 2). Between the pediatric and adult periods, two miRNAs were upregulated and three were downregulated (Table 3). An example of miRNA expression changes in each category of Table 2 & 3 is provided in dot plots of individual miRNA threshold cycle (C_T) values (Figure 5) (Note: An increase in C_T values indicate a decrease in miRNA expression. miRNAs that do not generate a C_T value are assigned a value of 40 indicating that it is undetected). Figure 5A shows an increase in

let-7a-5p between the fetal and pediatric/adult group whereas Figure 5B shows a decrease in miR-431-5p expression between these groups. Figure 5C & 5D depicts the gradual increase and decrease in expression of miR-34a-5p and miR-18a-5p, respectively, across the developmental periods.

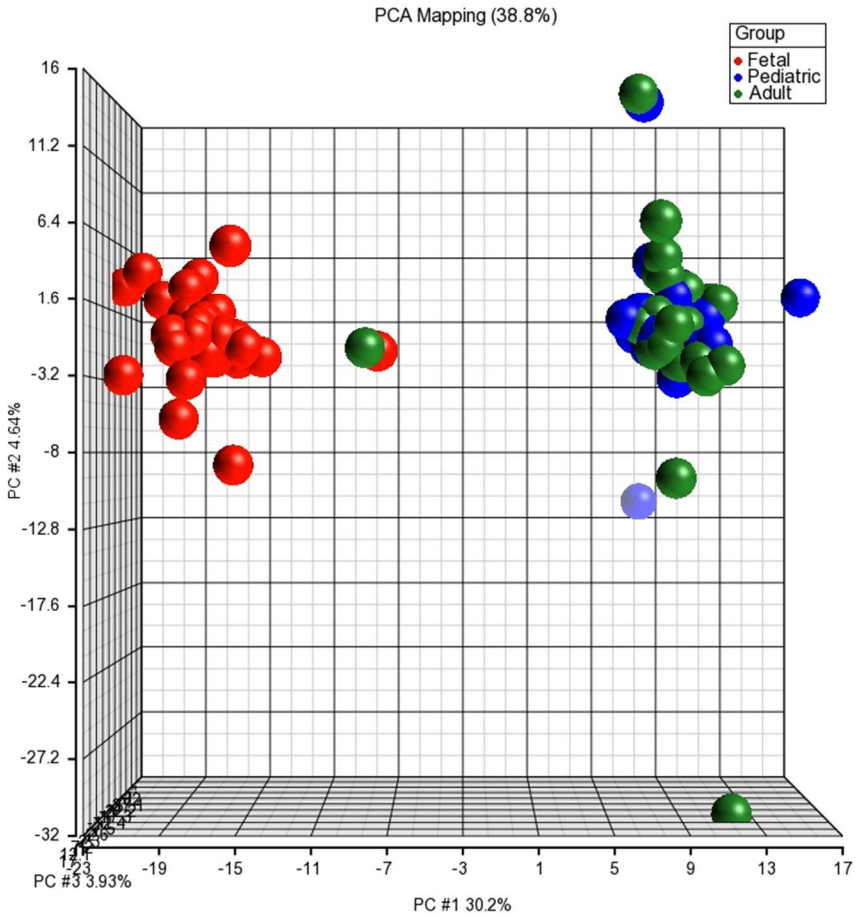

Figure 3: Principal components analysis of developmentally-regulated miRNAs

Principal components analysis of all 533 miRNAs measured using TaqMan OpenArray. Axes are principal components 1, 2, and 3. Fetal (Red), Pediatric (Blue), Adult (Green).

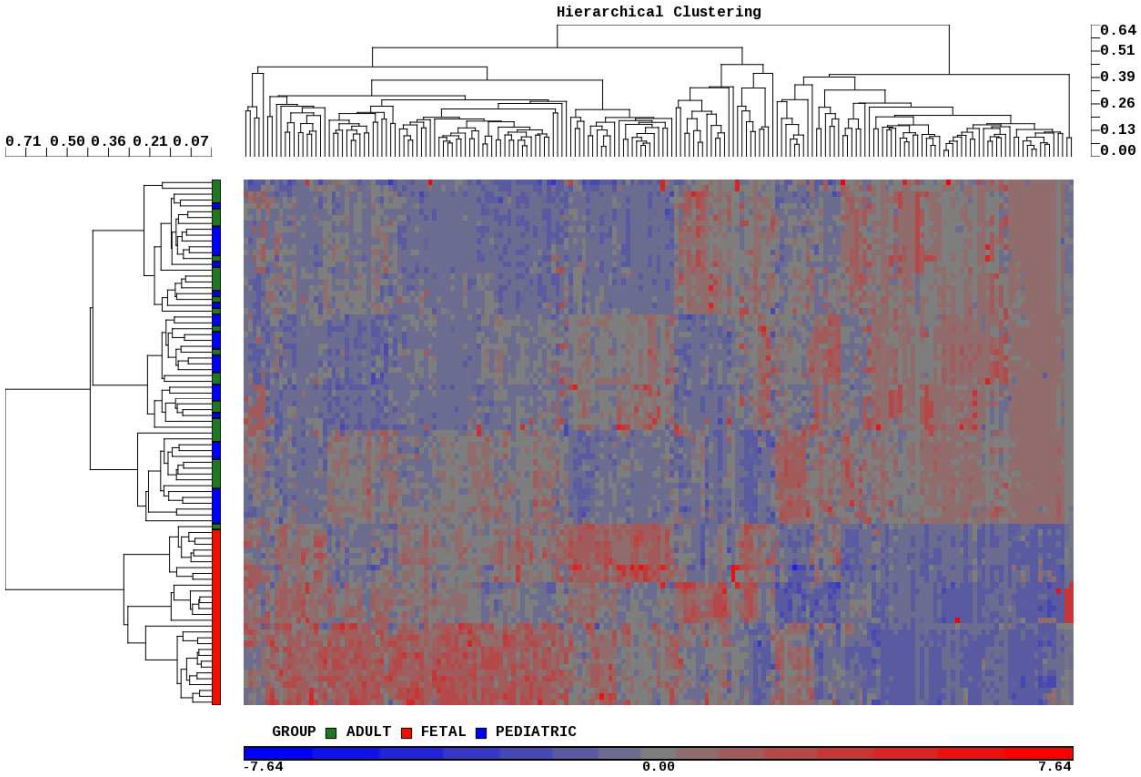

Figure 4: Heatmap of all developmentally-regulated miRNAs in human liver samples
Hierarchical clustering of miRNA expression levels using Spearman Rank Dissimilarity. *X*-axis: miRNAs. *Y*-axis: 90 samples across the 3 developmental periods. Fetal (Red), Pediatric (Blue), Adult (Green). Color scale below the figure shows increasing expression from blue to gray to red.

Table 1: miRNA naming using alternative designations

miRNA	Alternative Name	TaqMan Assay #	Sequence
let-7a-5p	let-7a	377	UGAGGUAGUAGGUUGUAUAGUU
let-7b-5p	let-7b	2619	UGAGGUAGUAGGUUGUGUGGUU
let-7e-5p	let-7e	2406	UGAGGUAGGAGGUUGUAUAGUU
let-7f-5p	let-7f	382	UGAGGUAGUAGAUUGUAUAGUU
let-7g-5p	let-7g	2282	UGAGGUAGUAGUUUGUACAGUU
miR-106a-5p	miR-106a	2169	AAAAGUGCUUACAGUGCAGGUAG
miR-10a-5p	miR-10a	387	UACCCUGUAGAUCCGAAUUUGUG
miR-10b-5p	miR-10b	2218	UACCCUGUAGAACCGAAUUUGUG
miR-10b-3p	miR-10b#	2315	ACAGAUUCGAUUCUAGGGGAAU
miR-122-3p	miR-122#	2130	AACGCCAUUAUCACACUAAAUA
miR-1244	miR-1244	2791	AAGUAGUUGGUUUGUAUGAGAUGGUU
miR-125b-5p	miR-125b	449	UCCCUGAGACCCUAACUUGUGA
miR-126-5p	miR-126#	451	CAUUAUUACUUUUGGUACGCG
miR-1271-5p	miR-1271	2779	CUUGGCACCUAGCAAGCACUCA
miR-1275	miR-1275	2840	GUGGGGGAGAGGCUGUC
miR-128a-3p	miR-128a	2216	UCACAGUGAACCGGUCUCUUU
miR-130a-3p	miR-130a	454	CAGUGCAAUGUUAAAAGGGCAU
miR-132-3p	miR-132	457	UAACAGUCUACAGCCAUGGUCG
miR-136-3p	miR-136#	2100	CAUCAUCGUCUCAAAUGAGUCU
miR-139-3p	miR-139-3p	2313	GGAGACGCGGCCCUGUUGGAGU
miR-139-5p	miR-139-5p	2289	UCUACAGUGCACGUGUCUCCAG
miR-140-3p	miR-140-3p	2234	UACCACAGGGUAGAACCACGG
miR-144-5p	miR-144#	2148	GGAUAUCAUCAUAUACUGUAAG
miR-148b-3p	miR-148b	471	UCAGUGCAUCACAGAACUUUGU
miR-154-3p	miR-154#	478	AAUCAUACACGGUUGACCUAUU
miR-18a-5p	miR-18a	2422	UAAGGUGCAUCUAGUGCAGAUAG
miR-20a-3p	miR-20a#	2437	ACUGCAUUAUGAGCACUUAAAG
miR-200a-3p	miR-200a	502	UAACACUGUCUGGUAACGAUGU
miR-200b-3p	miR-200b	2251	UAAUACUGCCUGGUAAUGAUGA
miR-219a-5p	miR-219	522	UGAUUGUCCAAACGCAAUUCU
miR-30a-3p	miR-30a-3p	416	CUUUCAGUCGGAUGUUUGCAGC
miR-34a-5p	miR-34a	426	UGGCAGUGUCUUAGCUGGUUGU
miR-382-5p	miR-382	572	GAAGUUGUUCGUGGUGGAUUCG
miR-409-3p	miR-409-3p	2332	GAAUGUUGCUCGGUGAACCCCU
miR-411-5p	miR-411	1610	UAGUAGACCGUAUAGCGUACG
miR-431-5p	miR-431	1979	UGUCUUGCAGGCCGUCAUGCA

miR-432-5p	miR-432	1026	UCUUGGAGUAGGUCAUUGGGUGG
miR-433-3p	miR-433	1028	AUCAUGAUGGGCUCCUCGGUGU
miR-483-3p	miR-483-3p	2339	UCACUCCUCUCCUCCCGUCUU
miR-485-3p	miR-485-3p	1277	GUCAUACACGGCUCUCCUCUCU
miR-487a-3p	miR-487a	1279	AAUCAUACAGGGACAUCCAGUU
miR-512-3p	miR-512-3p	1823	AAGUGCUGUCAUAGCUGAGGUC
miR-515-3p	miR-515-3p	2369	GAGUGCCUUCUUUUGGAGCGUU
miR-519a-3p	miR-519a	2415	AAAGUGCAUCCUUUUAGAGUGU
miR-519e-5p	miR-519e#	1166	UUCUCCAAAAGGGAGCACUUUC
miR-539-5p	miR-539	1286	GGAGAAAUUAUCCUUGGUGUGU
miR-625-5p	miR-625	2431	AGGGGGAAAGUUCUAUAGUCC
miR-668-3p	miR-668	1992	UGUCACUCGGCUCGGCCCACUAC
miR-889-3p	miR-889	2202	UUAAUAUCGGACAACCAUUGU

Table 2: List of differentially expressed miRNAs between fetal and pediatric samples

Upregulated			
miRNAs*	**p-value**	**FDR****	**Fold Change**
miR-497-5p	8.60E-27	2.90E-25	> 500
miR-139-5p	6.20E-26	2.00E-24	3.7
miR-29c-3p	2.00E-23	5.00E-22	7.9
miR-195-5p	1.80E-20	3.70E-19	34
miR-23b-3p	4.80E-19	8.90E-18	4.9
miR-579-3p	9.60E-19	1.60E-17	131.4
miR-576-3p	3.20E-18	5.30E-17	18.3
miR-29a-5p	1.80E-17	2.60E-16	21.2
miR-29b-2-5p	2.10E-17	3.00E-16	> 500
miR-511-5p	4.00E-17	5.40E-16	10
miR-145-3p	1.40E-16	1.80E-15	178.5
miR-22-5p	2.60E-16	3.20E-15	6.2
let-7a-5p	4.70E-16	5.50E-15	2.1
miR-505-3p	1.40E-15	1.60E-14	64.1
miR-505-5p	1.80E-15	1.90E-14	33.5
miR-29b-3p	2.30E-15	2.40E-14	7.4
miR-99a-3p	3.40E-15	3.40E-14	44
miR-628-3p	8.30E-15	7.80E-14	58.1
miR-27b-5p	9.40E-15	8.60E-14	5.5
miR-193b-5p	3.40E-14	2.90E-13	42.3
miR-10a-5p	4.90E-14	4.00E-13	3.4
miR-374a-3p	6.00E-14	4.60E-13	79.9
miR-590-5p	2.60E-13	1.90E-12	4
miR-132-3p	2.70E-13	2.00E-12	3.7
miR-146b-3p	1.40E-12	9.80E-12	43.3
miR-378a-5p	1.90E-12	1.20E-11	246.8
miR-885-5p	2.80E-12	1.80E-11	2.6
let-7b-5p	5.00E-12	3.20E-11	> 500
miR-30a-3p	5.50E-12	3.50E-11	3.3
miR-152-3p	5.80E-12	3.60E-11	2.5
miR-340-3p	6.40E-12	3.90E-11	4.1
miR-194-3p	2.30E-11	1.40E-10	12.4
miR-24-2-5p	2.40E-11	1.40E-10	92.9
miR-146b-5p	3.40E-11	2.00E-10	3.6
miR-590-3p	3.70E-11	2.10E-10	13.3

Upregulated cont'd			
miRNAs*	**p-value**	**FDR****	**Fold Change**
miR-193a-5p	5.00E-11	2.90E-10	2.4
miR-148b-5p	5.70E-11	3.20E-10	13.3
miR-125b-5p	6.80E-11	3.80E-10	2.2
miR-362-3p	6.90E-11	3.80E-10	8.5
miR-422a	1.20E-10	6.60E-10	242.7
miR-374a-5p	3.00E-10	1.50E-09	1.9
miR-455-5p	8.90E-10	4.20E-09	2.1
miR-211-5p	9.10E-10	4.30E-09	106.8
miR-151a-5p	1.40E-09	6.60E-09	4.3
miR-30e-3p	2.10E-09	9.60E-09	2
miR-24-3p	3.30E-09	1.50E-08	2
miR-192-3p	5.10E-09	2.30E-08	4.3
miR-27a-5p	5.60E-09	2.40E-08	10.8
miR-744-3p	9.00E-09	3.90E-08	4.1
miR-32-5p	1.20E-08	5.00E-08	22.8
miR-95-3p	1.40E-08	5.80E-08	27.6
miR-27a-3p	1.40E-08	6.10E-08	2.4
miR-383-5p	2.00E-08	8.60E-08	9.9
miR-592	2.30E-08	9.80E-08	13.1
let-7g-5p	3.10E-08	1.30E-07	1.7
miR-1275	3.30E-08	1.30E-07	3
miR-939-5p	3.60E-08	1.50E-07	61.3
miR-597-5p	3.90E-08	1.60E-07	24.9
miR-186-5p	5.90E-08	2.30E-07	1.8
miR-28-3p	1.60E-07	6.40E-07	2.2
miR-28-5p	2.00E-07	7.80E-07	2
miR-99a-5p	2.30E-07	8.60E-07	1.8
miR-122-3p	3.00E-07	1.10E-06	9.2
miR-502-3p	3.40E-07	1.20E-06	8.6
miR-26b-5p	6.50E-07	2.30E-06	1.9
miR-200a-3p	7.00E-07	2.40E-06	2.7
miR-628-5p	7.00E-07	2.40E-06	48.5
miR-455-3p	9.30E-07	3.20E-06	1.9
miR-21-5p	1.60E-06	5.20E-06	13.4
miR-452-5p	1.60E-06	5.30E-06	4.1
miR-148b-3p	4.30E-06	1.30E-05	1.8
miR-155-5p	4.60E-06	1.40E-05	7.1
miR-194-5p	6.90E-06	2.10E-05	1.8

Upregulated cont'd			
miRNAs*	**p-value**	**FDR****	**Fold Change**
miR-375	1.30E-05	3.60E-05	2.7
miR-143-3p	1.50E-05	4.20E-05	1.8
miR-1271-5p	2.30E-05	6.40E-05	4.2
miR-139-3p	2.40E-05	6.80E-05	19.5
miR-128a-3p	3.10E-05	8.70E-05	1.6
miR-223-5p	4.80E-05	1.30E-04	3.2
miR-26a-5p	5.40E-05	1.50E-04	1.7
miR-625-5p	6.30E-05	1.70E-04	3.2
miR-216b-5p	7.70E-05	2.10E-04	9.6
miR-423-5p	8.50E-05	2.30E-04	1.6
miR-26b-3p	1.10E-04	2.90E-04	4
miR-17-5p	1.20E-04	3.00E-04	469.2
miR-34a-5p	1.60E-04	4.10E-04	1.7
miR-31-5p	2.10E-04	5.20E-04	9.8
miR-212-3p	2.20E-04	5.60E-04	7.6
miR-10b-5p	5.60E-04	1.30E-03	9.1
miR-106a-5p	7.50E-04	1.80E-03	151.9
miR-199a-5p	9.40E-04	2.20E-03	1.7
miR-146a-5p	1.00E-03	2.30E-03	38
miR-126-5p	1.30E-03	3.00E-03	1.5
miR-330-3p	2.00E-03	4.60E-03	3.9
miR-320b	2.20E-03	4.90E-03	1.9
miR-150-5p	2.40E-03	5.30E-03	6.7
miR-10b-3p	2.80E-03	6.10E-03	17.3
miR-27b-3p	3.30E-03	7.20E-03	1.4
let-7f-5p	3.50E-03	7.60E-03	1.5
miR-331-3p	3.70E-03	8.00E-03	1.4
miR-424-5p	4.30E-03	9.10E-03	3.8
miR-140-3p	4.50E-03	9.50E-03	2.2
miR-145-5p	5.60E-03	1.20E-02	22.2
miR-532-3p	6.10E-03	1.30E-02	1.2
miR-142-5p	6.60E-03	1.40E-02	3.4
let-7e-5p	8.80E-03	1.80E-02	1.3
miR-671-3p	8.60E-03	1.80E-02	2.9
miR-30a-5p	9.60E-03	1.90E-02	1.5
miR-197-3p	1.20E-02	2.40E-02	1.3
miR-1244	1.80E-02	3.40E-02	1.9
miR-15a-3p	2.20E-02	4.10E-02	6.7

miR-199a-3p	2.20E-02	4.20E-02	1.4
miR-30d-5p	2.20E-02	4.20E-02	1.5
miR-19b-3p	2.70E-02	4.90E-02	12.7
Downregulated			
miRNAs	**p-value**	**FDR**	**Fold Change**
miR-431-5p	1.00E-58	5.50E-56	< -500
miR-668-3p	5.00E-42	1.30E-39	< -500
miR-539-5p	3.30E-36	4.30E-34	-101.6
miR-411-5p	8.30E-36	8.90E-34	-18.2
miR-409-3p	2.10E-34	1.60E-32	-30.8
miR-889-3p	4.70E-32	3.10E-30	-39
miR-433-3p	6.00E-32	3.60E-30	< -500
miR-483-3p	2.00E-30	1.10E-28	-52.6
miR-136-3p	3.20E-30	1.50E-28	-26.1
miR-512-3p	5.50E-30	2.50E-28	< -500
miR-432-5p	5.90E-28	2.20E-26	< -500
miR-485-3p	5.60E-28	2.20E-26	< -500
miR-382-5p	8.70E-28	3.10E-26	< -500
miR-487a-3p	3.80E-25	1.10E-23	< -500
miR-519e-5p	1.20E-24	3.40E-23	< -500
miR-130a-3p	3.10E-24	8.30E-23	-3.7
miR-515-3p	7.30E-23	1.80E-21	< -500
miR-154-3p	1.00E-22	2.30E-21	< -500
miR-144-5p	2.60E-21	5.80E-20	< -500
miR-519a-3p	2.20E-20	4.40E-19	< -500
miR-526b-5p	4.00E-20	7.60E-19	< -500
miR-377-5p	8.40E-19	1.50E-17	< -500
miR-221-3p	6.90E-18	1.10E-16	-3
miR-654-5p	2.30E-17	3.20E-16	< -500
miR-301a-3p	7.50E-17	1.00E-15	-4.9
miR-519d-3p	1.90E-16	2.40E-15	< -500
miR-494-3p	6.40E-16	7.20E-15	< -500
miR-487b-3p	7.30E-16	8.10E-15	-389.5
miR-18a-5p	2.30E-15	2.40E-14	-5.1
miR-370-3p	4.70E-15	4.50E-14	-55.2
miR-493-3p	1.60E-14	1.40E-13	< -500
miR-154-5p	1.70E-14	1.40E-13	< -500
miR-9-3p	2.80E-14	2.40E-13	-13.9
miR-323a-3p	5.40E-14	4.20E-13	< -500
miR-337-5p	8.00E-14	6.10E-13	-121.5

miR-543	1.60E-13	1.20E-12	-67
miR-411-3p	3.00E-13	2.10E-12	< -500
miR-758-3p	1.70E-12	1.10E-11	< -500
miR-654-3p	3.30E-11	1.90E-10	-118.7
miR-184	8.50E-11	4.60E-10	< -500
miR-206	1.60E-10	8.10E-10	-234.8
miR-324-5p	1.30E-09	6.00E-09	-2
miR-185-5p	2.80E-09	1.30E-08	-2.6
miR-376c-3p	3.10E-09	1.40E-08	< -500
miR-9-5p	3.90E-08	1.60E-07	-15.6
miR-410-3p	6.90E-08	2.70E-07	-98.7
miR-652-3p	1.00E-07	4.00E-07	-2
miR-1180-3p	1.10E-07	4.40E-07	-3.2
miR-106b-5p	2.40E-07	8.90E-07	-1.6
miR-20a-5p	4.40E-07	1.60E-06	-1.8
miR-127-3p	4.70E-07	1.70E-06	-19.4
miR-376a-3p	1.10E-06	3.90E-06	-30.5
miR-99b-5p	1.60E-06	5.20E-06	-1.7
miR-942-5p	2.50E-06	8.20E-06	-2.6
miR-106b-3p	3.30E-06	1.00E-05	-5.1
miR-19b-1-5p	5.00E-06	1.50E-05	-2.5
miR-337-3p	7.50E-06	2.20E-05	-62.9
miR-1247-5p	3.20E-05	8.80E-05	-117
miR-25-3p	8.90E-05	2.40E-04	-1.6
miR-181a-5p	1.00E-04	2.70E-04	-1.5
miR-369-3p	3.10E-04	7.70E-04	-51.7
miR-381-3p	4.20E-04	1.00E-03	-36.9
miR-20b-5p	9.20E-04	2.20E-03	-5.5
miR-93-3p	1.70E-03	4.00E-03	-1.8
miR-744-5p	2.60E-03	5.80E-03	-1.6
miR-335-5p	3.90E-03	8.40E-03	-1.5
miR-339-3p	9.50E-03	1.90E-02	-1.4
miR-222-3p	1.00E-02	2.00E-02	-1.6
miR-425-5p	1.00E-02	2.00E-02	-3.5
miR-16-5p	1.90E-02	3.60E-02	-1.3
miR-141-3p	2.50E-02	4.60E-02	-8.1
miR-483-5p	2.70E-02	4.90E-02	-4.4

*The alternative nomenclature for select miRNAs and TaqMan assay IDs are provided in Table 1, to allow relation of our data to that utilized in other reports using the # designation over the -3p or -5p designations.
**False discovery rate comparing fetal vs. pediatric

Note: A 2-fold change means there is a 2-fold higher increase in miRNA expression from fetal to pediatric human liver tissues.

Table 3: List of differentially expressed miRNAs between pediatric and adult samples

Downregulated			
miRNA	**p-value**	**FDR***	**Fold Change**
miR-18a-5p	1.4E-05	3.7E-03	-2.0
miR-20a-3p	7.8E-05	1.4E-02	-2.0
miR-219a-5p	1.7E-04	2.3E-02	-12.0
Upregulated			
miRNA	**p-value**	**FDR***	**Fold Change**
miR-34a-5p	1.6E-06	8.3E-04	2.1
miR-30a-3p	3.2E-04	3.4E-02	1.7

*False discovery rate comparing pediatric vs. adult

Note: A 2-fold change means there is a 2-fold higher increase in miRNA expression from pediatric to adult.

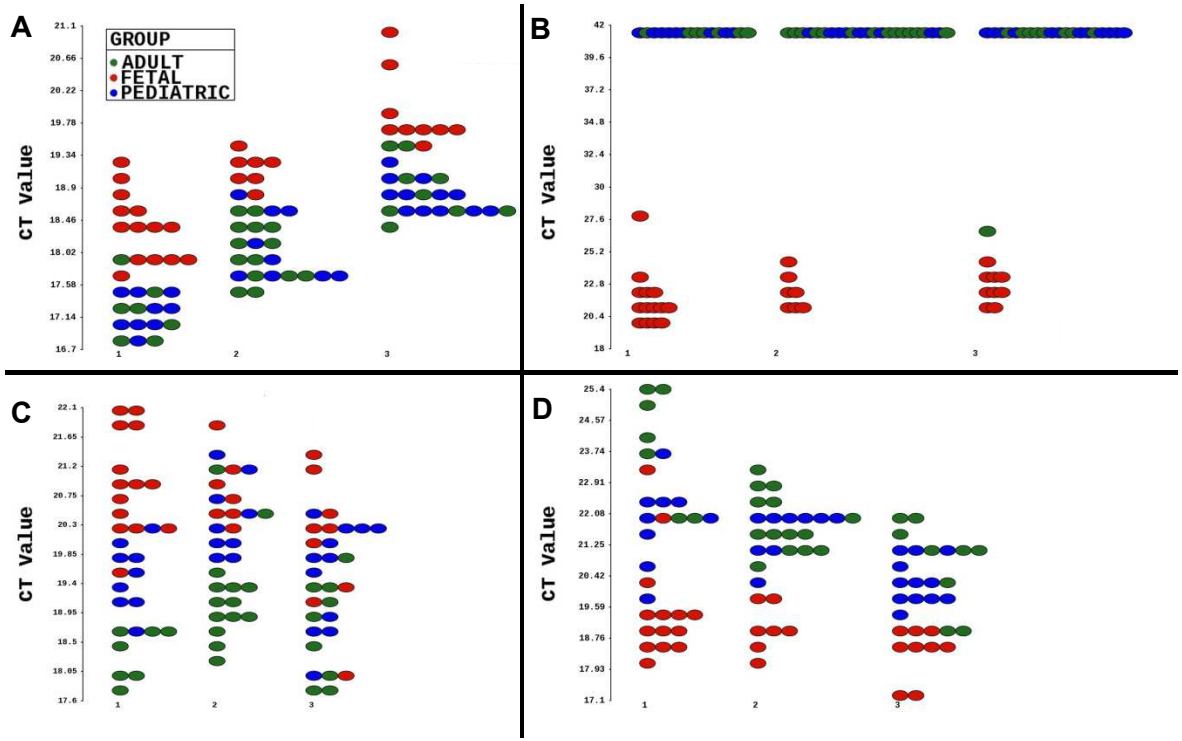

Figure 5: Dot plots of miRNAs that changed across the developmental periods

Dot plots of individual miRNA threshold cycle (C_T) values in the 90 samples. (Note: Increase in C_T value indicates a decrease in miRNA expression) A. let-7a-5p increasing expression between fetal and pediatric/adult groups. B. miR-431-5p decreasing expression between fetal and pediatric/adult groups. C. miR-34a-5p gradually increasing in expression with age. D. miR-18a-5p gradually decreasing in expression with age. *X*-axis: There are three batches across the 90 samples, 1, 2, 3 as the qPCR instrument could only analyze a max of 30 samples at a time. As a result, there is a batch effect that was corrected for in all statistical analyses. *Y*-axis: C_T Values. Fetal (Red), Pediatric (Blue), Adult (Green).

Inverse correlation of expression of miRNAs and pharmacogene mRNAs

Over 14,000 human genes were analyzed using RNA-seq in 30 randomly selected liver samples from our 90 human liver samples (10 samples per age group). Figure 6 displays the developmental expression patterns of 34 genes involved in drug absorption, distribution, metabolism, excretion (ADME); also included are several genes that regulate the expression of these ADME genes (Figure 6 & Table 4). Among those genes, expression of 28 mRNAs increased and expression of 3 decreased from fetal to pediatric and two increased and five decreased from pediatric to adult. *CYP2D6* and *UGT2B17* gene expression levels were among those that increased from pediatric to adult while *CYP1A1, CYP1A2, CYP2C19, GSTM1,* and *SLCO1B3* expression levels decreased from pediatric to adult. *CYP3A7, GSTP1*, and *SLC15A2* expression decreased from fetal to pediatric/adult while most of the others increased. These findings are consistent with previous findings regarding the developmental expression profiles for these pharmacogenes (de Wildt et al., 1999; Hines, 2008, 2013; Mooij et al., 2014).

A linear regression model was used to determine negative correlations between the expression levels of the developmentally changing miRNAs and the mRNA expression levels of pharmacogenes. In order to eliminate bias due to the difference in the expression levels of these miRNAs and mRNAs, we considered developmental periods as a cofactor while searching for inverse correlations between the miRNA and target genes. The negative estimates shown in Table 5 indicate the changes in mRNA expression. Estimates indicate the changes in mRNA expressed as RPKM (reads per kilobases per million) per one C_T value decrease in miRNA expression. More abundantly expressed mRNA in our data such as *CYP2E1* (RPKM values ranging from 3.3-3085) will result in larger estimated

changes of mRNA levels compared to genes with less abundant mRNA such as *ABCG2* (.4-7.5) (data not shown). We observed over 1000 negative correlations (Table 5).

In silico identification of miRNAs predicted to target the mRNA of top pharmacogenes

Predicted miRNA target analysis was performed using Ingenuity Pathway Analysis. This program identifies predicted and experimentally validated targets from multiple databases. Among the developmentally-regulated miRNAs and 34 pharmacogenes, 93 predictions and six experimentally validated targets were revealed involving 27 genes and 67 miRNAs (Table 6). Eighteen of these predictions overlapped with the negatively correlated miRNA-mRNA combinations (Table 5).

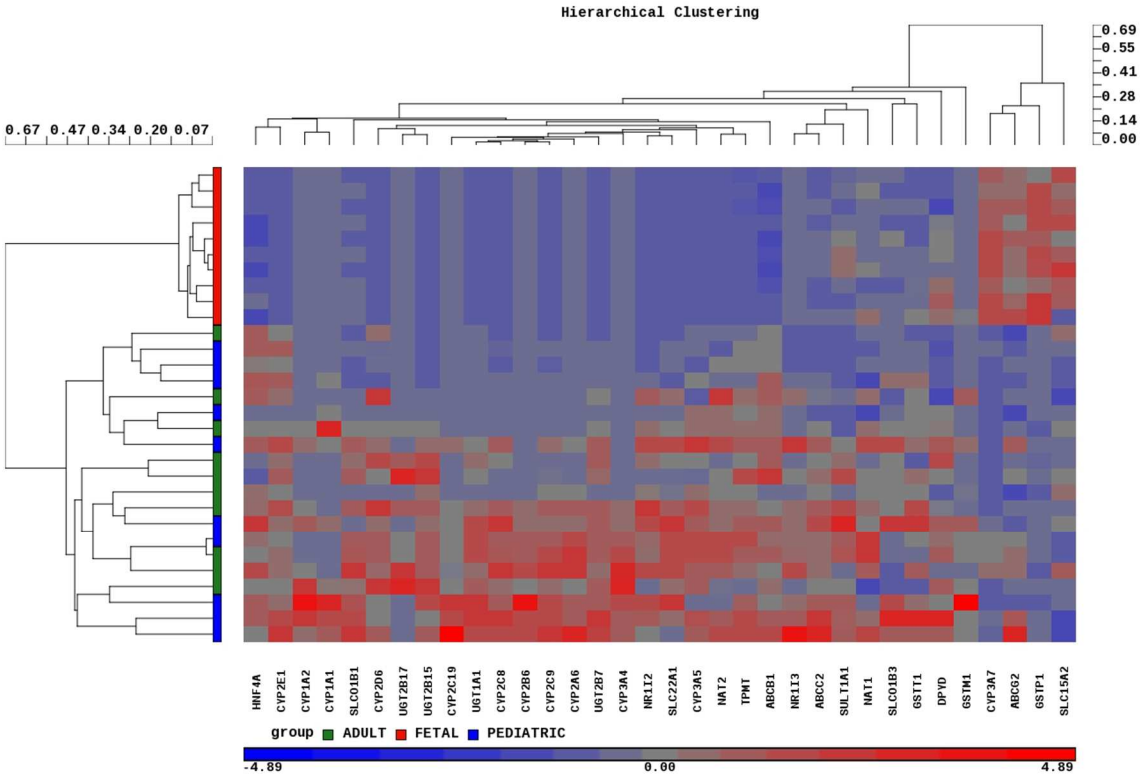

Figure 6: Heatmap of the mRNA expression of pharmacogenes across the developmental periods

Hierarchical clustering of ADME and regulatory gene mRNA using Spearman Rank Dissimilarity. *X*-axis: mRNAs. *Y*-axis: 30 samples across the 3 developmental periods (Red: Fetal, Blue: Pediatric, Green: Adult). Color scale below the figure shows increasing expression from blue to gray to red. **SLC22A2* and *SLC22A6* are excluded due to insufficient reads in the majority of samples.

Table 4: mRNA expression of pharmacogenes

	Fetal vs. Pediatric				Pediatric vs. Adult			
Gene	**logFC[1]**	**logCPM[2]**	**p-value**	**FDR[3]**	**logFC**	**logCPM**	**p-value**	**FDR**
ABCB1	3.1	5.8	3.0E-37	6.1E-36	0.0	6.5	9.9E-01	1.0
ABCC2	1.8	8.6	4.0E-15	2.9E-14	-0.5	8.9	1.1E-01	7.5E-01
ABCG2	-0.3	5.0	5.8E-02	9.4E-02	-0.4	4.5	2.8E-01	1.0
CYP1A1	6.8	6.4	2.2E-111	4.0E-109	-1.9	6.8	2.0E-04	1.4E-02
CYP1A2	8.7	7.4	4.4E-150	5.5E-147	-1.9	7.8	3.9E-05	3.9E-03
CYP2A6	8.2	7.7	2.8E-144	1.9E-141	-0.4	8.4	2.8E-01	1.0
CYP2B6	7.8	9.2	2.3E-143	1.4E-140	-0.9	9.7	8.5E-03	2.0E-01
CYP2C19	7.9	6.9	1.3E-132	3.8E-130	-2.5	7.0	1.9E-15	3.8E-12
CYP2C8	7.3	9.2	2.7E-133	8.1E-131	-0.5	9.9	1.6E-01	8.6E-01
CYP2C9	7.5	8.8	6.0E-134	1.9E-131	-0.5	9.5	2.4E-01	1.0
CYP2D6	4.9	5.2	1.6E-71	9.2E-70	0.9	6.6	1.4E-04	1.1E-02
CYP2E1	8.2	11.6	1.3E-159	3.2E-156	-0.4	12.2	2.0E-01	9.1E-01
CYP3A4	7.1	9.4	3.7E-128	9.8E-126	0.0	10.5	1.2E-01	7.7E-01
CYP3A5	3.8	8.7	7.8E-55	2.8E-53	-0.2	9.4	6.7E-01	1.0
CYP3A7	-3.2	9.8	8.4E-43	2.1E-41	0.4	7.5	5.2E-02	5.5E-01
DPYD	0.3	6.9	2.0E-01	2.7E-01	-0.1	6.9	7.6E-01	1.0
GSTM1	3.4	4.5	1.2E-40	2.8E-39	-2.1	4.6	1.4E-13	2.1E-10
GSTP1	-3.0	5.8	9.6E-35	1.8E-33	-0.2	3.5	6.6E-01	1.0
GSTT1	2.0	4.9	1.2E-16	9.8E-16	-0.8	5.1	2.2E-03	7.9E-02
HNF4A	1.1	6.8	5.4E-07	2.0E-06	-0.1	7.1	7.8E-01	1.0
NAT1	0.4	3.0	1.1E-01	1.6E-01	0.1	3.1	8.0E-01	1.0
NAT2	7.0	3.6	3.6E-80	2.6E-78	0.0	4.5	9.1E-01	1.0
NR1I2	3.8	5.1	2.4E-50	7.2E-49	0.1	5.9	9.0E-01	1.0
NR1I3	1.8	4.7	4.5E-14	3.1E-13	-0.5	5.0	9.9E-02	7.2E-01

SLC15A2	-1.1	2.4	1.1E-04	2.9E-04	0.7	1.9	5.9E-02	5.9E-01
SLC22A1	7.1	7.1	4.6E-124	1.1E-121	-0.1	7.9	6.8E-01	1.0
SLCO1B1	1.5	7.5	5.1E-10	2.6E-09	-0.1	7.9	9.6E-01	1.0
SLCO1B3	1.3	7.4	3.1E-09	1.5E-08	-1.0	7.3	1.6E-04	1.2E-02
SULT1A1	0.6	4.6	6.3E-03	1.3E-02	0.0	4.7	8.6E-01	1.0
TPMT	2.2	5.1	8.6E-21	9.0E-20	-0.2	5.6	4.5E-01	1.0
UGT1A1	8.1	8.3	5.4E-146	5.0E-143	-0.5	9.0	1.9E-01	9.0E-01
UGT2B15	4.4	5.7	1.9E-64	8.8E-63	0.7	6.9	8.6E-03	2.0E-01
UGT2B17	3.6	0.9	3.4E-21	3.6E-20	3.0	3.9	1.2E-23	8.2E-20
UGT2B7	4.5	6.6	2.0E-64	9.4E-63	-0.2	7.3	6.6E-01	1.0

[1] $\log_2$ fold change

[2] $\log_2$ counts per million

[3] false discovery rate

Table 5: Negative correlations between developmental miRNA and the mRNA of top pharmacogenes

	Gene	miRNA	p-value	FDR	Estimate*
Phase I	*CYP1A1*	miR-223-5p	4.44E-03	2.32E-02	-7.2
	CYP1A1	miR-27b-5p	8.83E-03	3.73E-02	-13.1
	CYP1A1	miR-497-5p	9.68E-03	3.95E-02	-4.2
	CYP1A2	miR-223-5p	4.86E-05	1.50E-03	-13.8
	CYP1A2	miR-27b-5p	2.59E-04	3.96E-03	-24.8
	CYP1A2	miR-592	4.27E-04	5.32E-03	-8.8
	CYP1A2	miR-744-3p	6.61E-04	6.72E-03	-13.5
	CYP1A2	miR-148b-5p	9.48E-04	8.48E-03	-9.7
	CYP1A2	miR-99a-3p	3.19E-03	1.87E-02	-7.1
	CYP1A2	miR-31-5p	3.49E-03	1.97E-02	-4.3
	CYP1A2	miR-199a-5p	4.92E-03	2.50E-02	-16.7
	CYP1A2	miR-497-5p	5.87E-03	2.82E-02	-6.4
	CYP1A2	miR-200a-3p	6.40E-03	2.98E-02	-21.1
	CYP1A2	miR-151a-5p	7.03E-03	3.18E-02	-9.5
	CYP1A2	miR-505-5p	8.58E-03	3.66E-02	-5.6
	CYP1A2	miR-30e-3p	8.75E-03	3.70E-02	-21.3
	CYP2A6	miR-505-5p	1.95E-05	8.58E-04	-20.2
	CYP2A6	miR-192-3p	2.54E-05	1.02E-03	-37.5
	CYP2A6	miR-625-5p	5.87E-05	1.66E-03	-18.3
	CYP2A6	miR-151a-5p	8.20E-05	2.02E-03	-31.8
	CYP2A6	miR-375	8.75E-05	2.09E-03	-25.4
	CYP2A6	miR-340-3p	1.05E-04	2.26E-03	-41.1
	CYP2A6	miR-99a-3p	1.20E-04	2.44E-03	-21.6
	CYP2A6	miR-194-3p	1.30E-04	2.56E-03	-24.7
	CYP2A6	miR-26b-3p	1.63E-04	2.94E-03	-31.0
	CYP2A6	miR-148b-5p	2.27E-04	3.59E-03	-26.0
	CYP2A6	miR-505-3p	3.66E-04	4.92E-03	-19.0
	CYP2A6	miR-195-5p	3.86E-04	5.04E-03	-28.7
	CYP2A6	miR-28-5p	4.11E-04	5.21E-03	-63.3
	CYP2A6	miR-576-3p	4.72E-04	5.64E-03	-23.4
	CYP2A6	miR-146b-3p	4.77E-04	5.67E-03	-19.2
	CYP2A6	miR-331-3p	4.85E-04	5.71E-03	-62.0
	CYP2A6	miR-452-5p	5.48E-04	6.13E-03	-29.4
	CYP2A6	miR-197-3p	6.45E-04	6.63E-03	-82.0
	CYP2A6	miR-324-5p	6.98E-04	6.95E-03	-79.3
	CYP2A6	miR-590-3p	7.41E-04	7.22E-03	-31.9
	CYP2A6	miR-497-5p	7.88E-04	7.46E-03	-18.5
	CYP2A6	miR-320b	8.53E-04	7.90E-03	-24.9
	CYP2A6	miR-335-5p	8.78E-04	7.99E-03	-71.4
	CYP2A6	miR-30e-3p	9.43E-04	8.45E-03	-63.9

Gene	miRNA	p-value	FDR	Estimate*
CYP2A6	miR-223-5p	1.01E-03	8.81E-03	-28.8
CYP2A6	miR-31-5p	1.27E-03	1.00E-02	-11.5
CYP2A6	miR-199a-5p	1.40E-03	1.07E-02	-45.8
CYP2A6	miR-152-3p	1.51E-03	1.12E-02	-73.0
CYP2A6	miR-22-5p	1.97E-03	1.35E-02	-25.9
CYP2A6	miR-301a-3p	2.00E-03	1.37E-02	-50.9
CYP2A6	miR-511-5p	2.19E-03	1.45E-02	-30.2
CYP2A6	miR-148b-3p	2.44E-03	1.55E-02	-57.2
CYP2A6	miR-221-3p	2.72E-03	1.66E-02	-79.2
CYP2A6	miR-216b-5p	3.53E-03	1.99E-02	-12.1
CYP2A6	miR-29b-3p	3.62E-03	2.01E-02	-48.6
CYP2A6	miR-28-3p	3.75E-03	2.07E-02	-43.5
CYP2A6	miR-592	4.14E-03	2.20E-02	-18.2
CYP2A6	miR-26b-5p	6.20E-03	2.91E-02	-107.7
CYP2A6	miR-193a-5p	6.62E-03	3.04E-02	-55.9
CYP2A6	miR-199a-3p	7.71E-03	3.39E-02	-40.6
CYP2A6	miR-30d-5p	8.58E-03	3.66E-02	-50.4
CYP2A6	miR-10a-5p	1.08E-02	4.27E-02	-44.2
CYP2A6	miR-590-5p	1.09E-02	4.28E-02	-67.1
CYP2A6	miR-27a-3p	1.15E-02	4.44E-02	-47.1
CYP2A6	miR-502-3p	1.23E-02	4.68E-02	-14.4
CYP2A6	miR-27b-5p	1.30E-02	4.84E-02	-44.4
CYP2A6	miR-378a-5p	1.31E-02	4.85E-02	-11.7
CYP2B6	miR-223-5p	1.93E-05	8.58E-04	-52.0
CYP2B6	miR-592	2.15E-05	9.14E-04	-36.7
CYP2B6	miR-505-5p	2.74E-05	1.05E-03	-29.5
CYP2B6	miR-151a-5p	3.28E-05	1.18E-03	-48.8
CYP2B6	miR-192-3p	3.40E-05	1.20E-03	-54.8
CYP2B6	miR-148b-5p	4.10E-05	1.35E-03	-41.6
CYP2B6	miR-99a-3p	6.21E-05	1.70E-03	-32.9
CYP2B6	miR-340-3p	1.96E-04	3.25E-03	-58.9
CYP2B6	miR-146b-3p	2.94E-04	4.24E-03	-29.2
CYP2B6	miR-26b-3p	3.18E-04	4.51E-03	-44.3
CYP2B6	miR-375	3.71E-04	4.95E-03	-34.8
CYP2B6	miR-194-3p	4.15E-04	5.21E-03	-34.3
CYP2B6	miR-31-5p	4.49E-04	5.46E-03	-18.2
CYP2B6	miR-497-5p	5.58E-04	6.16E-03	-28.0
CYP2B6	miR-30e-3p	5.73E-04	6.23E-03	-97.6
CYP2B6	miR-199a-5p	5.82E-04	6.23E-03	-72.0
CYP2B6	miR-195-5p	5.77E-04	6.23E-03	-41.4
CYP2B6	miR-625-5p	7.09E-04	7.02E-03	-23.8
CYP2B6	miR-576-3p	1.20E-03	9.73E-03	-32.6
CYP2B6	miR-221-3p	1.57E-03	1.15E-02	-122.4
CYP2B6	miR-28-5p	1.61E-03	1.17E-02	-85.4

Gene	miRNA	p-value	FDR	Estimate*
CYP2B6	miR-197-3p	1.71E-03	1.22E-02	-113.3
CYP2B6	miR-27b-5p	1.76E-03	1.24E-02	-80.0
CYP2B6	miR-744-3p	1.79E-03	1.26E-02	-46.0
CYP2B6	miR-335-5p	1.94E-03	1.33E-02	-99.6
CYP2B6	miR-29a-5p	2.13E-03	1.42E-02	-20.9
CYP2B6	miR-331-3p	2.27E-03	1.48E-02	-82.2
CYP2B6	miR-30d-5p	3.20E-03	1.87E-02	-82.2
CYP2B6	miR-452-5p	3.28E-03	1.90E-02	-38.1
CYP2B6	miR-320b	3.36E-03	1.93E-02	-33.1
CYP2B6	miR-324-5p	3.81E-03	2.09E-02	-102.8
CYP2B6	miR-152-3p	4.00E-03	2.15E-02	-99.5
CYP2B6	miR-199a-3p	5.38E-03	2.65E-02	-62.3
CYP2B6	miR-511-5p	6.18E-03	2.90E-02	-40.5
CYP2B6	miR-505-3p	6.24E-03	2.92E-02	-22.6
CYP2B6	miR-22-5p	6.29E-03	2.93E-02	-34.4
CYP2B6	miR-590-3p	9.22E-03	3.82E-02	-38.0
CYP2B6	miR-29b-3p	9.58E-03	3.92E-02	-65.0
CYP2B6	miR-216b-5p	9.90E-03	4.01E-02	-16.0
CYP2B6	miR-27a-3p	9.98E-03	4.04E-02	-70.7
CYP2B6	miR-148b-3p	1.03E-02	4.12E-02	-73.2
CYP2B6	miR-27a-5p	1.18E-02	4.54E-02	-29.6
CYP2C19	miR-452-5p	1.54E-04	2.82E-03	-18.2
CYP2C19	miR-27a-3p	5.19E-04	5.90E-03	-35.4
CYP2C19	miR-26b-3p	1.58E-03	1.16E-02	-15.6
CYP2C19	miR-505-3p	1.85E-03	1.29E-02	-9.8
CYP2C19	miR-199a-3p	2.73E-03	1.66E-02	-25.9
CYP2C19	miR-31-5p	3.09E-03	1.82E-02	-6.2
CYP2C19	miR-200a-3p	4.07E-03	2.18E-02	-31.4
CYP2C19	miR-195-5p	4.12E-03	2.19E-02	-13.9
CYP2C19	miR-199a-5p	5.54E-03	2.71E-02	-23.5
CYP2C19	miR-192-3p	5.68E-03	2.75E-02	-15.5
CYP2C19	miR-497-5p	5.92E-03	2.83E-02	-9.0
CYP2C19	miR-505-5p	7.23E-03	3.24E-02	-8.1
CYP2C19	miR-186-5p	8.74E-03	3.70E-02	-47.3
CYP2C19	miR-223-5p	9.05E-03	3.77E-02	-13.7
CYP2C19	miR-216b-5p	9.40E-03	3.86E-02	-6.3
CYP2C19	miR-143-3p	1.24E-02	4.68E-02	-38.7
CYP2C8	miR-223-5p	8.74E-06	5.15E-04	-74.4
CYP2C8	miR-99a-3p	3.29E-05	1.18E-03	-47.1
CYP2C8	miR-148b-5p	4.84E-05	1.50E-03	-57.6
CYP2C8	miR-505-5p	1.14E-04	2.36E-03	-38.7
CYP2C8	miR-197-3p	1.62E-04	2.93E-03	-182.7
CYP2C8	miR-151a-5p	2.32E-04	3.66E-03	-62.3
CYP2C8	miR-199a-5p	2.60E-04	3.96E-03	-105.1

Gene	miRNA	p-value	FDR	Estimate*
CYP2C8	miR-30e-3p	2.63E-04	3.97E-03	-142.4
CYP2C8	miR-375	2.93E-04	4.24E-03	-49.2
CYP2C8	miR-497-5p	2.91E-04	4.24E-03	-40.5
CYP2C8	miR-216b-5p	3.26E-04	4.58E-03	-29.4
CYP2C8	miR-590-3p	3.29E-04	4.60E-03	-69.1
CYP2C8	miR-340-3p	5.57E-04	6.16E-03	-77.4
CYP2C8	miR-331-3p	6.27E-04	6.51E-03	-125.7
CYP2C8	miR-192-3p	6.69E-04	6.77E-03	-65.7
CYP2C8	miR-27b-5p	6.99E-04	6.95E-03	-119.0
CYP2C8	miR-505-3p	6.99E-04	6.95E-03	-37.6
CYP2C8	miR-31-5p	7.26E-04	7.15E-03	-24.6
CYP2C8	miR-625-5p	7.55E-04	7.31E-03	-33.0
CYP2C8	miR-22-5p	9.85E-04	8.67E-03	-56.1
CYP2C8	miR-590-5p	9.99E-04	8.73E-03	-172.0
CYP2C8	miR-29b-3p	1.02E-03	8.84E-03	-110.7
CYP2C8	miR-152-3p	1.28E-03	1.00E-02	-152.3
CYP2C8	miR-195-5p	1.47E-03	1.11E-02	-54.2
CYP2C8	miR-28-5p	1.88E-03	1.31E-02	-117.6
CYP2C8	miR-146b-3p	2.03E-03	1.38E-02	-35.8
CYP2C8	miR-592	2.17E-03	1.43E-02	-39.8
CYP2C8	miR-511-5p	2.98E-03	1.77E-02	-60.6
CYP2C8	miR-200a-3p	3.06E-03	1.81E-02	-115.2
CYP2C8	miR-320b	3.14E-03	1.84E-02	-46.4
CYP2C8	miR-532-3p	3.44E-03	1.96E-02	-226.9
CYP2C8	miR-576-3p	3.45E-03	1.96E-02	-41.7
CYP2C8	miR-27a-5p	3.48E-03	1.97E-02	-47.0
CYP2C8	miR-374a-3p	3.74E-03	2.06E-02	-30.2
CYP2C8	miR-26b-3p	4.99E-03	2.52E-02	-50.4
CYP2C8	miR-335-5p	5.08E-03	2.55E-02	-127.5
CYP2C8	miR-502-3p	6.59E-03	3.04E-02	-32.0
CYP2C8	miR-452-5p	7.80E-03	3.41E-02	-48.7
CYP2C8	miR-24-3p	8.38E-03	3.60E-02	-74.8
CYP2C8	miR-194-3p	8.84E-03	3.73E-02	-37.2
CYP2C8	miR-132-3p	1.32E-02	4.88E-02	-113.9
CYP2C8	miR-324-5p	1.34E-02	4.95E-02	-125.0
CYP2C8	miR-148b-3p	1.34E-02	4.95E-02	-98.8
CYP2C8	miR-378a-5p	1.34E-02	4.95E-02	-24.0
CYP2C9	miR-99a-3p	2.62E-05	1.04E-03	-37.7
CYP2C9	miR-505-5p	3.34E-05	1.19E-03	-32.4
CYP2C9	miR-223-5p	5.31E-05	1.58E-03	-55.3
CYP2C9	miR-192-3p	5.88E-05	1.66E-03	-59.3
CYP2C9	miR-148b-5p	8.85E-05	2.10E-03	-44.6
CYP2C9	miR-497-5p	1.25E-04	2.51E-03	-33.6
CYP2C9	miR-151a-5p	1.26E-04	2.52E-03	-51.0

Gene	miRNA	p-value	FDR	Estimate*
CYP2C9	miR-375	1.32E-04	2.57E-03	-40.7
CYP2C9	miR-340-3p	1.50E-04	2.79E-03	-66.0
CYP2C9	miR-199a-5p	1.93E-04	3.25E-03	-84.8
CYP2C9	miR-197-3p	2.20E-04	3.54E-03	-142.8
CYP2C9	miR-195-5p	2.60E-04	3.96E-03	-48.0
CYP2C9	miR-31-5p	2.61E-04	3.96E-03	-20.7
CYP2C9	miR-30e-3p	4.15E-04	5.21E-03	-110.2
CYP2C9	miR-216b-5p	4.16E-04	5.21E-03	-23.1
CYP2C9	miR-625-5p	4.41E-04	5.39E-03	-27.1
CYP2C9	miR-331-3p	4.92E-04	5.75E-03	-101.3
CYP2C9	miR-26b-3p	5.48E-04	6.13E-03	-47.5
CYP2C9	miR-505-3p	5.55E-04	6.16E-03	-30.3
CYP2C9	miR-146b-3p	6.05E-04	6.42E-03	-31.0
CYP2C9	miR-452-5p	6.09E-04	6.42E-03	-47.8
CYP2C9	miR-28-5p	7.45E-04	7.25E-03	-99.8
CYP2C9	miR-592	8.34E-04	7.76E-03	-33.9
CYP2C9	miR-29b-3p	1.06E-03	9.05E-03	-87.7
CYP2C9	miR-590-3p	1.07E-03	9.05E-03	-51.0
CYP2C9	miR-576-3p	1.09E-03	9.16E-03	-36.3
CYP2C9	miR-27b-5p	1.13E-03	9.39E-03	-91.5
CYP2C9	miR-152-3p	1.16E-03	9.55E-03	-121.8
CYP2C9	miR-194-3p	1.45E-03	1.10E-02	-34.9
CYP2C9	miR-320b	1.63E-03	1.18E-02	-38.9
CYP2C9	miR-335-5p	2.26E-03	1.48E-02	-108.9
CYP2C9	miR-511-5p	2.49E-03	1.58E-02	-48.8
CYP2C9	miR-22-5p	2.89E-03	1.74E-02	-41.0
CYP2C9	miR-27a-3p	2.89E-03	1.74E-02	-88.7
CYP2C9	miR-590-5p	2.94E-03	1.76E-02	-125.6
CYP2C9	miR-200a-3p	3.27E-03	1.90E-02	-91.0
CYP2C9	miR-502-3p	5.17E-03	2.58E-02	-26.0
CYP2C9	miR-148b-3p	5.73E-03	2.77E-02	-86.4
CYP2C9	miR-324-5p	5.76E-03	2.78E-02	-109.4
CYP2C9	miR-27a-5p	6.02E-03	2.85E-02	-35.4
CYP2C9	miR-221-3p	7.44E-03	3.30E-02	-117.6
CYP2C9	miR-199a-3p	7.77E-03	3.41E-02	-66.3
CYP2C9	miR-24-3p	8.38E-03	3.60E-02	-59.4
CYP2C9	miR-374a-3p	1.02E-02	4.10E-02	-21.6
CYP2C9	miR-28-3p	1.03E-02	4.13E-02	-64.0
CYP2C9	miR-532-3p	1.05E-02	4.18E-02	-160.5
CYP2C9	miR-193a-5p	1.05E-02	4.18E-02	-86.9
CYP2C9	miR-378a-5p	1.13E-02	4.38E-02	-19.5
CYP2C9	miR-26b-5p	1.34E-02	4.94E-02	-161.3
CYP2D6	miR-216b-5p	4.65E-07	7.27E-05	-3.5
CYP2D6	miR-497-5p	1.32E-05	6.82E-04	-4.3

Gene	miRNA	p-value	FDR	Estimate*
CYP2D6	miR-29b-3p	3.10E-05	1.13E-03	-12.4
CYP2D6	miR-502-3p	7.10E-05	1.85E-03	-4.1
CYP2D6	miR-374a-3p	9.78E-05	2.18E-03	-3.6
CYP2D6	miR-99a-3p	1.08E-04	2.31E-03	-4.2
CYP2D6	miR-31-5p	1.44E-04	2.70E-03	-2.5
CYP2D6	miR-30e-3p	2.14E-04	3.48E-03	-13.5
CYP2D6	miR-532-3p	2.39E-04	3.73E-03	-25.5
CYP2D6	miR-340-3p	2.74E-04	4.10E-03	-7.5
CYP2D6	miR-511-5p	2.83E-04	4.19E-03	-6.7
CYP2D6	miR-22-5p	3.39E-04	4.71E-03	-5.6
CYP2D6	miR-145-3p	4.98E-04	5.80E-03	-2.6
CYP2D6	miR-195-5p	5.25E-04	5.95E-03	-5.4
CYP2D6	miR-375	5.79E-04	6.23E-03	-4.4
CYP2D6	miR-320b	6.79E-04	6.84E-03	-4.9
CYP2D6	miR-590-5p	1.03E-03	8.88E-03	-16.1
CYP2D6	miR-28-5p	1.06E-03	9.04E-03	-11.5
CYP2D6	miR-590-3p	1.06E-03	9.04E-03	-6.0
CYP2D6	miR-132-3p	1.31E-03	1.02E-02	-13.3
CYP2D6	miR-152-3p	1.37E-03	1.05E-02	-14.2
CYP2D6	miR-579-3p	1.48E-03	1.11E-02	-4.5
CYP2D6	miR-199a-5p	1.58E-03	1.16E-02	-8.8
CYP2D6	miR-10b-3p	1.69E-03	1.21E-02	-2.3
CYP2D6	miR-24-3p	1.82E-03	1.27E-02	-8.1
CYP2D6	miR-505-3p	2.01E-03	1.37E-02	-3.3
CYP2D6	miR-452-5p	2.10E-03	1.41E-02	-5.2
CYP2D6	miR-505-5p	2.13E-03	1.42E-02	-3.0
CYP2D6	miR-331-3p	2.16E-03	1.43E-02	-10.8
CYP2D6	miR-592	2.30E-03	1.49E-02	-3.7
CYP2D6	miR-34a-5p	2.32E-03	1.51E-02	-13.3
CYP2D6	miR-30a-5p	2.35E-03	1.52E-02	-9.5
CYP2D6	miR-29c-3p	2.54E-03	1.60E-02	-9.9
CYP2D6	miR-576-3p	3.52E-03	1.98E-02	-3.9
CYP2D6	miR-223-5p	4.09E-03	2.19E-02	-5.0
CYP2D6	miR-155-5p	4.92E-03	2.50E-02	-6.1
CYP2D6	miR-200a-3p	5.25E-03	2.61E-02	-10.3
CYP2D6	miR-27b-5p	5.81E-03	2.80E-02	-9.4
CYP2D6	miR-197-3p	5.82E-03	2.80E-02	-13.2
CYP2D6	miR-148b-5p	5.84E-03	2.81E-02	-4.0
CYP2D6	miR-27b-3p	6.27E-03	2.93E-02	-9.4
CYP2D6	miR-625-5p	8.98E-03	3.76E-02	-2.5
CYP2D6	miR-30a-3p	1.22E-02	4.66E-02	-8.5
CYP2D6	miR-335-5p	1.23E-02	4.67E-02	-10.8
CYP2D6	miR-151a-5p	1.24E-02	4.69E-02	-4.2
CYP2D6	miR-125b-5p	1.30E-02	4.84E-02	-13.0

Gene	miRNA	p-value	FDR	Estimate*
CYP2E1	miR-216b-5p	1.53E-07	4.76E-05	-149.5
CYP2E1	miR-502-3p	5.54E-06	3.70E-04	-187.0
CYP2E1	miR-29b-3p	1.16E-05	6.48E-04	-539.2
CYP2E1	miR-31-5p	6.36E-05	1.73E-03	-109.7
CYP2E1	miR-125b-5p	7.89E-05	1.96E-03	-795.4
CYP2E1	miR-152-3p	1.03E-04	2.25E-03	-691.2
CYP2E1	miR-219a-5p	1.03E-04	2.25E-03	-131.8
CYP2E1	miR-497-5p	1.29E-04	2.55E-03	-165.7
CYP2E1	miR-24-3p	1.36E-04	2.61E-03	-397.0
CYP2E1	miR-199a-5p	1.49E-04	2.78E-03	-424.2
CYP2E1	miR-200a-3p	1.78E-04	3.09E-03	-546.1
CYP2E1	miR-452-5p	1.88E-04	3.21E-03	-252.3
CYP2E1	miR-29c-3p	2.08E-04	3.39E-03	-489.4
CYP2E1	miR-132-3p	4.62E-04	5.58E-03	-597.3
CYP2E1	miR-99a-3p	6.38E-04	6.58E-03	-159.4
CYP2E1	miR-532-3p	6.46E-04	6.64E-03	-1009.7
CYP2E1	miR-331-3p	6.64E-04	6.73E-03	-491.0
CYP2E1	miR-579-3p	6.90E-04	6.90E-03	-200.6
CYP2E1	miR-505-3p	7.10E-04	7.02E-03	-147.4
CYP2E1	miR-590-3p	7.17E-04	7.08E-03	-258.7
CYP2E1	miR-195-5p	7.28E-04	7.15E-03	-223.2
CYP2E1	miR-34a-5p	7.49E-04	7.27E-03	-604.7
CYP2E1	miR-27a-3p	8.34E-04	7.76E-03	-481.5
CYP2E1	miR-27b-5p	8.72E-04	7.99E-03	-460.1
CYP2E1	miR-28-5p	9.82E-04	8.67E-03	-484.0
CYP2E1	miR-23b-3p	1.34E-03	1.04E-02	-561.4
CYP2E1	miR-27b-3p	1.47E-03	1.11E-02	-447.5
CYP2E1	miR-30e-3p	1.48E-03	1.11E-02	-500.1
CYP2E1	miR-155-5p	1.60E-03	1.17E-02	-283.2
CYP2E1	miR-145-3p	1.71E-03	1.22E-02	-101.3
CYP2E1	miR-143-3p	1.78E-03	1.25E-02	-656.8
CYP2E1	miR-27a-5p	2.12E-03	1.41E-02	-192.2
CYP2E1	miR-375	2.40E-03	1.54E-02	-167.3
CYP2E1	miR-505-5p	2.47E-03	1.57E-02	-125.1
CYP2E1	miR-223-5p	2.70E-03	1.66E-02	-216.1
CYP2E1	miR-374a-3p	2.77E-03	1.68E-02	-121.6
CYP2E1	miR-378a-5p	3.25E-03	1.89E-02	-109.7
CYP2E1	miR-511-5p	3.49E-03	1.97E-02	-234.2
CYP2E1	miR-151a-5p	3.63E-03	2.02E-02	-201.7
CYP2E1	miR-186-5p	3.79E-03	2.08E-02	-721.6
CYP2E1	miR-29b-2-5p	4.53E-03	2.35E-02	-100.8
CYP2E1	miR-193a-5p	4.70E-03	2.42E-02	-467.9
CYP2E1	miR-590-5p	5.00E-03	2.52E-02	-590.6
CYP2E1	miR-10b-3p	5.76E-03	2.78E-02	-87.2

Gene	miRNA	p-value	FDR	Estimate*
CYP2E1	miR-628-3p	5.83E-03	2.80E-02	-117.9
CYP2E1	miR-340-3p	7.26E-03	3.25E-02	-246.1
CYP2E1	miR-21-5p	7.48E-03	3.32E-02	-168.1
CYP2E1	miR-26b-5p	9.37E-03	3.86E-02	-832.0
CYP2E1	miR-423-5p	9.64E-03	3.94E-02	-438.2
CYP2E1	miR-30a-3p	1.01E-02	4.06E-02	-365.1
CYP2E1	miR-625-5p	1.11E-02	4.36E-02	-102.0
CYP2E1	miR-26b-3p	1.17E-02	4.53E-02	-179.8
CYP2E1	miR-146b-3p	1.24E-02	4.69E-02	-117.1
CYP2E1	miR-197-3p	1.30E-02	4.84E-02	-506.6
CYP3A4	miR-375	8.52E-05	2.07E-03	-67.7
CYP3A4	miR-99a-3p	9.52E-05	2.17E-03	-58.3
CYP3A4	miR-340-3p	1.89E-04	3.22E-03	-106.4
CYP3A4	miR-505-5p	2.94E-04	4.24E-03	-47.7
CYP3A4	miR-576-3p	4.02E-04	5.15E-03	-63.0
CYP3A4	miR-148b-5p	4.05E-04	5.17E-03	-67.2
CYP3A4	miR-590-3p	4.83E-04	5.70E-03	-87.5
CYP3A4	miR-192-3p	5.51E-04	6.16E-03	-86.1
CYP3A4	miR-30e-3p	5.79E-04	6.23E-03	-176.0
CYP3A4	miR-31-5p	6.10E-04	6.42E-03	-32.2
CYP3A4	miR-320b	6.92E-04	6.90E-03	-67.3
CYP3A4	miR-223-5p	1.06E-03	9.05E-03	-76.6
CYP3A4	miR-151a-5p	1.30E-03	1.02E-02	-72.4
CYP3A4	miR-22-5p	1.39E-03	1.07E-02	-70.8
CYP3A4	miR-592	1.71E-03	1.22E-02	-52.5
CYP3A4	miR-194-3p	2.01E-03	1.37E-02	-55.5
CYP3A4	miR-27b-5p	2.43E-03	1.55E-02	-140.6
CYP3A4	miR-497-5p	2.62E-03	1.63E-02	-45.1
CYP3A4	miR-331-3p	2.72E-03	1.66E-02	-146.0
CYP3A4	miR-511-5p	2.73E-03	1.66E-02	-78.9
CYP3A4	miR-195-5p	3.44E-03	1.96E-02	-65.4
CYP3A4	miR-29b-3p	3.56E-03	2.00E-02	-129.7
CYP3A4	miR-199a-5p	4.32E-03	2.27E-02	-111.3
CYP3A4	miR-625-5p	4.49E-03	2.33E-02	-37.1
CYP3A4	miR-28-5p	4.81E-03	2.46E-02	-140.2
CYP3A4	miR-146b-3p	5.54E-03	2.71E-02	-42.3
CYP3A4	miR-152-3p	6.52E-03	3.01E-02	-170.9
CYP3A4	miR-26b-3p	7.04E-03	3.18E-02	-62.9
CYP3A4	miR-335-5p	7.33E-03	3.27E-02	-158.8
CYP3A4	miR-324-5p	7.64E-03	3.37E-02	-173.0
CYP3A4	miR-200a-3p	8.15E-03	3.53E-02	-135.3
CYP3A4	miR-197-3p	8.69E-03	3.70E-02	-175.5
CYP3A4	miR-30d-5p	8.90E-03	3.74E-02	-133.9
CYP3A4	miR-505-3p	8.93E-03	3.75E-02	-39.2

Gene	miRNA	p-value	FDR	Estimate*
CYP3A4	miR-29a-5p	1.02E-02	4.09E-02	-32.3
CYP3A4	miR-590-5p	1.04E-02	4.17E-02	-179.9
CYP3A4	miR-216b-5p	1.24E-02	4.69E-02	-28.1
CYP3A4	miR-221-3p	1.33E-02	4.91E-02	-179.0
CYP3A5	miR-216b-5p	6.33E-06	4.08E-04	-8.1
CYP3A5	miR-590-3p	1.23E-05	6.51E-04	-18.7
CYP3A5	miR-590-5p	4.74E-05	1.49E-03	-47.4
CYP3A5	miR-29b-3p	7.33E-05	1.88E-03	-30.0
CYP3A5	miR-99a-3p	1.53E-04	2.82E-03	-10.3
CYP3A5	miR-378a-5p	2.36E-04	3.70E-03	-7.8
CYP3A5	miR-497-5p	2.62E-04	3.96E-03	-9.5
CYP3A5	miR-152-3p	5.26E-04	5.95E-03	-37.8
CYP3A5	miR-27b-5p	6.80E-04	6.84E-03	-27.9
CYP3A5	miR-28-5p	9.32E-04	8.38E-03	-29.0
CYP3A5	miR-340-3p	1.11E-03	9.22E-03	-17.3
CYP3A5	miR-532-3p	1.15E-03	9.48E-03	-58.0
CYP3A5	miR-199a-5p	1.16E-03	9.53E-03	-22.4
CYP3A5	miR-22-5p	1.22E-03	9.81E-03	-12.9
CYP3A5	miR-151a-5p	1.27E-03	1.00E-02	-13.1
CYP3A5	miR-374a-3p	1.69E-03	1.21E-02	-7.6
CYP3A5	miR-148b-5p	1.80E-03	1.26E-02	-11.0
CYP3A5	miR-505-5p	1.84E-03	1.28E-02	-7.6
CYP3A5	miR-195-5p	1.85E-03	1.29E-02	-12.5
CYP3A5	miR-30e-3p	2.02E-03	1.37E-02	-29.1
CYP3A5	miR-576-3p	2.57E-03	1.60E-02	-10.0
CYP3A5	miR-375	2.71E-03	1.66E-02	-9.9
CYP3A5	miR-200a-3p	2.91E-03	1.75E-02	-27.1
CYP3A5	miR-625-5p	3.09E-03	1.82E-02	-6.9
CYP3A5	miR-320b	3.23E-03	1.88E-02	-10.8
CYP3A5	miR-192-3p	3.49E-03	1.97E-02	-13.6
CYP3A5	miR-23b-3p	3.59E-03	2.00E-02	-30.9
CYP3A5	miR-132-3p	3.73E-03	2.06E-02	-30.5
CYP3A5	miR-511-5p	3.84E-03	2.09E-02	-13.9
CYP3A5	miR-26b-5p	4.42E-03	2.31E-02	-53.7
CYP3A5	miR-331-3p	4.89E-03	2.49E-02	-25.0
CYP3A5	miR-27a-3p	5.07E-03	2.55E-02	-24.8
CYP3A5	miR-452-5p	5.96E-03	2.84E-02	-11.7
CYP3A5	miR-505-3p	5.97E-03	2.84E-02	-7.4
CYP3A5	miR-31-5p	6.14E-03	2.89E-02	-4.8
CYP3A5	miR-502-3p	6.46E-03	3.00E-02	-7.5
CYP3A5	miR-34a-5p	6.87E-03	3.12E-02	-30.0
CYP3A5	miR-193a-5p	7.08E-03	3.19E-02	-26.8
CYP3A5	miR-27b-3p	8.09E-03	3.51E-02	-22.9
CYP3A5	miR-148b-3p	8.51E-03	3.64E-02	-24.4

	Gene	miRNA	p-value	FDR	Estimate*
	CYP3A5	miR-223-5p	9.29E-03	3.84E-02	-11.4
	CYP3A5	miR-24-3p	1.00E-02	4.06E-02	-17.1
	CYP3A5	miR-27a-5p	1.05E-02	4.18E-02	-9.8
	CYP3A5	miR-194-5p	1.25E-02	4.72E-02	-34.7
	CYP3A7	miR-431-5p	2.97E-11	6.88E-08	-34.4
	CYP3A7	miR-668-3p	1.25E-10	2.17E-07	-42.0
	CYP3A7	miR-889-3p	8.14E-08	3.33E-05	-94.7
	CYP3A7	miR-539-5p	1.43E-07	4.74E-05	-93.8
	CYP3A7	miR-485-3p	1.64E-07	4.76E-05	-24.3
	CYP3A7	miR-493-3p	2.78E-07	5.69E-05	-36.5
	CYP3A7	miR-512-3p	2.67E-07	5.69E-05	-26.1
	CYP3A7	miR-487a-3p	4.48E-07	7.27E-05	-33.6
	CYP3A7	miR-483-3p	5.47E-07	7.46E-05	-73.1
	CYP3A7	miR-487b-3p	1.80E-06	1.76E-04	-61.4
	CYP3A7	miR-382-5p	3.14E-06	2.54E-04	-25.7
	CYP3A7	miR-519a-3p	6.53E-06	4.17E-04	-29.4
	CYP3A7	miR-433-3p	8.21E-06	4.88E-04	-31.2
	CYP3A7	miR-323a-3p	1.26E-05	6.60E-04	-50.0
	CYP3A7	miR-154-3p	7.48E-05	1.90E-03	-28.1
	CYP3A7	miR-18a-5p	1.12E-04	2.35E-03	-109.7
	CYP3A7	miR-654-5p	1.38E-04	2.63E-03	-26.2
	CYP3A7	miR-19b-1-5p	1.75E-04	3.07E-03	-105.6
	CYP3A7	miR-526b-5p	1.86E-04	3.20E-03	-38.2
	CYP3A7	miR-370-3p	2.03E-04	3.35E-03	-28.9
	CYP3A7	miR-144-5p	2.08E-04	3.39E-03	-35.4
	CYP3A7	miR-411-5p	3.42E-04	4.71E-03	-98.7
	CYP3A7	miR-483-5p	6.10E-04	6.42E-03	-110.9
	CYP3A7	miR-410-3p	6.81E-04	6.85E-03	-27.4
	CYP3A7	miR-758-3p	6.86E-04	6.89E-03	-24.6
	CYP3A7	miR-494-3p	1.02E-03	8.84E-03	-26.5
	CYP3A7	miR-519d-3p	1.87E-03	1.30E-02	-23.0
	CYP3A7	miR-409-3p	1.92E-03	1.32E-02	-79.0
	CYP3A7	miR-130a-3p	2.56E-03	1.60E-02	-188.2
	CYP3A7	miR-136-3p	3.02E-03	1.79E-02	-82.6
	CYP3A7	miR-519e-5p	3.54E-03	1.99E-02	-21.9
	CYP3A7	miR-376a-3p	4.96E-03	2.51E-02	-70.1
	CYP3A7	miR-432-5p	4.96E-03	2.51E-02	-24.2
	CYP3A7	miR-16-5p	6.89E-03	3.12E-02	-78.4
	CYP3A7	miR-19b-3p	9.38E-03	3.86E-02	-83.1
	CYP3A7	miR-377-5p	1.01E-02	4.08E-02	-30.7
	CYP3A7	miR-184	1.07E-02	4.25E-02	-19.2
Phase II	*DPYD*	miR-223-5p	1.12E-02	4.38E-02	-0.6
	GSTM1	miR-744-3p	6.33E-07	8.15E-05	-6.9
	GSTM1	miR-592	3.46E-05	1.20E-03	-3.9

Gene	miRNA	p-value	FDR	Estimate*
GSTM1	miR-29a-5p	1.39E-04	2.64E-03	-2.7
GSTM1	miR-374a-3p	2.93E-03	1.75E-02	-2.4
GSTM1	miR-223-5p	6.77E-03	3.09E-02	-3.9
GSTM1	miR-497-5p	1.12E-02	4.38E-02	-2.3
GSTP1	miR-431-5p	3.57E-13	2.48E-09	-4.7
GSTP1	miR-668-3p	2.62E-11	6.88E-08	-5.7
GSTP1	miR-483-3p	5.16E-10	5.98E-07	-10.9
GSTP1	miR-382-5p	5.05E-10	5.98E-07	-4.0
GSTP1	miR-889-3p	4.98E-09	4.33E-06	-13.2
GSTP1	miR-493-3p	1.27E-07	4.66E-05	-5.0
GSTP1	miR-487a-3p	1.43E-07	4.74E-05	-4.6
GSTP1	miR-512-3p	2.45E-07	5.69E-05	-3.5
GSTP1	miR-485-3p	2.58E-07	5.69E-05	-3.2
GSTP1	miR-539-5p	3.66E-07	6.36E-05	-12.3
GSTP1	miR-487b-3p	9.26E-07	1.09E-04	-8.3
GSTP1	miR-654-5p	1.68E-06	1.70E-04	-4.1
GSTP1	miR-370-3p	2.16E-06	1.96E-04	-4.6
GSTP1	miR-519a-3p	5.11E-06	3.52E-04	-4.0
GSTP1	miR-323a-3p	5.39E-06	3.66E-04	-6.9
GSTP1	miR-154-3p	1.18E-05	6.49E-04	-4.0
GSTP1	miR-433-3p	1.96E-05	8.58E-04	-4.0
GSTP1	miR-18a-5p	5.66E-05	1.63E-03	-15.1
GSTP1	miR-758-3p	8.76E-05	2.09E-03	-3.7
GSTP1	miR-519d-3p	9.35E-05	2.15E-03	-3.7
GSTP1	miR-432-5p	1.22E-04	2.46E-03	-4.2
GSTP1	miR-526b-5p	1.34E-04	2.59E-03	-5.2
GSTP1	miR-411-5p	1.82E-04	3.14E-03	-13.6
GSTP1	miR-184	2.36E-04	3.70E-03	-3.5
GSTP1	miR-494-3p	2.78E-04	4.14E-03	-3.8
GSTP1	miR-19b-1-5p	3.86E-04	5.04E-03	-13.5
GSTP1	miR-409-3p	3.96E-04	5.10E-03	-11.7
GSTP1	miR-483-5p	8.12E-04	7.61E-03	-14.5
GSTP1	miR-410-3p	1.08E-03	9.11E-03	-3.6
GSTP1	miR-127-3p	1.16E-03	9.55E-03	-3.3
GSTP1	miR-130a-3p	1.17E-03	9.57E-03	-26.7
GSTP1	miR-144-5p	1.21E-03	9.78E-03	-4.3
GSTP1	let-7f-5p	2.30E-03	1.49E-02	-7.4
GSTP1	miR-19b-3p	5.50E-03	2.69E-02	-11.8
GSTP1	miR-515-3p	5.99E-03	2.84E-02	-3.2
GSTP1	miR-20b-5p	8.77E-03	3.71E-02	-3.0
GSTP1	miR-376c-3p	9.21E-03	3.81E-02	-1.8
GSTT1	miR-223-5p	9.91E-04	8.69E-03	-3.4
GSTT1	miR-197-3p	3.48E-03	1.97E-02	-8.4
GSTT1	miR-148b-5p	7.99E-03	3.48E-02	-2.3

Gene	miRNA	p-value	FDR	Estimate*
NAT1	miR-452-5p	4.33E-03	2.27E-02	-0.1
NAT1	miR-590-5p	5.98E-03	2.84E-02	-0.4
NAT1	miR-197-3p	8.15E-03	3.53E-02	-0.4
NAT1	miR-216b-5p	8.29E-03	3.57E-02	-0.1
NAT2	miR-216b-5p	2.58E-07	5.69E-05	-1.0
NAT2	miR-29b-3p	2.74E-05	1.05E-03	-3.7
NAT2	miR-497-5p	3.10E-05	1.13E-03	-1.2
NAT2	miR-532-3p	4.83E-05	1.50E-03	-8.1
NAT2	miR-197-3p	7.44E-05	1.90E-03	-5.2
NAT2	miR-502-3p	3.29E-04	4.60E-03	-1.1
NAT2	miR-99a-3p	3.76E-04	5.00E-03	-1.2
NAT2	miR-590-3p	5.19E-04	5.90E-03	-1.9
NAT2	miR-28-5p	5.63E-04	6.16E-03	-3.5
NAT2	miR-511-5p	5.79E-04	6.23E-03	-1.9
NAT2	miR-340-3p	6.62E-04	6.72E-03	-2.1
NAT2	miR-452-5p	7.84E-04	7.45E-03	-1.6
NAT2	miR-374a-3p	8.65E-04	7.97E-03	-0.9
NAT2	miR-590-5p	8.72E-04	7.99E-03	-4.8
NAT2	miR-199a-5p	8.86E-04	8.04E-03	-2.7
NAT2	miR-195-5p	1.02E-03	8.83E-03	-1.5
NAT2	miR-132-3p	1.19E-03	9.68E-03	-4.0
NAT2	miR-22-5p	1.36E-03	1.05E-02	-1.5
NAT2	miR-30e-3p	2.11E-03	1.41E-02	-3.4
NAT2	miR-378a-5p	2.16E-03	1.43E-02	-0.8
NAT2	miR-505-5p	2.69E-03	1.65E-02	-0.9
NAT2	miR-320b	2.70E-03	1.66E-02	-1.3
NAT2	miR-331-3p	3.00E-03	1.78E-02	-3.1
NAT2	miR-375	3.58E-03	2.00E-02	-1.1
NAT2	miR-625-5p	3.78E-03	2.08E-02	-0.8
NAT2	miR-34a-5p	4.79E-03	2.46E-02	-3.7
NAT2	miR-152-3p	5.17E-03	2.58E-02	-3.7
NAT2	miR-148b-5p	5.28E-03	2.62E-02	-1.2
NAT2	miR-579-3p	5.68E-03	2.75E-02	-1.2
NAT2	miR-146b-3p	5.89E-03	2.83E-02	-0.9
NAT2	miR-29c-3p	5.91E-03	2.83E-02	-2.7
NAT2	miR-24-3p	6.02E-03	2.85E-02	-2.1
NAT2	miR-505-3p	6.59E-03	3.04E-02	-0.9
NAT2	miR-592	6.98E-03	3.16E-02	-1.0
NAT2	miR-145-3p	7.37E-03	3.28E-02	-0.6
NAT2	miR-151a-5p	7.42E-03	3.30E-02	-1.3
NAT2	miR-335-5p	7.62E-03	3.36E-02	-3.4
NAT2	miR-31-5p	7.72E-03	3.39E-02	-0.6
NAT2	miR-223-5p	1.07E-02	4.23E-02	-1.3
NAT2	miR-193a-5p	1.08E-02	4.27E-02	-3.0

Gene	miRNA	p-value	FDR	Estimate*
NAT2	miR-155-5p	1.21E-02	4.62E-02	-1.6
NAT2	miR-29b-2-5p	1.27E-02	4.76E-02	-0.6
TPMT	miR-216b-5p	1.14E-08	7.96E-06	-0.6
TPMT	miR-29b-3p	1.59E-07	4.76E-05	-2.4
TPMT	miR-497-5p	4.61E-07	7.27E-05	-0.8
TPMT	miR-502-3p	7.06E-07	8.78E-05	-0.8
TPMT	miR-99a-3p	1.09E-06	1.25E-04	-0.8
TPMT	miR-452-5p	2.62E-06	2.25E-04	-1.2
TPMT	miR-505-5p	9.11E-06	5.28E-04	-0.7
TPMT	miR-511-5p	1.06E-05	5.99E-04	-1.3
TPMT	miR-340-3p	1.26E-05	6.60E-04	-1.4
TPMT	miR-199a-5p	1.36E-05	6.90E-04	-1.8
TPMT	miR-195-5p	1.42E-05	7.13E-04	-1.1
TPMT	miR-28-5p	1.96E-05	8.58E-04	-2.3
TPMT	miR-590-3p	1.88E-05	8.58E-04	-1.2
TPMT	miR-30e-3p	2.17E-05	9.14E-04	-2.4
TPMT	miR-331-3p	2.78E-05	1.06E-03	-2.2
TPMT	miR-375	4.31E-05	1.40E-03	-0.8
TPMT	miR-320b	5.41E-05	1.59E-03	-0.9
TPMT	miR-152-3p	6.08E-05	1.68E-03	-2.8
TPMT	miR-151a-5p	6.13E-05	1.69E-03	-1.0
TPMT	miR-625-5p	6.72E-05	1.78E-03	-0.6
TPMT	miR-148b-5p	7.26E-05	1.87E-03	-0.9
TPMT	miR-223-5p	9.33E-05	2.15E-03	-1.0
TPMT	miR-31-5p	9.77E-05	2.18E-03	-0.4
TPMT	miR-193a-5p	1.00E-04	2.22E-03	-2.4
TPMT	miR-505-3p	1.25E-04	2.51E-03	-0.6
TPMT	miR-532-3p	1.32E-04	2.57E-03	-4.3
TPMT	miR-22-5p	1.32E-04	2.57E-03	-1.0
TPMT	miR-592	2.49E-04	3.84E-03	-0.7
TPMT	miR-34a-5p	2.88E-04	4.24E-03	-2.5
TPMT	miR-24-3p	2.93E-04	4.24E-03	-1.5
TPMT	miR-219a-5p	3.22E-04	4.55E-03	-0.5
TPMT	miR-146b-3p	3.55E-04	4.82E-03	-0.6
TPMT	miR-197-3p	4.35E-04	5.37E-03	-2.7
TPMT	miR-374a-3p	4.38E-04	5.38E-03	-0.5
TPMT	miR-192-3p	4.97E-04	5.80E-03	-1.0
TPMT	miR-576-3p	6.31E-04	6.54E-03	-0.7
TPMT	miR-29c-3p	7.61E-04	7.33E-03	-1.8
TPMT	miR-579-3p	7.67E-04	7.36E-03	-0.8
TPMT	miR-148b-3p	7.87E-04	7.46E-03	-2.0
TPMT	miR-27b-3p	8.64E-04	7.97E-03	-1.8
TPMT	miR-27b-5p	1.02E-03	8.83E-03	-1.8
TPMT	miR-26b-3p	1.06E-03	9.04E-03	-0.9

Gene	miRNA	p-value	FDR	Estimate*
TPMT	miR-23b-3p	1.37E-03	1.05E-02	-2.2
TPMT	miR-26b-5p	1.55E-03	1.15E-02	-3.8
TPMT	miR-27a-3p	1.62E-03	1.18E-02	-1.8
TPMT	miR-186-5p	2.20E-03	1.45E-02	-3.0
TPMT	miR-194-3p	2.24E-03	1.47E-02	-0.7
TPMT	miR-28-3p	2.46E-03	1.56E-02	-1.4
TPMT	miR-335-5p	2.50E-03	1.58E-02	-2.1
TPMT	miR-378a-5p	2.71E-03	1.66E-02	-0.4
TPMT	miR-301a-3p	2.95E-03	1.76E-02	-1.6
TPMT	miR-27a-5p	3.36E-03	1.93E-02	-0.7
TPMT	miR-125b-5p	3.69E-03	2.05E-02	-2.4
TPMT	miR-590-5p	3.83E-03	2.09E-02	-2.4
TPMT	miR-29b-2-5p	4.10E-03	2.19E-02	-0.4
TPMT	miR-30a-3p	4.31E-03	2.27E-02	-1.6
TPMT	miR-194-5p	5.33E-03	2.64E-02	-2.5
TPMT	miR-145-3p	6.08E-03	2.87E-02	-0.4
TPMT	miR-200a-3p	7.24E-03	3.24E-02	-1.6
TPMT	miR-10a-5p	9.00E-03	3.77E-02	-1.4
TPMT	miR-132-3p	1.28E-02	4.80E-02	-1.7
UGT1A1	miR-223-5p	1.60E-08	9.68E-06	-35.6
UGT1A1	miR-148b-5p	3.31E-08	1.77E-05	-29.0
UGT1A1	miR-505-5p	1.78E-07	4.76E-05	-19.6
UGT1A1	miR-99a-3p	3.56E-07	6.35E-05	-22.3
UGT1A1	miR-151a-5p	3.95E-07	6.70E-05	-32.2
UGT1A1	miR-375	2.03E-06	1.91E-04	-24.7
UGT1A1	miR-30e-3p	3.06E-06	2.53E-04	-70.3
UGT1A1	miR-340-3p	3.85E-06	2.94E-04	-39.7
UGT1A1	miR-192-3p	5.42E-06	3.66E-04	-33.7
UGT1A1	miR-497-5p	6.28E-06	4.08E-04	-19.7
UGT1A1	miR-199a-5p	7.93E-06	4.75E-04	-50.4
UGT1A1	miR-625-5p	1.02E-05	5.83E-04	-16.7
UGT1A1	miR-31-5p	1.14E-05	6.41E-04	-12.4
UGT1A1	miR-592	1.41E-05	7.11E-04	-21.5
UGT1A1	miR-27b-5p	2.00E-05	8.68E-04	-58.7
UGT1A1	miR-331-3p	2.75E-05	1.05E-03	-60.8
UGT1A1	miR-576-3p	3.33E-05	1.19E-03	-22.8
UGT1A1	miR-590-3p	3.57E-05	1.23E-03	-31.8
UGT1A1	miR-195-5p	3.85E-05	1.29E-03	-27.4
UGT1A1	miR-22-5p	4.26E-05	1.39E-03	-27.5
UGT1A1	miR-28-5p	5.94E-05	1.67E-03	-59.6
UGT1A1	miR-26b-3p	6.08E-05	1.68E-03	-27.8
UGT1A1	miR-505-3p	6.43E-05	1.73E-03	-17.7
UGT1A1	miR-320b	6.64E-05	1.78E-03	-24.4
UGT1A1	miR-152-3p	8.55E-05	2.07E-03	-73.7

Gene	miRNA	p-value	FDR	Estimate*
UGT1A1	miR-194-3p	9.78E-05	2.18E-03	-21.4
UGT1A1	miR-511-5p	1.04E-04	2.26E-03	-31.1
UGT1A1	miR-146b-3p	1.04E-04	2.26E-03	-17.8
UGT1A1	miR-29b-3p	1.30E-04	2.56E-03	-51.7
UGT1A1	miR-216b-5p	1.43E-04	2.70E-03	-12.8
UGT1A1	miR-335-5p	2.47E-04	3.82E-03	-65.9
UGT1A1	miR-452-5p	3.30E-04	4.60E-03	-25.9
UGT1A1	miR-502-3p	3.38E-04	4.70E-03	-16.7
UGT1A1	miR-197-3p	6.25E-04	6.50E-03	-70.2
UGT1A1	miR-27a-5p	8.01E-04	7.53E-03	-21.8
UGT1A1	miR-200a-3p	8.78E-04	7.99E-03	-52.6
UGT1A1	miR-148b-3p	1.00E-03	8.74E-03	-52.3
UGT1A1	miR-374a-3p	1.08E-03	9.11E-03	-13.8
UGT1A1	miR-324-5p	1.16E-03	9.56E-03	-65.5
UGT1A1	miR-29a-5p	1.17E-03	9.57E-03	-12.6
UGT1A1	miR-221-3p	1.24E-03	9.93E-03	-72.0
UGT1A1	miR-301a-3p	1.33E-03	1.03E-02	-44.9
UGT1A1	miR-24-3p	1.70E-03	1.22E-02	-36.0
UGT1A1	miR-30d-5p	1.75E-03	1.24E-02	-50.0
UGT1A1	miR-193a-5p	2.25E-03	1.47E-02	-52.8
UGT1A1	miR-194-5p	3.32E-03	1.92E-02	-70.7
UGT1A1	miR-27a-3p	3.33E-03	1.92E-02	-45.8
UGT1A1	miR-199a-3p	3.34E-03	1.92E-02	-37.7
UGT1A1	miR-10a-5p	3.92E-03	2.13E-02	-42.0
UGT1A1	miR-28-3p	3.97E-03	2.14E-02	-36.9
UGT1A1	miR-26b-5p	4.63E-03	2.39E-02	-94.8
UGT1A1	miR-378a-5p	5.90E-03	2.83E-02	-11.0
UGT1A1	miR-532-3p	6.81E-03	3.11E-02	-88.0
UGT1A1	miR-186-5p	7.54E-03	3.34E-02	-71.2
UGT1A1	miR-590-5p	7.59E-03	3.35E-02	-59.8
UGT1A1	miR-27b-3p	7.76E-03	3.41E-02	-40.7
UGT1A1	miR-30a-3p	8.66E-03	3.68E-02	-39.3
UGT1A1	miR-744-3p	9.76E-03	3.97E-02	-22.6
UGT1A1	miR-30a-5p	1.13E-02	4.41E-02	-36.1
UGT1A1	miR-219a-5p	1.24E-02	4.69E-02	-9.7
UGT1A1	miR-339-3p	1.32E-02	4.90E-02	-40.0
UGT2B15	miR-497-5p	6.63E-06	4.19E-04	-4.5
UGT2B15	miR-99a-3p	1.62E-05	7.77E-04	-4.6
UGT2B15	miR-30e-3p	4.70E-05	1.48E-03	-14.6
UGT2B15	miR-374a-3p	7.56E-05	1.90E-03	-3.7
UGT2B15	miR-340-3p	9.30E-05	2.15E-03	-8.1
UGT2B15	miR-223-5p	1.33E-04	2.58E-03	-6.3
UGT2B15	miR-29b-3p	1.54E-04	2.82E-03	-11.7
UGT2B15	miR-592	1.66E-04	2.98E-03	-4.4

Gene	miRNA	p-value	FDR	Estimate*
UGT2B15	miR-216b-5p	1.75E-04	3.07E-03	-2.9
UGT2B15	miR-320b	1.98E-04	3.27E-03	-5.3
UGT2B15	miR-511-5p	2.10E-04	3.42E-03	-6.9
UGT2B15	miR-576-3p	3.06E-04	4.37E-03	-4.7
UGT2B15	miR-502-3p	3.12E-04	4.43E-03	-3.8
UGT2B15	miR-22-5p	3.43E-04	4.71E-03	-5.7
UGT2B15	miR-375	3.42E-04	4.71E-03	-4.6
UGT2B15	miR-505-5p	3.55E-04	4.82E-03	-3.5
UGT2B15	miR-148b-5p	5.47E-04	6.13E-03	-4.8
UGT2B15	miR-31-5p	5.48E-04	6.13E-03	-2.4
UGT2B15	miR-331-3p	7.56E-04	7.31E-03	-11.8
UGT2B15	miR-744-3p	7.63E-04	7.33E-03	-6.5
UGT2B15	miR-195-5p	8.50E-04	7.88E-03	-5.3
UGT2B15	miR-151a-5p	1.02E-03	8.84E-03	-5.4
UGT2B15	miR-505-3p	1.10E-03	9.21E-03	-3.5
UGT2B15	miR-27b-5p	1.15E-03	9.50E-03	-10.9
UGT2B15	miR-29a-5p	1.17E-03	9.57E-03	-2.9
UGT2B15	miR-152-3p	1.18E-03	9.59E-03	-14.5
UGT2B15	miR-199a-5p	1.22E-03	9.82E-03	-9.0
UGT2B15	miR-30a-3p	1.41E-03	1.08E-02	-10.6
UGT2B15	miR-194-3p	1.53E-03	1.13E-02	-4.1
UGT2B15	miR-26b-3p	1.69E-03	1.21E-02	-5.2
UGT2B15	miR-192-3p	1.80E-03	1.26E-02	-5.8
UGT2B15	miR-219a-5p	1.95E-03	1.34E-02	-2.7
UGT2B15	miR-145-3p	2.05E-03	1.39E-02	-2.4
UGT2B15	miR-579-3p	2.59E-03	1.62E-02	-0.9
UGT2B15	miR-590-3p	2.97E-03	1.77E-02	-5.6
UGT2B15	miR-145-3p	3.09E-03	1.82E-02	-0.5
UGT2B15	miR-200a-3p	3.73E-03	2.06E-02	-10.7
UGT2B15	miR-186-5p	3.78E-03	2.08E-02	-17.4
UGT2B15	miR-28-5p	4.21E-03	2.23E-02	-10.4
UGT2B15	miR-452-5p	5.16E-03	2.58E-02	-4.8
UGT2B15	miR-24-3p	5.38E-03	2.65E-02	-7.4
UGT2B15	miR-34a-5p	6.15E-03	2.90E-02	-12.3
UGT2B15	miR-27b-3p	6.36E-03	2.96E-02	-9.5
UGT2B15	miR-30a-5p	6.47E-03	3.00E-02	-1.9
UGT2B15	miR-625-5p	6.72E-03	3.08E-02	-2.6
UGT2B15	miR-579-3p	6.77E-03	3.09E-02	-4.0
UGT2B15	miR-30a-5p	8.12E-03	3.52E-02	-8.6
UGT2B15	miR-29c-3p	8.32E-03	3.58E-02	-1.9
UGT2B15	miR-26b-5p	8.46E-03	3.63E-02	-20.3
UGT2B15	miR-125b-5p	8.77E-03	3.71E-02	-2.9
UGT2B15	miR-335-5p	9.01E-03	3.77E-02	-11.4
UGT2B15	miR-30a-3p	9.10E-03	3.79E-02	-1.9

Gene	miRNA	p-value	FDR	Estimate*
UGT2B15	miR-378a-5p	1.07E-02	4.25E-02	-2.3
UGT2B15	miR-95-3p	1.15E-02	4.45E-02	-0.7
UGT2B15	miR-30d-5p	1.18E-02	4.54E-02	-9.5
UGT2B15	miR-29c-3p	1.19E-02	4.57E-02	-8.6
UGT2B15	miR-197-3p	1.23E-02	4.67E-02	-12.3
UGT2B15	miR-193a-5p	1.25E-02	4.71E-02	-10.1
UGT2B15	miR-219a-5p	1.32E-02	4.88E-02	-0.5
UGT2B15	miR-29b-2-5p	1.33E-02	4.92E-02	-2.2
UGT2B17	miR-579-3p	2.63E-03	1.63E-02	-0.8
UGT2B17	miR-145-3p	3.13E-03	1.84E-02	-0.4
UGT2B17	miR-30a-5p	6.74E-03	3.08E-02	-1.7
UGT2B17	miR-29c-3p	8.12E-03	3.52E-02	-1.7
UGT2B17	miR-125b-5p	8.21E-03	3.55E-02	-2.6
UGT2B17	miR-30a-3p	8.96E-03	3.76E-02	-1.7
UGT2B17	miR-95-3p	1.17E-02	4.53E-02	-0.7
UGT2B17	miR-219a-5p	1.31E-02	4.85E-02	-0.4
UGT2B7	miR-216b-5p	4.03E-06	2.95E-04	-4.5
UGT2B7	miR-497-5p	8.95E-06	5.23E-04	-6.0
UGT2B7	miR-223-5p	2.75E-05	1.05E-03	-9.1
UGT2B7	miR-99a-3p	3.08E-05	1.13E-03	-6.0
UGT2B7	miR-148b-5p	7.74E-05	1.94E-03	-7.2
UGT2B7	miR-27b-5p	8.62E-05	2.08E-03	-17.0
UGT2B7	miR-29b-3p	9.44E-05	2.16E-03	-16.1
UGT2B7	miR-199a-5p	1.12E-04	2.35E-03	-14.0
UGT2B7	miR-502-3p	1.15E-04	2.38E-03	-5.4
UGT2B7	miR-30e-3p	1.53E-04	2.82E-03	-18.6
UGT2B7	miR-31-5p	1.54E-04	2.82E-03	-3.4
UGT2B7	miR-505-5p	1.60E-04	2.91E-03	-4.8
UGT2B7	miR-452-5p	1.71E-04	3.04E-03	-8.2
UGT2B7	miR-340-3p	1.95E-04	3.25E-03	-10.5
UGT2B7	miR-151a-5p	2.74E-04	4.10E-03	-7.9
UGT2B7	miR-152-3p	3.53E-04	4.81E-03	-21.1
UGT2B7	miR-195-5p	3.69E-04	4.95E-03	-7.6
UGT2B7	miR-375	3.86E-04	5.04E-03	-6.2
UGT2B7	miR-590-3p	4.34E-04	5.36E-03	-8.7
UGT2B7	miR-331-3p	4.51E-04	5.47E-03	-16.3
UGT2B7	miR-374a-3p	4.69E-04	5.62E-03	-4.5
UGT2B7	miR-505-3p	5.80E-04	6.23E-03	-4.8
UGT2B7	miR-200a-3p	6.36E-04	6.57E-03	-16.5
UGT2B7	miR-28-5p	6.91E-04	6.90E-03	-16.1
UGT2B7	miR-320b	7.29E-04	7.16E-03	-6.6
UGT2B7	miR-192-3p	7.37E-04	7.20E-03	-8.3
UGT2B7	miR-22-5p	9.81E-04	8.67E-03	-7.1
UGT2B7	miR-511-5p	1.09E-03	9.14E-03	-8.3

	Gene	miRNA	p-value	FDR	Estimate*
	UGT2B7	miR-592	1.14E-03	9.44E-03	-5.3
	UGT2B7	miR-625-5p	1.26E-03	9.99E-03	-4.1
	UGT2B7	miR-24-3p	1.28E-03	1.01E-02	-11.3
	UGT2B7	miR-590-5p	1.73E-03	1.23E-02	-21.0
	UGT2B7	miR-146b-3p	1.93E-03	1.33E-02	-4.6
	UGT2B7	miR-378a-5p	2.44E-03	1.55E-02	-3.6
	UGT2B7	miR-197-3p	2.65E-03	1.64E-02	-19.4
	UGT2B7	miR-27a-3p	2.69E-03	1.66E-02	-14.3
	UGT2B7	miR-576-3p	2.92E-03	1.75E-02	-5.4
	UGT2B7	miR-26b-3p	3.42E-03	1.96E-02	-6.6
	UGT2B7	miR-186-5p	3.49E-03	1.97E-02	-23.6
	UGT2B7	miR-532-3p	4.05E-03	2.17E-02	-28.5
	UGT2B7	miR-193a-5p	4.25E-03	2.25E-02	-15.3
	UGT2B7	miR-26b-5p	4.80E-03	2.46E-02	-29.0
	UGT2B7	miR-219a-5p	5.20E-03	2.60E-02	-3.3
	UGT2B7	miR-27a-5p	5.34E-03	2.64E-02	-5.7
	UGT2B7	miR-27b-3p	6.06E-03	2.87E-02	-12.8
	UGT2B7	miR-145-3p	6.28E-03	2.93E-02	-2.9
	UGT2B7	miR-148b-3p	7.37E-03	3.28E-02	-13.5
	UGT2B7	miR-125b-5p	8.00E-03	3.48E-02	-18.7
	UGT2B7	miR-335-5p	8.59E-03	3.66E-02	-15.4
	UGT2B7	miR-30a-3p	9.32E-03	3.85E-02	-12.0
	UGT2B7	miR-132-3p	1.21E-02	4.63E-02	-14.6
	UGT2B7	miR-194-5p	1.24E-02	4.69E-02	-18.9
	UGT2B7	miR-29c-3p	1.26E-02	4.73E-02	-11.4
Transporters	*ABCB1*	miR-502-3p	2.35E-07	5.69E-05	-1.2
	ABCB1	miR-216b-5p	6.62E-07	8.38E-05	-0.8
	ABCB1	miR-219a-5p	2.10E-06	1.95E-04	-0.9
	ABCB1	miR-29b-3p	2.80E-06	2.35E-04	-3.2
	ABCB1	miR-497-5p	4.93E-06	3.47E-04	-1.1
	ABCB1	miR-24-3p	2.52E-05	1.02E-03	-2.4
	ABCB1	miR-579-3p	2.74E-05	1.05E-03	-1.3
	ABCB1	miR-511-5p	5.56E-05	1.61E-03	-1.7
	ABCB1	miR-199a-5p	8.69E-05	2.08E-03	-2.5
	ABCB1	miR-145-3p	8.67E-05	2.08E-03	-0.7
	ABCB1	miR-34a-5p	9.16E-05	2.15E-03	-3.9
	ABCB1	miR-29c-3p	1.14E-04	2.36E-03	-2.9
	ABCB1	miR-30e-3p	1.39E-04	2.64E-03	-3.3
	ABCB1	miR-31-5p	1.74E-04	3.07E-03	-0.6
	ABCB1	miR-374a-3p	1.96E-04	3.25E-03	-0.8
	ABCB1	miR-378a-5p	2.50E-04	3.84E-03	-0.7
	ABCB1	miR-155-5p	2.63E-04	3.97E-03	-1.8
	ABCB1	miR-590-3p	3.04E-04	4.36E-03	-1.6
	ABCB1	miR-200a-3p	3.56E-04	4.82E-03	-3.0

Gene	miRNA	p-value	FDR	Estimate*
ABCB1	miR-99a-3p	3.89E-04	5.06E-03	-0.9
ABCB1	miR-152-3p	4.05E-04	5.17E-03	-3.7
ABCB1	miR-331-3p	4.13E-04	5.21E-03	-2.9
ABCB1	miR-125b-5p	5.14E-04	5.88E-03	-4.1
ABCB1	miR-195-5p	5.62E-04	6.16E-03	-1.3
ABCB1	miR-27b-5p	6.22E-04	6.48E-03	-2.7
ABCB1	miR-21-5p	7.37E-04	7.20E-03	-1.2
ABCB1	miR-320b	8.70E-04	7.99E-03	-1.1
ABCB1	miR-27b-3p	8.79E-04	7.99E-03	-2.7
ABCB1	miR-28-5p	9.49E-04	8.48E-03	-2.8
ABCB1	miR-223-5p	1.01E-03	8.77E-03	-1.3
ABCB1	miR-452-5p	1.06E-03	9.05E-03	-1.3
ABCB1	miR-30a-3p	1.25E-03	9.98E-03	-2.5
ABCB1	miR-505-3p	1.33E-03	1.03E-02	-0.8
ABCB1	miR-532-3p	1.50E-03	1.12E-02	-5.4
ABCB1	miR-132-3p	1.50E-03	1.12E-02	-3.2
ABCB1	miR-375	1.53E-03	1.13E-02	-1.0
ABCB1	miR-505-5p	1.73E-03	1.23E-02	-0.7
ABCB1	miR-22-5p	1.80E-03	1.26E-02	-1.2
ABCB1	miR-340-3p	1.88E-03	1.31E-02	-1.6
ABCB1	miR-23b-3p	2.24E-03	1.47E-02	-3.1
ABCB1	miR-151a-5p	2.38E-03	1.53E-02	-1.2
ABCB1	miR-592	3.69E-03	2.04E-02	-0.9
ABCB1	miR-30a-5p	3.97E-03	2.14E-02	-2.2
ABCB1	miR-193a-5p	4.80E-03	2.46E-02	-2.7
ABCB1	miR-27a-5p	4.86E-03	2.48E-02	-1.0
ABCB1	miR-95-3p	6.55E-03	3.02E-02	-0.9
ABCB1	miR-197-3p	7.60E-03	3.35E-02	-3.1
ABCB1	miR-301a-3p	7.65E-03	3.37E-02	-2.1
ABCB1	miR-625-5p	7.95E-03	3.47E-02	-0.6
ABCB1	miR-423-5p	9.30E-03	3.85E-02	-2.5
ABCB1	miR-628-3p	9.31E-03	3.85E-02	-0.6
ABCB1	miR-576-3p	9.68E-03	3.95E-02	-0.8
ABCB1	miR-29b-2-5p	1.02E-02	4.11E-02	-0.5
ABCB1	miR-148b-5p	1.04E-02	4.17E-02	-0.9
ABCB1	miR-186-5p	1.11E-02	4.35E-02	-3.7
ABCB1	miR-28-3p	1.23E-02	4.67E-02	-1.8
ABCB1	miR-330-3p	1.26E-02	4.73E-02	-0.5
ABCC2	miR-223-5p	6.16E-05	1.69E-03	-9.6
ABCC2	miR-505-3p	1.27E-04	2.53E-03	-5.7
ABCC2	miR-452-5p	2.04E-04	3.35E-03	-8.9
ABCC2	miR-148b-5p	2.37E-04	3.70E-03	-7.4
ABCC2	miR-497-5p	3.73E-04	4.97E-03	-5.5
ABCC2	miR-505-5p	4.76E-04	5.67E-03	-5.0

Gene	miRNA	p-value	FDR	Estimate*
ABCC2	miR-199a-5p	5.02E-04	5.82E-03	-14.1
ABCC2	miR-27a-3p	6.12E-04	6.42E-03	-17.4
ABCC2	miR-192-3p	6.49E-04	6.65E-03	-9.1
ABCC2	miR-216b-5p	6.54E-04	6.68E-03	-3.9
ABCC2	miR-625-5p	8.68E-04	7.98E-03	-4.5
ABCC2	miR-99a-3p	9.39E-04	8.44E-03	-5.5
ABCC2	miR-197-3p	1.08E-03	9.11E-03	-22.7
ABCC2	miR-151a-5p	1.16E-03	9.56E-03	-7.8
ABCC2	miR-195-5p	1.37E-03	1.05E-02	-7.6
ABCC2	miR-26b-3p	1.80E-03	1.26E-02	-7.6
ABCC2	miR-331-3p	2.08E-03	1.40E-02	-16.0
ABCC2	miR-186-5p	2.77E-03	1.68E-02	-26.3
ABCC2	miR-375	2.90E-03	1.74E-02	-5.8
ABCC2	miR-27b-5p	3.34E-03	1.92E-02	-14.7
ABCC2	miR-590-5p	3.47E-03	1.97E-02	-21.6
ABCC2	miR-146b-3p	3.72E-03	2.06E-02	-4.7
ABCC2	miR-27a-5p	3.78E-03	2.08E-02	-6.5
ABCC2	miR-152-3p	3.83E-03	2.09E-02	-19.3
ABCC2	miR-31-5p	3.99E-03	2.14E-02	-3.0
ABCC2	miR-148b-3p	4.08E-03	2.18E-02	-15.6
ABCC2	miR-28-5p	4.74E-03	2.44E-02	-15.1
ABCC2	miR-200a-3p	4.84E-03	2.47E-02	-15.3
ABCC2	miR-30e-3p	5.26E-03	2.61E-02	-15.9
ABCC2	miR-199a-3p	5.59E-03	2.72E-02	-12.0
ABCC2	miR-340-3p	5.67E-03	2.75E-02	-8.9
ABCC2	miR-29b-3p	6.42E-03	2.98E-02	-13.1
ABCC2	miR-590-3p	8.27E-03	3.57E-02	-7.4
ABCC2	miR-10a-5p	8.77E-03	3.71E-02	-13.0
ABCC2	miR-335-5p	1.06E-02	4.22E-02	-16.3
ABCC2	miR-576-3p	1.27E-02	4.77E-02	-5.0
ABCG2	miR-668-3p	4.08E-03	2.18E-02	-0.2
ABCG2	miR-431-5p	9.03E-03	3.77E-02	-0.2
ABCG2	miR-512-3p	1.09E-02	4.29E-02	-0.1
SLC15A2	miR-493-3p	3.63E-05	1.24E-03	-0.033
SLC15A2	miR-433-3p	5.35E-05	1.58E-03	-0.030
SLC15A2	miR-889-3p	1.19E-04	2.44E-03	-0.1
SLC15A2	miR-431-5p	1.67E-04	2.99E-03	-0.025
SLC15A2	miR-154-3p	1.77E-04	3.09E-03	-0.028
SLC15A2	miR-485-3p	1.92E-04	3.25E-03	-0.020
SLC15A2	miR-487b-3p	2.17E-04	3.51E-03	-0.1
SLC15A2	miR-668-3p	2.90E-04	4.24E-03	-0.031
SLC15A2	miR-539-5p	3.82E-04	5.03E-03	-0.1
SLC15A2	miR-758-3p	4.15E-04	5.21E-03	-0.026
SLC15A2	miR-409-3p	8.76E-04	7.99E-03	-0.1

Gene	miRNA	p-value	FDR	Estimate*
SLC15A2	miR-410-3p	1.05E-03	8.98E-03	-0.028
SLC15A2	miR-323a-3p	1.20E-03	9.70E-03	-0.041
SLC15A2	miR-144-5p	2.08E-03	1.40E-02	-0.032
SLC15A2	miR-411-5p	2.16E-03	1.43E-02	-0.1
SLC15A2	miR-130a-3p	2.57E-03	1.60E-02	-0.2
SLC15A2	miR-19b-1-5p	4.30E-03	2.27E-02	-0.1
SLC15A2	miR-519d-3p	4.35E-03	2.28E-02	-0.022
SLC15A2	miR-487a-3p	5.93E-03	2.83E-02	-0.022
SLC15A2	miR-654-3p	6.19E-03	2.91E-02	-0.041
SLC15A2	miR-136-3p	6.49E-03	3.01E-02	-0.1
SLC15A2	miR-654-5p	6.52E-03	3.01E-02	-0.021
SLC15A2	miR-184	8.03E-03	3.49E-02	-0.021
SLC15A2	miR-512-3p	8.33E-03	3.58E-02	-0.016
SLC15A2	miR-526b-5p	8.50E-03	3.64E-02	-0.030
SLC15A2	miR-432-5p	9.03E-03	3.77E-02	-0.024
SLC15A2	miR-18a-5p	1.21E-02	4.62E-02	-0.1
SLC15A2	miR-494-3p	1.29E-02	4.82E-02	-0.022
SLC22A1	miR-374a-3p	1.07E-06	1.24E-04	-10.3
SLC22A1	miR-99a-3p	1.30E-06	1.44E-04	-12.1
SLC22A1	miR-592	4.20E-06	3.01E-04	-12.5
SLC22A1	miR-22-5p	9.43E-06	5.42E-04	-16.2
SLC22A1	miR-30e-3p	1.49E-05	7.36E-04	-37.3
SLC22A1	miR-497-5p	2.07E-05	8.93E-04	-10.6
SLC22A1	miR-148b-5p	3.05E-05	1.13E-03	-13.6
SLC22A1	miR-223-5p	3.78E-05	1.28E-03	-16.3
SLC22A1	miR-340-3p	4.54E-05	1.45E-03	-20.3
SLC22A1	miR-216b-5p	5.01E-05	1.53E-03	-7.5
SLC22A1	miR-151a-5p	9.96E-05	2.21E-03	-15.0
SLC22A1	miR-29a-5p	1.06E-04	2.27E-03	-8.1
SLC22A1	miR-29b-3p	2.62E-04	3.96E-03	-27.8
SLC22A1	miR-744-3p	3.22E-04	4.55E-03	-16.6
SLC22A1	miR-320b	3.43E-04	4.71E-03	-12.5
SLC22A1	miR-505-5p	3.45E-04	4.73E-03	-8.4
SLC22A1	miR-511-5p	5.41E-04	6.09E-03	-15.9
SLC22A1	miR-590-3p	5.77E-04	6.23E-03	-15.5
SLC22A1	miR-197-3p	9.17E-04	8.27E-03	-38.2
SLC22A1	miR-375	9.66E-04	8.59E-03	-10.6
SLC22A1	miR-30a-3p	1.69E-03	1.21E-02	-25.5
SLC22A1	miR-532-3p	1.79E-03	1.25E-02	-55.4
SLC22A1	miR-576-3p	1.83E-03	1.27E-02	-10.2
SLC22A1	miR-199a-5p	1.89E-03	1.31E-02	-21.4
SLC22A1	miR-194-3p	2.25E-03	1.47E-02	-9.8
SLC22A1	miR-502-3p	2.34E-03	1.51E-02	-8.1
SLC22A1	miR-27b-5p	2.59E-03	1.61E-02	-25.0

Gene	miRNA	p-value	FDR	Estimate*
SLC22A1	miR-30d-5p	2.61E-03	1.62E-02	-27.0
SLC22A1	miR-152-3p	2.65E-03	1.64E-02	-33.3
SLC22A1	miR-331-3p	2.65E-03	1.64E-02	-26.1
SLC22A1	miR-625-5p	2.70E-03	1.66E-02	-6.9
SLC22A1	miR-145-3p	3.44E-03	1.96E-02	-5.6
SLC22A1	miR-28-5p	3.58E-03	2.00E-02	-25.8
SLC22A1	miR-31-5p	3.79E-03	2.08E-02	-5.0
SLC22A1	miR-195-5p	4.84E-03	2.47E-02	-11.3
SLC22A1	miR-590-5p	5.37E-03	2.65E-02	-34.6
SLC22A1	miR-192-3p	5.46E-03	2.68E-02	-12.8
SLC22A1	miR-335-5p	7.72E-03	3.39E-02	-28.2
SLC22A1	miR-30a-5p	8.21E-03	3.55E-02	-20.9
SLC22A1	miR-505-3p	8.48E-03	3.64E-02	-7.0
SLC22A1	miR-378a-5p	8.74E-03	3.70E-02	-5.9
SLC22A1	miR-29b-2-5p	1.09E-02	4.28E-02	-5.4
SLC22A2	miR-144-5p	4.32E-03	2.27E-02	-0.005
SLC22A2	miR-654-5p	4.39E-03	2.29E-02	-0.004
SLC22A2	miR-889-3p	4.71E-03	2.42E-02	-0.011
SLC22A2	miR-433-3p	4.83E-03	2.47E-02	-0.004
SLC22A2	miR-487a-3p	7.29E-03	3.26E-02	-0.004
SLC22A2	miR-431-5p	7.82E-03	3.42E-02	-0.003
SLC22A2	miR-668-3p	9.50E-03	3.90E-02	-0.004
SLC22A2	miR-18a-5p	1.21E-02	4.63E-02	-0.014
SLC22A2	miR-539-5p	1.31E-02	4.86E-02	-0.010
SLC22A2	miR-526b-5p	1.36E-02	5.00E-02	-0.005
SLCO1B1	miR-452-5p	5.97E-05	1.67E-03	-7.8
SLCO1B1	miR-99a-3p	1.60E-04	2.91E-03	-5.0
SLCO1B1	miR-216b-5p	2.04E-04	3.35E-03	-3.5
SLCO1B1	miR-199a-5p	2.90E-04	4.24E-03	-12.0
SLCO1B1	miR-192-3p	3.83E-04	5.03E-03	-7.8
SLCO1B1	miR-195-5p	4.38E-04	5.38E-03	-6.7
SLCO1B1	miR-505-5p	4.76E-04	5.67E-03	-4.1
SLCO1B1	miR-375	4.89E-04	5.73E-03	-5.5
SLCO1B1	miR-31-5p	5.63E-04	6.16E-03	-2.9
SLCO1B1	miR-331-3p	1.09E-03	9.18E-03	-13.9
SLCO1B1	miR-29b-3p	1.25E-03	9.94E-03	-12.5
SLCO1B1	miR-148b-5p	1.30E-03	1.02E-02	-5.5
SLCO1B1	miR-26b-3p	1.35E-03	1.04E-02	-6.5
SLCO1B1	miR-151a-5p	1.35E-03	1.04E-02	-6.4
SLCO1B1	miR-197-3p	1.36E-03	1.05E-02	-18.4
SLCO1B1	miR-340-3p	1.43E-03	1.09E-02	-8.3
SLCO1B1	miR-223-5p	1.66E-03	1.20E-02	-6.6
SLCO1B1	miR-625-5p	1.78E-03	1.25E-02	-3.6
SLCO1B1	miR-497-5p	2.05E-03	1.39E-02	-4.1

Gene	miRNA	p-value	FDR	Estimate*
SLCO1B1	miR-27a-3p	2.28E-03	1.48E-02	-13.1
SLCO1B1	miR-320b	2.36E-03	1.52E-02	-5.5
SLCO1B1	miR-505-3p	2.50E-03	1.58E-02	-3.9
SLCO1B1	miR-146b-3p	2.56E-03	1.60E-02	-4.0
SLCO1B1	miR-30e-3p	2.65E-03	1.64E-02	-14.0
SLCO1B1	miR-28-5p	2.83E-03	1.71E-02	-13.0
SLCO1B1	miR-592	3.12E-03	1.84E-02	-4.4
SLCO1B1	miR-576-3p	4.11E-03	2.19E-02	-4.7
SLCO1B1	miR-511-5p	4.22E-03	2.23E-02	-6.7
SLCO1B1	miR-200a-3p	4.59E-03	2.38E-02	-12.7
SLCO1B1	miR-148b-3p	5.00E-03	2.53E-02	-12.7
SLCO1B1	miR-502-3p	5.91E-03	2.83E-02	-3.7
SLCO1B1	miR-24-3p	6.15E-03	2.90E-02	-8.9
SLCO1B1	miR-27b-5p	6.34E-03	2.96E-02	-11.4
SLCO1B1	miR-152-3p	6.86E-03	3.12E-02	-15.1
SLCO1B1	miR-301a-3p	7.12E-03	3.20E-02	-10.7
SLCO1B1	miR-193a-5p	8.98E-03	3.76E-02	-12.8
SLCO1B1	miR-335-5p	9.10E-03	3.79E-02	-13.7
SLCO1B1	miR-199a-3p	9.13E-03	3.79E-02	-9.4
SLCO1B1	miR-590-5p	9.20E-03	3.81E-02	-16.2
SLCO1B1	miR-590-3p	9.68E-03	3.95E-02	-6.0
SLCO1B1	miR-324-5p	1.04E-02	4.17E-02	-14.8
SLCO1B1	miR-194-3p	1.12E-02	4.37E-02	-4.2
SLCO1B1	miR-221-3p	1.17E-02	4.53E-02	-16.1
SLCO1B1	miR-186-5p	1.17E-02	4.53E-02	-18.7
SLCO1B1	miR-26b-5p	1.18E-02	4.55E-02	-23.7
SLCO1B1	miR-194-5p	1.34E-02	4.94E-02	-16.9
SLCO1B3	miR-223-5p	4.02E-04	5.15E-03	-4.5
SLCO1B3	miR-27b-5p	1.04E-03	8.91E-03	-8.3
SLCO1B3	miR-148b-5p	5.77E-03	2.78E-02	-3.0
SLCO1B3	miR-199a-5p	6.34E-03	2.96E-02	-5.9
SLCO1B3	miR-200a-3p	1.09E-02	4.28E-02	-7.2
SULT1A1	miR-223-5p	8.63E-04	7.97E-03	-1.0
SULT1A1	miR-148b-5p	9.68E-04	8.59E-03	-0.8
SULT1A1	miR-99a-3p	1.71E-03	1.22E-02	-0.6
SULT1A1	miR-30e-3p	2.26E-03	1.48E-02	-2.0
SULT1A1	miR-625-5p	2.47E-03	1.57E-02	-0.5
SULT1A1	miR-505-3p	2.97E-03	1.77E-02	-0.6
SULT1A1	miR-22-5p	3.18E-03	1.86E-02	-0.8
SULT1A1	miR-151a-5p	3.42E-03	1.95E-02	-0.8
SULT1A1	miR-505-5p	4.16E-03	2.20E-02	-0.5
SULT1A1	miR-375	6.61E-03	3.04E-02	-0.6
SULT1A1	miR-497-5p	6.64E-03	3.05E-02	-0.5
SULT1A1	miR-199a-5p	7.96E-03	3.47E-02	-1.3

	Gene	miRNA	p-value	FDR	Estimate*
	SULT1A1	miR-340-3p	8.34E-03	3.58E-02	-1.0
	SULT1A1	miR-320b	8.74E-03	3.70E-02	-0.7
	SULT1A1	miR-26b-3p	9.20E-03	3.81E-02	-0.8
	SULT1A1	miR-592	1.01E-02	4.09E-02	-0.6
	SULT1A1	miR-301a-3p	1.19E-02	4.57E-02	-1.4
	SULT1A1	miR-194-3p	1.23E-02	4.67E-02	-0.6
	SULT1A1	miR-29a-5p	1.35E-02	4.99E-02	-0.4
Regulatory	*HNF4A*	miR-374a-3p	1.21E-05	6.50E-04	-1.1
	HNF4A	miR-502-3p	1.88E-05	8.58E-04	-1.2
	HNF4A	miR-216b-5p	4.60E-05	1.47E-03	-0.8
	HNF4A	miR-497-5p	5.02E-05	1.53E-03	-1.1
	HNF4A	miR-29b-3p	5.81E-05	1.66E-03	-3.4
	HNF4A	miR-532-3p	5.94E-05	1.67E-03	-7.6
	HNF4A	miR-30e-3p	9.36E-05	2.15E-03	-3.9
	HNF4A	miR-132-3p	1.19E-04	2.44E-03	-4.3
	HNF4A	miR-145-3p	1.27E-04	2.53E-03	-0.8
	HNF4A	miR-152-3p	1.37E-04	2.62E-03	-4.5
	HNF4A	miR-590-3p	1.95E-04	3.25E-03	-1.9
	HNF4A	miR-99a-3p	1.96E-04	3.25E-03	-1.1
	HNF4A	miR-29b-2-5p	2.26E-04	3.59E-03	-0.8
	HNF4A	miR-30a-3p	3.83E-04	5.03E-03	-3.2
	HNF4A	miR-223-5p	4.07E-04	5.18E-03	-1.6
	HNF4A	miR-579-3p	4.29E-04	5.33E-03	-1.4
	HNF4A	miR-22-5p	4.49E-04	5.46E-03	-1.5
	HNF4A	miR-155-5p	5.18E-04	5.90E-03	-2.0
	HNF4A	miR-31-5p	8.75E-04	7.99E-03	-0.6
	HNF4A	miR-27b-5p	1.08E-03	9.11E-03	-3.0
	HNF4A	miR-125b-5p	1.23E-03	9.85E-03	-4.5
	HNF4A	miR-511-5p	1.26E-03	1.00E-02	-1.7
	HNF4A	miR-592	1.45E-03	1.10E-02	-1.1
	HNF4A	miR-340-3p	1.72E-03	1.22E-02	-1.9
	HNF4A	miR-331-3p	2.21E-03	1.45E-02	-3.0
	HNF4A	miR-28-5p	2.39E-03	1.54E-02	-3.0
	HNF4A	miR-30a-5p	2.45E-03	1.56E-02	-2.6
	HNF4A	miR-151a-5p	2.63E-03	1.63E-02	-1.4
	HNF4A	miR-24-3p	2.81E-03	1.70E-02	-2.2
	HNF4A	miR-505-5p	3.11E-03	1.83E-02	-0.8
	HNF4A	miR-199a-5p	3.20E-03	1.87E-02	-2.3
	HNF4A	miR-29c-3p	3.22E-03	1.88E-02	-2.7
	HNF4A	miR-27a-5p	3.47E-03	1.97E-02	-1.2
	HNF4A	miR-219a-5p	3.57E-03	2.00E-02	-0.7
	HNF4A	miR-744-3p	3.59E-03	2.00E-02	-1.6
	HNF4A	miR-375	4.99E-03	2.52E-02	-1.0
	HNF4A	miR-505-3p	5.17E-03	2.58E-02	-0.8

Gene	miRNA	p-value	FDR	Estimate*
HNF4A	miR-320b	7.14E-03	3.21E-02	-1.1
HNF4A	miR-27b-3p	7.97E-03	3.48E-02	-2.6
HNF4A	miR-195-5p	9.36E-03	3.86E-02	-1.2
HNF4A	miR-148b-5p	9.54E-03	3.91E-02	-1.0
HNF4A	miR-34a-5p	1.00E-02	4.05E-02	-3.2
HNF4A	miR-197-3p	1.11E-02	4.36E-02	-3.4
HNF4A	miR-143-3p	1.16E-02	4.48E-02	-3.6
HNF4A	miR-29a-5p	1.32E-02	4.89E-02	-0.6
NR1I2	miR-216b-5p	7.30E-06	4.53E-04	-0.7
NR1I2	miR-497-5p	1.58E-05	7.61E-04	-1.0
NR1I2	miR-374a-3p	2.57E-05	1.03E-03	-0.8
NR1I2	miR-99a-3p	4.38E-05	1.41E-03	-1.0
NR1I2	miR-592	1.45E-04	2.71E-03	-1.0
NR1I2	miR-223-5p	2.34E-04	3.68E-03	-1.3
NR1I2	miR-30e-3p	4.27E-04	5.32E-03	-2.9
NR1I2	miR-29b-3p	5.01E-04	5.82E-03	-2.4
NR1I2	miR-148b-5p	5.69E-04	6.21E-03	-1.1
NR1I2	miR-22-5p	6.77E-04	6.84E-03	-1.2
NR1I2	miR-197-3p	7.31E-04	7.16E-03	-3.5
NR1I2	miR-340-3p	8.66E-04	7.97E-03	-1.6
NR1I2	miR-532-3p	9.99E-04	8.73E-03	-5.2
NR1I2	miR-151a-5p	1.24E-03	9.93E-03	-1.2
NR1I2	miR-199a-5p	2.00E-03	1.36E-02	-1.9
NR1I2	miR-590-5p	2.16E-03	1.43E-02	-3.4
NR1I2	miR-505-5p	2.41E-03	1.54E-02	-0.7
NR1I2	miR-152-3p	3.54E-03	1.99E-02	-2.9
NR1I2	miR-502-3p	3.57E-03	2.00E-02	-0.7
NR1I2	miR-195-5p	3.62E-03	2.01E-02	-1.0
NR1I2	miR-27b-5p	3.93E-03	2.13E-02	-2.2
NR1I2	miR-511-5p	4.32E-03	2.27E-02	-1.2
NR1I2	miR-590-3p	4.32E-03	2.27E-02	-1.2
NR1I2	miR-28-5p	4.50E-03	2.33E-02	-2.3
NR1I2	miR-744-3p	5.69E-03	2.76E-02	-1.2
NR1I2	miR-30a-3p	5.96E-03	2.84E-02	-2.0
NR1I2	miR-29a-5p	6.07E-03	2.87E-02	-0.5
NR1I2	miR-320b	6.50E-03	3.01E-02	-0.9
NR1I2	miR-29b-2-5p	6.82E-03	3.11E-02	-0.5
NR1I2	miR-10b-3p	7.32E-03	3.27E-02	-0.4
NR1I2	miR-186-5p	8.04E-03	3.50E-02	-3.5
NR1I2	miR-625-5p	8.90E-03	3.74E-02	-0.6
NR1I2	miR-331-3p	9.86E-03	4.00E-02	-2.1
NR1I2	miR-145-3p	9.87E-03	4.00E-02	-0.5
NR1I2	miR-125b-5p	1.00E-02	4.05E-02	-3.0
NR1I2	miR-31-5p	1.04E-02	4.17E-02	-0.4

Gene	miRNA	p-value	FDR	Estimate*
NR1I2	miR-375	1.19E-02	4.56E-02	-0.8
NR1I3	miR-197-3p	4.69E-04	5.62E-03	-7.4
NR1I3	miR-216b-5p	5.66E-04	6.18E-03	-1.2
NR1I3	miR-452-5p	2.21E-03	1.45E-02	-2.3
NR1I3	miR-590-5p	4.67E-03	2.41E-02	-6.5
NR1I3	miR-27a-3p	6.28E-03	2.93E-02	-4.4
NR1I3	miR-505-3p	1.01E-02	4.06E-02	-1.3
NR1I3	miR-532-3p	1.14E-02	4.42E-02	-8.5
NR1I3	miR-199a-5p	1.20E-02	4.59E-02	-3.3
NR1I3	miR-497-5p	1.29E-02	4.81E-02	-1.3

*****Estimates indicate the changes in mRNA expressed as RPKM (reads per kilobases per million) per one threshold cycle decrease in miRNA expression.

Note: Decrease in threshold cycle is an increase in miRNA expression. For example, an estimate of -40.0 means that for every one threshold cycle decrease in miRNA expression, the correlated mRNA decreased 40 RPKM. In other words, the miRNA and mRNA are negatively correlated.

Table 6: List of miRNA-mRNA predicted targets

miRNA	Seed Sequence	mRNA	Source	Confidence
miR-455-3p	CAGUCCA	*ABCB1*	TargetScan Human	Moderate (predicted)
let-7a-5p	GAGGUAG	*ABCC2*	TargetScan Human	Moderate (predicted)
miR-106a-5p	AAAGUGC	*ABCG2*	TargetScan Human	Moderate (predicted)
miR-154-3p	AUCAUAC	*ABCG2*	TargetScan Human	Moderate (predicted)
miR-512-3p	AGUGCUG	*ABCG2*	TargetScan Human	Moderate (predicted)
miR-519a-3p	AAGUGCA	*ABCG2*	miRecords	Experimentally Observed
miR-125b-5p	CCCUGAG	*CYP1A1*	miRecords	Experimentally Observed
miR-146b-3p	GCCCUGU	*CYP1A1*	TargetScan Human	High (predicted)
miR-193a-5p	GGGUCUU	*CYP1A1*	TargetScan Human	Moderate (predicted)
miR-143-3p	GAGAUGA	*CYP1A2*	TargetScan Human	Moderate (predicted)
miR-320b	AAAGCUG	*CYP1A2*	TargetScan Human	High (predicted)
miR-431-5p	GUCUUGC	*CYP1A2*	TargetScan Human	Moderate (predicted)
miR-668-3p	GUCACUC	*CYP1A2*	TargetScan Human	Moderate (predicted)
miR-942-5p	CUUCUCU	*CYP2A6*	TargetScan Human	Moderate (predicted)
miR-1275	UGGGGGA	*CYP2B6*	TargetScan Human	Moderate (predicted)
miR-29b-3p	AGCACCA	*CYP2B6*	TargetScan Human	Moderate (predicted)
miR-483-3p	CACUCCU	*CYP2B6*	TargetScan Human	Moderate (predicted)
miR-625-5p	GGGGGAA	*CYP2B6*	TargetScan Human	Moderate (predicted)
miR-744-5p	GCGGGGC	*CYP2B6*	TargetScan Human	Moderate (predicted)
miR-939-5p	GGGGAGC	*CYP2B6*	TargetScan Human	Moderate (predicted)
miR-143-3p	GAGAUGA	*CYP2C9*	TargetScan Human	Moderate (predicted)
miR-155-5p	UAAUGCU	*CYP2C9*	TargetScan Human	Moderate (predicted)
miR-369-3p	AUAAUAC	*CYP2C9*	TargetScan Human	Moderate (predicted)
miR-150-5p	CUCCCAA	*CYP3A4*	TargetScan Human	Moderate (predicted)

miRNA	Seed Sequence	mRNA	Source	Confidence
miR-455-3p	CAGUCCA	*CYP3A4*	TargetScan Human	Moderate (predicted)
miR-21-5p	AGCUUAU	*CYP3A5*	TargetScan Human	Moderate (predicted)
miR-539-5p	GAGAAAU	*CYP3A7*	TargetScan Human	Moderate (predicted)
miR-106a-5p	AAAGUGC	*DPYD*	TargetScan Human	Moderate (predicted)
miR-1271-5p	UUGGCAC	*DPYD*	TargetScan Human	Moderate (predicted)
miR-199a-3p	CAGUAGU	*DPYD*	TargetScan Human	Moderate (predicted)
miR-25-3p	AUUGCAC	*DPYD*	TargetScan Human	High (predicted)
miR-31-5p	GGCAAGA	*DPYD*	TargetScan Human	Moderate (predicted)
miR-34a-5p	GGCAGUG	*DPYD*	TargetScan Human	High (predicted)
miR-376a-3p	UCAUAGA	*DPYD*	TargetScan Human	Moderate (predicted)
miR-425-5p	AUGACAC	*DPYD*	TargetScan Human	High (predicted)
miR-494-3p	GAAACAU	*DPYD*	TargetScan Human	Moderate (predicted)
miR-519a-3p	AAGUGCA	*DPYD*	TargetScan Human	Moderate (predicted)
miR-519e-5p	UCUCCAA	*DPYD*	TargetScan Human	Moderate (predicted)
miR-628-5p	UGCUGAC	*DPYD*	TargetScan Human	Moderate (predicted)
miR-151a-5p	CGAGGAG	*GSTM1*	TargetScan Human	Moderate (predicted)
miR-1247-5p	CCCGUCC	*HNF4A*	TargetScan Human	Moderate (predicted)
miR-143-3p	GAGAUGA	*HNF4A*	TargetScan Human	Moderate (predicted)
miR-216b-5p	AAUCUCU	*HNF4A*	TargetScan Human	Moderate (predicted)
miR-34a-5p	GGCAGUG	*HNF4A*	TargetScan Human	Experimentally Observed
miR-483-5p	AGACGGG	*HNF4A*	TargetScan Human	Moderate (predicted)
miR-532-3p	CUCCCAC	*HNF4A*	TargetScan Human	Moderate (predicted)
miR-625-5p	GGGGGAA	*HNF4A*	TargetScan Human	Moderate (predicted)
miR-668-3p	GUCACUC	*HNF4A*	TargetScan Human	Moderate (predicted)
miR-151a-5p	CGAGGAG	*NAT1*	TargetScan Human	Moderate (predicted)
miR-29b-3p	AGCACCA	*NAT1*	TargetScan Human	High (predicted)

Table 6 cont'd

miRNA	Seed Sequence	mRNA	Source	Confidence
miR-320b	AAAGCUG	*NAT1*	TargetScan Human	Moderate (predicted)
miR-628-5p	UGCUGAC	*NAT2*	TargetScan Human	Moderate (predicted)
miR-142-5p	AUAAAGU	*NR1I2*	TargetScan Human	Moderate (predicted)
miR-148b-3p	CAGUGCA	*NR1I2*	miRecords	Experimentally Observed
miR-18a-5p	AAGGUGC	*NR1I2*	TargetScan Human	High (predicted)
miR-219a-5p	GAUUGUC	*NR1I2*	TargetScan Human	Moderate (predicted)
miR-34a-5p	GGCAGUG	*NR1I2*	TargetScan Human	Moderate (predicted)
miR-576-3p	AGAUGUG	*NR1I2*	TargetScan Human	Moderate (predicted)
miR-132-3p	AACAGUC	*SLC15A2*	TargetScan Human	Moderate (predicted)
miR-184	GGACGGA	*SLC15A2*	TargetScan Human	Moderate (predicted)
miR-206	GGAAUGU	*SLC15A2*	TargetScan Human	High (predicted)
miR-23b-3p	UCACAUU	*SLC15A2*	TargetScan Human	High (predicted)
miR-376a-3p	UCAUAGA	*SLC15A2*	TargetScan Human	High (predicted)
miR-519a-3p	AAGUGCA	*SLC15A2*	TargetScan Human	Moderate (predicted)
miR-576-3p	AGAUGUG	*SLC15A2*	TargetScan Human	Moderate (predicted)
miR-1275	UGGGGGA	*SLC22A1*	TargetScan Human	Moderate (predicted)
miR-150-5p	CUCCCAA	*SLC22A2*	TargetScan Human	Moderate (predicted)
miR-155-5p	UAAUGCU	*SLC22A2*	TargetScan Human	Moderate (predicted)
miR-181a-5p	ACAUUCA	*SLC22A2*	TargetScan Human	Moderate (predicted)
miR-382-5p	AAGUUGU	*SLC22A2*	TargetScan Human	Moderate (predicted)
miR-431-5p	GUCUUGC	*SLC22A2*	TargetScan Human	Moderate (predicted)
miR-452-5p	ACUGUUU	*SLC22A2*	TargetScan Human	Moderate (predicted)
miR-211-5p	UCCCUUU	*SLC22A6*	TargetScan Human	High (predicted)
miR-331-3p	CCCCUGG	*SLC22A6*	TargetScan Human	Moderate (predicted)

miRNA	Seed Sequence	mRNA	Source	Confidence
miR-654-5p	GGUGGGC	*SLC22A6*	TargetScan Human	Moderate (predicted)
miR-139-5p	CUACAGU	*SLCO1B1*	TargetScan Human	Moderate (predicted)
miR-194-5p	GUAACAG	*SLCO1B1*	TargetScan Human	Moderate (predicted)
miR-206	GGAAUGU	*SLCO1B1*	TargetScan Human	High (predicted)
miR-511-5p	UGUCUUU	*SLCO1B1*	TargetScan Human	Moderate (predicted)
miR-576-3p	AGAUGUG	*SLCO1B1*	TargetScan Human	Moderate (predicted)
miR-526b-5p	UCUUGAG	*SULT1A1*	TargetScan Human	Moderate (predicted)
miR-10a-5p	ACCCUGU	*TPMT*	TargetScan Human	Moderate (predicted)
miR-185-5p	GGAGAGA	*TPMT*	TargetScan Human	Moderate (predicted)
miR-206	GGAAUGU	*TPMT*	TargetScan Human	Moderate (predicted)
miR-28-5p	AGGAGCU	*TPMT*	TargetScan Human	Moderate (predicted)
miR-526b-5p	UCUUGAG	*TPMT*	TargetScan Human	Moderate (predicted)
miR-885-5p	CCAUUAC	*TPMT*	TargetScan Human	High (predicted)
miR-9-5p	CUUUGGU	*TPMT*	TargetScan Human	Moderate (predicted)
miR-141-3p	AACACUG	*UGT1A1*	TargetScan Human	Moderate (predicted)
miR-148b-3p	CAGUGCA	*UGT1A1*	TargetScan Human	Moderate (predicted)
miR-376a-3p	UCAUAGA	*UGT1A1*	TargetScan Human	Moderate (predicted)
miR-125b-5p	CCCUGAG	*UGT2B15*	miRecords	Experimentally Observed
miR-376c-3p	ACAUAGA	*UGT2B15*	TargetScan Human	Moderate (predicted)
miR-382-5p	AAGUUGU	*UGT2B15*	TargetScan Human	Moderate (predicted)
miR-125b-5p	CCCUGAG	*UGT2B17*	miRecords	Experimentally Observed
miR-376c-3p	ACAUAGA	*UGT2B17*	TargetScan Human	Moderate (predicted)
miR-382-5p	AAGUUGU	*UGT2B17*	TargetScan Human	Moderate (predicted)
miR-409-3p	AAUGUUG	*UGT2B17*	TargetScan Human	Moderate (predicted)
miR-494-3p	GAAACAU	*UGT2B17*	TargetScan Human	Moderate (predicted)

Discussion

The expression of pharmacogenes are known to be altered throughout development, especially during the early and late developmental stages in humans. For example, *CYP3A7* is the predominant *CYP* gene expressed in the fetal liver, but its expression becomes undetectable in most children (Lacroix et al., 1997). Data also shows that expression of select *UGTs* and transporters increases in older children and adults compared to neonates and younger children (Miller et al., 1976; Mooij et al., 2014). However, the mechanisms that control these changes are not well understood. Recently, there is emerging evidence that hepatic miRNA expression changes with age in humans and rodents (Mimura et al., 2014; Rieger et al., 2013). Data from our study are in alignment with the emerging evidence that changes in hepatic miRNA expression may contribute to the known developmental changes in these drug disposition genes (Burgess et al., 2015). Since these findings, miRNAs have been shown to play a role in skeletal muscle development and developmental changes in the small intestines, hypothalamus, ear, and heart (Bianchi et al., 2017; Doubi-Kadmiri et al., 2016; Liang et al., 2016; Torres et al., 2015; Zhang et al., 2015).

Our data indicate that miRNA expression in the human liver is age-dependent; this is consistent with observations of developmental changes of hepatic miRNA expression patterns in rats (Mimura et al., 2014). Specifically, miRNAs 29c-3p, 195-5p, and 497-5p were significantly upregulated and 301a-3p, 106b-5p, 185-5p, and 539-5p downregulated between the human fetal and pediatric livers which is in agreement with miRNAs that changed with age in rat liver tissue; exceptions were miRNAs 148b-3p and let-7a-5p, which revealed opposite findings. Other miRNAs Mimura et al. found to change in aging rat liver were consistent with our data, but not significant after FDR-corrected.

The extent of mRNA induction or repression between developmental stages varied greatly, particularly between fetal and pediatric. Since drug metabolism and disposition is enzyme and transporter specific, these differences most certainly contribute to the variability in the developmental changes in drug metabolism and disposition. Furthermore, interindividual variability in the rate of change in the expression of these genes also likely contributes to the interindividual variability in drug efficacy and toxicity. There was substantial variability in the expression of many of the miRNAs during each of the developmental periods. This may be a result of the interindividual variability in the timing of the developmental changes. These developmental changes in miRNA expression are most likely not due to a discrete incremental change amongst individuals but more of a continual change over time; one that likely occurs in every individual, but at various rates and to variable extents. This may contribute to the variable rates of changes in hepatic drug disposition.

A limitation to our study is that we do not have serial samples within individuals or broad coverage of time points during the various developmental stages. Hence, the exact timing of some of the changes cannot be determined from our data. Since liver biopsies within individuals would not be ethical, such a study is not feasible in human subjects. However, more liver samples less than one year of age, post-puberty, and adult livers to compare against the geriatric age groups, in addition to knowledge of menopausal status will be useful in determining if altered miRNA expression is more heavily influenced by these developmental events. Especially in children less than one year of age, as many known changes in drug metabolism enzymes have been observed in this age range from older children. Also, due to limited sample materials, we were not able to measure protein expression by Western blot analysis or activity of the drug disposition genes. Since miRNAs can affect protein translation without substantial effects on mRNA levels, our

miRNA-mRNA correlations may miss some gene-specific effects and will need to be tested in individual experiments.

Our data support that these changes in hepatic miRNA expression throughout the developmental periods are important in regulating the mRNA expression of phase I and II enzymes, drug transporters, and regulatory genes. Six of these developmentally-regulated miRNAs have previously been experimentally validated to target *ABCG2, CYP1A1, HNF4A, NR1I2, UGT2B15* and *UGT2B17* (Ramamoorthy et al., 2012; Shi et al., 2007; Takagi et al., 2008; To et al., 2008). Twenty-seven miRNAs, undetectable during fetal development, were expressed in the pediatric and adults samples. Additionally, 43 miRNAs expressed during the fetal period were not expressed in pediatric and adult livers. The changes in hepatic miRNA expression from pediatric to adult periods may also contribute to changes in hepatic pharmacogene expression as several of these miRNA changes were correlated with changes in hepatic mRNA expression.

Previously, hepatic expression of miR-34a-5p, miR-200a-3p, and miR-200b-3p was associated with age in a Caucasian, mostly adult, population from Europe (Rieger et al., 2013). In our data, miR-34a-5p was upregulated 1.7- and 2.1-fold from fetal to pediatric to adult and miR-200a-3p increased 2.7-fold from fetal to pediatric (Table 2 and 3). However, correlations of miRNAs and mRNAs between the two cohorts varied. For example, in both studies miR-28-3p negatively correlated with *CYP2C9* mRNA, whereas miR-148b-3p was negatively correlated with *CYP2C9* mRNA in our study (Table 5), but was described to be positively correlated with *CYP2C9* by Rieger et al (Rieger et al., 2013). This could be due to a number of reasons as liver sample demographics varied between the studies as one population is based in Europe and the other, the United States. It has been shown that

environmental factors such as diet, smoking and drinking can alter miRNA expression in tissues (Rieger et al., 2013; Wilson et al., 2017).

In conclusion, our data clearly demonstrates that there are major changes in hepatic miRNA expression between the developmental periods. These changes are most marked between fetal and pediatric ages; however, there were also notable changes between the pediatric and adult periods. Several of these miRNAs have either been validated to target pharmacogenes, as shown in Table 6, or are predicted to target these genes. These data strongly suggest that hepatic miRNA expression contributes to the clinical variability in hepatic drug disposition. The marked change in miRNA expression between the fetal and pediatric/adult groups may contribute to the high susceptibility of fetuses to adverse drug events. These developmental changes in miRNA expression may also contribute to changes in hepatic functions other than drug metabolism, such as cholesterol metabolism. Collectively, this information suggests that age-dependent miRNAs significantly impact a variety of human liver functions. Additional studies are warranted to: validate the hepatic miRNA-mRNA interactions; and determine indirect effects of miRNAs on pharmacogenes as well as the effects of SNPs on creating or abolishing miRNA target sites that control these genes.

CHAPTER 2

Developmentally-regulated microRNA regulation of pharmacogenes

Introduction

Our studies in the previous chapter demonstrated that the hepatic expression of many miRNAs change during development. Several of these are predicted to regulate drug disposition genes. This discovery may explain part of the known developmental changes that occur in drug disposition. To follow up on these studies, we have begun validating the predicted miRNA-mRNA interactions. These validation experiments are important in determining exactly how these developmentally-regulated miRNAs contribute to changes in drug disposition gene expression by allowing us to understand which gene/genes a miRNA is targeting. With this knowledge, we will be able to predict the effects of miRNA expression changes that can occur from various diseases and environmental exposures (Gupta et al., 2014; Ramamoorthy et al., 2013; Tao et al., 2013).

In this study, we focused on the miRNA regulation of *CYP2B6* and *CYP1A2*. We used several cell culture models, such as the transfection of predicted miRNAs and measuring gene expression and activity. These data suggest that developmentally-regulated miRNAs have the ability to alter gene expression of drug disposition genes.

Materials and Methods

Cell culture maintenance

HeLa, HepG2, and HEK293 cells supplied from ATCC (Manassas, VA) were thawed from liquid nitrogen storage. Cells were maintained according to manufacturer's protocol using DMEM with 4.5 g/L glucose, L-glutamine & sodium pyruvate from Corning cellgro (Manassas, VA) supplemented with 10% fetal bovine serum from Atlanta Biologicals (Flowery Branch, GA). Approximately one million cells were used for freezing cell lines

and stored in liquid nitrogen using Recovery Cell Culture Freezing Medium from Gibco (Grand Island, NY). Cryopreserved HepaRG cells were supplied by BioPredic International (Gibco, USA). Cells were maintained according to manufacturer's protocol using Williams' E Medium (Gibco, Grand Island, NY), supplemented with 10% fetal bovine serum (Atlanta Biologicals, Flowery Branch, GA), GlutaMax Supplement, HepaRG Maintenance/Metabolism Medium Supplement or HepaRG Thaw, Plate & General Purpose Medium Supplement (Gibco, Frederick, MD), ITS (Corning cellgro, Manassas, VA), Penicillin-Streptomycin Solution (GE Healthcare Life Sciences, Logan, UT). All cell lines were tested for mycoplasma contamination using Mycoplasma Detection Kit through Biotool (Houston, TX). Cells were rinsed using 1x phosphate buffered saline (Corning cellgro, Manassas, VA) and trypsinized using 1x TrypLE Express from Gibco (Grand Island, NY). Cells were stored at 37°C, 5% CO_2 in Thermo Forma Series II Water-Jacketed CO_2 Incubator.

E. coli transformations

TALE-TF, pIS-0 (Addgene, Cambridge, MA) (Yekta et al 2004), and *Renilla* luciferase reporter pGL4.74 (Promega, Madison, WI) plasmids were all transformed in One Shot OmniMax 2 TI Chemically Competent *E. coli* (Invitrogen, Carlsbald, CA). Briefly, *E.coli* was thawed on ice. Plasmids were diluted to 1 ng/µL and 1 µL was added to *E. coli*, incubated on ice for 30 minutes, heat-shocked for 30 seconds at 42°C, and placed on ice for 2 minutes. Next, 250 µL of SOC medium was added to each vial and shaken for 1 hour at 225 rpm at 37°C. Transformation mix was diluted 1:50 into LB Medium Miller (Alfa Aesar, Ward Hill, MA) or LB Broth (Amresco, Solon, OH) and 20 µL spread on ampicillin-resistant agar plates. Ampicillin (100 mg/mL) was purchased from Sigma Aldrich (St. Louis, MO). Plated bacteria were incubated overnight at 37°C. TALE-TF plasmids were purified using Qiagen HiSpeed Plasmid Maxi Kit (Valencia, CA). Single colonies were

selected and cultured in 4 mLs of ampicillin-resistant LB media overnight. *Renilla* luciferase and pIS-0 firefly luciferase plasmids were isolated using the NucleoSpin Plasmid (NoLid) DNA purification kit (Macherey-Nagel, Düren, Germany). DNA was quantified using Qubit dsDNA BR Assay Kit (Invitrogen, Eugene, OR). Plasmids stored at -20°C.

Transfections

HeLa (cervical cancer), HepG2 (liver carcinoma), and HEK293 (embryonic kidney) cells were seeded at 90,000 cells/well in a 24 well plate. Cells were transfected 24-48 hours after seeding, depending on when cells reach ~80% confluency. HepaRG (liver carcinoma) cells are plated at 400,000 cells/well in 24 well plates. Media was changed every two days and cells were transfected Day 6 after seeding. All cells were transfected using Lipofectamine 2000 or Lipofectamine 3000 Transfection Kits (Invitrogen, Carlsbad, CA) using OPTI-MEM I 1x (Gibco, Grand Island, NY).

TALE-TFs used to validated miRNA targeting of CYPs

Four TALE-TFs were synthesized per target, *CYP2B6* and *CYP1A2* (GeneCopoeia, Rockville, MD).

CYP2B6 TALE-TF target sites:

1) TAATGCTTCCTGGATGATGA, 2) TGGATGAAATTTTATAACAG

3) TGGAGGCTGCAGCAGGGTGC, 4) TCTTCCTTGCACTCCTCACA.

CYP1A2 TALE-TF target sites:

1) TCCACACCAGCCATTACA, 2) TGGCCCAAGGCCAAGAGT

3) TCAGGAGTGGCTGGAACA, 4) TCTCTTTAGGATGCAAAA.

Both 500 ng of individual TALE-TFs transfected per well for TALE-TF and 500 ng of total TALE-TFs transfected per well (125 ng of four TALE-TFs) were used for validation experiments. The combination of four TALE-TFs was used for all other experiments and cotransfected with 18 pmoles per well of Miridian microRNA mimics, Hairpin inhibitors or Negative Control #1 (GE Dharmacon, Chicago, IL). Negative Control #1 is cel-miR-67 which has been shown to be functional in *C. elegans* but predicted not to target any human genes. MicroRNA mimics and inhibitors were diluted to 20 μM working solutions, aliquoted to minimize freeze thaws, and stored at -80°C. Three technical replicates were done per biological replicate.

Transfection in HepaRG cells

Three different experiments were performed in HepaRG cells. First, 18 pmoles for each of seven miRNAs predicted to target *CYP2B6* were transfected. Second, 18 pmoles for each of four different miRNAs predicted to target CYP1A2 were transfected. Third, for the developmental miRNA transfection experiment discussed in future directions, 18 pmoles for 18 different developmentally-regulated miRNAs were transfected per well in 24 well plates (Table 7). Lipofectamine 3000 reagent was scaled up according to the manufacturers protocol (Seven miRNAs: 3.4 μL, Four miRNAs: 1.9 μL, Eighteen miRNAs: 8.6 μL). Three technical replicates were done in each of three biological replicates.

Table 7: List of miRNA mimics and inhibitors used

Catalog No.	Gene Symbol	Type	Gene Targeted*
C-301407-00	hsa-miR-1275	Mimic	*CYP2B6/SLC22A1*
C-300608-03	hsa-miR-141-3p	Mimic	*UGT1A1*
C-300611-05	hsa-miR-143-3p	Mimic	*CYP1A2/2C9/HNF4A*
C-300634-03	hsa-miR-154-3p	Mimic	*ABCG2*
C-300644-03	hsa-miR-206	Mimic	*SLC15A2/SLCO1B1/TPMT*
C-300578-05	hsa-miR-221-3p	Mimic	*
C-300504-07	hsa-miR-29a-3p	Mimic	*CYP2B6*
C-300520-05	hsa-miR-29b-3p	Mimic	*CYP2B6*
C-300657-03	hsa-miR-301a-3p	Mimic	*
C-301308-00	hsa-miR-320b	Mimic	*CYP1A2/NAT*
C-300704-03	hsa-miR-324-5p	Mimic	*
C-300708-05	hsa-miR-335-5p	Mimic	*
C-301185-01	hsa-miR-339-3p	Mimic	*
C-300675-03	hsa-miR-369-3p	Mimic	*CYP2C9*
C-300857-01	hsa-miR-376a-3p	Mimic	*DPYD/SLC15A2/UGT1A1*
C-300674-05	hsa-miR-376c-3p	Mimic	*UGT2B15/17*
C-300691-03	hsa-miR-382-5p	Mimic	*SLC22A2*
C-300729-03	hsa-miR-431-5p	Mimic	*CYP1A2/SLC22A2*
C-300742-05	hsa-miR-483-3p	Mimic	*CYP2B6*
C-300769-03	hsa-miR-512-3p	Mimic	*ABCG2*
C-300835-05	hsa-miR-519a-3p	Mimic	*ABCG2/DPYD/SLC15A2*
C-300951-03	hsa-miR-625-5p	Mimic	*CYP2B6/HNF4A*
C-301001-01	hsa-miR-668-3p	Mimic	*CYP1A2/HNF4A*
C-301242-01	hsa-miR-744-5p	Mimic	*CYP2B6*
C-301268-01	hsa-miR-939-5p	Mimic	*CYP2B6*
IH-301407-01	hsa-miR-1275	Inhibitor	*CYP2B6/SLC22A1*
IH-300611-06	hsa-miR-143-3p	Inhibitor	*CYP1A2/2C9/HNF4A*
IH-300504-08	hsa-miR-29a-3p	Inhibitor	*CYP2B6*
IH-300521-07	hsa-miR-29b-3p	Inhibitor	*CYP2B6*
IH-301308-01	hsa-miR-320b	Inhibitor	*CYP1A2/NAT*
IH-300729-05	hsa-miR-431-5p	Inhibitor	*CYP1A2/SLC22A2*
IH-300742-06	hsa-miR-483-3p	Inhibitor	*CYP2B6*
IH-300951-04	hsa-miR-625-5p	Inhibitor	*CYP2B6/HNF4A*
IH-301001-03	hsa-miR-668-3p	Inhibitor	*CYP1A2/HNF4A*
IH-301242-02	hsa-miR-744-5p	Inhibitor	*CYP2B6*
IH-301268-02	hsa-miR-939-5p	Inhibitor	*CYP2B6*
CN-001000-01	cel-miR-67	Control	None

***** These miRNAs were negatively correlated with increased gene expression from liver expression studies but were not predicted to target these specific genes. They were included in the experiment where 18 miRNAs were transfected in adult HepaRG cells.

RNA isolation and storage

RNA was isolated 48 hours after transfection with plasmids, miRNAs, or plasmid-miRNA combinations using Qiagen RNeasy Mini Kit or Qiagen miRNeasy Mini Kit. An on-column DNase digest was performed using Qiagen RNase-Free DNAse Set (Valencia, CA). RNA concentrations were measured using Invitrogen Qubit RNA BR Assay on the Qubit fluorometer (Invitrogen, Eugene, OR).

cDNA and quantitative PCR

cDNA was made using Qiagen QuantiTect Reverse Transcription Kit (Valencia, CA). Within each experiment, the RNA input was consistent among samples within each experiment. Reverse transcription reactions run according to manufacturer's protocol using the Applied Biosystems GeneAmp PCR System 9700. TaqMan Gene Expression Assays for *CYP2B6* (Hs04183483_g1, FAM-labelled), *CYP1A2* (Hs00167927_m1, FAM-labelled), and *GAPDH* (Hs02786624_g1, VIC-labelled) and TaqMan Universal Master Mix II, with UNG (Applied Biosystems, Foster City, CA) were used to measure gene expression according to the manufacturer's protocol in 20 µL reaction on the BioRad Thermal Cycler and Applied Biosystems QuantStudio 12K Flex.

Statistical analysis for quantitative PCR

The Delta Delta C_T (ddC_T) method was used to calculate changes in *CYP2B6* and *CYP1A2* mRNA expression when validating TALE-TF activity and miRNA ability to alter mRNA expression in HeLa, HepG2, and HepaRG cells. Delta Delta C_T= experimental (average C_T of *CYP* – average C_T of *GAPDH*) – control (average C_T of *CYP* – average C_T of

GAPDH). Fold changes are calculated 2^ddC_T and log_2 transformed. Paired t-tests were used to assess the changes in mRNA expression using the dC_T values. All analyses performed using Graphpad Prism 6 (La Jolla, CA), with *p*-values <0.05 considered statistically significant.

Measurement of mRNA expression in HepaRG cells

Library preparation and sequencing

The concentration and quality of total RNA samples was first assessed using Agilent 2100 Bioanalyzer. A RIN (RNA Integrity Number) of five or higher was required to pass the quality control. Then five hundred nanograms of RNA per sample were used to prepared single-indexed strand-specific cDNA library using TruSeq Stranded mRNA Library Prep Kit (Illumina). The resulting libraries were assessed for its quantity and size distribution using Qubit and Agilent 2100 Bioanalyzer. One and a half picomolar pooled libraries were sequenced with 2×75 bp paired-end configuration on NextSeq500 (Illumina) using NextSeq 500/550 High Output Kit. A Phred quality score (Q score) was used to measure the quality of sequencing. More than 90% of the sequencing reads reached Q30 (99.9% base call accuracy).

Sequence alignment and gene counts

The sequencing data were first assessed using FastQC (v.0.11.5, Babraham Bioinformatics, Cambridge, UK) for quality control. Then all sequenced libraries were mapped to the human genome (UCSC hg19) using STAR RNA-seq aligner (v.2.5) (Dobin et al., 2013) with the following parameter: "--outSAMmapqUnique 60". The reads distribution across the genome was assessed using bamutils (from ngsutils v.0.5.9) (Breese and Liu, 2013). Uniquely mapped sequencing reads were assigned to hg19 refGene genes using featureCounts (subread v.1.5.1) (Liao et al., 2014) with the following

parameters: “-s 2 –p –Q 10”. Genes with read count per million (CPM) < 0.5 in more than 3 of the samples were removed. The data was normalized using TMM (trimmed mean of M values) method. Differential expression analysis was performed using edgeR (v.3.12.1) (McCarthy et al., 2012; Robinson et al., 2010). False discovery rate (FDR) was computed from *p*-values using the Benjamini-Hochberg procedure.

In vitro drug probe assay and LC/MS/MS methods

Reagents

Bupropion, phenacetin, nevirapine, efavirenz and 8-hydroxyefavirenz were obtained from Toronto Research Chemicals Inc. (North York, ON, Canada). All other chemicals were high-performance liquid chromatography grade.

Drug probe assay

To measure CYP2B6 and CYP1A2 activity in HepaRG cells, a final concentration of 100 µM bupropion (CYP2B6) or 200 µM phenacetin (CYP1A2) in 500 µLs was added Day 8, two days after transfection with synthetic miRNAs. Drug probe was incubated on cells for one hour. Media was removed and stored in -80°C until extraction for quantification of parent and metabolites.

Bupropion extraction

A liquid-liquid extraction was performed according to (Ward et al., 2003) by using 500 µL of media obtained from HepaRG cell drug probe assay and 25 µL of nevirapine internal standard (500 ng/µL). Then, 500 µL of Gly/NaOH pH 11.13 solution was added and vortexed. Six milliliters of ethyl acetate was added, vortexed, and shaken for 5 minutes. Samples were centrifuged at 3,600 rpm for 10 minutes and 4°C on an Allegra 6R Benchtop centrifuge (Beckman Coulter, Brea, CA) to remove the organic layer. Supernatants were

dried and reconstituted in 100 µL MeOH 0.1% formic acid 1:1 (mobile phase) for mass spectrometry analysis.

LC-MS/MS quantification

The liquid chromatography/tandem mass spectrometry (LC/MS/MS) method for detection and quantification of EFV and 8-hydroxy efavirenz was developed to obtain the best selectivity and sensitivity (Ward et al., 2003). Some alterations were made to adapt to bupropion and hydroxyl-bupropion detection and quantification (Ogburn et al., 2010). The analysis was performed on an API 3200 triple-quadrupole mass spectrometry (Applied Biosystem/MDS Sciex, Foster City, CA) equipped with a turbo ion spray source. The HPLC system consists of two LC-20AD pumps, a SIL-20AHT UFLC autosampler, a DGU-20A3 degasser and a CBM-20A controller (Shimadzu, Columbia, MD), all controlled by Analyst 1.5.1 software (Applied Biosystem/MDS Sciex, Foster City, CA) in conjunction with Windows XP (Microsoft, Redmond, WA). The chromatographic separation of EFV and 8-hydroxy efaviranz was performed on a Phenomenex (Torance, CA) Luna C_{18} column (150 × 4.6 mm, 5 µm particle size). The injection volume was 10 µL. Before and after each injection, the needle was washed with ACN/H_2O (75/25, v/v). Mobile phase (0.8 ml/min) was (A) methanol: formic acid (0.1% in water) (1/99, v/v) and (B) methanol: formic acid (0.1% in water) (99/1, v/v) using the following gradient: starting from 25% B, linear gradient to 90% B between 0.01 and 16 min, then re-equilibrated to initial conditions between 16.01 min and 20.00 min; the separation of bupropion and 8-hydroxy bupropion was almost the same as EFV except the gradient from 90% A to 90% B within 10 min, then re-equilibrated until 14 min.

Statistical analysis for drug concentrations

Metabolite parent ratios were calculated using the following formula: [(Metabolite Analyte Peak/IS Peak Area Counts) ÷ (Parent Analyte Peak/IS Peak Area Counts)]. Values were $\log_{10}$ transformed. Technical triplicates were done for three or four biological replicates. Technical triplicates were averaged and paired t-tests were performed between the combined miRNA-treated and control-treated HepaRG cells. All analyses performed using Graphpad Prism 6 (La Jolla, CA), with *p*-values <0.05 considered statistically significant.

Results

TALE-TFs induce expression of CYPs

Among the miRNAs that were developmentally-regulated, we wanted to begin validating the miRNA-mRNA predictions observed in Chapter 1. Since expression of *CYP2B6* and *CYP1A2* was not expressed at quantifiable levels in HeLa or HepG2 cells, we utilized transcription activator-like effector-transcription factors (TALE-TFs), to induce gene expression in these cell culture models. We did not use primary human hepatocytes, as they originate from a pool of donors and may increase variability in miRNA targeting due to genetic variation effects. Primary human hepatocytes are also expensive, difficult to transfect, and have unknown histories (e.g. medication use, disease). TALE-TF proteins can be designed to induce the expression of any gene through a repeat variable di-amino acid code targeting sequences near the promoter region of the gene of interest. The protein coils around the targeted DNA sequence. Transcription activation is facilitated by the attached viral protein 64 (VP64) transcription factor as depicted in Figure 7.

Four TALE-TFs were designed to target *CYP2B6*. These TALE-TFs each target a 20 bp sequence within or near the promoter region of *CYP2B6* to facilitate the recruitment of transcription factors to increase transcription. When TALE-TFs (T1, T2) were transfected

into HeLa cells individually, *CYP2B6* expression was increased 18- and 7-fold, respectively. TALE-TFs 3 and 4 had no effect of *CYP2B6* expression; however, when all four were transfected simultaneously, *CYP2B6* expression increased 121-fold (Figure 8). In HepG2 cells, *CYP2B6* expression was increased 50-, 33-,15-, 14-fold for the four individual TALE-TFs and 70-fold when combined.

Four TALE-TFs were also designed to target *CYP1A2*. The combination of all four TALE-TFs increased expression 164- and 189-fold in HeLa and HepG2 cells respectively (Figure 8). They were not tested individually since all four usually work better than individual transfections, which was consistent with our results for *CYP2B6* induction.

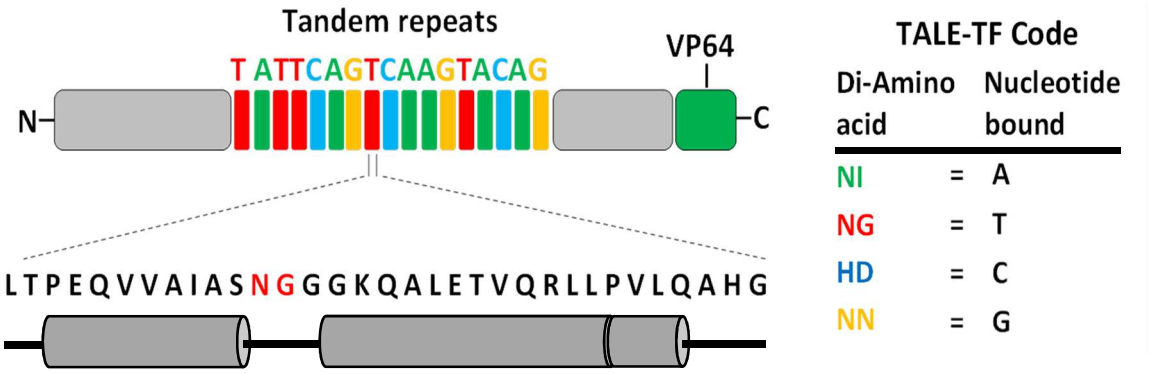

Figure 7: TALE-TF protein structure and code

TALE-TFs can induce the expression of target genes by binding to regions near the promoter through a central tandem repeating domain consisting of ~34 amino acid repeats. The residues at the 12th and 13th position of each repeat creates a code that determines which base pair it will bind.

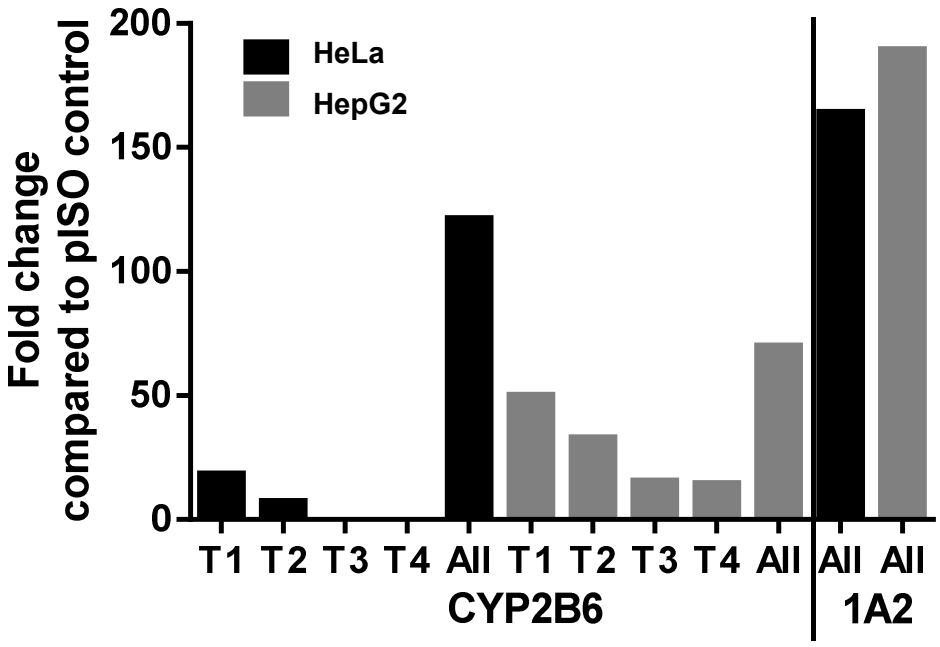

Figure 8: Induction of *CYP* expression using TALE-TFs

TALE-TFs were used to induce expression of *CYP2B6* and *CYP1A2*. *X*-axis: Individual TALE-TFs (T1-4) and all four TALE-TFs (All) in either HeLa cells (black bars) or HepG2 cells (gray bars). *Y*-axis: Fold-change compared to control pIS-0 plasmid. The control plasmid is a luciferase plasmid that does not affect *CYP* expression.

miRNA regulation of CYP2B6

After induction of *CYP2B6* gene expression in HeLa cells, miRNAs predicted to target *CYP2B6* mRNA and their inhibitors were used to validate predictions. MicroRNAs that target *CYP2B6* through degradation of mRNA should result in decreased *CYP2B6* mRNA. Inhibitors function through perfect complimentary binding to sequester its target miRNA and prevent it from having an effect. MicroRNAs 744-5p and 1275 significantly downregulated *CYP2B6* mRNA 3.6-fold (p<0.001) and 2.6-fold (p<0.05). In all other miRNAs, the decrease in *CYP2B6* mRNA was not significant. Inhibitors for endogenous miR-29b-3p and miR-744-5p significantly increased *CYP2B6* mRNA expression 2.4- and 2.3-fold respectively (p<0.05) (Figure 9).

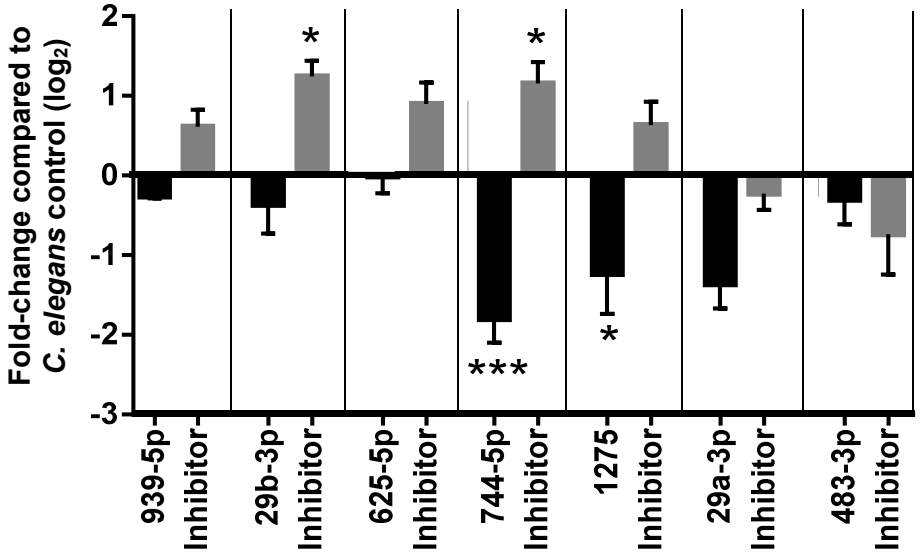

Figure 9: miRNA regulation of *CYP2B6* in HeLa cells

Predicted miRNAs or their inhibitors transfected in HeLa cells. *X*-axis: miRNA mimics (black bars) and inhibitors (gray bars). MicroRNAs 29a-3p and 483-3p experiments were performed earlier using Lipofectamine 2000 instead of Lipofectamine 3000. *Y*-axis: $\log_2$ fold-changes compared to *C. elegans* miRNA negative control. Errors bars are standard error of mean. (*=p<0.05, **=p<0.01, ***=p<0.001)

When comparing the combination of miRNA regulation, all seven miRNAs were transfected simultaneously in HeLa and HepG2 cells. In HeLa cells, there were no significant changes among the mimics, but the combined inhibitors significantly decreased *CYP2B6* expression 5.7-fold (p<0.05) (Figure 10). Similar results were observed in HepG2 cells with inhibitors decreasing *CYP2B6* expression 4.3-fold (p<0.01).

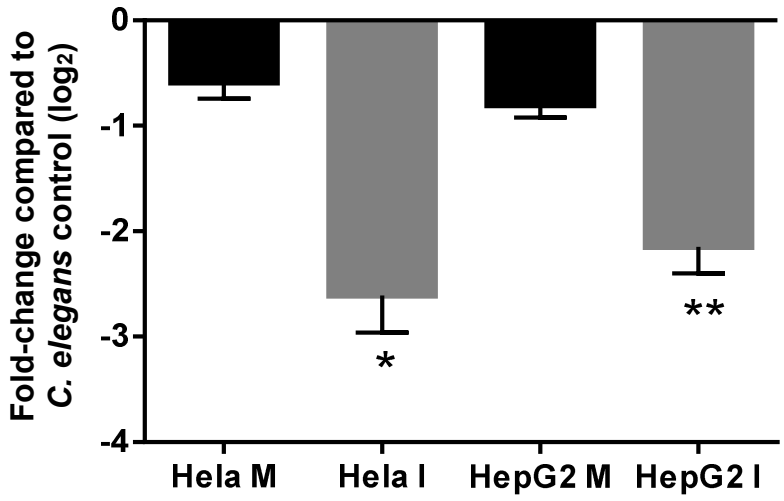

Figure 10: Regulation of *CYP2B6* mRNA in HeLa and HepG2 cells transfected with seven miRNAs predicted to target *CYP2B6* mRNA

Seven miRNA mimics and inhibitors transfected together in HeLa and HepG2 cells. *X*-axis: miRNA mimics (M: black bars) and inhibitors (I: gray bars). *Y*-axis: $\log_2$ fold-change compared to *C. elegans* miRNA negative control. Error bars are standard error of mean. (*=p<0.05, **=p<0.01)

miRNA regulation of CYP2B6 in HepaRG cells

Due to cell-type specific differences and inability to measure CYP2B6 enzyme activity in HeLa and HepG2 cells, even after TALE-TF induction, future experiments were conducted in HepaRG cells. HepaRG cells are a human hepatic cell line that exhibit characteristics of primary human hepatocytes, such as expression of *CYP* genes, nuclear receptors, and drug transporters.

When all seven miRNAs predicted to target *CYP2B6* were transfected in HepaRG cells, mRNA expression was significantly decreased 1.3-fold (p=0.0078). No changes were observed in CYP2B6 activity as measured by bupropion hydroxylation (Figure 11).

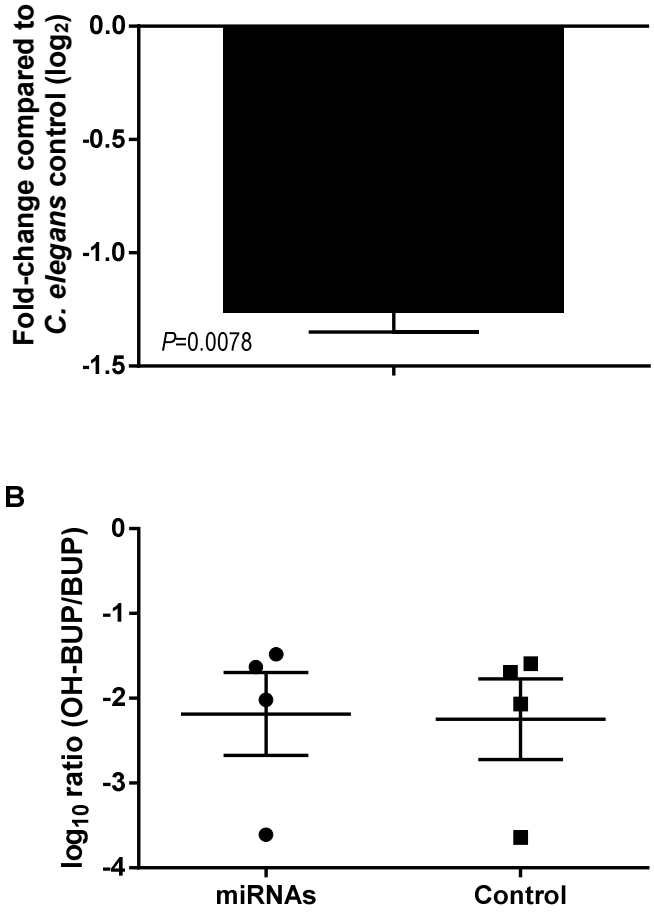

Figure 11: miRNA regulation of *CYP2B6* expression and activity in HepaRG cells

A. *CYP2B6* mRNA expression and **B.** activity measured by bupropion conversion to hydroxybupropion in HepaRG cells after miRNA regulation. Individual dots represent biological replicates paired with their control. Error bars are standard error of mean.

miRNA regulation of CYP1A2

After induction of *CYP1A2* gene expression in HeLa cells with the TALE-TFs, miRNAs predicted to target *CYP1A2* and their inhibitors were used to validate predictions. None of the miRNA mimics significantly reduced *CYP1A2* expression, but independently, three inhibitors significantly increased *CYP1A2* expression (431-5p: 2.6-fold, 143-3p: 2.1-fold, 320b: 2.4-fold (p<0.05)) (Figure 12).

When comparing the combination of miRNA regulation, all four miRNAs were transfected simultaneously in HeLa and HepG2 cells. In HeLa cells, there were no significant changes among the mimics and inhibitors (Figure 13), but both were in the overall direction as the individually transfected miRNAs as shown in Figure 12. However, in HepG2 cells, the inhibitors significantly downregulated *CYP1A2* mRNA expression (3.6-fold, $p<0.05$) suggesting that there are cell-type specific differences in miRNA regulation.

When tested in HepaRG cells, *CYP1A2* mRNA expression was not quantifiable by qPCR; however, because these cells were verified to have CYP1A2 activity, future experiments will focus on measuring the effect of the miRNAs on CYP1A2 activity as measured by the conversion of phenacetin to acetaminophen.

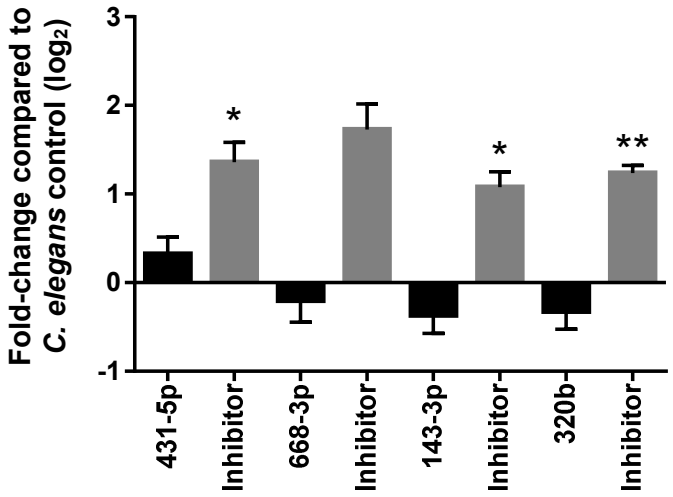

Figure 12: miRNA regulation of *CYP1A2* in HeLa cells

Predicted miRNAs or their inhibitors transfected in HeLa cells. *X*-axis: miRNA mimics (black bars) and inhibitors (gray bars). *Y*-axis: $\log_2$ fold changes compared to *C. elegans* miRNA negative control. Errors bars are standard error of mean. (*=p<0.05, **=p<0.01)

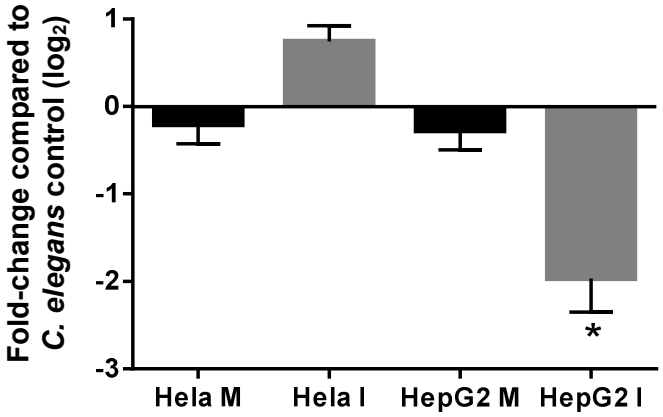

Figure 13: Combined miRNA regulation of *CYP1A2* in HeLa and HepG2 cells

Combined four miRNA mimics and inhibitors transfected in HeLa and HepG2 cells. *X*-axis: miRNA mimics (M: black bars) and inhibitors (I: gray bars). *Y*-axis: $\log_2$ fold change compared to C. elegans miRNA negative control. Error bars are standard error of mean. (*=p<0.05)

Discussion

Our studies identified developmentally-regulated miRNAs that are capable of regulating *CYP* gene expression. Validating miRNA-mRNA interactions provides additional support that the developmentally-regulated miRNAs observed in Chapter 1 likely have important roles in the ontogeny of the hepatic drug metabolism. These hepatic miRNAs can contribute to known developmental changes in pharmacogenes through the degradation of mRNA or through repression of translation, both mechanisms allowing for a reduction in activity.

MicroRNAs were transfected into HeLa or HepG2 cells and gene expression of the target mRNA was measured; however, because these cell lines do not express the *CYP* genes, TALE-TFs were used to induce endogenous gene expression. TALE-TF induction increased gene expression levels to more physiological levels versus levels observed with over expression plasmids. A combination of four TALE-TFs targeting the promoter region of *CYP2B6*, increased *CYP2B6* expression synergistically compared to individual TALE-TFs. This synergistic regulation of gene expression is expected of TALE-TFs as the increase in transcription activators allows for increased binding and stabilization for proteins involved in transcription (Carey et al., 1990; Perez-Pinera et al., 2013). As a result, when validating *CYP1A2*, four different TALE-TFs were also used to increase gene expression in HeLa and HepG2 cells.

Seven developmentally-regulated miRNAs were predicted to target *CYP2B6*. Gene expression was significantly decreased by two miRNAs, miR-1275 and miR-744-5p. When transfected with their inhibitors, *CYP2B6* gene expression increased with miR-744-5p and miR-29b-3p. This suggests that endogenous miR-744-5p and miR-29b-3p must be present in HeLa cells as inhibitors sequester endogenous miRNAs through perfect

complimentary binding. When the combination of seven miRNA inhibitors was transfected, an unexpected decrease in *CYP2B6* mRNA expression was observed in HeLa and HepG2 cells. It is known that a single miRNA can have multiple targets, so observed changes can be due to other factors such as the inhibitors sequestering miRNAs responsible for targeting upstream transcription factors and repressor elements. It is of note that measuring gene expression using qPCR is limited to detecting only mRNA degradation by miRNAs as opposed to their ability to repress translation. A combination of techniques is necessary to fully characterize miRNA ability to target a particular mRNA.

CYP2B6 has been validated to be targeted by miR-25-3p in HepaRG cells via reporter gene assays and electrophoretic mobility shift assays (Jin et al., 2016). The *Jin et al* group discovered the connection between *CYP2B6* mRNA and miR-25-3p expression through inverse correlations in human hepatocytes. This particular miRNA was found to decrease in expression between fetal and pediatric human liver tissues (1.6-fold decrease: Table 2); however, it was not predicted to target *CYP2B6* using our prediction methods or found to be negatively correlated in our data.

Next, we tested the combination of miRNAs in HepaRG cells, a cell line that expressed *CYP2B6* and that had been validated to have CYP2B6 activity (Rubin et al., 2015). HepaRG cells are emerging as a popular cell line for validating miRNA-mRNA interactions in comparison to primary human hepatocytes, due to their consistency between batches as HepaRG cells originate from a single human source (Jin et al., 2016; Yu et al., 2015; Zeng et al., 2017). Primary human hepatocytes are usually pooled from various donors, introducing variability into experiments such as genetic variant effects which can lead to variable drug metabolism. In our experiments, *CYP2B6* mRNA expression levels significantly decreased upon miRNA transfection compared to the control, but CYP2B6

activity levels were not changed. This could suggest that either the decrease in mRNA levels was not large enough to affect CYP2B6 activity or the transfection period was not long enough for protein levels to be affected. In primary human hepatocytes, the half-life for *CYP2B6* mRNA was approximately 38 hours and 68 hours for enzyme activity (Dixit et al., 2016).

CYP1A2 was predicted to be targeted by four developmentally-regulated miRNAs. These miRNAs did not downregulate *CYP1A2* gene expression in HeLa cells. However, individual inhibitors increased expression. This suggests that these miRNAs may be endogenously present in HeLa cells at levels high enough, that additional miRNAs did not have an additional effect. Furthermore, cell-type specific differences in miRNA regulation became apparent when *CYP1A2* mRNAs levels were significantly decreased in HepG2 cells but increased in HeLa cells when the combination of inhibitors was added. This prompted us to continue validations in HepaRG cells as this cell line was more representative of the human liver; however, *CYP1A2* mRNA levels could not be detected in HepaRG cells, although these cells have been shown to have CYP1A2 activity (Rubin et al., 2015). This could be due to variability in processing of HepaRG cells on the supplier or on our behalf. Future studies will address phenacetin-O-deethlaytion as a measure of CYP1A2 activity by incubating phenacetin in the cell culture media in conjunction with transfected miRNAs in addition to measuring mRNA and protein levels.

MicroRNA regulation is difficult to interpret without proof of miRNA binding, so novel techniques including Argonaute 2 high-throughput sequencing of RNA isolated by cross-linked immunoprecipitation (Ago2-HITS-CLIP), will prove as a valuable unbiased approach to determine miRNA-mRNA interactions (Bottini et al., 2017; Spengler et al., 2016). This tool captures the Argonaute protein bound to the miRNA and its target,

followed by sequencing to decipher direct binding of miRNAs and their targets. This is critical as miRNAs can have multiple targets and have been shown to bind to their targets via non-canonical pathways (Duursma et al., 2008; Orom et al., 2008). This is a limitation of using prediction algorithms and tools to predict miRNA-mRNA interactions as they focus on seed sequence binding within the 3'UTR of target genes.

Furthermore, as the post-transcriptional activity of miRNAs have been extensively studied, very little is known about how miRNAs themselves are regulated. Studies pertaining to miRNA stability will be critical for understanding differential expression and miRNA activity in different human cell lines and tissues. It is known that miRNAs show tissue-specific regulation, which infer that a regulatory network exists (Biemar et al., 2005). Such a network remains to be elucidated. Their expression levels may also be regulated by RNA-binding proteins and the various proteins that process miRNAs into mature miRNAs as shown previously in Figure 1. It is known that double-stranded RNA binding proteins bind their targets based on structure rather than sequence, so this may serve as a mechanism for why miRNAs are differentially expressed among cell types. Competition with other RNA binding proteins and the differential expression of these proteins can explain these differences in miRNA expression across cell types (Habig et al., 2007). As the regulation of miRNAs become well-studied, it will enable better understanding of miRNAs as regulators themselves.

Collectively, our data show that miRNAs have the potential to alter gene expression of drug disposition genes. To better address the effects of miRNA regulation, selection of appropriate cell lines are necessary as cell-type specific differences can make it difficult to extrapolate results. HepaRG cells are a useful tool for drug metabolism and miRNA studies as they have been characterized to express drug disposition genes and eliminate

the genetic variability that may arise from the pooled primary human hepatocytes. However, there is also a need for understanding the expression levels of miRNAs in the different cell lines and human tissues, as this information becomes useful for the interpretation of the synthetic miRNA and miRNA inhibitor experiments. However, to best understand miRNA regulation, better characterization of miRNAs themselves are warranted.

CHAPTER 3

Variants in the CYP2B6 3'UTR alter in vitro and in vivo CYP2B6 activity: potential role of microRNAs

Introduction

MicroRNAs have been shown to negatively regulate drug disposition gene expression. However, due to miRNA regulation via perfect complimentary binding in the 'seed' sequence region 7-8 nucleotides in length, genetic variants in this region have the potential to alter miRNA regulation. Pharmacogenetics, the study of genetic differences that can affect an individual's response to drugs, has primarily focused on genetic variations in the promoter and coding region of drug disposition genes; however, emerging evidence has shown that genetic variations in the 3'UTR may contribute to variability in drug response by altering miRNA regulation. For example, miR-34a-5p has been previously validated to target hepatic nuclear factor 4α (*HNF4A*), a master regulator of many drug disposition genes (Ramamoorthy et al., 2012; Wirsing et al., 2011). Furthermore, a SNP in the 3'UTR of *HNF4A* (rs11574744) abolished the miRNA target sites of both miR-34a-5p. This SNP prevented the ability of miR-34a-5p to downregulate *HNF4A* and appeared to be associated with altered CYP2D6 activity in a cohort previously phenotyped with the *CYP2D6* probe drug, dextromethorphan (Ramamoorthy et al., 2012). This SNP is also present only in African Americans, as we know that these genetic variants can occur at differing frequencies among populations.

We hypothesize that genetic variants in the 3'UTR of *CYP2B6* contribute to the variability in CYP2B6 activity among humans. In this study, we retrospectively sequenced the *CYP2B6* 3'UTR of healthy human volunteers with previously characterized efavirenz pharmacokinetics. Efavirenz has been shown to be a suitable probe drug substrate to measure CYP2B6 activity *in vitro* and *in vivo* (Administration, 2012). C_{max} and AUC_{0-48}

ratios (8-hydroxy-efavirenz/efavirenz) (8-OH-EFV/EFV) have been demonstrated to reflect CYP2B6 activity (Jiang et al., 2013; Xu et al., 2013). Functional variants in the *CYP2B6* 3'UTR observed *in vivo* were validated through *in vitro* models. Our findings suggest that genetic variants in the 3'UTR may explain additional variation in drug metabolism and disposition (Burgess et al., 2017).

Materials and Methods

CYP2B6 activity in healthy volunteers

Data from 200 healthy non-pregnant female (n=83) and male (n=117) volunteers (18-55 years old) administered a single efavirenz dose, a probe drug substrate of CYP2B6 activity, was obtained from the single dose phase of three previous studies, published and unpublished (Desta et al., 2016; Robarge et al., 2017). These studies were approved by the Indiana University School of Medicine Institutional Review Board, conducted at the Indiana University School of Medicine Clinical Research Center and registered at http://www.clinicaltrials.gov (trial identifiers NCT00668395, NCT01104376, and NCT02401256). After written informed consent, volunteers were thoroughly screened using medical history, physical examination, and laboratory tests such as electrocardiography, HIV test, urinalysis and blood tests. During this screen, venous blood was drawn for DNA isolation. Dietary restrictions and inclusion and exclusion criteria have been previously reported (Michaud et al., 2014; Michaud et al., 2012).

These open label studies were retrospectively used to evaluate the association of single dose efavirenz pharmacokinetics with the *CYP2B6* 3'UTR variants. Briefly, plasma samples were taken pre-dose and at 0.5, 1, 1.5, 2, 2.5, 3, 4, 6, 8, 10, 12, 16, 24, 48, 72 and 144 hours after single dose efavirenz administration. Participants from two studies (127 participants total) were administered 600 mg of efavirenz and 73 participants from

another study were administered 100 mg of efavirenz (Sustiva, Bristol-Myers Squibb). Plasma efavirenz and 8-hydroxy-efavirenz concentrations were measured using a validated LC-MS/MS protocol as previously described (Robarge et al., 2017). Non-compartmental analysis of data was performed using Phoenix® WinNonlin® (version 7.0, Pharsight Corp., Cary, NC) to determine C_{max} (maximal plasma concentration) and AUC_{0-48} (area under the plasma concentration time curve from zero to 48 hours). C_{max} was assessed directly from the concentration-time profile and AUC_{0-48} was determined using the trapezoidal rule with linear up/log down interpolation.

CYP2B6 activity in human liver microsomes (HLMs)

HLMs were prepared by differential centrifugation, as described by Lu and Levin (1972) (Lu and Levin, 1972). *In vitro* microsomal incubations were performed according to Pearce et al 2015 (Pearce et al., 2016). Briefly, HLMs (30 µg of microsomal protein), potassium phosphate buffer (50 mM, pH 7.4), $MgCl_2$ (3 mM), EDTA (1 mM), and bupropion (500 µM) were incubated at the final concentrations listed. Reactions were initiated by the addition of a NADPH-generating system, consisting of NADP (1 mM), glucose-6-phosphate (5 mM), and glucose-6-phosphate dehydrogenase (1 U/ml), incubated at 37°C in a Thermo Forma Benchtop Orbital Shaker (Marietta, OH) and terminated after 30 minutes by the addition of 50 µL of ice-cold acetonitrile. Incubations were performed in triplicate. Bupropion stock solutions were dissolved in methanol; however, the concentration of methanol present in the incubation mixtures did not exceed 0.25%. Hydroxyl-bupropion and bupropion were resolved by isocratic, reversed-phase high-performance liquid chromatography based on a modification of the method by Faucette et al. 2000 (Faucette et al., 2000) as described previously (Pearce et al., 2016).

Genotyping and sequencing in healthy volunteers

Genomic DNA extracted from whole blood was used for genotyping (coding region variants) and Sanger sequencing of the 3'UTR. *CYP2B6* genotyping was performed using TaqMan Genotyping Assays for rs3745274 (516G>T, Q172H) and rs28399499 (983T>C, I328T) (Life Technologies, Foster City, CA) according to the protocol provided. PCR was performed on BioRad iCycler and QuantStudio 12K Flex real-time PCR instruments. *CYP2B6* rs2279343 (785A>G, K262R) genotyping was performed by first amplifying exon 5 with primers 5'-CTCTCTCCCTGTGACCTGCTA-3' (forward) and 5'-CTCCCTCTGTCTTTCATTCTGTC-3' (reverse) (Integrated DNA Technologies, Coralville, IA) as described by Lang et al. (Lang et al., 2001), then using 1 µL exon 5 PCR amplification product as a template for a custom TaqMan Genotyping Assay as previously described (Michaud et al., 2014).

To sequence the 3'UTR region, this region was first amplified by adding the following reagents to each reaction: 1 µL of DNA (10 ng), 12 µL CloneAmp HiFi PCR Premix (CloneTech, Mountain View, CA), 10 µL ultrapure distilled water and 1 µL of each primer (final concentration: [0.4 µM]) (Integrated DNA Technologies, Coralville, IA). The primer sequences used were 5'-GGCAAAATACCCCCAACATA-3' (forward) and 5'-AGAGTTGGCATTGAGGTGAGAG-3' (reverse) (Swart and Dandara, 2014). The PCR amplification conditions were 98°C for 5 minutes, 40 cycles at 98°C for 10 seconds, 69.5°C for 15 seconds, and 72°C for 2 minutes. Final extension was 72°C for 7 minutes. PCR purification was performed using a QIAquick PCR Purification Kit (Qiagen, Valencia, CA) according to the user manual. DNA concentrations were measured with a Qubit dsDNA BR Assay Kit (Invitrogen, Eugene, OR) according to the user manual. Samples were prepared for sequencing using 10 µL of DNA (50 ng) and 2 µL of one of four different

primers [1.7 μM] and Sanger sequenced by ACGT (Germantown, MD). The 1.8 kb PCR product was sequenced in its entirety using the primers mentioned above and forward and reverse primers 5'-CTAAGCCTTGCTCTGTCTCC-3' (forward) and 5'-GGAGAATCACTTGAACCCAGG-3' (reverse).

Genotyping and sequencing in human liver tissue samples

Genomic DNA extracted from 90 human liver samples was used for genotyping (coding region) and Sanger sequencing (3'UTR region). This protocol is different from the genotyping and sequencing of the healthy human volunteers, because the human liver microsomes were processed independently in a collaborating laboratory. Genotyping of coding region variants was performed on Applied Biosystems 7900 HT Real-Time PCR System or QuantStudio 12K Flex real-time PCR instruments using Life Technologies TaqMan assays for *CYP2B6* rs3745274 (516G>T, Q172H) and rs28399499 (983T>C, I328T) (Life Technologies, Foster City, CA). To detect *CYP2B6* rs2279343 (785A>G, K262R) a high-resolution melting (HRM) assay was performed as previously described (Twist et al., 2013).

To sequence the 3'UTR, this region was first amplified by adding the following reagents to each reaction: 1 μL of DNA (15 ng), 4 μL KAPA LR Hotstart 2X, 2.4 μL ultrapure distilled water and 0.3 μL of each primer (final concentration: [0.375 μM]) (Integrated DNA Technologies, Coralville, IA). The primer sequences used were 5'-AATCTGTTGCAGTGGACATTTG-3' (forward) and 5'-AGAGTTGGCATTGAGGTGAGA-3' (reverse). The PCR amplification conditions were 94°C for 3 minutes, 48 cycles at 94°C for 10 seconds, 61.5°C for 15 seconds, and 68°C for 2 minutes. Final extension was 68°C for 7 minutes. PCR purification was performed using ExoSAP-IT (USB, Cleveland, OH).

A 1:20 dilution of the purified PCR product was used for sequencing, performed with BigDye terminator v3.1 and the STeP cycle sequencing protocol (Platt et al., 2007). Briefly, three cycle steps were performed: 1) at 95°C for 10 sec, 50°C for 5 sec and 60°C for 1 min 15 sec for a total 15 cycles, 2) at 95°C for 10 sec, 50°C for 5 sec and 60°C for 1 min 30 sec, a total of 5 cycles and 3) at 95°C for 10 sec, 50°C for 5 sec and 60°C for 2 min for 15 cycles. The sequence reactions were cleaned up with AxyPrep Mag DyeClean (Axygen, Corning Life Sciences, Tewksbury, MA) and electrophoresis was performed on a 3730xl DNA Analyzer (Life Technologies, Foster City, CA). The 1962 bp PCR product was sequenced in its entirety using the following forward primers 5'-TGTGTCTGGGCTTAGGGAC-3', 5'-GTGATTCACCCACCTTAGCC-3', 5'-GTCTCAGCTCCCAAGTAGCTG-3', and the reverse primers 5'-CAGGTCTCTCAGAGGCAGG-3', 5'-AGTTCGAGACCAGCCTGG-3', 5'-CCAGCTCCTCCAGAGGC-3' and 5'-GCAGCTGGGAATGAGGA-3'.

As a quality control, genotyping was repeated in random samples and genotyping and sequencing results were verified by a second person to assure accurate interpretation of the data. Sequences were analyzed using Sequencher (v.5.4.5, Gene Codes Corporation, Ann Arbor, MI) and BioEdit (v.7.2.5) (Hall, 1999) after alignment to the *CYP2B6* reference sequence with GenBank Accession Number NC_000019.10.

CYP2B6 allele, genotype, haplotype, diplotype analyses

CYP2B6 star allele designations were assigned in accordance with the Human Cytochrome P450 Allele Nomenclature Database (http://cypalleles.ki.se/). Allele and genotype frequencies, Hardy-Weinberg equilibrium analysis, and linkage disequilibrium analysis were performed using SHEsis (Shi and He, 2005). Haplotype construction was

performed using PHASE version 2.1.1 (Stephens and Donnelly, 2003; Stephens et al., 2001). Haplotype and diplotype Venn diagrams were generated using BioVenn (Hulsen et al., 2008).

In silico microRNA predictions

The PolymiRTS Database 3.0 (accessed June 2014) was used to identify SNPs predicted to create or abolish miRNA target sites for *CYP2B6* (Bhattacharya et al., 2014). For the dinucleotide variant, rs70950385, manual seed sequence alignment was performed.

In vitro luciferase assay to test effects of the rs70950385 (CA) variant on microRNA targeting

The pIS-0 firefly luciferase vector (Yekta et al., 2004) (Addgene, Cambridge, MA) was used to study 3'UTR function in relation to miRNA regulation. The oligo containing either the wild-type (5'-GCCGTGTAATTCTAGGAGCTCGTCACACACTGCTGTAGTCTTCCCC**AG**TCCTCATCGTTCTAGAGTCGGGGC-3') or variant (5'-GCCGTGTAATTCTAGGAGC TCGTCACACACTGCTGTAGTCTTCCCC**CA**TCCTCATCGTTCTAGAGTCGGGGC-3') miRNA target sites for the rs70950385 SNP (Integrated DNA Technologies, Coralville, IA) were amplified and then cloned into the pIS-0 vector 3'UTR using the NEBuilder HiFi DNA assembly system as instructed by the user manual (New England BioLabs, Ipswich, MA). The plasmids were then transformed into One Shot OmniMax 2 TI Chemically Competent *E. coli* (Invitrogen, Carlsbad, CA) and plated on ampicillin-treated agar plates. Individual colonies were selected and grown in ampicillin-treated liquid culture overnight. Plasmid DNA was isolated using a NucleoSpin Plasmid (NoLid) DNA Purification Kit (Macherey-Nagel, Düren, Germany) and quantified using a DNA dsDNA BR Assay Kit (Qiagen, Invitrogen, Eugene, OR). DNA was subsequently sequenced using the 5'-

GTGGTTTGTCCAAACTCATC-3' reverse primer to ensure clones with the correct wild-type and variant sequences were selected.

HepG2 human liver carcinoma cells were seeded at a density of 90,000 cells per well in 24 well plates and cultured for 48 hours. HepG2 cells were then transfected using Lipofectamine 3000 (Life Technologies, Foster City, CA) for 48 hours with each plasmid (500 ng/well) with or without the miRNAs (hsa-miR-625-5p and hsa-miR-1275; final concentration: [30 pM]) (GE Dharmacon, Chicago, IL) predicted to target the *CYP2B6* 3'UTR region encompassing the genetic variant. *Renilla* luciferase reporter pGL4.74 (10 ng/well) was used as the transfection control. *C. elegans* cel-miR-67 was employed as a negative control. Luciferase activity was measured with the Dual-Glo Luciferase Assay as instructed by the user manual (Promega, Madison, WI).

Statistical analyses for* CYP2B6 *3'UTR study

Efavirenz C_{max}, AUC_{0-48} metabolite:parent ratios, and bupropion hydroxylase activity (untransformed data) were analyzed among each genotype, haplotype, or diplotype using Kruskal-Wallis followed by Dunn's post-hoc tests. *In vitro* luciferase assay results were analyzed using paired ratio t-tests. All analyses were performed using Graphpad Prism version 6 (La Jolla, CA); *p*-values <0.05 were considered statistically significant.

Results

Association of CYP2B6 3'UTR SNPs with efavirenz C_{max} and AUC_{0-48} metabolite:parent ratios in healthy volunteers

Among 200 healthy volunteers sequenced for *CYP2B6* 3'UTR variants, 187 volunteers had a complete set of efavirenz metabolism data and 197 were genotyped for *CYP2B6*6* and *CYP2B6*18*. Of the 197 volunteers for whom *CYP2B6* genotyping data were available, 47% were normal metabolizers, 42% intermediate metabolizers, and 11% were classified as poor metabolizers (Table 8). Plasma efavirenz C_{max} and AUC_{0-48} ratios (8-OH-EFV/EFV) were used for the analysis.

Twenty-five variants were observed in the 3'UTR of this population; however, only seven variants were observed at a frequency that allowed us to assess pharmacokinetic differences among the genotypes (Table 9). Among the normal metabolizers, altered efavirenz metabolism was detected in subjects with the following 3'UTR variants: rs3181842, rs7246465, rs707265, rs70950385, and rs1042389 (Figure 14; Table 10). The rs70950385 and rs1042389 variants were in complete linkage disequilibrium (r^2=1.0, D'=1.0) in our cohort and thus not shown separately (Figure 15). For rs3181842, an increase in CYP2B6 activity, as shown by the C_{max} ratio, was detected between the T/T and C/C genotypes (43.9% increase; p<0.01) and AUC ratio between volunteers with T/T versus T/C (31.9% increase; p<0.05) and C/C genotypes (70.6% increase; p<0.0001) (Figure 14A; Table 10). An increase in CYP2B6 activity was observed among volunteers carrying the rs7246465 variant allele (C_{max}: C/C vs. T/T [40.0% increase; p<0.01]; AUC: C/C vs. C/T [38.0% increase; p<0.01] and T/T [67.9% increase; p<0.0001]) and rs707265 (C_{max}: G/G vs. G/A [20.0% increase; p<0.05] and A/A [46.6% increase; p<0.01]; AUC: G/G vs. G/A [34.2% increase; p<0.05] and A/A [72.4% increase; p<0.0001]) (Figure 14B,E; Table 10). These two variants were in partial linkage disequilibrium in our study cohort

(r^2=0.80, D'=0.91) (Figure 15). The rs70950385 variant allele was associated with a decrease in CYP2B6 activity using C_{max} between AG/AG vs. CA/CA (32.6%; p<0.01) and AG/CA vs. CA/CA genotypes (25.4%; p<0.05) and AUC between AG/AG and CA/CA genotypes (32.7%; p<0.05) (Figure 14F; Table 10). Comparable changes in efavirenz metabolism among the 3'UTR variants were also observed when all volunteers were included, even those with *CYP2B6*6* and *CYP2B6*18* alleles (Figure 16; Table 11).

Table 8: CYP2B6 star allele frequency

Metabolizer Status	Observed Star Alleles	Count (%)
Normal	*1/*1, *1/*2, *1/*4	92 (47)
Intermediate	*1/*6, *4/*6, *1/*18	83 (42)
Poor	*6/*6, *6/*18,*18/*18	22 (11)

* No genotyping data for 3 volunteers

Table 9: CYP2B6 3'UTR variant frequencies in healthy volunteers

SNP	Chromosome 19 Position[1]	MAF	HWE	Genotype (n)		
rs34749331	41016899	0.005	Yes	G/G (198)	G/A (2)	
rs139818840[2]	41017033	0.055	Yes	7/7 (179)	7/8 (20)	8/8 (1)
rs528886765	41017103	0.003	Yes	C/C (199)	C/T (1)	
rs3181842	41017111	0.343	Yes	T/T (89)	T/C (85)	C/C (26)
rs28969414	41017171	0.037	Yes	T/T (185)	T/A (15)	
rs28969415	41017172	0.037	Yes	A/A (185)	G/A (15)	
rs553398143	41017187	0.003	Yes	C/C (199)	C/T (1)	
rs28969416	41017188	0.003	Yes	A/A (199)	A/G (1)	
rs535525152	41017191	0.003	Yes	C/C (199)	C/T (1)	
rs764949833	41017192	0.003	Yes	A/A (199)	A/G (1)	
rs150701000	41017208	0.007	Yes	A/A (197)	A/G (3)	
rs185153760	41017249	0.005	Yes	G/G (198)	G/A (2)	
rs142189613	41017333	0.003	Yes	G/G (199)	G/A (1)	
rs7260525	41017349	0.117	Yes	A/A (156)	A/G (41)	G/G (3)
rs7246465	41017398	0.323	No	C/C (99)	C/T (73)	T/T (28)
novel variant	41017895	0.003	Yes	C/C (199)	C/T (1)	
rs28969420	41017899	0.050	No	G/G (166)	G/T (24)	T/T (10)
rs145450819	41017916	0.005	Yes	C/C (198)	C/G (2)	
rs567303715	41018016	0.003	Yes	C/C (199)	C/G (1)	
rs28969421	41018082	0.010	No	G/G (197)	G/A (2)	A/A (1)
rs1038376	41018104	0.333	Yes	A/A (89)	A/T (89)	T/T (22)
rs707265	41018182	0.318	Yes	G/G (101)	G/A (71)	A/A (28)
rs70950385	41018226	0.228	Yes	AG/AG (122)	AG/CA (65)	CA/CA (13)

rs1042389	41018248	0.228	Yes	C/C (122)	C/T (65)	T/T (13)
rs538901499	41018270	0.010	Yes	A/A (198)	A/G (2)	

[1] Chromosome position is according to GenBank Accession Number NC_000019.10 [GRCh37.p17 108 annotation]

[2] rs139818840 variant includes 7 or 8 AT repeats

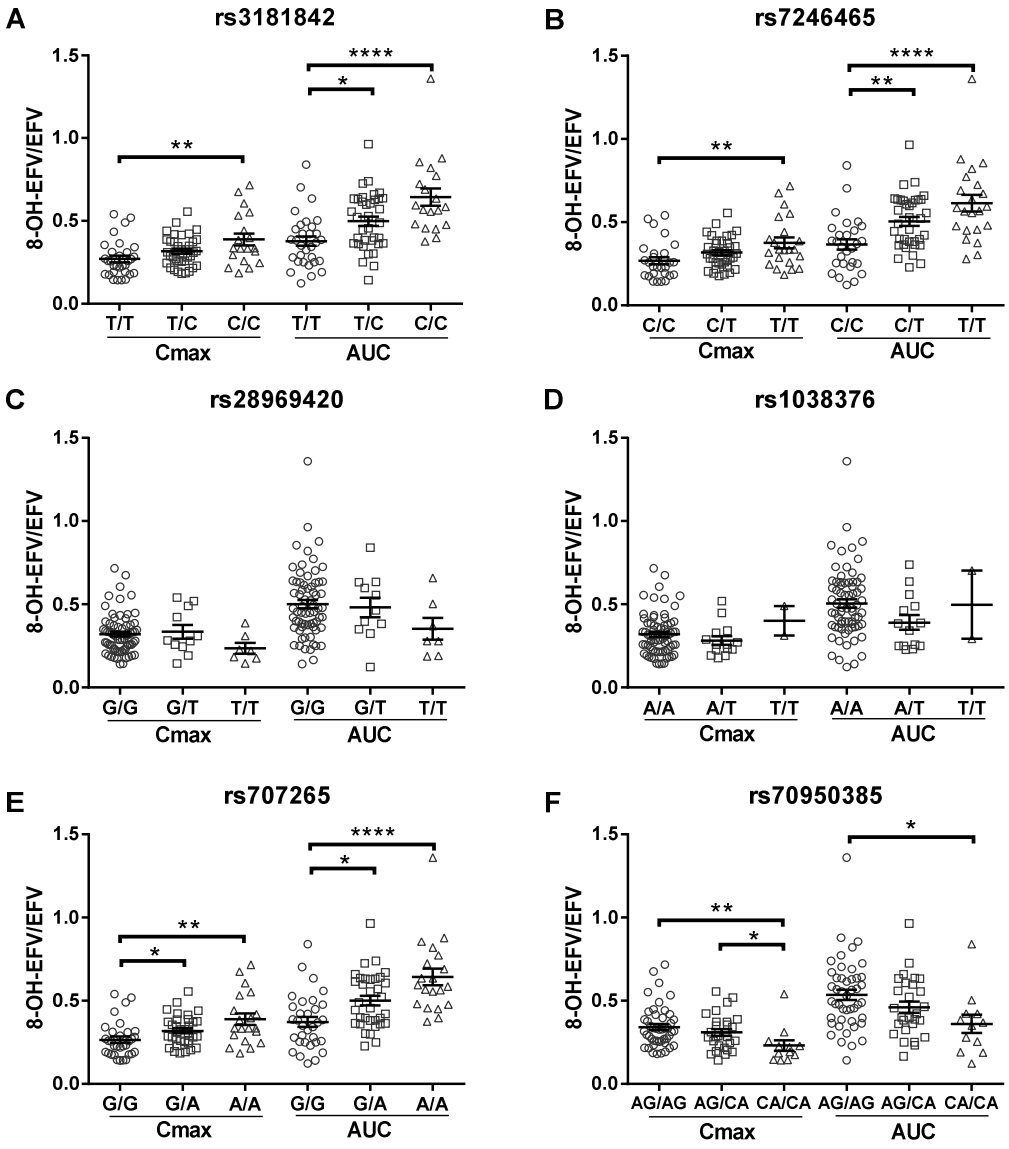

Figure 14: Association of *CYP2B6* 3'UTR variants with efavirenz metabolism in healthy volunteers with *CYP2B6* genotypes predicting normal metabolism (n=86)

Efavirenz C_{max} and AUC metabolite:parent ratios (8-OH-EFV/EFV) among normal metabolizers; subjects with *CYP2B6*6* and **18* alleles excluded. *X*-axis: *CYP2B6* 3'UTR genotypes **F.** rs70950385 variant is in complete LD with rs1042389 (data not shown separately). *Y*-axis: 8-hydroxy-efavirenz/efavirenz ratio[#]. (*=p<0.05, **=p<0.01, ***=p<0.001, ****=p<0.0001). [#] Higher 8-OH-EFV/EFV ratios mean higher CYP2B6 activity.

Table 10: Association of *CYP2B6* 3'UTR variants with efavirenz metabolism in healthy volunteers without any *CYP2B6*6* and *CYP2B6*18* alleles (n=86)

* Ratio=(8-OH-EFV/EFV)

	n	Mean Cmax Ratio*	Lower 95% CI	Upper 95% CI	Mean AUC Ratio*	Lower 95% CI	Upper 95% CI
rs3181842							
T/T	31	0.270	0.230	0.310	0.378	0.319	0.437
T/C	36	0.317	0.286	0.349	0.498	0.440	0.556
C/C	19	0.389	0.312	0.465	0.645	0.533	0.756
rs7246465							
C/C	28	0.268	0.225	0.312	0.365	0.301	0.429
C/T	36	0.317	0.285	0.348	0.504	0.450	0.559
T/T	22	0.376	0.308	0.443	0.614	0.508	0.719
rs28969420							
G/G	68	0.321	0.292	0.351	0.502	0.451	0.552
G/T	11	0.335	0.244	0.427	0.482	0.351	0.614
T/T	7	0.236	0.158	0.315	0.353	0.193	0.514
rs1038376							
A/A	70	0.320	0.290	0.350	0.506	0.456	0.556
A/T	14	0.284	0.227	0.341	0.391	0.296	0.487
T/T	2	0.402	-0.729	1.532	0.498	-2.107	3.103
rs707265							
G/G	32	0.266	0.227	0.305	0.374	0.314	0.433
G/A	34	0.319	0.288	0.351	0.501	0.444	0.559
A/A	20	0.390	0.318	0.462	0.644	0.539	0.749
rs70950385							
AG/AG	46	0.342	0.305	0.380	0.536	0.473	0.599
AG/CA	28	0.309	0.268	0.351	0.461	0.392	0.531
CA/CA	12	0.231	0.161	0.301	0.361	0.241	0.481

Cmax=maximum concentration

AUC=area under the curve 0-48 hours

CI=confidence intervals

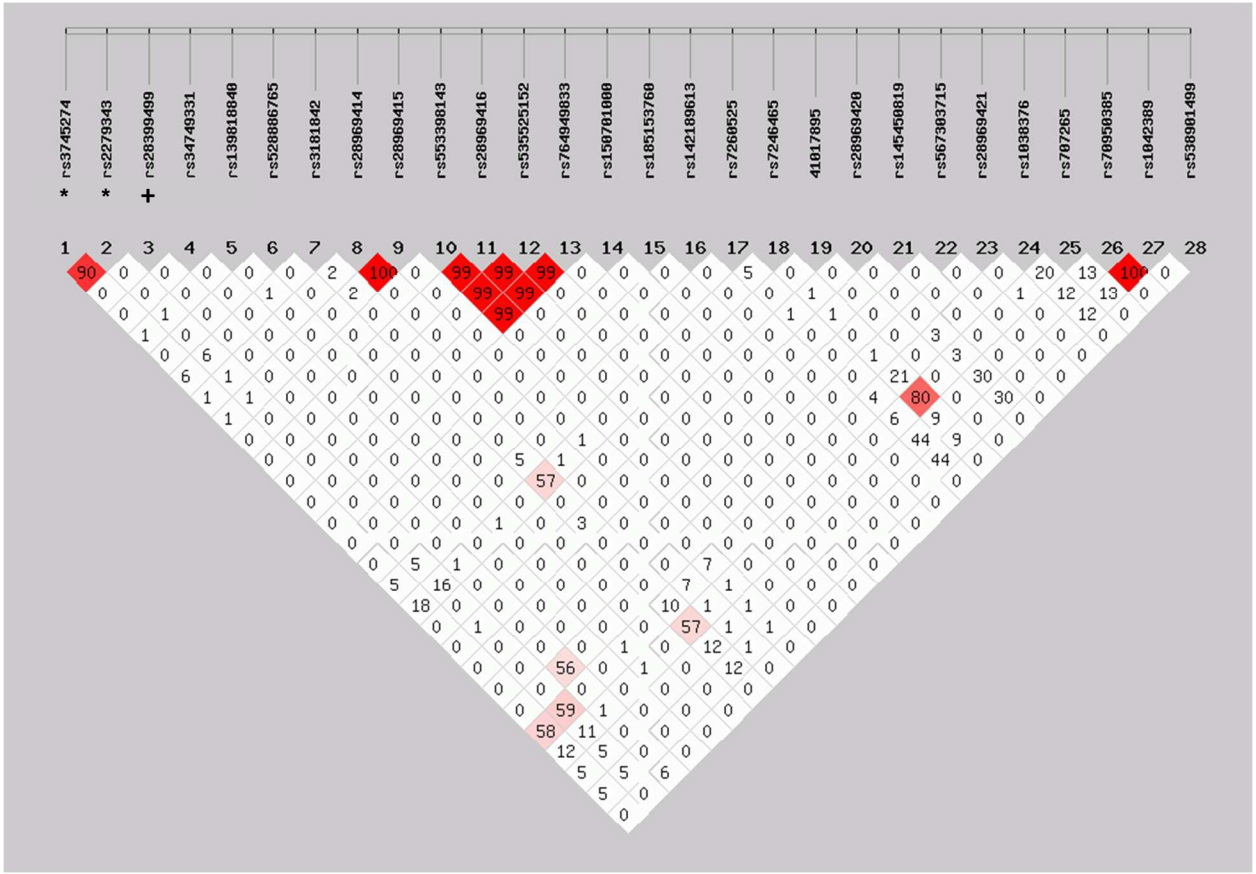

Figure 15: r^2 linkage disequilibrium diagram of *CYP2B6* variants genotyped in samples from all four studies (3 clinical trials and one liver sample set) The r^2 values for *CYP2B6* 3'UTR variants and *CYP2B6*6* (SNP 1 and 2) and *CYP2B6*18* (SNP 3).
*****SNP 1 (516G>T) and 2 (785A>G) denote *CYP2B6*6*, **+**SNP 3 (983T>C) denotes *CYP2B6*18*

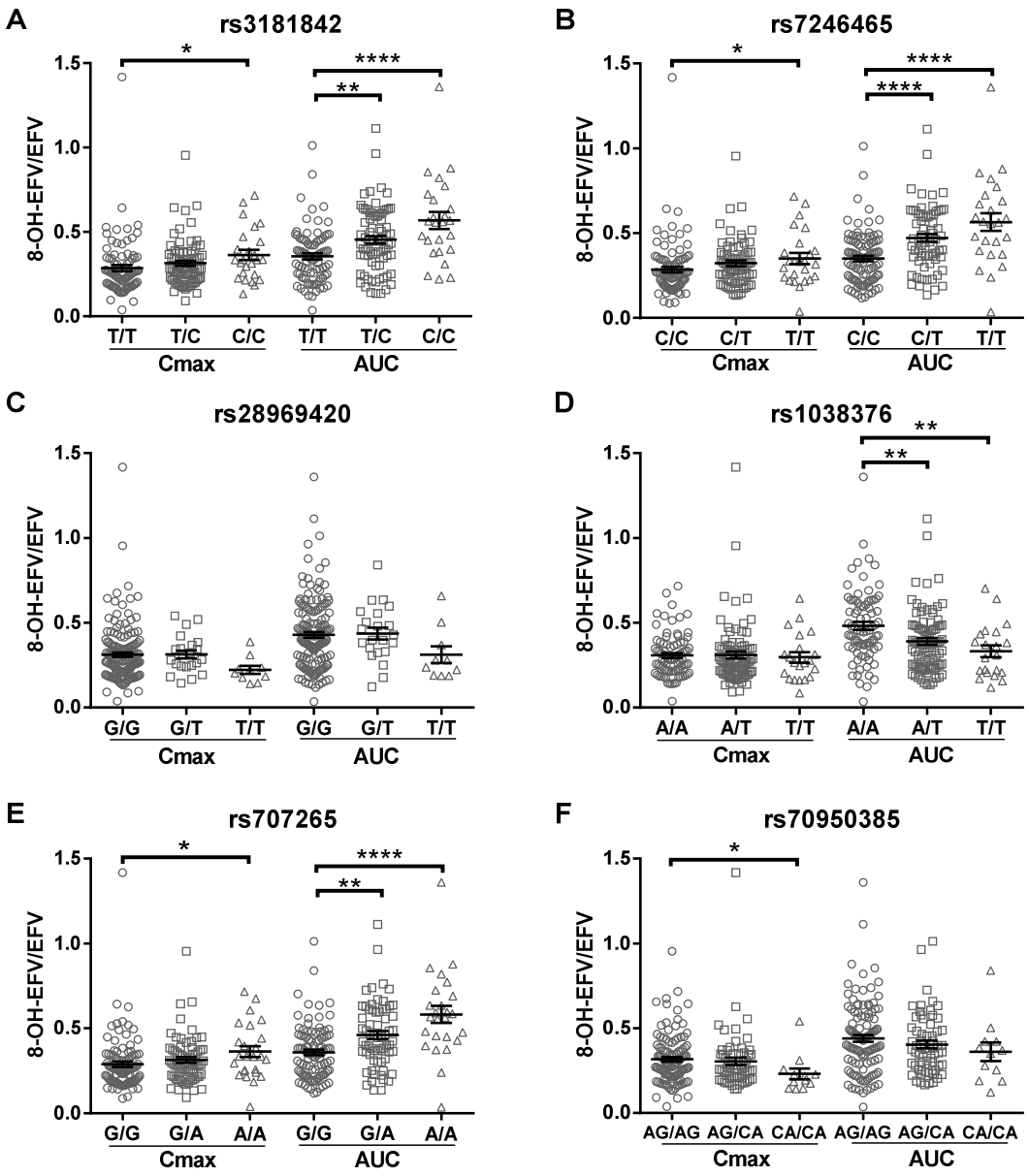

Figure 16: Association of *CYP2B6* 3'UTR variants with efavirenz metabolism in healthy volunteer population (n=187)

Efavirenz Cmax and AUC metabolite:parent ratios among all volunteers. *X*-axis: *CYP2B6* 3'UTR genotypes **F.** rs70950385 variant is in complete LD with rs1042389 (data not shown separately). *Y*-axis: #8-hydroxy-efavirenz/efavirenz ratio. (*=p<0.05, **=p<0.01, ****=p<0.0001). # Higher 8-OH-EFV/EFV ratios mean higher CYP2B6 activity.

Table 11: Association of *CYP2B6* 3'UTR variants with efavirenz metabolism in all volunteers including those with *CYP2B6*6* and *CYP2B6*18* alleles (n=187)

	n	Mean Cmax Ratio*	Lower 95% CI	Upper 95% CI	Mean AUC Ratio*	Lower 95% CI	Upper 95% CI
rs3181842							
T/T	86	0.286	0.249	0.322	0.355	0.321	0.390
T/C	76	0.314	0.283	0.346	0.454	0.410	0.498
C/C	25	0.364	0.300	0.428	0.568	0.464	0.671
rs7246465							
C/C	94	0.285	0.252	0.319	0.351	0.319	0.383
C/T	68	0.323	0.289	0.357	0.472	0.427	0.518
T/T	25	0.351	0.284	0.418	0.566	0.457	0.674
rs28969420							
G/G	155	0.312	0.286	0.339	0.429	0.396	0.462
G/T	22	0.314	0.265	0.363	0.437	0.364	0.510
T/T	10	0.224	0.169	0.278	0.312	0.200	0.424
rs1038376							
A/A	81	0.308	0.279	0.336	0.482	0.435	0.529
A/T	85	0.311	0.271	0.350	0.391	0.351	0.430
T/T	21	0.296	0.232	0.361	0.333	0.261	0.405
rs707265							
G/G	97	0.289	0.256	0.321	0.358	0.327	0.390
G/A	65	0.315	0.280	0.350	0.461	0.412	0.509
A/A	25	0.363	0.296	0.431	0.582	0.478	0.686
rs70950385							
AG/AG	113	0.317	0.289	0.344	0.440	0.401	0.479
AG/CA	63	0.305	0.261	0.349	0.405	0.360	0.450
CA/CA	12	0.231	0.161	0.301	0.361	0.241	0.481

* Ratio= (8-OH-EFV/EFV)

Cmax=maximum concentration

AUC=area under the curve 0-48 hours

CI=confidence intervals

To assess the changes in efavirenz metabolism among combinations of variants, haplotype and diplotype analyses were performed. A significant overall change was detected among the C_{max} ratios between the different haplotypes, but no significant changes were detected after post-hoc analysis (Table 12). A decrease in CYP2B6 activity as measured by AUC ratios were observed between haplotype 4 versus 2 (p<0.01), 12 (p<0.0001), 13 (p<0.05), and 24 (p<0.01) (Table 12). Haplotypes 2, 4, 12, 13, and 24 distinguished from the wild-type variations in the following 3'UTR variants: rs3181842, rs7260525, rs7246465, rs28969420, rs1038376, rs707265, rs70950385, and rs1042389. A significant overall change was also observed in AUC ratios between the different diplotypes, but no significant changes were observed after post-hoc analysis. The sample size for many haplotypes and diplotypes were too small to assess, i.e. many haplotypes and diplotypes were observed only within one of the metabolizer groups (Figure 17). Out of the 38 inferred 3'UTR haplotypes, two haplotypes were found among volunteers or samples that did not have *CYP2B6*6* and **18* genotyping data for. Of the remaining 36 haplotypes, 8, 9, and 3 were unique to normal, intermediate, and poor metabolizers, respectively, whereas 16 overlapped (Figure 17A). Haplotype 4 was detected among only genotypic normal and intermediate metabolizers, whereas haplotype 2, 12, and 13 were detected among all three groups; however, haplotype 24 (associated with decreased CYP2B6 activity) was also specific to genotypic normal and intermediate metabolizers suggesting the 3'UTR variants contribute to the variability in CYP2B6 activity (data not shown). Out of the 76 predicted diplotypes, 33, 21, and 8 were unique to normal, intermediate, and poor metabolizers, respectively, whereas 14 overlapped (Figure 17B). There were no diplotypes overlapping between the normal and poor metabolizer groups.

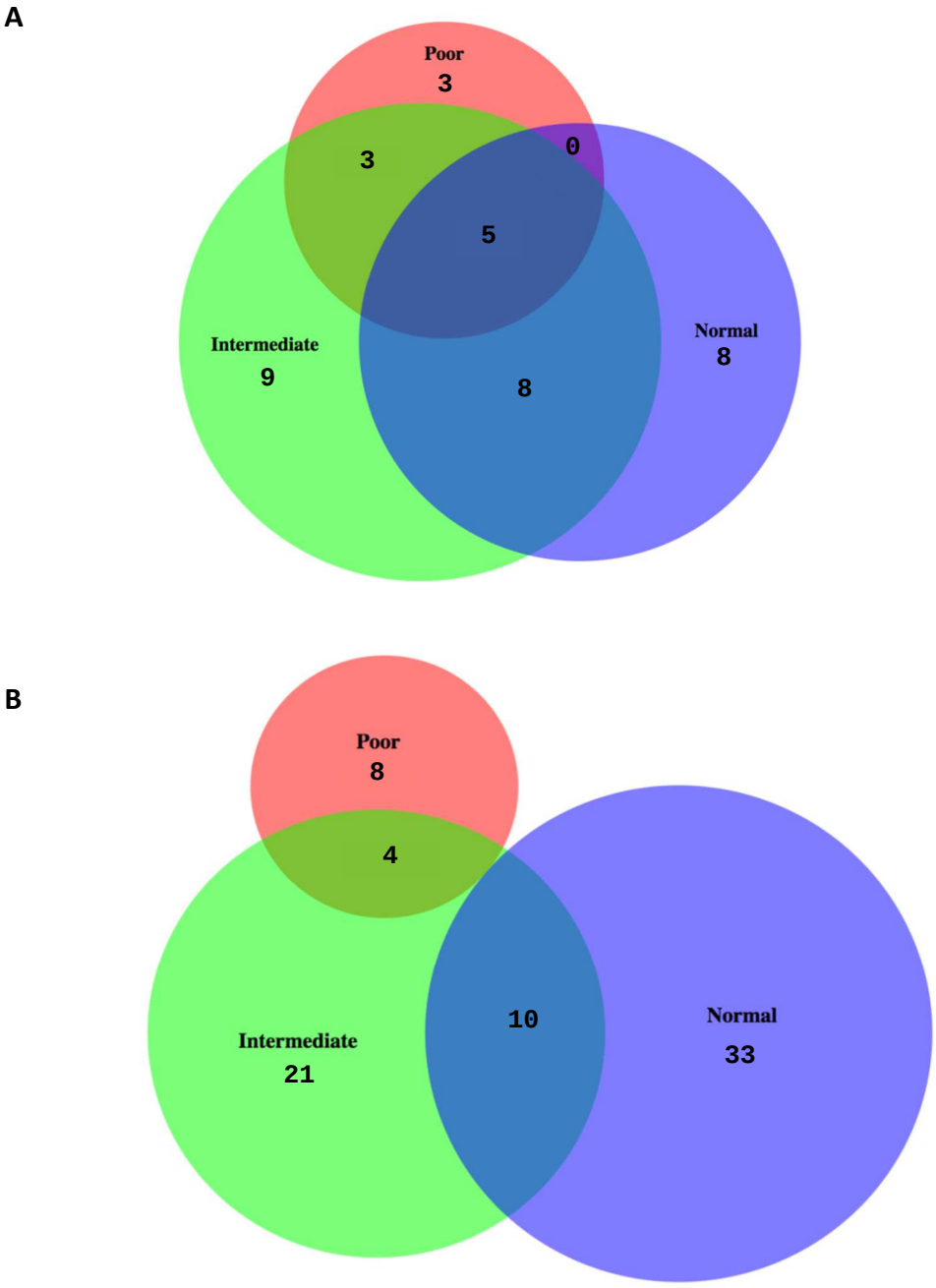

Figure 17: Venn diagrams of haplotypes and diplotypes observed in all studies

The Venn diagrams depict the number of haplotypes **(A)** and diplotypes **(B)** within each CYP2B6 metabolizer group, as assigned by *CYP2B6*6* and *CYP2B6*18*. Normal (blue), intermediate (green), and poor (red) metabolizers.

Table 12: CYP2B6 3'UTR variant haplotype association with CYP2B6 activity in healthy volunteers and human liver microsomes

Haplotype ID	Haplotype**	Count	Mean Cmax (8-OH-EFV/EFV)	Mean AUC_{0-48} (8-OH-EFV/EFV)	Mean OH-BUP Rates (pmol/mg protein/min)
1	G7CCTACACAAGGACCGCCGAGAGTA	7	0.25±0.07	0.33±0.19	265.7±167.6
2*	G7CCTACACAAGGACCGCCGTGAGTA	25	0.27±0.03	0.33±0.03*	453.5±375.3
3	G7CCTACACAAGGACCGCGGAGAGTA	1	0.36	0.38	-
4*	G7CCTACACAAGGATCGCCGAAAGTA	128	0.35±0.02	0.55±0.03*	572.0±135.8
5	G7CCTACACAAGGATCTCCGAAAGTA	1	0.39	0.66	-
6	G7CCTACACAAGGATCTCCGAGCACA	1	-	-	
7	G7CCTACACAAGGGCCGCCGAGCACA	1	-	-	32.79
8	G7CTTACACAAGGACCGCCGAAAGTA	5	0.30±0.06	0.46±0.09	125.2
9	G7CTTACACAAGGACCGCCGAGAGTA	62	0.29±0.02	0.40±0.03	480.8±104.4
10	G7CTTACACAAGGACCGCCGAGCACA	7	0.30±0.06	0.40±0.03	-
11	G7CTTACACAAGGACCGCCGTAAGTA	1	0.52	0.59	-
12*	G7CTTACACAAGGACCGCCGTGAGTA	128	0.31±0.02	0.38±0.02*	512.1±106.1
13*	G7CTTACACAAGGACCTCCGAGCACA	50	0.28±0.01	0.39±0.03*	153.3±61.7
14	G7CTTACACAAGGACTGCCGTGAGTA	1	0.34	0.60	-
15	G7CTTACACAAGGATCGCCGAAAGTA	6	0.26±0.05	0.32±0.08	967.3±582.5
16	G7CTTACACAAGGATCGCCGAAAGTG	2	0.35±0.10	0.38±0.003	-
17	G7CTTACACAAGGATCGCCGAGAGTA	6	0.36±0.04	0.56±0.07	116.5
18	G7CTTACACAAGGATCGCCAAAAGTA	3	0.038	0.04	67.0
19	G7CTTACACAAGGATCGGCGAGAGTA	4	0.27	0.34	623.5±545.3
20	G7CTTACACAAGGATCTCCGAGAGTA	1	0.18	0.28	-

21	G7CTTACACAAGGATCTCCGAGCACA	2	0.22	0.28	-
22	G7CTTACACAAGGATCTCCAAAAGTA	2	0.17±0.03	0.21±0.02	-
23	G7CTTACACAAGGGCCGCCGAAAGTA	1	-	-	-
24*	G7CTTACACAAGGGCCGCCGAGCACA	65	0.29±0.03	0.40±0.03*	403.9±137.6
25	G7CTTACACAAGGGCCGCCGTGAGTA	1	0.30	0.38	-
26	G7CTTACACAAGGGTCGCCGAGCACA	1	-	-	-
27	G7CTTACACAAGAACCGCCGTGAGTA	1	0.45	0.39	-
28	G7CTTACACAAAGACCGCCGAAAGTA	1	0.28	0.49	-
29	G7CTTACACAAAGACCGCCGAGAGTA	1	0.36	0.46	-
30	G7CTTACACAGGGACCGCCGAGAGTA	3	0.24±0.03	0.33	-
31	G7CTTATGTGAGGACCGCCGAGAGTA	1	-	-	33.2
32	G7CTTATGTGAGGACCGCCGTGAGTA	1	0.26	0.39	-
33	G7CTAGCACAAGGACCGCCGAGAGTA	1	-	-	68.65
34	G7CTAGCACAAGGACCGCCGTGAGTA	22	0.28±0.03	0.37±0.05	342.4±168.6
35	G7TCTACACAAGGACCGCCGAGAGTA	1	-	-	42.46
36	G7TCTACACAAGGACCTCCGTGAGTA	1	0.23	0.23	-
37	G8CCTACACAAGGATCGCCGAAAGTA	32	0.32±0.04	0.51±0.05	444.8±162.7
38	A7CTTACACAAGGACCGCCGAAAGTA	3	0.09	0.14	-

***** Haplotypes that are statistically significant versus haplotype 4 when comparing AUC ratios.

****** The order of variants composing the haplotypes are corresponding with the individual variants listed in Table 1 as follows: rs34749331, rs139818840, rs528886765, rs3181842, rs28969414, rs28969415, rs553398143, rs28969416, rs535525152, rs764949833, rs150701000, rs185153760, rs142189613, rs7260525, rs7246465, novel variant, rs28969420, rs145450819, rs567303715, rs28969421, rs1038376, rs707265, rs70950385 (AG>CA), rs1042389, rs538901499.

3'UTR SNPs association with altered CYP2B6 activity in human liver microsomes

To further evaluate the changes observed in our healthy volunteer population, DNA from 90 human liver microsomal preparations isolated from pediatric and adult liver tissue samples were sequenced and characterized for CYP2B6 activity by measuring bupropion hydroxylation (one sample had an undetectable bupropion hydroxylation rate). In this tissue panel, based on the *CYP2B6*6* and *CYP2B6*18* genotypes, there were 51 genotypic normal, 31 intermediate, 4 poor metabolizers. The *CYP2B6*6* and *CYP2B6*18* genotypes of 4 samples were unknown (data not shown). A decrease in CYP2B6 activity was observed among samples with the rs70950385 homozygous (AG/AG) genotype (543.3 pmol/mg protein/min) versus carriers of the CA allele (326.3 pmol/mg protein/min) in the panel (39.9% decrease; $p<0.05$ based on untransformed data) (Figure 18 – $\log_2$-transformed velocities for visualization purposes; Table 13). Differences were not significant in normal metabolizers, likely because there were too few samples in this subset. The rs70950385 and rs1042389 variants were also in complete linkage disequilibrium in this sample population ($r^2=1.0$, D=1.0) (Figure 15). There were no statistically significant changes for any of the other variants, haplotypes, and diplotypes, as their frequencies were low (Figure 19 and Table 13).

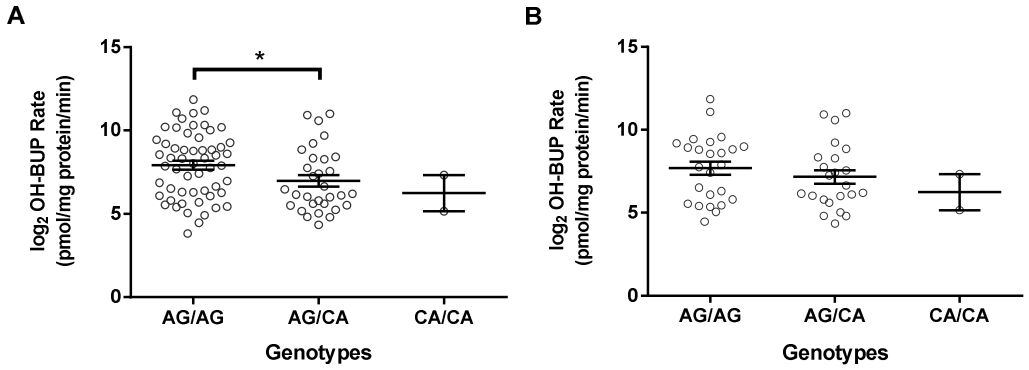

Figure 18: Association of *CYP2B6* rs70950385 with bupropion metabolism in human liver microsomes

Bupropion hydroxylation activity observed in human liver microsomes among **A.** all samples and **B.** normal metabolizers (i.e. volunteers with no *CYP2B6*6* and *CYP2B6*18* alleles). *X*-axis: Genotype (rs70950385 in complete linkage disequilibrium with rs1042389). *Y*-axis: $\log_2$ transformed rate of hydroxyl-bupropion (pmol/mg protein/min). (*=p<0.05) Note: Data was $\log_2$-transformed for visual purposes only.

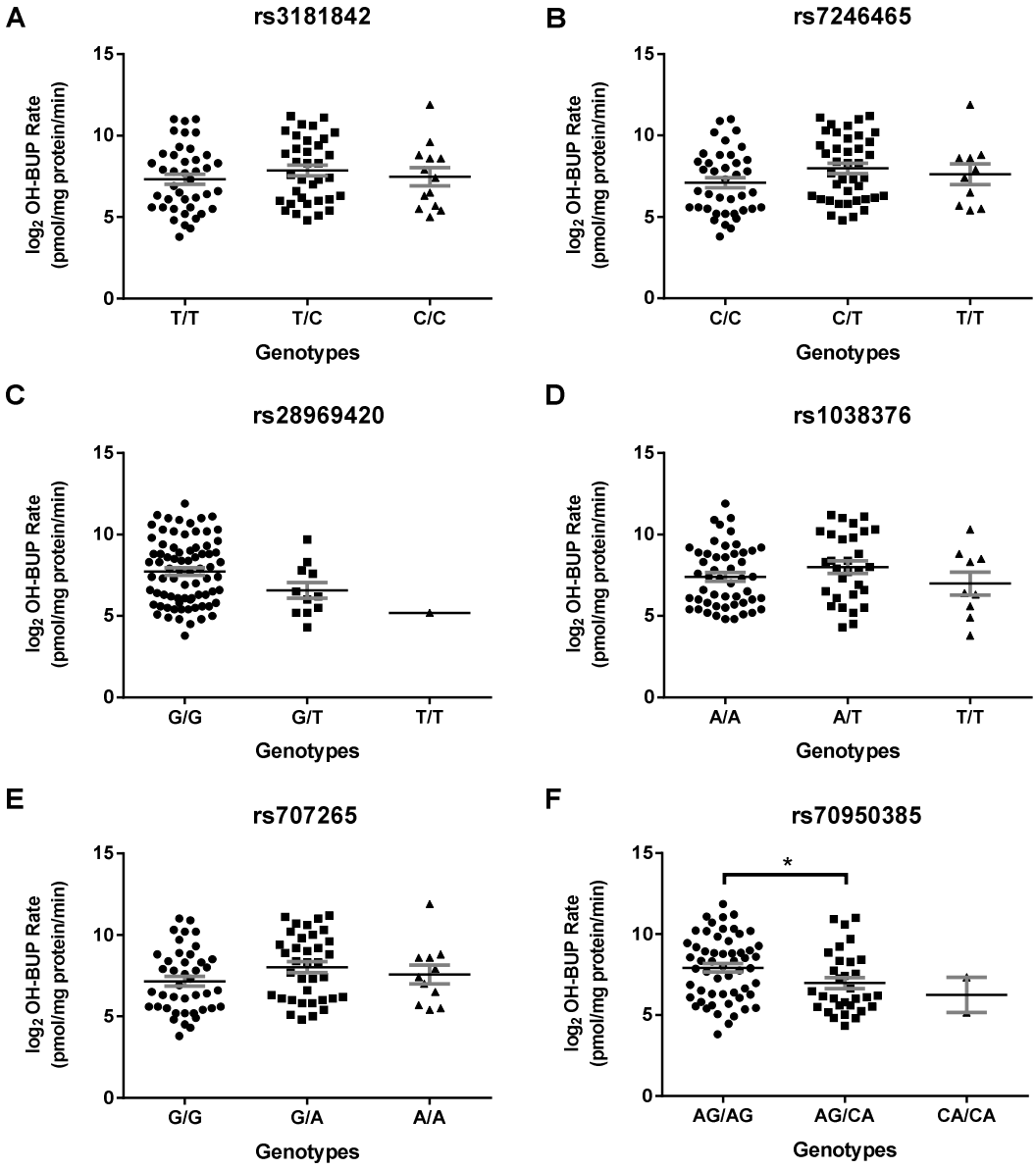

Figure 19: Association of *CYP2B6* 3'UTR variants with bupropion metabolism in human liver microsomes (n=89)

Bupropion hydroxylation rates among normal metabolizers; subjects with *CYP2B6*6* and **18* alleles excluded. *X*-axis: *CYP2B6* 3'UTR genotypes. *Y*-axis: log_2 transformed bupropion hydroxylation rate (pmol/mg protein/min). **F.** rs70950385 variant is in complete LD with rs1042389 (data not shown separately).

Table 13: Association of *CYP2B6* 3'UTR variants with bupropion metabolism in human liver microsomes (n=89)

	Normal Metabolizers				Total Population			
	n	Mean Bupropion Hydroxylation Rate*	Lower 95% CI	Upper 95% CI	n	Mean Bupropion Hydroxylation Rate*	Lower 95% CI	Upper 95% CI
rs3181842								
T/T	17	414.6	-35.98	865.2	41	392.5	213.9	571.1
T/C	21	365.5	117.8	613.2	35	520.1	302.7	737.5
C/C	12	539.1	84.06	994.1	13	495.6	-103.3	1095
rs7246465								
C/C	18	376.2	68.53	683.9	39	331.6	171	492.3
C/T	23	387	158	616	40	555.8	345.8	765.8
T/T	9	613.3	-288.4	1515	10	557.2	-244.1	1358
rs28969420								
G/G	43	471.4	242.2	700.7	77	503.6	345.8	661.5
G/T	6	147.4	26.47	268.3	11	174.7	15.62	333.8
T/T	1	35.7	-	-	1	35.72	-	-
rs1038376								
A/A	45	415.6	210.2	620.9	50	402.9	214.3	591.5
A/T	5	498.5	-663.5	1660	30	596.9	331.2	862.7
T/T	0	-	-	-	9	298.3	-13.09	609.6
rs707265								
G/G	18	376.2	68.53	683.9	42	340.4	185.4	495.4
G/A	23	387	158	616	36	576.2	348.8	803.7
A/A	9	613.3	-288.4	1515	11	517.9	-201.3	1237
rs70950385								
AG/AG	25	494.1	162	826.2	56	543.3	350.8	735.8

AG/CA	23	375.8	112.6	639	31	326.3	126.3	526.3
CA/CA	2	98.3	-697.1	893.7	2	98.33	-697.2	893.9

*pmol/mg protein/min

CI= confidence intervals

The rs70950385 (CA) variant allele alters luciferase activity due to altered miR-1275 regulation

The rs70950385 variant (AG>CA) is a combination of rs12979270 (A>C) and rs12979898 (G>A). Those two SNPs were in complete linkage disequilibrium in our total population. The rs12979270 (A>C) was predicted by PolymiRTS to create miRNA target site for miR-625-5p (Figure 20A) through perfect complimentary alignment within the seed sequence region, nucleotides 2-8 from the 5' end of the miRNA. Manual seed sequence comparisons revealed the dinucleotide variant created an additional base pair match for the first nucleotide of miR-1275 (Figure 20B). So, we tested the effect of the variant by cloning either the wild-type or the variant sequence into the 3'UTR of the luciferase plasmid. We would expect to see a decrease in luciferase activity compared to the wild-type luciferase plasmid, if the CA variant created a binding site for predicted miRNAs. When this mechanism was tested in a luciferase model in HepG2 cells without co-transfection of predicted miRNAs, there were no differences in luciferase activity between the plasmid containing the wild-type and variant miRNA target sites with *C. elegans* negative control miRNA or no miRNA transfection controls (Figure 21A). However, when transfected with the miRNAs whose binding was predicted to be altered by the variant, miR-1275 reduced luciferase activity by 11.3% (p=0.0035) in the presence of the variant allele compared to the wild-type allele (Figure 21B). MicroRNA 625-5p did not impact luciferase activity suggesting that the CA allele did not create a binding site for this predicted miRNA.

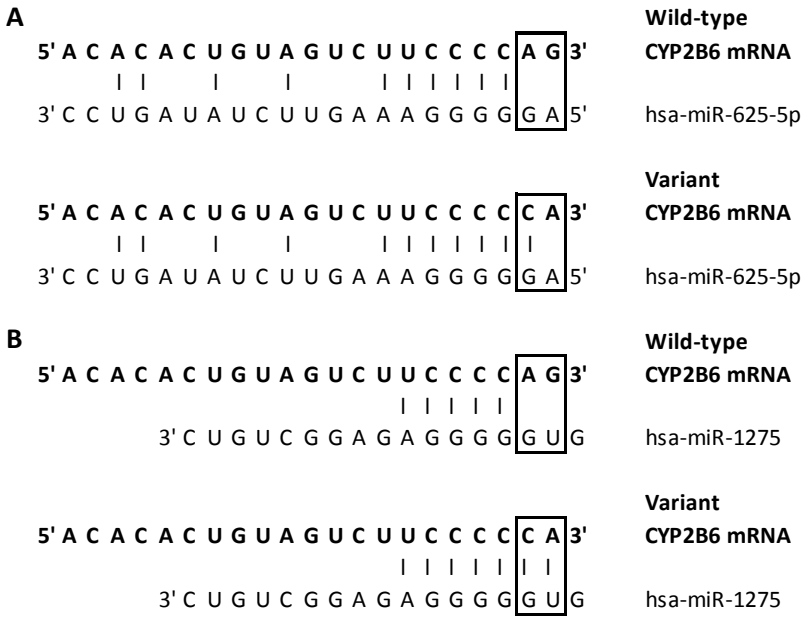

Figure 20: rs70950385 creates miR-625-5p and miR-1275 target site in *CYP2B6* 3'UTR

Proposed mechanism for miRNA **A.** 625-5p and **B.** 1275 binding to the *CYP2B6* 3'UTR among carriers of the rs70950385 (CA) allele.

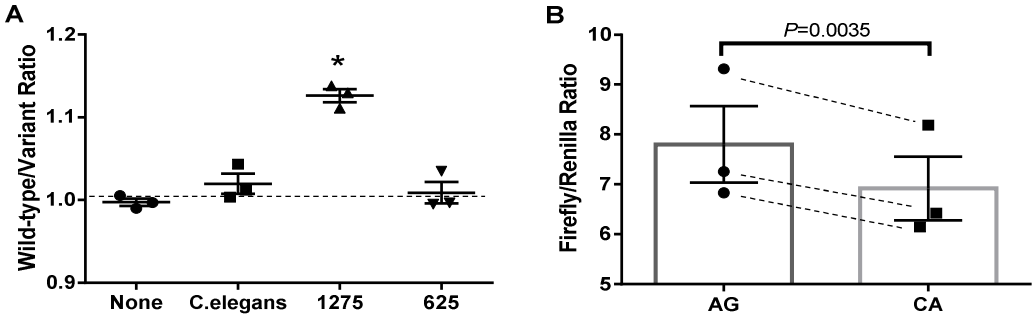

Figure 21: miRNA regulation of a predicted target site within *CYP2B6* 3'UTR in vitro
MicroRNA regulation of *CYP2B6* through measurement of luciferase activity in pIS-0 plasmids containing either the reference (wild-type) or variant miRNA target sites. **A.** *X*-axis: Luciferase plasmids were co-transfected with the following miRNAs: none (no transfected miRNAs), *C. elegans* (negative control cel-miR-67), miR-1275, and miR-625. *Y*-axis: Wild-type (firefly/*Renilla* luciferase) / Variant (firefly/*Renilla* luciferase). A ratio of 1=no change, >1=wild-type had higher luciferase activity, <1=variant had higher luciferase activity. **B.** *X*-axis*:* Plasmids containing either the wild-type 3'UTR sequence (5'-GCCGTGTAATTCTAGGAGCTCGTCACACACTGCTGTAGTCTTCCCC**AG**TCCTCA TCGTTCTAGAGTCGGGGC-3') or variant (5'-GCCGTGTAATTCTAGGAGCTCGTCAC ACACTGCTGTAGTCTTCCCC**CA**TCCTCATCGTTCTAGAGTCGGGGC-3') co-transfected with miR-1275. *Y*-axis: Firefly/*Renilla* luciferase ratio. (*=p<0.05)

Discussion

Variability in the pharmacokinetics of efavirenz and other drugs that undergo CYP2B6-mediated metabolism has been attributed to genetic variants in the *CYP2B6* coding region; however, variability in clinical response and adverse events are not completely explained by these genetic differences. Data from this study indicates that genetic variations in the 3'UTR of *CYP2B6* have an effect on CYP2B6 activity, independent of CYP2B6 metabolizer status (assigned based on *CYP2B6*6* and **18*). There were 25 unique variants detected in the 3'UTR of *CYP2B6* in our study population. Of these variants, seven were observed at a frequency that allowed us to assess differences in efavirenz pharmacokinetics between the homozygous and heterozygous volunteers. The rs3181842, rs7246465, and rs707265 had a similar increase in CYP2B6 activity for homozygous volunteers (Figure 14 A,B, and E). These three variants were not predicted to remove or create a miRNA target site through the PolymiRTS database at the time the database was accessed. Although the mechanism behind these observed changes are unknown, the mechanism may be related to only one of the variants as there is partial linkage disequilibrium among the three variants. The rs3181842 vs. rs7246465, rs3181842 vs. rs707265, and rs7246465 vs. rs707265 have r^2 values of 0.58, 0.58, and 0.80 respectively (Figure 15).

The rs70950385 and rs1042389 variants were shown to be in complete LD in our volunteers and the human liver microsome samples. These two variants conveyed decreased CYP2B6 activity among efavirenz pharmacokinetics in subjects genotyped as normal metabolizers. They were also associated with a decrease in bupropion hydroxylation in the human liver microsome panel. The rs1042389 variant has previously been associated with a decrease in median efavirenz plasma concentration among black South African HIV/AIDS patients in a study assessing the effect of 3'UTR variants on

efavirenz response (Swart and Dandara, 2014). The rs70950385 and rs1042389 SNPs were shown to be in complete LD in this population as well. We propose that the observed decrease in CYP2B6 activity is mediated by miRNA regulation owing to the rs70950385 variant creating a miRNA target site for miR-1275. This hypothesis is further corroborated by our *in vitro* data (Figure 21). In HepG2 cells treated with miR-1275 that expressed the variant (CA) miRNA target site, reduced luciferase activity was observed compared to cells that expressed the reference (wild-type) (AG) miRNA target site. This suggests that this miRNA has the ability to reduce protein activity either through degradation of mRNA or through repressing translation. Previously, we showed that miR-1275 expression is increased in pediatric and adult human livers compared to fetal livers, unequivocally demonstrating that this miRNA is expressed in the human liver (Burgess et al., 2015). These data suggest that this miRNA may play a role in regulating CYP2B6 activity; however, further studies are warranted to validate that this is the underlying mechanism as opposed to other mechanisms, such as variant-induced structural changes in the mRNA that may affect its stability.

No significant changes in efavirenz pharmacokinetics were observed among the 3'UTR variants within the genetic intermediate and poor metabolizers in our human volunteer population for any variant with the exception of rs7246465 (C/T vs. T/T; $p<0.05$) (data not shown). All other variants yielded similar trends. This is likely due to inadequate sample numbers among the intermediate and poor metabolizer groups to detect these changes. Alternatively, this observation may be due to a limited effect size of the 3'UTR variants in the presence of coding region variants known to reduce CYP2B6 activity. The rs70950385 homozygous variant and other genotypes were only detected in normal metabolizers in our population. Interestingly, many 3'UTR haplotypes and diplotypes were unique to the

metabolizer status. This may be due to partial LD with the *CYP2B6*6* and *CYP2B6*18* alleles or that our sample size was too small to detect an overlap.

This study shows that 3'UTR variants impact drug metabolism. Although the mechanisms are not known for all altered efavirenz pharmacokinetics associated with 3'UTR variants in *CYP2B6*, miRNA regulation is a likely contributor. Limitations on linking the other variants to miRNAs may be due to the limitations of miRNA prediction algorithms and tools which focus mostly on the seed sequence region as the main mechanism for miRNA binding. As in the case of rs70950385, our data suggest that miRNA regulation may explain, at least in part, the decreased CYP2B6 activity in healthy volunteers carrying the variant allele, as corroborated by our in vitro data. Although pharmacogenetics has primarily focused on genetic variants in the coding and promoter regions, our findings, i.e. that genetic variants in the 3'UTR contribute to variability in drug response, will open up the field to consider 3'UTR variants as a source of variability in the activities of many drug disposition genes.

CHAPTER 4

Novel high-throughput bioassay to functionally test genetic variants in microRNA target sites

Introduction

Due to the large number of variants in the 3'UTR predicted to alter miRNA regulation of drug disposition genes, the traditional individual variant-miRNA validation assays will prove to be costly and time-consuming. Although individual luciferase assays remain the gold-standard for validations, a more high-throughput way to functionally test these variants will aid in the selection of candidate variants to test individually. Our lab created such an assay, PASSPORT-sequencing (Parallel ASSessment of POlymorphisms in miRNA Target sites), that will allow hundreds of variants to be tested simultaneously in multiple cell lines. In this study, we use PASSPORT-seq to test over 100 wild-type-variant pairs in four different cell lines. Our findings support the emerging role of variants in miRNA target sites in altering miRNA regulation.

Materials and Methods

PASSPORT-sequencing

Selection of miRNA variants

SNPs to test in the high-throughput bioassay were selected from the PolymiRTS database for variants that were predicted to alter binding of our list of developmentally-regulated miRNAs to our pharmacogenes of interests. Additional variants were obtained from SNPs identified by our sequencing of the 3'UTRs of the 30 human liver tissues. TargetScan was used to identify miRNA binding within these sequenced samples. Lastly, several variants that showed allele-specific expression in this sequenced dataset were selected. There were 119 SNPs identified in the assay: 55 from the RNA-sequencing data (17 of those showing allele-specific expression); and 64 within the PolymiRTS database.

Test sequence design

The 5' and 3' flanking regions for each of the 119 variants were extracted from dbSNP. A 32-nucleotide region containing either the wild-type or variant allele flanked by 9 nucleotides on the 3' end and 22 nucleotides on the 5' end was used as the test sequence. Since it is known that miRNAs are 17-22 nucleotides in the length, the 9 nucleotides on the 3' end allow the targeting miRNA to fully bind whether the variant is at nucleotide positions 1 or 8 of the target mRNA. Two hundred and thirty-eight of these 32-nucleotide regions were created to test the 119 SNPs (Table 14). Universal primer binding regions were added on both sides of each test region, 5'-GTAATTCTAGGAGCTC and 3'-CGTTCTAGAGTCGGG resulting in a final 63 base pair oligonucleotide. These 238 test oligonucleotides were commercially synthesized as pooled single-stranded oligonucleotides (Oligomix, LC Sciences, Houston, TX). The oligonucleotides were amplified using the universal primer regions by PCR with CloneAmp HiFi PCR Premix (CloneTech, Mountain View, CA).

Plasmid library preparation

The pIS-0 vector was linearized using *Sac*I-HF and *Bmt*I-HF restriction endonucleases (New England Biolabs, Ipswich, MA) and purified using QIAquick PCR spin columns (Qiagen, Germantown, MD). The linearized plasmid was mixed with 2 µL of unpurified double-stranded pooled oligonucleotides and plasmid assembly was performed using NEBuilder HiFi DNA assembly kit (NEB, Ipswich, MA) according to manufacturer's instructions. The universal primers matched the ends of the linearized pIS-0 plasmid and were used to amplify the test oligonucleotides, serving as the flanking homology regions for the NEBuilder assembly. Next, 2 µL of assembled product was transformed into One Shot OmniMax 2 TI Chemically Competent *E. coli* (Invitrogen, Carlsbald, CA).

Transformed cells were plated on six 10 cm LB-agar plates containing 100 µg/mL ampicillin. After overnight incubation, all colonies were harvested and added to 12 mL LB-broth containing 100 µg/mL ampicillin. The liquid culture was grown at 37°C for five hours, and plasmids were isolated using 10 QIAprep Spin Miniprep Columns (Qiagen, Germantown, MD) according to manufacturer's protocol. All plasmids isolated were combined to create the plasmid library for future experiments. DNA concentrations were measured using Qubit dsDNA BR Assay Kit (Invitrogen, Eugene, OR).

Cloning efficiency and plasmid representation

To assess representation of the 238 constructs in the plasmid library, 18 individual colonies were selected from the transformed bacteria plates and were grown in four mLs LB-broth containing 100 µg/mL ampicillin. Plasmids were isolated from each liquid culture using QIAprep Spin Miniprep Columns (Qiagen, Germantown, MD). Samples were Sanger sequenced using the reverse primer 5'-GTGGTTTGTCCAAACTCATC-3' (ACGT, Wheeling, IL). Target site representation was also determined from Next-generation sequencing of the plasmid pool described below. All wild-type and variant sequences were detected in the sequencing run.

Cell culture transfection

The pool of luciferase plasmids was transfected into HeLa, HepG2, HEK293, and HepaRG cells at 500 ng total plasmid for 48 hours as described previously for each cell line. After 48 hours, cells were lysed and total RNA was isolated and quantified for RNA-sequencing. cDNA was synthesized from 800 ng of total RNA using the QuantiTect Reverse Transcription Kit (Qiagen, Germantown, MD).

Molecular barcoding

PCR amplification was used to barcode the miRNA target sites within the 3'UTR of the luciferase gene using the flanking universal primer regions. Two microliters of cDNA and one picogram of the input plasmid pool were used as the PCR templates in separate reactions. A unique 6-nucleotide molecular barcode was added to the 5' end of both the forward and reverse primer. Five replicates of the input pool, five biological replicates for four different cell lines resulted in 25 unique pair of barcodes as listed in Table 15. The barcoded PCR products were purified using MinElute PCR Purification Kit (Qiagen, Germantown, MD). DNA was quantified and equimolar concentrations of each PCR product were combined to form the sequencing pool.

Next-generation sequencing

Pooled PCR products were sequenced using a modified protocol for Ion Proton system (Thermo Fisher Scientific, Waltham, MA). Briefly, the sequencing library was created by end polishing the barcoded PCR products, followed by adapter ligation and amplification. The resulting library was quantified and its quality assessed by Agilent Bioanalyzer (Agilent Technologies, Santa Clara, CA). Eight microliters of the 100 pM library was then applied to Ion Sphere Particles to prepare the sequencing template. The template was amplified using Ion OneTouch 2. The Ion Sphere Particles with the amplified template were loaded onto an IonPI chip and sequenced on the Ion Proton system per manufacturer's instructions. Approximately 41 million reads were generated from the sequencing run. Raw reads were generated as fastq files for bioinformatic analysis.

Bioinformatics and statistical analysis

The raw reads were aligned to the reference library containing the 238 test sequences (TMAP- Ion Torrent Suite, Thermo Fisher Scientific, Waltham, MA). The reads that aligned

to the reference library were filtered to retain reads with a mapping quality greater than 20. These reads were further filtered to include only those sequences with perfect barcodes at both ends.

Differential expression analysis was done by comparing the expression of each variant allele to the respective reference allele for all 119 SNPs. To account for differences in the concentrations of the variant and reference plasmids that were used for the transfections, the plasmid input correction factor for each target site was calculated as the average of the number of reads from the variant plasmid divided by the number of reads from the reference plasmid across 5 replicates of the plasmids. The reads from the variant alleles for all biological replicates were divided by the input correction factor. The corrected read counts were fit into a generalized linear model using EdgeR (Robinson et al., 2010) assuming a negative binomial distribution. Biological replicates and the genotype were used as covariates. The *p*-values and $\log_2$ fold-change of the variant alleles compared to the respective reference alleles were derived using likelihood ratio test on the genotype variable in the generalized linear model. The *p*-values were corrected for a false discovery rate (FDR) using the Benjamini and Hochberg algorithm (Benjamini and Hochberg, 1995).

Table 14: Wild type and variant miRNA sequences inserted into firefly luciferase plasmids

No.	RS no.	Wild-type Sequence	No.	Variant Sequence	SNP
1	rs10580	CCCCAACACCA CCCCTTGCCCA ACCAATGCAC	120	CCCCAACACCA CCCCTTGCCCA GCCAATGCAC	AG
2	rs4352283	ATCAGGTGCCA AGCCCTGTTCTA GGTGCTGGG	121	ATCAGGTGCCA AGCCCTGTTCT CGGTGCTGGG	AC
3	rs11581122	TCTACTTAGAAG GCTTGGGGCCC AGGGTAATG	122	TCTACTTAGAAG GCTTGGGGCCT AGGGTAATG	CT
4	rs5875	CCCCACCCACT CCTATACCATGA CATCAGTGT	123	CCCCACCCACT CCTATACCATGT CATCAGTGT	AT
5	rs28382751	GGAGGCCGAGG CGGGCAGATCA ACTGAGGTCG	124	GGAGGCCGAG GCGGGCAGATC ACCTGAGGTCG	AC
6	rs3947	GGGGCCACAGT CAGCTGGGGCA ACAGGTACTC	125	GGGGCCACAGT CAGCTGGGGCA GCAGGTACTC	AG
7	rs3134615	TACTGCTGCCTC TTTCCCACCTGC CTCATCTC	126	TACTGCTGCCT CTTTCCCACCTT CCTCATCTC	GT
8	rs186026692	AGACATCATCAA GTGGAGAGAAA TCATAGTTT	127	AGACATCATCA AGTGGAGAGAA GTCATAGTTT	AG
9	rs200253092	TTTGTTTATATTT TCCCATTTGGAC TGTAACT	128	TTTGTTTATATT TTCCCATTTGAA CTGTAACT	GA
10	rs200519094	AGAGAAATCATA GTTTAAACTGCA TTATAAAT	129	AGAGAAATCAT AGTTTAAACTGT ATTATAAAT	CT
11	rs201524771	ATTATGAAGAGG TATCTGTTTAAC ATTTCCTC	130	ATTATGAAGAG GTATCTGTTTAC CATTTCCTC	AC
12	rs202026600	ATTAAAAAGTAT TTAACATCTCTT ACAGTCAG	131	ATTAAAAAGTAT TTAACATCTCAT ACAGTCAG	TA
13	rs28364275	GAACTCTGACTG TATGAGATGTTA AATACTTT	132	GAACTCTGACT GTATGAGATGT CAAATACTTT	TC
14	rs28364280	ACTGCCTTGCTA AAAGATTATAGA AGTAGCAA	133	ACTGCCTTGCT AAAAGATTATAA AAGTAGCAA	GA

Table 14 cont'd

No.	RS no.	Wild-type Sequence	No.	Variant Sequence	SNP
15	rs150176505	GAAACCCCTCG ATTGTCTACCTC GATCGTACT	134	GAAACCCCTCG ATTGTCTACCTT GATCGTACT	CT
16	rs139156785	TTGGGAGCTGC CAAGAGTGAAG GGAAGAGACA	135	TTGGGAGCTGC CAAGAGTGAAG AGAAGAGACA	GA
17	rs17861086	AAGGTAATTGAA ATACCCCCCCG TCACTCCAG	136	AAGGTAATTGA AATACCCCCCC CTCACTCCAG	GC
18	rs35427048	AGGGAAGAGAC AGCCCAGGATA CTGGCACAGA	137	AGGGAAGAGAC AGCCCAGGATA TTGGCACAGA	CT
19	rs4986884	TGTAAGACCCTT ATTGCTGTCCTG GAGGGGCT	138	TGTAAGACCCT TATTGCTGTCC CGGAGGGGCT	TC
20	rs11636419	GGAGGATCATTT GAGCCCAGGAA TTGGAAAGC	139	GGAGGATCATT TGAGCCCAGGA GTTGGAAAGC	AG
21	rs17861162	ATTACAGGTGTG AGCCACGGTGC CCGGCCCAC	140	ATTACAGGTGT GAGCCACGGTG GCCGGCCCAC	CG
22	rs8192733	GAGGGAAGAGA AGAAACAGAAG GGGCTCAGTT	141	GAGGGAAGAGA AGAAACAGAAG CGGCTCAGTT	GC
23	rs1038376	GATCCACCCAC CTCAGTGTTCCA AAGTGCTGA	142	GATCCACCCAC CTCAGTGTTCC TAAGTGCTGA	AT
24	rs1042389	AGTCCTCATTCC CAGCTGCCTCTT CCTACTGC	143	AGTCCTCATTC CCAGCTGCCTC CTCCTACTGC	TC
25	rs28399502	GCTTCCTTCCCC TCCATGGCACC AGTTGTCTG	144	GCTTCCTTCCC CTCCATGGCAC AAGTTGTCTG	CA
26	rs28969420	TAAGCCTTGCTC TGTCTCCCAGG CTGGAGTGC	145	TAAGCCTTGCT CTGTCTCCCAG TCTGGAGTGC	GT
27	rs3181842	CTGGAGTGCAG TGGCGTGATCT CGGCTCACTG	146	CTGGAGTGCAG TGGCGTGATCT TGGCTCACTG	CT
28	rs4803420	ctaaattttgtatttttagG TGGTCTTGAACT	147	ctaaattttgtatttttag GTGTTCTTGAA CT	GT
29	rs707265	TTGAATGCTATT TTTGAGGTTCAT GCCTGTTG	148	TTGAATGCTATT TTTGAGGTTCG TGCCTGTTG	AG
30	rs7246465	ATTCACATAACA TAAAATTAGCTG TTTTAAAG	149	ATTCACATAACA TAAAATTAGCC GTTTTAAAG	TC

31	rs7260525	gtcaccgtgcccagcC ATGTATATATAT AAtt	150	gtcaccgtgcccagcC ATGTATGTATAT AAtt	AG
32	rs1058932	GAATGCTAGCC CATCTGGCTGC CGATCTGCTA	151	GAATGCTAGCC CATCTGGCTGC TGATCTGCTA	CT
33	rs9332242	TGCCTTTTCTCA CCTGTCATCTCA CATTTTCC	152	TGCCTTTTCTCA CCTGTCATCTG ACATTTTCC	CG
34	rs2480256	CCCCGCTTTCAA ACAAGTTTTCAA ATTGTTTG	153	CCCCGCTTTCA AACAAGTTTTCG AATTGTTTG	AG
35	rs2480257	GAACCCCCCGC TTTCAAACAAGA TTTCAAATT	154	GAACCCCCCGC TTTCAAACAAGT TTTCAAATT	AT
36	rs56307258	CCCCCGCTTTCA AACAAGTTTTCA AATTGTTT	155	CCCCCGCTTTC AAACAAGTTTTA AAATTGTTT	CA
37	rs7081484	AGTGTGTGGAG GACACCCTGAA CCCCCCGCTT	156	AGTGTGTGGAG GACACCCTGAA TCCCCCGCTT	CT
38	rs28371763	GAGTGAGACTC AGTCTTAAAAAT ATATGCCTT	157	GAGTGAGACTC AGTCTTAAAAAA ATATGCCTT	TA
39	rs15524	GGAGAATGAGT TATTCTAAGGAT TTCTACTTT	158	GGAGAATGAGT TATTCTAAGGAC TTCTACTTT	TC
40	rs17161788	ATGAGTTATTCT AAGGATTTCTAC TTTGGTCT	159	ATGAGTTATTCT AAGGATTTCTG CTTTGGTCT	AG
41	rs10211	CACAATGCACGT ACAGAATCCCC GATTATTTA	160	CACAATGCACG TACAGAATCCC TGATTATTTA	CT
42	rs12360	TAAGGACTTCTG GTTTGCTCTTCA AGAAAGCT	161	TAAGGACTTCT GGTTTGCTCTTT AAGAAAGCT	CT
43	rs139849737	TGCTGGGGAAG TAGATTTGGCTT CTCTGCTTC	162	TGCTGGGGAAG TAGATTTGGCT CCTCTGCTTC	TC
44	rs183800671	TCCTATTTTTATT AATGATTGTCGT TGAAATT	163	TCCTATTTTTAT TAATGATTGTG GTTGAAATT	CG
45	rs17470762	AATATAATGTTG ATAATATATATTA AGTGTGC	164	AATATAATGTTG ATAATATATACT AAGTGTGC	TC
46	rs184161277	TCTTTCCAAATT AAAACAAATATA CATTTTCT	165	TCTTTCCAAATT AAAACAAATACA CATTTTCT	TC

Table 14 cont'd

No.	RS no.	Wild-type Sequence	No.	Variant Sequence	SNP
47	rs188501488	AAATTAAAGGTA ATTTTTAATGTTA AAATGTT	166	AAATTAAAGGTA ATTTTTAATGAT AAAATGTT	TA
48	rs2151562	AGAACAGAATTT ATTAGAAACTTA CTAAAATT	167	AGAACAGAATTT ATTAGAAACTCA CTAAAATT	TC
49	rs291592	AGATCCTGGTTA CCACTCTTTTGC TGTGCACA	168	AGATCCTGGTT ACCACTCTTTTA CTGTGCACA	GA
50	rs291593	CCACTCTTTTGC TGTGCACATACG GGCTCTGA	169	CCACTCTTTTGC TGTGCACATAT GGGCTCTGA	CT
51	rs41285690	TCTCCTCTTCAT GGCATCTTCAAT ATGAATCT	170	TCTCCTCTTCAT GGCATCTTCAG TATGAATCT	AG
52	rs55696854	GTTGATAATATA TATTAAGTGTGC CAAATCAG	171	GTTGATAATATA TATTAAGTGTTC CAAATCAG	GT
53	rs56160474	GGATGTTCACTG CCAGTTGTCTTA TGTGAAAA	172	GGATGTTCACT GCCAGTTGTCT CATGTGAAAA	TC
54	rs201925035	TCCTTTCTCCAG GACCAATAAAAT TTCTAAGA	173	TCCTTTCTCCAG GACCAATAAAC TTTCTAAGA	AC
55	rs4630	CCAGAAAGCAG GAATGGCTTGC CTAAGACTTG	174	CCAGAAAGCAG GAATGGCTTGC TTAAGACTTG	CT
56	rs11086926	GTGCTTCTCCTC TCCTAGCCCCT GTCATGGTG	175	GTGCTTCTCCT CTCCTAGCCCC GGTCATGGTG	TG
57	rs114764820	CTCATCCTCCTT CTTCAGGGACTT GGGTGGGT	176	CTCATCCTCCTT CTTCAGGGACC TGGGTGGGT	TC
58	rs11574744	TGGCCTAAGGG CCACATCCCACT GCCACCCTT	177	TGGCCTAAGGG CCACATCCCAC AGCCACCCTT	TA
59	rs11574745	GAAGCCACTGC CTTCACCTTCAC CTTCATCCA	178	GAAGCCACTGC CTTCACCTTCAT CTTCATCCA	CT
60	rs183246640	GGAACACCAGG CTGAGGTCCTG ATCAGCTTCA	179	GGAACACCAGG CTGAGGTCCTG GTCAGCTTCA	AG
61	rs189107638	TCCTGTTTGCTG ATAAATATTAAG GAGAATTC	180	TCCTGTTTGCT GATAAATATTAG GGAGAATTC	AG

62	rs200905283	AAGGATGAAGG GCCCGAGAACA TGGCCTAAGG	181	AAGGATGAAGG GCCCGAGAACA AGGCCTAAGG	TA
63	rs3212210	AGAACAGCCTG AGCCAAGGCCT AGTGGTAGTA	182	AGAACAGCCTG AGCCAAGGCCT CGTGGTAGTA	AC
64	rs41280258	GGCCCGAGAAC ATGGCCTAAGG GCCACATCCC	183	GGCCCGAGAAC ATGGCCTAAGG ACCACATCCC	GA
65	rs41282030	CTACTGCCTTGG ACAACTTTTCTC ATGTTGAA	184	CTACTGCCTTG GACAACTTTTCC CATGTTGAA	TC
66	rs6103734	caactaggaagtggct gagtcaGgacttgaac	185	caactaggaagtggct gagtcaAgacttgaac	GA
67	rs4986993	TGAATTCCTAGA AAAGTTTTATTG GTAGATGA	186	TGAATTCCTAGA AAAGTTTTATGG GTAGATGA	TG
68	rs45539742	ATAAAGGCATTT TAAGGATGGCC TGTGATTAT	187	ATAAAGGCATTT TAAGGATGGCG TGTGATTAT	CG
69	rs10460826	TGCCCCCCACC CCCAGTTCAGTC TGTAGGGAG	188	TGCCCCCCACC CCCAGTTCAGT GTGTAGGGAG	CG
70	rs10511395	TTCCGAGCTGCT TTGTGGGCTCC AGGCCTGTA	189	TTCCGAGCTGC TTTGTGGGCTC AAGGCCTGTA	CA
71	rs1054190	ATTTGAACACAT TATTAAGCACCG ATAATAGG	190	ATTTGAACACAT TATTAAGCACTG ATAATAGG	CT
72	rs1054191	GTGGATGCTGA GCTGTGATGGC GGGCACTGGG	191	GTGGATGCTGA GCTGTGATGGC AGGCACTGGG	GA
73	rs113594465	CAGCCAGACCC AGAGCCCTCTG AGCCGCCACT	192	CAGCCAGACCC AGAGCCCTCTG GGCCGCCACT	AG
74	rs12107248	ACAAGGCTACG CTGACAATCAGT TAAACACAC	193	ACAAGGCTACG CTGACAATCAG ATAAACACAC	TA
75	rs12721615	AAATTTTTTTGC ATTTTCACAAAT TATACTTT	194	AAATTTTTTTGC ATTTTCACAAGT TATACTTT	AG
76	rs149397784	CAGGAAGGACA TGGGTGCCCCC CACCCCCAGT	195	CAGGAAGGACA TGGGTGCCCCC AACCCCCAGT	CA
77	rs185946310	CGCTTCCTGAGT CTTTTCATTGCT ACCTCTAA	196	CGCTTCCTGAG TCTTTTCATTGT TACCTCTAA	CT
78	rs200737867	GCTGCCCTTGG GTGACACCTCC GAGAGGCAGC	197	GCTGCCCTTGG GTGACACCTCC AAGAGGCAGC	GA

Table 14 cont'd

No.	RS no.	Wild-type Sequence	No.	Variant Sequence	SNP
79	rs2472683	GGGTACCCAAG TGAAGGTTCCCA AGGACATGA	198	GGGTACCCAAG TGAAGGTTCCC GAGGACATGA	AG
80	rs3732358	GTAGCTGAGCG GCTGCCCTTGG GTGACACCTC	199	GTAGCTGAGCG GCTGCCCTTGG ATGACACCTC	GA
81	rs3732359	AAGGGACCAAG CGACCAAGGAT GGGCCATCTG	200	AAGGGACCAAG CGACCAAGGAT AGGCCATCTG	GA
82	rs3732360	CAGGCCTGTAC TCATCGGCAGG CGCATGAGTA	201	CAGGCCTGTAC TCATCGGCAGG TGCATGAGTA	CT
83	rs3814057	TATATAAGGCAT TCCACACCTAAG AACTAGTT	202	TATATAAGGCAT TCCACACCTAC GAACTAGTT	AC
84	rs3814058	AAATGTAGCCCT GGGTTTAATGTC AAATCAAG	203	AAATGTAGCCC TGGGTTTAATG CCAAATCAAG	TC
85	rs6438550	AAAAACAAACAG AAACACAAACGA TTTGGATC	204	AAAAACAAACA GAAACACAAAC AATTTGGATC	GA
86	rs76580593	TTTCCTTTTAAA AGGCCCTGTGG TCTGGGGAG	205	TTTCCTTTTAAA AGGCCCTGTGT TCTGGGGAG	GT
87	rs112532686	TGAAAAAATGTG GACACACAAATT GGAAAAGA	206	TGAAAAAATGT GGACACACAAA CTGGAAAAGA	TC
88	rs114029015	GAGAAGTTATAT CTCTCTGATTAT GATAGTAT	207	GAGAAGTTATAT CTCTCTGATTGT GATAGTAT	AG
89	rs13860	CTTCAGTTTTAA TGACAAGCATTT CAGAAATA	208	CTTCAGTTTTAA TGACAAGCATC TCAGAAATA	TC
90	rs180751034	CAAACAATGCAC TTCTGTTAATGC AGTGTAAG	209	CAAACAATGCA CTTCTGTTAATT CAGTGTAAG	GT
91	rs185103906	AGGTTCCTATCA AAATTTGTGGGA GTAGGGAT	210	AGGTTCCTATC AAAATTTGTGGT AGTAGGGAT	GT
92	rs189039600	GTTTAAATTAAC ATGTACGCTGCA GAACATTG	211	GTTTAAATTAAC ATGTACGCTGA AGAACATTG	CA
93	rs189331203	ATTCTTCTTAGC CTCTATGGCGCT GGTCTATG	212	ATTCTTCTTAGC CTCTATGGCGT TGGTCTATG	CT

94	rs9457846	GCACCTGAGAG AGATGTTTTGCG GCGATGTCG	213	GCACCTGAGAG AGATGTTTTGCA GCGATGTCG	GA
95	rs4149087	CACAGAGTTTGA ACTATAATACTA AGGCCTGA	214	CACAGAGTTTG AACTATAATACG AAGGCCTGA	TG
96	rs4149088	AGGCCTGAAGT CTAGCTTGGATA TATGCTACA	215	AGGCCTGAAGT CTAGCTTGGAT GTATGCTACA	AG
97	rs71581985	CTTCTGTGTTTC CAAACAGCATTG CATTGATT	216	CTTCTGTGTTTC CAAACAGCATG GCATTGATT	TG
98	rs71581986	GGATATATGCTA CAATAATATCTG TTACTCAC	217	GGATATATGCT ACAATAATATCC GTTACTCAC	TC
99	rs79775553	CTTCTGCTTCTG TGTTTCCAAACA GCATTGCA	218	CTTCTGCTTCTG TGTTTCCAAAGA GCATTGCA	CG
100	rs189727189	CCTGTAGCCAG TCAGAAATGAGC TTATTCATA	219	CCTGTAGCCAG TCAGAAATGAG TTTATTCATA	CT
101	rs79132805	TTTCTACTGGAC CCATGGAAGTG GATTAAGAA	220	TTTCTACTGGAC CCATGGAAGTA GATTAAGAA	GA
102	rs1042157	AATAAAATATGA ATTGAGGGCCC GGGACGGTA	221	AATAAAATATGA ATTGAGGGCCT GGGACGGTA	CT
103	rs6839	GAGCTGTGAGA GGGGCTCCTGG AGTCACTGCA	222	GAGCTGTGAGA GGGGCTCCTGG GGTCACTGCA	AG
104	rs1142365	GAAAagcaaccccgt ctctactAaaaatacaa	223	GAAAagcaaccccg tctctactGaaaataca a	AG
105	rs144017186	GAGGCTGACAA GACATATCTCTC GGGAGAGTA	224	GAGGCTGACAA GACATATCTCT GGGGAGAGTA	CG
106	rs1802650	TGCACCTGGCC TGACATTCTTTA TGAAATTTA	225	TGCACCTGGCC TGACATTCTTTT TGAAATTTA	AT
107	rs189810658	GGCTAATTTTTT TGTATTTTTACT AGAGACGG	226	GGCTAATTTTTT TGTATTTTTAGT AGAGACGG	CG
108	rs55661878	AAACAATCTATA TGGAACAAACAT TCCCAAAT	227	AAACAATCTATA TGGAACAAACG TTCCCAAAT	AG
109	rs55818790	TAAAAAAATATT TCAAAATGCAAT GCATATTA	228	TAAAAAAATATT TCAAAATGCAG TGCATATTA	AG
110	rs55839603	TTCAAGGTGGTC CCAAAAGTTATA TAAAAGAT	229	TTCAAGGTGGT CCCAAAAGTTA CATAAAAGAT	TC

No.	RS no.	Wild-type Sequence	No.	Variant Sequence	SNP
111	rs9465100	TTTACttttatgtagagacaggGtctcacttt	230	TTTACttttatgtagagacaggAtctcacttt	GA
112	rs1042640	CGGGATTCAAAGGTGGTCCCACGGCTGCCCCT	231	CGGGATTCAAAGGTGGTCCCACCGCTGCCCCT	GC
113	rs10929303	TGAATATGTATCGTGCCCCCTCTGGTGTCTTT	232	TGAATATGTATCGTGCCCCCTCCGGTGTCTTT	TC
114	rs8330	ATGGTCAGTCCTCATCTCTGTCGTGCTTCATA	233	ATGGTCAGTCCTCATCTCTGTCCTGCTTCATA	GC
115	rs35791822	AAATACAATGGGGGGAAGGATAGCATTTGGAG	234	AAATACAATGGGGGGAAGGATATCATTTGGAG	GT
116	rs138053056	GTAGACAATGGCTCTGACTCCCCGCAACTTC	235	GTAGACAATGGCTCTGACTCCCTGCAACTTC	CT
117	rs146050194	GGAGCTGGTATCACAGGCGTCCCCCACCACG	236	GGAGCTGGTATCACAGGCGTCCTCCACCACG	CT
118	rs183641079	CTCCAAATGTTTTCATTATCTCCCCCCCAAC	237	CTCCAAATGTTTTCATTATCTCTCCCCCAAC	CT
119	rs12979270	ACACACTGCTGTAGTCTTCCCCAGTCCTCAT	238	ACACACTGCTGTAGTCTTCCCCCGTCCTCAT	AC

*Empty vector sequence (if no miRNA target site was inserted) [26 bp]: TATACGCGTCTCAAGCTTACTGCTAG

Table 15: Barcodes and primers in 5'>3' direction

No	Sample	5' Barcode *and Primer* (27 nt)	3' Barcode *and Primer** (25 nt)
1	HeLa Rep 1	**ACATGT***GCCGTGTA ATTCTAGGAGCTC*	**ACAACC***CCGCCCCGA CTCTAGAACG*
2	HeLa Rep 2	**ACCTTT***GCCGTGTA ATTCTAGGAGCTC*	**ACGGTT***CCGCCCCGA CTCTAGAACG*
3	HeLa Rep 3	**AGAAGG***GCCGTGT AATTCTAGGAGCTC*	**AGACGT***CCGCCCCGA CTCTAGAACG*
4	HeLa Rep 4	**AGTGGA***GCCGTGT AATTCTAGGAGCTC*	**AGTTAC***CCGCCCCGA CTCTAGAACG*
5	HeLa Rep 5	**ATCAAC***GCCGTGTA ATTCTAGGAGCTC*	**ATGCAC***CCGCCCCGA CTCTAGAACG*
6	HEK Rep 1	**ATGTTG***GCCGTGTA ATTCTAGGAGCTC*	**CAATAC***CCGCCCCGA CTCTAGAACG*
7	HEK Rep 2	**CACAAG***GCCGTGT AATTCTAGGAGCTC*	**CATCTA***CCGCCCCGA CTCTAGAACG*
8	HEK Rep 3	**CCAAAT***GCCGTGTA ATTCTAGGAGCTC*	**CGTTTC***CCGCCCCGA CTCTAGAACG*
9	HEK Rep 4	**CTATGG***GCCGTGTA ATTCTAGGAGCTC*	**CTCCTT***CCGCCCCGA CTCTAGAACG*
10	HEK Rep 5	**GAAACC***GCCGTGT AATTCTAGGAGCTC*	**GACAAT***CCGCCCCGA CTCTAGAACG*
11	HepG2 Rep 1	**GCACTA***GCCGTGTA ATTCTAGGAGCTC*	**GCGTTT***CCGCCCCGA CTCTAGAACG*
12	HepG2 Rep 2	**GGTCTA***GCCGTGTA ATTCTAGGAGCTC*	**GTAATC***CCGCCCCGA CTCTAGAACG*
13	HepG2 Rep 3	**GTAGAG***GCCGTGT AATTCTAGGAGCTC*	**GTTAGT***CCGCCCCGA CTCTAGAACG*
14	HepG2 Rep 4	**TAACCC***GCCGTGTA ATTCTAGGAGCTC*	**TACAGA***CCGCCCCGA CTCTAGAACG*
15	HepG2 Rep 5	**TAGAAC***GCCGTGTA ATTCTAGGAGCTC*	**TATGCC***CCGCCCCGA CTCTAGAACG*
16	HepaRG Rep 1	**TCAAAG***GCCGTGTA ATTCTAGGAGCTC*	**TCCATA***CCGCCCCGA CTCTAGAACG*
17	HepaRG Rep 2	**TCGATT***GCCGTGTA ATTCTAGGAGCTC*	**TCTACC***CCGCCCCGA CTCTAGAACG*
18	HepaRG Rep 3	**TGCTAG***GCCGTGTA ATTCTAGGAGCTC*	**TGAACC***CCGCCCCGA CTCTAGAACG*
19	HepaRG Rep 4	**TTCGAA***GCCGTGTA ATTCTAGGAGCTC*	**TTAACG***CCGCCCCGA CTCTAGAACG*
20	HepaRG Rep 5	**AAACAC***GCCGTGT AATTCTAGGAGCTC*	**TTCTGG***CCGCCCCGA CTCTAGAACG*
21	Plasmid Input 1	**TAAGAC***GCCGTGTA ATTCTAGGAGCTC*	**TGCTCA***CCGCCCCGA CTCTAGAACG*

22	Plasmid Input 2	***TGGGAT****GCCGTGTA* *ATTCTAGGAGCTC*	**TCTTAG***CCGCCCCGA* *CTCTAGAACG*
23	Plasmid Input 3	**TCTGCT***GCCGTGTA* *ATTCTAGGAGCTC*	**AAGAAC***CCGCCCCGA* *CTCTAGAACG*
24	Plasmid Input 4	**AACGGT***GCCGTGT* *AATTCTAGGAGCTC*	**AACTTC***CCGCCCCGA* *CTCTAGAACG*
25	Plasmid Input 5	***AATGTG****GCCGTGTA* *ATTCTAGGAGCTC*	**GCAGAA***CCGCCCCGA* *CTCTAGAACG*

*Please note that the 3' barcode as shown above will be read on the complimentary (bottom) strand. The reverse compliment of the 3' barcode will be seen on the main (top) strand.

Results

Our bioinformatic predictions identified hundreds of variants in the 3'UTR in pharmacogenes that could alter miRNA regulation. It is not practical to test all these variants individually using the traditional luciferase reporter assay. As a novel approach to functionally test the large number of variants in the 3'UTR that could affect gene expression, we modified the luciferase reporter assay to develop PASSPORT-seq (Parallel Assessment of Polymorphisms in miRNA Target Sites sequencing) (Figure 22). PASSPORT-seq is a high-throughput bioassay that can functionally test hundreds of variants in miRNA target sites in parallel, as well as the functional testing of these variants in different cell lines to subject miRNA target sites to different miRNA environments. We synthesized and cloned 238 miRNA target sites into the pIS-0 luciferase plasmid; each contained either the wild-type or variant miRNA target site (119 wild-type-variant pairs). The pool of 238 plasmids was then transfected into four cell lines and the luciferase gene expression was measured by next-generation sequencing. The difference in mRNA expression between the wild-type and variant plasmids indicate a functional variant in miRNA target sites.

We tested 119 variants in HeLa (cervical cancer), HepG2 (liver carcinoma), HEK293 (embryonic kidney), and HepaRG (liver carcinoma). Out of the 119 wild-type and variant pairs tested, 38 variants resulted in FDR-significantly altered expression in at least one cell line (Table 16). Twenty-one variants were observed to have increased expression, whereas, 17 variants had decreased expression compared to the wild-type allele. There were many differences and similarities in wild-type versus variant expression levels between the cell lines. Only four variants were FDR-significant and 34 went in the same direction among all four cell lines when considering SNPs that were FDR-significant in at

least one cell line (Figure 23). These differences between cell lines, most likely reflect differences in the miRNA expression profiles between these different cell types.

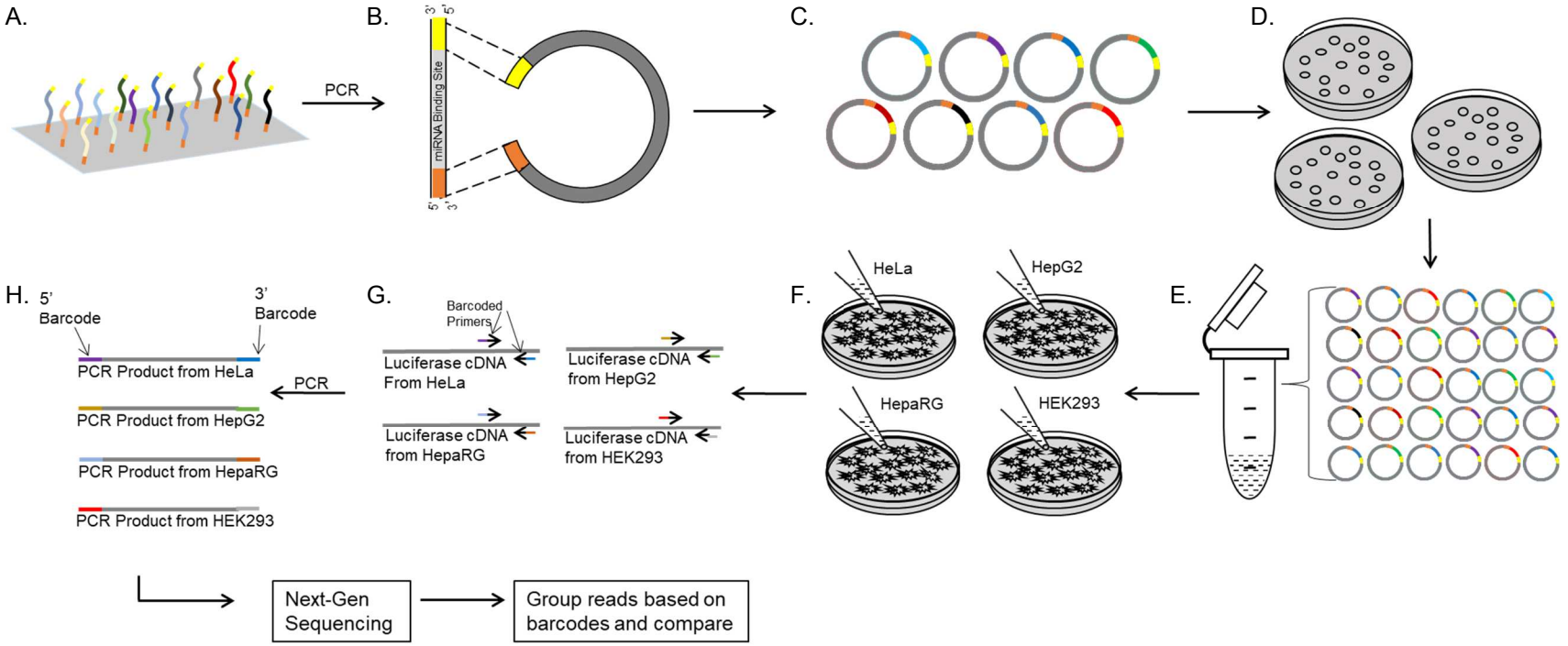

Figure 22: PASSPORT-sequencing workflow

PASSPORT-sequencing workflow: A) 119 wild-type and variant miRNA target regions each with the same 15-20 bp flanking sequence were synthesized as an oligonucleotide pool B) using the flanking universal sequences, the oligonucleotide pool was amplified and made double stranded by PCR. The pIS-0 plasmid was linearized by restriction enzymes. C) The double stranded oligonucleotides were inserted into the linear plasmid using the NEBuilder gene assembly system. D) Chemically competent bacteria were transformed with the plasmid pool containing the test miRNA target regions. Transformed bacteria were plated on 4 plates. E) All colonies from the plates were harvested, combined and scaled up in liquid culture. Plasmids were isolated from the liquid culture. F) Four cell lines were

transfected with the plasmid pool and incubated for 48 hours after which cDNA was prepared from total RNA. G) miRNA target regions were amplified using universal primers that were uniquely barcoded for replicates within cell lines and for the input plasmid pool. H) The barcoded PCR products were combined to form the sequencing pool.

Table 16: 3'UTR variants predicted to alter miRNA targeting among four cell lines

SNP	Wild-type	Variant	HEK293 (Var/WT) logFC*	HeLa (Var/WT) logFC	HepG2 (Var/WT) logFC	HepaRG (Var/WT) logFC
rs11086926	T	G	0.94	0.73	0.81	1.29
rs7081484	C	T	0.44	0.16	0.38	0.72
rs5875	A	T	-0.03	0.27	0.11	0.62
rs139156785	G	A	0.42	0.36	0.11	0.61
rs45539742	C	G	0.47	0.23	0.23	0.57
rs12721615	A	G	0.17	0.11	0.22	0.55
rs7246465	T	C	0.19	0.11	0.23	0.54
rs2480256	A	G	0.55	0.39	0.44	0.51
rs1058932	C	T	0.17	-0.01	0.08	0.49
rs7260525	A	G	0.14	0.55	0.42	0.45
rs3947	A	G	0.70	0.30	0.52	0.45
rs202026600	T	A	0.12	0.15	0.32	0.42
rs10929303	T	C	0.14	0.10	0.11	0.41
rs17161788	A	G	0.12	0.11	0.15	0.40
rs3814057	A	C	0.27	0.15	0.29	0.38
rs55818790	A	G	0.22	0.20	0.19	0.35
rs13860	T	C	0.32	0.48	0.54	0.34
rs112532686	T	C	0.12	0.27	0.24	0.34
rs28382751	A	C	0.35	0.27	0.31	0.31
rs189810658	C	G	0.28	0.21	0.31	0.31
rs1038376	A	T	0.22	0.22	0.37	0.29

Table 16 cont'd

SNP	Wild-type	Variant	HEK293 (Var/WT) logFC	HeLa (Var/WT) logFC	HepG2 (Var/WT) logFC	HepaRG (Var/WT) logFC
rs4803420	G	T	-0.27	-0.29	-0.47	0.28
rs1042640	G	C	0.27	0.14	0.36	0.26
rs17470762	T	C	0.11	0.09	0.02	0.25
rs4149088	A	G	0.28	0.12	0.16	0.25
rs9465100	G	A	0.15	0.27	0.19	0.25
rs71581985	T	G	0.35	0.04	0.14	0.23
rs146050194	C	T	0.31	0.06	0.24	0.21
rs56160474	T	C	0.35	0.27	0.29	0.20
rs15524	T	C	0.29	0.27	0.39	0.19
rs1142365	A	G	0.25	0.04	0.17	0.18
rs183800671	C	G	0.26	0.11	0.23	0.17
rs4352283	A	C	0.08	0.09	0.31	0.16
rs3732359	G	A	0.02	-0.15	0.01	0.16
rs79132805	G	A	-0.13	0.10	0.07	0.16
rs185946310	C	T	0.10	0.01	-0.15	0.16
rs707265	A	G	0.16	0.22	0.19	0.15
rs41285690	A	G	0.41	0.23	0.18	0.15
rs2472683	A	G	0.32	0.13	0.16	0.15
rs3732358	G	A	0.28	0.13	0.18	0.15
rs184161277	T	C	0.12	0.10	0.17	0.14
rs8192733	G	C	0.46	0.28	0.37	0.14
rs201925035	A	C	0.26	0.30	0.21	0.13
rs3212210	A	C	0.30	0.06	-0.04	0.11

rs139849737	T	C	0.17	0.12	0.09	0.11
rs180751034	G	T	-0.19	-0.07	-0.13	0.08
rs79775553	C	G	0.10	0.08	0.10	0.07
rs201524771	A	C	0.14	-0.10	0.12	0.06
rs3814058	T	C	0.20	0.16	0.13	0.06
rs200737867	G	A	-0.07	-0.14	0.18	0.06
rs11574745	C	T	0.23	0.01	0.11	0.04
rs2151562	T	C	0.17	-0.02	0.07	0.03
rs56307258	C	A	0.21	0.16	0.04	0.03
rs41280258	G	A	0.17	0.38	-0.07	0.03
rs1042157	C	T	0.11	0.23	0.31	0.02
rs8330	G	C	0.08	0.21	0.07	0.02
rs28364280	G	A	-0.14	-0.08	-0.26	0.01
rs138053056	C	T	0.12	0.15	0.28	0.01
rs114764820	T	C	0.18	0.18	0.11	0.00
rs10580	A	G	0.15	0.10	0.28	0.00
rs41282030	T	C	0.07	0.06	-0.04	-0.01
rs114029015	A	G	0.22	0.13	0.19	-0.01
rs28364275	T	C	0.10	0.09	0.08	-0.03
rs188501488	T	A	0.16	0.12	0.06	-0.03
rs183641079	C	T	0.33	-0.18	0.05	-0.05
rs11574744	T	A	0.10	0.07	0.07	-0.08
rs185103906	G	T	0.08	0.02	0.07	-0.08
rs4986993	T	G	0.19	-0.09	-0.13	-0.08
rs189107638	A	G	0.13	0.06	0.13	-0.09
rs28969420	G	T	0.07	0.17	-0.01	-0.11
rs200519094	C	T	0.02	-0.04	-0.08	-0.11

Table 16 cont'd

SNP	Wild-type	Variant	HEK293 (Var/WT) logFC	HeLa (Var/WT) logFC	HepG2 (Var/WT) logFC	HepaRG (Var/WT) logFC
rs11636419	A	G	0.12	-0.05	-0.06	-0.12
rs17861086	G	C	-0.12	-0.25	-0.02	-0.12
rs12360	C	T	-0.13	-0.04	0.03	-0.13
rs4630	C	T	-0.06	-0.01	-0.20	-0.13
rs1054191	G	A	-0.05	-0.04	0.09	-0.14
rs200905283	T	A	0.02	-0.09	-0.26	-0.14
rs149397784	C	A	0.10	0.06	0.02	-0.15
rs3134615	G	T	-0.23	-0.13	-0.30	-0.15
rs6438550	G	A	0.00	0.09	-0.06	-0.16
rs12107248	T	A	0.14	0.15	-0.01	-0.17
rs291593	C	T	-0.18	-0.26	-0.22	-0.17
rs9457846	G	A	-0.14	-0.03	-0.06	-0.17
rs10460826	C	G	0.06	0.05	0.07	-0.18
rs28399502	C	A	-0.14	-0.12	-0.17	-0.22
rs76580593	G	T	-0.08	0.05	-0.19	-0.24
rs1042389	T	C	-0.03	0.00	-0.09	-0.24
rs1802650	A	T	0.06	-0.11	-0.21	-0.26
rs10511395	C	A	-0.22	-0.21	-0.26	-0.28
rs189727189	C	T	-0.18	-0.10	-0.18	-0.28
rs6103734	G	A	0.04	-0.01	-0.03	-0.29
rs4149087	T	G	0.07	0.06	0.19	-0.30
rs183246640	A	G	-0.26	-0.31	-0.25	-0.32
rs291592	G	A	-0.31	-0.15	-0.22	-0.32

rs11581122	C	T	-0.12	-0.32	-0.27	-0.33
rs2480257	A	T	0.02	-0.13	-0.06	-0.33
rs71581986	T	C	-0.07	-0.05	-0.03	-0.33
rs4986884	T	C	-0.33	-0.08	-0.41	-0.33
rs144017186	C	G	-0.35	-0.15	-0.36	-0.35
rs3732360	C	T	-0.15	-0.20	-0.29	-0.36
rs10211	C	T	-0.40	-0.10	-0.05	-0.37
rs55696854	G	T	-0.31	-0.22	-0.44	-0.37
rs35427048	C	T	0.11	-0.10	0.19	-0.39
rs150176505	C	T	-0.40	-0.22	-0.35	-0.39
rs189039600	C	A	-0.15	-0.40	-0.51	-0.41
rs28371763	T	A	-0.51	-0.33	-0.47	-0.42
rs189331203	C	T	-0.52	-0.41	-0.44	-0.42
rs200253092	G	A	-0.07	-0.14	0.06	-0.43
rs9332242	C	G	0.14	0.10	0.10	-0.48
rs3181842	C	T	-0.19	-0.16	-0.07	-0.48
rs1054190	C	T	-0.44	-0.15	-0.33	-0.49
rs55839603	T	C	0.14	0.12	0.05	-0.50
rs186026692	A	G	-0.01	0.01	-0.06	-0.56
rs35791822	G	T	-0.37	-0.24	-0.37	-0.56
rs55661878	A	G	-0.28	-0.19	-0.26	-0.58
rs6839	A	G	-0.59	-0.47	-0.69	-0.61
rs17861162	C	G	-0.42	-0.30	-0.39	-0.64
rs12979270	A	C	-0.03	-0.02	-0.12	-0.71
rs113594465	A	G	-0.84	-0.95	-0.98	-1.49

* logFC= $\log_2$ fold change

FDR Negative FC	p-value Negative FC	Not Sig Negative FC
FDR Positive FC	p-value Positive FC	Not Sig Positive FC

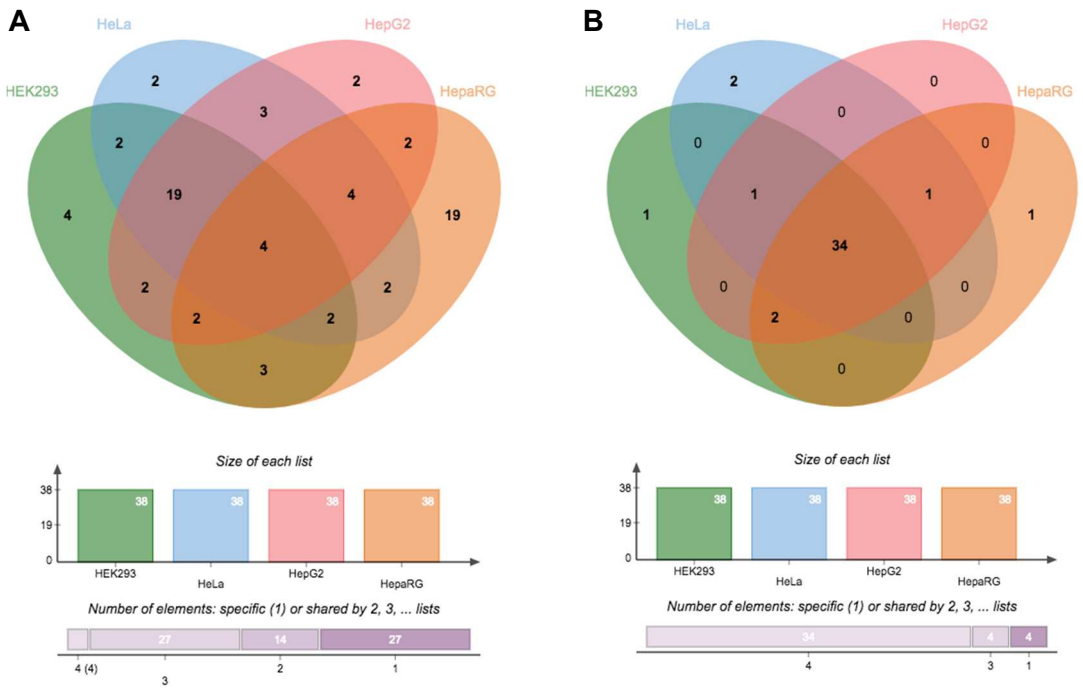

Figure 23: Significance and directionality overlap between four cell lines among variants that were FDR-significant in at least one cell line

The number of variants that overlap between the four different cells by **A.** FDR-significance or **B.** directionality among variants that were FDR-significant in at least one cell line.

Discussion

Due to the large number of 3'UTR genetic variants predicted to alter miRNA regulation, a more high-throughput way to functionally test these variants is necessary versus traditional individual luciferase assays as previously performed (Figure 21). Our lab created PASSPORT-seq to test hundreds of variants simultaneously in multiple cell lines (Figure 22). As a result, we functionally tested 119 wild-type-variant pairs to determine if the variant resulted in differential expression in HeLa, HepG2, Hek293, and HepaRG cells. These variants were predicted to alter miRNA binding using prediction tools such as PolymiRTS and from allele specific expression analysis in our RNA-seq data of 30 human liver tissues discussed in Chapter 1. This high-throughput assay allows us to better select candidate SNP pairs for further validation.

This high-throughput assay will be useful for the testing of 3'UTR variants in any set of genes of interests, including variants that affect the 3'UTR though the binding of repression elements other than miRNAs. A major benefit of PASSPORT-seq is that it enables you test hundreds of variants in a couple of weeks. The testing of the wild-type and variant sequence plasmids within the same transfected well of cells, eliminates much of the variability within biological replicates. Data from this high-throughput assay highlight effects at the transcript level as miRNAs are known to lead to the degradation of target mRNA. Although a limitation of this assay is that protein levels are not measured, which may increase the number of false negatives (i.e. variants that alter miRNA's ability to repress translation), it is also an advantage in that additional experiments are not needed to dissect whether the mechanism is on mRNA stability or translation. Subsequent individual luciferase assays will determine if protein activity is altered.

Other limitations of this assay include testing the miRNA target sites out of context, as only a 32-base pair region is tested. As a result, any effects regarding structural changes, such as mRNA secondary structures that may make the 3'UTR more or less accessible to miRNAs, will not be captured. The same holds true for individual luciferase experiments, so studies involving the full length mRNA with and without the variant miRNA binding sites will aid in determining the variant effect on mRNA regulation. Such a study can be performed utilizing CRISPR-Cas9, a tool that can be used to manipulate the DNA of genes of interest. However, PASSPORT-seq should prove to be a time-efficient way to functional test hundreds of 3'UTR variants, aiding in the selection of variants for further testing using other methods.

CONCLUSION

Collectively, our studies provide evidence that hepatic miRNA expression changes during the developmental periods. These changes have the potential to impact and explain known developmental changes in hepatic gene expression and subsequent processes, such as drug metabolism, as miRNAs are able to negatively regulate protein expression through the degradation of mRNA or translational repression. Better characterization of these developmental changes in hepatic miRNA expression can be obtained through measuring expression levels at more narrow age intervals, as well as during periods of well-documented physiological changes such as less than one year old, pre/post-puberty and menopause, and in geriatric populations. However, more liver samples will be needed at these various intervals for assessment. These changes in miRNA expression can then be linked to corresponding alterations in hepatic gene expression between the developmental periods, but further testing is warranted to elucidate the meaning of these changes.

In the case of drug metabolism, alterations in mRNA expression can be mediated through targeting not only enzymes directly involved in the biotransformation of drugs, but through the targeting of upstream transcription factors. This complexity of miRNA regulation becomes difficult to interpret as upstream transcription factors have multiple downstream targets and miRNAs themselves have multiple targets. Studies regarding miRNA stability, differential expression in various tissues and cell lines, and factors that are responsible for the regulation of miRNAs will aid in the interpretation of miRNA-related experiments. In the case of miRNA inhibitors, if the endogenous miRNA is not expressed in the cell culture model, then no effect would be observed with the inhibitor as there is no miRNA to be sequestered. Knowledge of these miRNA expression profiles in different cell lines is a way to address this limitation and may explain cell-type specific differences in gene regulation.

Furthermore, an array of techniques is necessary to validate the role of miRNAs in contributing to these developmental changes in pharmacogenes. Measuring mRNA and protein activity after miRNA and/or inhibitor treatment are only a few ways to validate miRNA-mRNA interactions. Measuring protein activity is crucial as miRNAs can prevent the translation of mRNA to protein, a consequence that is not captured when measuring mRNA expression alone. Proof of miRNA binding will also be a highly valuable area to explore as techniques are being developed to measure miRNA-mRNA interactions in an unbiased approach that is not limited to the seed sequence and other canonical binding requirements.

Our studies have also shown that genetic variations in the 3'UTR have the potential to further impact miRNA targeting and provide evidence for the inter-individual variability in drug pharmacokinetic profiles. As the field of pharmacogenetics has primarily focused on genetic variants in the coding and promoter regions, our findings will open up the field to consider 3'UTR variants as a source of variability in the activities of many pharmacogenes. Furthermore, studies that prove more definitively that miRNAs bind to these target sites will be able to confirm miRNAs as a source of variability as opposed to variant-induced structural changes in the mRNA that may affect its accessibility and stability. Also, more popularly used techniques to validate miRNA-variant interactions, involve cloning a section of the miRNA binding site into a luciferase plasmid. However, removing the binding site out of context prevents the assessment of structural changes and alterations by other repressor elements. To overcome these limitations in studying genetic variation effects on miRNA regulation, tools such as CRISPR-Cas9 will prove useful in manipulating a gene of interest while maintaining other contextual factors.

Overall, this research uncovers the fact that these miRNA expression profiles differ between fetal, pediatric, and adult human livers, suggesting epigenetic regulation by miRNAs as a potential mechanism for the regulation of gene expression in the human liver. Our studies provide evidence that hepatic miRNAs, in part, may be a contributor of these known developmental changes in pharmacogenes and changes in the pharmacokinetic profiles of various drugs. Additional studies are necessary to better understand the connection between these developmentally-regulated miRNAs and altered hepatic gene expression across the developmental stages. Through uncovering how miRNAs are regulated, better understanding of the mechanisms by which these developmental changes occur will follow.

FUTURE DIRECTIONS

Conversion of liver cell gene expression by miRNAs

Our current findings have provided evidence that miRNA expression changes throughout development, revealing new questions to be answered. It has been well known that large changes occur among the expression of hepatic drug disposition genes during liver development. It would be important to determine if these developmentally-regulated miRNAs are directly linked to developmental drug disposition gene changes. In order to link developmentally-regulated hepatic miRNAs to gene expression changes in the liver, 18 of the 72 hepatic miRNAs downregulated from fetal to pediatric were transfected into HepaRG cells (an adult cell line) and RNA and protein was isolated to measure pharmacogene expression using RNA-sequencing and mass-spectrometry based proteomic methods.

The goal was to determine if the HepaRG cells revert back to a more fetal-like gene expression state when transfected with miRNA that was highly expressed in fetal liver tissues. Preliminary results show that the highly expressed fetal miRNAs altered mRNA expression profiles in adult HepaRG cells compared to *C. elegans* cel-miR-67 negative control (Figure 24 and 25) as there were 683 genes significantly upregulated and 480 downregulated after fetal miRNA transfection. However, bioinformatics analysis is necessary to compare these changes between the fetal and pediatric changes discussed in Chapter 1, as our comparator is fetal liver tissue and not the *C. elegans* miRNA negative control. Next, this experiment can either be repeated with the remaining 54 downregulated miRNAs and changes can be bioinformatically combined to assess the entire effects of all 72 miRNAs or a custom library of the 72 miRNAs can be transfected at lower concentrations per miRNA so that all miRNA interactions can be assessed in the same

biological replicate. Information from this study will further improve our fundamental understanding of miRNAs role in the ontogeny of hepatic pharmacogenes.

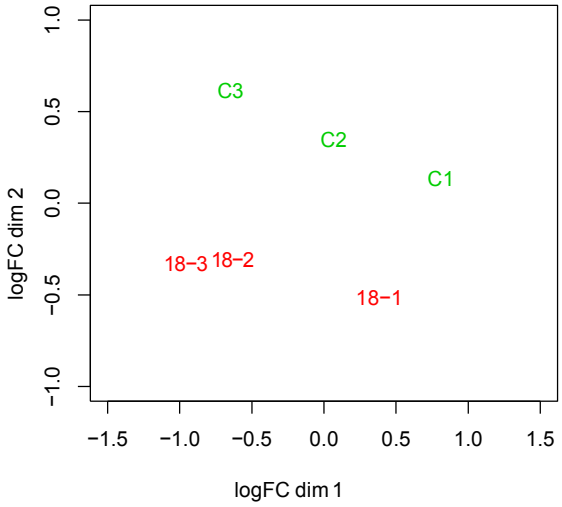

Figure 24: Multiple dimensional scaling plot comparing mRNA expression profiles of HepaRG cells transfected with fetal miRNAs or control (*C.elegans*) miRNA

Multi-dimensional scaling plot shows the level of similarity between the two groups of transfected cells. *X*-axis: $\log_2$ fold change for dimension 1 (dim 1). *Y*-axis: $\log_2$ fold change for dimension 2 (dim 2). 18-1, 18-2, 18-3 are biological replicates for HepaRG cells transfected with a combination of fetally miRNAs. C1, C2, C3 are biological replicates for HepaRG cells transfected with control miRNAs.

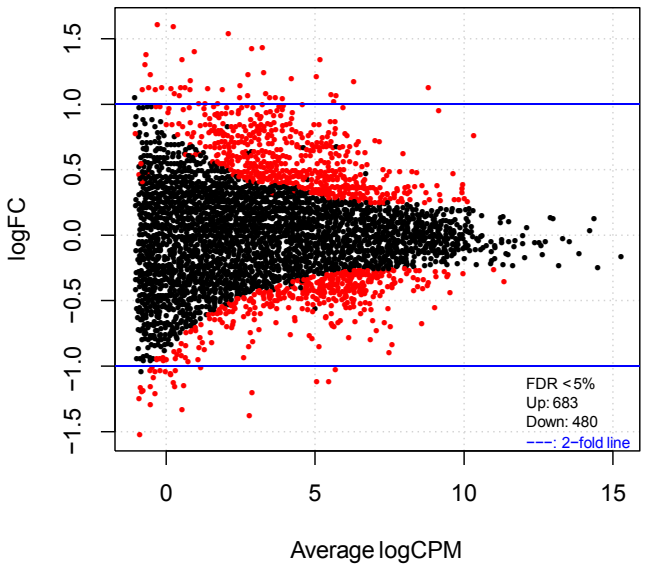

Figure 25: Bland-Altman plot comparing mRNA expression profiles of HepaRG cells transfected with fetal miRNAs or control (*C.elegans*) miRNA

Bland-Altman plot as a representation of the mRNA expression data. *X*-axis: Average logCPM (log_2 counts per million); *Y*-axis: log_2 fold change. The blue line represents a 2-fold change. Black dots are genes that are not significantly different between the fetal miRNA-treated and control-treated HepaRG cells. Red dots are statistically significant after FDR correction.

Assessing the effects of 3'UTR polymorphisms on miRNA regulation

In continuation of our study assessing the effects of polymorphisms in miRNA target sites in Chapter 4, individual luciferase assays to assess 3'UTR variants is necessary to validate our high-throughput assay findings. Due to the large number of variants predicted to alter miRNA regulation, the high-throughput assay aided in the selection of candidate SNPs to test individually. The clinical implications of these candidate polymorphisms in the 3'UTR can be followed up in human pharmacokinetic clinical trials through collaborative efforts as described in Chapter 3. Utilizing pharmacokinetic data of the drug disposition gene/genes of interests, will help determine if the 3'UTR variant accounts for variability in enzyme activity. Information from these studies will further progress utilizing genetic testing to predict patient response to drugs.

A novel approach to validate genetic variant effects on gene expression is to utilize the CRISPR-Cas9 genome editing system (Yu et al., 2016). This technique will allow for genetic variation comparisons within the same cell line. This is critical as cell-specific differences exist such as miRNA expression profiles, gene expression, and genetic differences within the 3'UTR. For example, the rs70950385 variant discussed in Chapter 3, differs between the cell lines. We sequenced the 3'UTR of *CYP2B6* in HeLa, HepG2, and HepaRG cells. For the rs70950385 variant that had been previously shown to alter miRNA targeting of miR-1275, HeLa cells were homozygous for the CA allele, whereas the HepG2 and HepaRG cells are heterozygous.

To precisely alter this variant in the 3'UTR, we transfect the platinum Cas9 protein, guide RNA (gRNA), and single-stranded oligo into HeLa cells using a lipid-based transfection. The gRNA 'AGGCAGCTGGGAATGAGGAT' will guide the Cas9 protein to create a double

strand break near our site of interest. A single-stranded oligo harboring the precise 3'UTR edit 5'-EEAACCTGGGCCAAGGGGGCTTTTTGATAGACGGAAGCAGTA GGAGGAGGCAGCTGGGAATGAGGACTGGGGAAGACTACAGCAGTGTGTGACTGTE ET-3' will serve as a template for the cellular homology-directed repair pathway. Transfected cells are then plated individually, cultured and DNA is isolated for sequencing to determine if gene editing was achieved. So, by utilizing the CRISPR-Cas9 genome editing system, we are able to use HeLa cells which are (CA/CA) and create stable lines that are either heterozygous or homozygous (AG/AG) and compare *CYP2B6* gene expression changes when miR-1275 is transfected. This will provide additional evidence that miR-1275 targets *CYP2B6* and that the rs70950385 variant is associated with decreased CYP2B6 activity.

miRNAs as biomarkers for predicting patient response and outcomes

Lastly, the miRNAs focused on in this project were expressed in liver tissue samples; however, it is known that miRNAs are found in the blood and can circulate between tissues via exosomes (Conde-Vancells et al., 2008; Kogure et al., 2011; Vickers et al., 2011). As liver biopsies are not feasible for predicting patient outcomes, it is necessary to understand how miRNAs are secreted between the different cell types as well as patterns in plasma miRNA levels. Individual or groups of miRNAs can serve as biomarkers for many biological disease states and progression such as breast cancer and diagnosis of liver disease, as well as for predicting patient response to drugs (Cortez et al., 2012; Dickinson et al., 2013; Fayyad-Kazan et al., 2013; Murakami et al., 2012; Salomon et al., 2017). For example, miR-150 and miR-342 were shown to be down-regulated in the plasma of patients with acute myeloblastic leukemia compared to healthy controls. These two miRNAs combined were able to discriminate AML patients with a sensitivity and specificity of 73% and 78%, respectively (Fayyad-Kazan et al., 2013). The use of miRNAs as biomarkers is an

emerging field as over 400 clinical trials have been conducted or are currently ongoing focused on miRNAs as biomarkers and screening mechanisms for a wide range of indications focused on diabetes, liver, kidney, and heart disease, cancers, etc. (ClinicalTrials.gov). Collectively, these studies will further our understanding of miRNAs role in various physiological processes, as well as provide information on how miRNAs circulate between cells and their involvement in drug metabolism, disease progression and diagnosis.

REFERENCES

Adkins, J.C., and Noble, S. (1998). Efavirenz. Drugs *56*, 1055-1064; discussion 1065-1056.

Administration, F.a.D. (2012). Guidance for industry: drug interaction studies-study design, data analysis, implications for dosing, and labeling recommendations. Center for Drug Evaluation and Research (CDER), Rockville.

Agarwal, V., Bell, G.W., Nam, J.W., and Bartel, D.P. (2015). Predicting effective microRNA target sites in mammalian mRNAs. Elife *4*.

Anderson, M.S., Cote, J., Liu, Y., Stypinski, D., Auger, P., Hohnstein, A., Rasmussen, S., Johnson-Levonas, A.O., and Gutstein, D.E. (2013). Effects of Rifampin, a potent inducer of drug-metabolizing enzymes and an inhibitor of OATP1B1/3 transport, on the single dose pharmacokinetics of anacetrapib. Journal of clinical pharmacology *53*, 746-752.

Aueviriyavit, S., Furihata, T., Morimoto, K., Kobayashi, K., and Chiba, K. (2007). Hepatocyte nuclear factor 1 alpha and 4 alpha are factors involved in interindividual variability in the expression of UGT1A6 and UGT1A9 but not UGT1A1, UGT1A3 and UGT1A4 mRNA in human livers. Drug Metab Pharmacokinet *22*, 391-398.

Baes, M., Gulick, T., Choi, H.S., Martinoli, M.G., Simha, D., and Moore, D.D. (1994). A new orphan member of the nuclear hormone receptor superfamily that interacts with a subset of retinoic acid response elements. Molecular and cellular biology *14*, 1544-1552.

Belanger, A.S., Tojcic, J., Harvey, M., and Guillemette, C. (2010). Regulation of UGT1A1 and HNF1 transcription factor gene expression by DNA methylation in colon cancer cells. BMC Mol Biol *11*, 9.

Benjamini, Y., Drai, D., Elmer, G., Kafkafi, N., and Golani, I. (2001). Controlling the false discovery rate in behavior genetics research. Behavioural brain research *125*, 279-284.

Benjamini, Y., and Hochberg, Y. (1995). Controlling the False Discovery Rate - a Practical and Powerful Approach to Multiple Testing. J Roy Stat Soc B Met *57*, 289-300.

Bertz, R.J., and Granneman, G.R. (1997). Use of in vitro and in vivo data to estimate the likelihood of metabolic pharmacokinetic interactions. Clinical pharmacokinetics *32*, 210-258.

Bhattacharya, A., Ziebarth, J.D., and Cui, Y. (2014). PolymiRTS Database 3.0: linking polymorphisms in microRNAs and their target sites with human diseases and biological pathways. Nucleic acids research *42*, D86-91.

Bianchi, M., Renzini, A., Adamo, S., and Moresi, V. (2017). Coordinated Actions of MicroRNAs with other Epigenetic Factors Regulate Skeletal Muscle Development and Adaptation. Int J Mol Sci *18*.

Biemar, F., Zinzen, R., Ronshaugen, M., Sementchenko, V., Manak, J.R., and Levine, M.S. (2005). Spatial regulation of microRNA gene expression in the Drosophila embryo.

Proceedings of the National Academy of Sciences of the United States of America *102*, 15907-15911.

Blake, M.J., Castro, L., Leeder, J.S., and Kearns, G.L. (2005). Ontogeny of drug metabolizing enzymes in the neonate. Seminars in fetal & neonatal medicine *10*, 123-138.

Blake, M.J., Gaedigk, A., Pearce, R.E., Bomgaars, L.R., Christensen, M.L., Stowe, C., James, L.P., Wilson, J.T., Kearns, G.L., and Leeder, J.S. (2007). Ontogeny of dextromethorphan O- and N-demethylation in the first year of life. Clinical pharmacology and therapeutics *81*, 510-516.

Bosma, P.J., Chowdhury, J.R., Bakker, C., Gantla, S., de Boer, A., Oostra, B.A., Lindhout, D., Tytgat, G.N., Jansen, P.L., Oude Elferink, R.P.*, et al.* (1995). The genetic basis of the reduced expression of bilirubin UDP-glucuronosyltransferase 1 in Gilbert's syndrome. The New England journal of medicine *333*, 1171-1175.

Bottini, S., Hamouda-Tekaya, N., Tanasa, B., Zaragosi, L.E., Grandjean, V., Repetto, E., and Trabucchi, M. (2017). From benchmarking HITS-CLIP peak detection programs to a new method for identification of miRNA-binding sites from Ago2-CLIP data. Nucleic acids research *45*, e71.

Breese, M.R., and Liu, Y. (2013). NGSUtils: a software suite for analyzing and manipulating next-generation sequencing datasets. Bioinformatics *29*, 494-496.

Brennecke, J., Stark, A., Russell, R.B., and Cohen, S.M. (2005). Principles of microRNA-target recognition. PLoS Biol *3*, e85.

Brueckner, B., Stresemann, C., Kuner, R., Mund, C., Musch, T., Meister, M., Sultmann, H., and Lyko, F. (2007). The human let-7a-3 locus contains an epigenetically regulated microRNA gene with oncogenic function. Cancer Res *67*, 1419-1423.

Burgess, K.S., Ipe, J., Swart, M., Metzger, I.F., Lu, J., Gufford, B.T., Thong, N., Desta, Z., Gaedigk, R., Pearce, R.*, et al.* (2017). Variants in the CYP2B6 3'UTR alter in vitro and in vivo CYP2B6 activity: Potential role of microRNAs. Clinical pharmacology and therapeutics.

Burgess, K.S., Philips, S., Benson, E.A., Desta, Z., Gaedigk, A., Gaedigk, R., Segar, M.W., Liu, Y., and Skaar, T.C. (2015). Age-related changes in microRNA expression and pharmacogenes in human liver. Clinical pharmacology and therapeutics.

Caraco, Y., Sheller, J., and Wood, A.J. (1999). Impact of ethnic origin and quinidine coadministration on codeine's disposition and pharmacodynamic effects. The Journal of pharmacology and experimental therapeutics *290*, 413-422.

Carey, M., Lin, Y.S., Green, M.R., and Ptashne, M. (1990). A mechanism for synergistic activation of a mammalian gene by GAL4 derivatives. Nature *345*, 361-364.

Clarke, D.J., Moghrabi, N., Monaghan, G., Cassidy, A., Boxer, M., Hume, R., and Burchell, B. (1997). Genetic defects of the UDP-glucuronosyltransferase-1 (UGT1) gene that cause familial non-haemolytic unconjugated hyperbilirubinaemias. Clin Chim Acta *266*, 63-74.

Conde-Vancells, J., Rodriguez-Suarez, E., Embade, N., Gil, D., Matthiesen, R., Valle, M., Elortza, F., Lu, S.C., Mato, J.M., and Falcon-Perez, J.M. (2008). Characterization and comprehensive proteome profiling of exosomes secreted by hepatocytes. J Proteome Res *7*, 5157-5166.

Cortez, M.A., Welsh, J.W., and Calin, G.A. (2012). Circulating microRNAs as noninvasive biomarkers in breast cancer. Recent Results Cancer Res *195*, 151-161.

Crews, K.R., Gaedigk, A., Dunnenberger, H.M., Klein, T.E., Shen, D.D., Callaghan, J.T., Kharasch, E.D., Skaar, T.C., and Clinical Pharmacogenetics Implementation, C. (2012). Clinical Pharmacogenetics Implementation Consortium (CPIC) guidelines for codeine therapy in the context of cytochrome P450 2D6 (CYP2D6) genotype. Clinical pharmacology and therapeutics *91*, 321-326.

Cuzzolin, L., Atzei, A., and Fanos, V. (2006). Off-label and unlicensed prescribing for newborns and children in different settings: a review of the literature and a consideration about drug safety. Expert opinion on drug safety *5*, 703-718.

Czajka-Oraniec, I., and Simpson, E.R. (2010). Aromatase research and its clinical significance. Endokrynol Pol *61*, 126-134.

Czech, B., and Hannon, G.J. (2011). Small RNA sorting: matchmaking for Argonautes. Nat Rev Genet *12*, 19-31.

Dannenberg, L.O., and Edenberg, H.J. (2006). Epigenetics of gene expression in human hepatoma cells: expression profiling the response to inhibition of DNA methylation and histone deacetylation. BMC Genomics *7*, 181.

de Wildt, S.N., Kearns, G.L., Leeder, J.S., and van den Anker, J.N. (1999). Cytochrome P450 3A: ontogeny and drug disposition. Clinical pharmacokinetics *37*, 485-505.

Desmeules, J., Gascon, M.P., Dayer, P., and Magistris, M. (1991). Impact of environmental and genetic factors on codeine analgesia. Eur J Clin Pharmacol *41*, 23-26.

Desta, Z., Metzger, I.F., Thong, N., Lu, J.B., Callaghan, J.T., Skaar, T.C., Flockhart, D.A., and Galinsky, R.E. (2016). Inhibition of Cytochrome P450 2B6 Activity by Voriconazole Profiled Using Efavirenz Disposition in Healthy Volunteers. Antimicrob Agents Chemother *60*, 6813-6822.

Desta, Z., Saussele, T., Ward, B., Blievernicht, J., Li, L., Klein, K., Flockhart, D.A., and Zanger, U.M. (2007). Impact of CYP2B6 polymorphism on hepatic efavirenz metabolism in vitro. Pharmacogenomics *8*, 547-558.

Dickinson, B.A., Semus, H.M., Montgomery, R.L., Stack, C., Latimer, P.A., Lewton, S.M., Lynch, J.M., Hullinger, T.G., Seto, A.G., and van Rooij, E. (2013). Plasma microRNAs serve as biomarkers of therapeutic efficacy and disease progression in hypertension-induced heart failure. Eur J Heart Fail *15*, 650-659.

Dixit, V., Moore, A., Tsao, H., and Hariparsad, N. (2016). Application of Micropatterned Cocultured Hepatocytes to Evaluate the Inductive Potential and Degradation Rate of Major

Xenobiotic Metabolizing Enzymes. Drug metabolism and disposition: the biological fate of chemicals *44*, 250-261.

Dluzen, D.F., Sun, D., Salzberg, A.C., Jones, N., Bushey, R.T., Robertson, G.P., and Lazarus, P. (2014). Regulation of UDP-glucuronosyltransferase 1A1 expression and activity by microRNA 491-3p. The Journal of pharmacology and experimental therapeutics *348*, 465-477.

Dobin, A., Davis, C.A., Schlesinger, F., Drenkow, J., Zaleski, C., Jha, S., Batut, P., Chaisson, M., and Gingeras, T.R. (2013). STAR: ultrafast universal RNA-seq aligner. Bioinformatics *29*, 15-21.

Doubi-Kadmiri, S., Benoit, C., Benigni, X., Beaumont, G., Vacher, C.M., Taouis, M., Baroin-Tourancheau, A., and Amar, L. (2016). Substantial and robust changes in microRNA transcriptome support postnatal development of the hypothalamus in rat. Sci Rep *6*, 24896.

Duursma, A.M., Kedde, M., Schrier, M., le Sage, C., and Agami, R. (2008). miR-148 targets human DNMT3b protein coding region. Rna *14*, 872-877.

Eap, C.B., Crettol, S., Rougier, J.S., Schlapfer, J., Sintra Grilo, L., Deglon, J.J., Besson, J., Croquette-Krokar, M., Carrupt, P.A., and Abriel, H. (2007). Stereoselective block of hERG channel by (S)-methadone and QT interval prolongation in CYP2B6 slow metabolizers. Clinical pharmacology and therapeutics *81*, 719-728.

Ellard, S., and Colclough, K. (2006). Mutations in the genes encoding the transcription factors hepatocyte nuclear factor 1 alpha (HNF1A) and 4 alpha (HNF4A) in maturity-onset diabetes of the young. Hum Mutat *27*, 854-869.

Evans, W.E., and Relling, M.V. (1999). Pharmacogenomics: translating functional genomics into rational therapeutics. Science *286*, 487-491.

Faucette, S.R., Hawke, R.L., Lecluyse, E.L., Shord, S.S., Yan, B., Laethem, R.M., and Lindley, C.M. (2000). Validation of bupropion hydroxylation as a selective marker of human cytochrome P450 2B6 catalytic activity. Drug metabolism and disposition: the biological fate of chemicals *28*, 1222-1230.

Fayyad-Kazan, H., Bitar, N., Najar, M., Lewalle, P., Fayyad-Kazan, M., Badran, R., Hamade, E., Daher, A., Hussein, N., ElDirani, R.*, et al.* (2013). Circulating miR-150 and miR-342 in plasma are novel potential biomarkers for acute myeloid leukemia. J Transl Med *11*, 31.

Fisel, P., Schaeffeler, E., and Schwab, M. (2016). DNA Methylation of ADME Genes. Clinical pharmacology and therapeutics *99*, 512-527.

Friedman, R.C., Farh, K.K., Burge, C.B., and Bartel, D.P. (2009). Most mammalian mRNAs are conserved targets of microRNAs. Genome Res *19*, 92-105.

Frueh, F.W., Amur, S., Mummaneni, P., Epstein, R.S., Aubert, R.E., DeLuca, T.M., Verbrugge, R.R., Burckart, G.J., and Lesko, L.J. (2008). Pharmacogenomic biomarker

information in drug labels approved by the United States food and drug administration: prevalence of related drug use. Pharmacotherapy *28*, 992-998.

Gammal, R.S., Court, M.H., Haidar, C.E., Iwuchukwu, O.F., Gaur, A.H., Alvarellos, M., Guillemette, C., Lennox, J.L., Whirl-Carrillo, M., Brummel, S.S.*, et al.* (2016). Clinical Pharmacogenetics Implementation Consortium (CPIC) Guideline for UGT1A1 and Atazanavir Prescribing. Clinical pharmacology and therapeutics *99*, 363-369.

Goldberg, A.D., Allis, C.D., and Bernstein, E. (2007). Epigenetics: a landscape takes shape. Cell *128*, 635-638.

Goodwin, B., Hodgson, E., D'Costa, D.J., Robertson, G.R., and Liddle, C. (2002). Transcriptional regulation of the human CYP3A4 gene by the constitutive androstane receptor. Molecular pharmacology *62*, 359-365.

Griffiths-Jones, S., Hui, J.H., Marco, A., and Ronshaugen, M. (2011). MicroRNA evolution by arm switching. EMBO Rep *12*, 172-177.

Guengerich, F.P. (2008). Cytochrome p450 and chemical toxicology. Chem Res Toxicol *21*, 70-83.

Gupta, P., Cairns, M.J., and Saksena, N.K. (2014). Regulation of gene expression by microRNA in HCV infection and HCV-mediated hepatocellular carcinoma. Virology journal *11*, 64.

Habig, J.W., Dale, T., and Bass, B.L. (2007). miRNA editing--we should have inosine this coming. Molecular cell *25*, 792-793.

Hall, T.A. (1999). BioEdit: a user-friendly biological sequence alignment editor and analysis program for Windows 95/98/NT. Paper presented at: Nucleic acids symposium series.

Hillgren, K.M., Keppler, D., Zur, A.A., Giacomini, K.M., Stieger, B., Cass, C.E., Zhang, L., and International Transporter, C. (2013). Emerging transporters of clinical importance: an update from the International Transporter Consortium. Clinical pharmacology and therapeutics *94*, 52-63.

Hines, R.N. (2007). Ontogeny of human hepatic cytochromes P450. Journal of biochemical and molecular toxicology *21*, 169-175.

Hines, R.N. (2008). The ontogeny of drug metabolism enzymes and implications for adverse drug events. Pharmacology & therapeutics *118*, 250-267.

Hines, R.N. (2013). Developmental expression of drug metabolizing enzymes: impact on disposition in neonates and young children. International journal of pharmaceutics *452*, 3-7.

Hofmann, M.H., Blievernicht, J.K., Klein, K., Saussele, T., Schaeffeler, E., Schwab, M., and Zanger, U.M. (2008). Aberrant splicing caused by single nucleotide polymorphism c.516G>T [Q172H], a marker of CYP2B6*6, is responsible for decreased expression and

activity of CYP2B6 in liver. The Journal of pharmacology and experimental therapeutics *325*, 284-292.

Holliday, R. (2006). Epigenetics: a historical overview. Epigenetics *1*, 76-80.

Homer, N., Merriman, B., and Nelson, S.F. (2009). BFAST: an alignment tool for large scale genome resequencing. PloS one *4*, e7767.

Hsieh, T.Y., Shiu, T.Y., Huang, S.M., Lin, H.H., Lee, T.C., Chen, P.J., Chu, H.C., Chang, W.K., Jeng, K.S., Lai, M.M.*, et al.* (2007). Molecular pathogenesis of Gilbert's syndrome: decreased TATA-binding protein binding affinity of UGT1A1 gene promoter. Pharmacogenet Genomics *17*, 229-236.

Hulsen, T., de Vlieg, J., and Alkema, W. (2008). BioVenn - a web application for the comparison and visualization of biological lists using area-proportional Venn diagrams. BMC Genomics *9*, 488.

Ingelman-Sundberg, M., and Rodriguez-Antona, C. (2005). Pharmacogenetics of drug-metabolizing enzymes: implications for a safer and more effective drug therapy. Philos Trans R Soc Lond B Biol Sci *360*, 1563-1570.

Jiang, F., Desta, Z., Shon, J.H., Yeo, C.W., Kim, H.S., Liu, K.H., Bae, S.K., Lee, S.S., Flockhart, D.A., and Shin, J.G. (2013). Effects of clopidogrel and itraconazole on the disposition of efavirenz and its hydroxyl metabolites: exploration of a novel CYP2B6 phenotyping index. Br J Clin Pharmacol *75*, 244-253.

Jin, Y., Yu, D., Tolleson, W.H., Knox, B., Wang, Y., Chen, S., Ren, Z., Deng, H., Guo, Y., and Ning, B. (2016). MicroRNA hsa-miR-25-3p suppresses the expression and drug induction of CYP2B6 in human hepatocytes. Biochem Pharmacol *113*, 88-96.

Jones, P.A., and Baylin, S.B. (2007). The epigenomics of cancer. Cell *128*, 683-692.

Jover, R., Moya, M., and Gomez-Lechon, M.J. (2009). Transcriptional regulation of cytochrome p450 genes by the nuclear receptor hepatocyte nuclear factor 4-alpha. Curr Drug Metab *10*, 508-519.

Juan, L., Wang, G., Radovich, M., Schneider, B.P., Clare, S.E., Wang, Y., and Liu, Y. (2013). Potential roles of microRNAs in regulating long intergenic noncoding RNAs. BMC medical genomics *6 Suppl 1*, S7.

Kacevska, M., Ivanov, M., and Ingelman-Sundberg, M. (2012). Epigenetic-dependent regulation of drug transport and metabolism: an update. Pharmacogenomics *13*, 1373-1385.

Kearns, G.L., Abdel-Rahman, S.M., Alander, S.W., Blowey, D.L., Leeder, J.S., and Kauffman, R.E. (2003). Developmental pharmacology--drug disposition, action, and therapy in infants and children. The New England journal of medicine *349*, 1157-1167.

Kharasch, E.D., Regina, K.J., Blood, J., and Friedel, C. (2015). Methadone Pharmacogenetics: CYP2B6 Polymorphisms Determine Plasma Concentrations, Clearance, and Metabolism. Anesthesiology *123*, 1142-1153.

Kim, B., Lee, J., Shin, K.H., Lee, S., Yu, K.S., Jang, I.J., and Cho, J.Y. (2017). Identification of omega- or (omega-1)-hydroxylated medium-chain acylcarnitines as novel urinary biomarkers for CYP3A activity. Clinical pharmacology and therapeutics.

Klein, K., Lang, T., Saussele, T., Barbosa-Sicard, E., Schunck, W.H., Eichelbaum, M., Schwab, M., and Zanger, U.M. (2005). Genetic variability of CYP2B6 in populations of African and Asian origin: allele frequencies, novel functional variants, and possible implications for anti-HIV therapy with efavirenz. Pharmacogenet Genomics *15*, 861-873.

Klingenberg, M. (1958). Pigments of rat liver microsomes. Arch Biochem Biophys *75*, 376-386.

Kogure, T., Lin, W.L., Yan, I.K., Braconi, C., and Patel, T. (2011). Intercellular nanovesicle-mediated microRNA transfer: a mechanism of environmental modulation of hepatocellular cancer cell growth. Hepatology *54*, 1237-1248.

Krek, A., Grun, D., Poy, M.N., Wolf, R., Rosenberg, L., Epstein, E.J., MacMenamin, P., da Piedade, I., Gunsalus, K.C., Stoffel, M.*, et al.* (2005). Combinatorial microRNA target predictions. Nat Genet *37*, 495-500.

Lacroix, D., Sonnier, M., Moncion, A., Cheron, G., and Cresteil, T. (1997). Expression of CYP3A in the human liver--evidence that the shift between CYP3A7 and CYP3A4 occurs immediately after birth. European journal of biochemistry / FEBS *247*, 625-634.

Lambert, N.J., Gu, S.G., and Zahler, A.M. (2011). The conformation of microRNA seed regions in native microRNPs is prearranged for presentation to mRNA targets. Nucleic acids research *39*, 4827-4835.

Lang, T., Klein, K., Fischer, J., Nussler, A.K., Neuhaus, P., Hofmann, U., Eichelbaum, M., Schwab, M., and Zanger, U.M. (2001). Extensive genetic polymorphism in the human CYP2B6 gene with impact on expression and function in human liver. Pharmacogenetics *11*, 399-415.

Lee, R.C., Feinbaum, R.L., and Ambros, V. (1993). The C. elegans heterochronic gene lin-4 encodes small RNAs with antisense complementarity to lin-14. Cell *75*, 843-854.

Lehmann, J.M., McKee, D.D., Watson, M.A., Willson, T.M., Moore, J.T., and Kliewer, S.A. (1998). The human orphan nuclear receptor PXR is activated by compounds that regulate CYP3A4 gene expression and cause drug interactions. J Clin Invest *102*, 1016-1023.

Lesko, L.J., and Zineh, I. (2010). DNA, drugs and chariots: on a decade of pharmacogenomics at the US FDA. Pharmacogenomics *11*, 507-512.

Lewis, B.P., Burge, C.B., and Bartel, D.P. (2005). Conserved seed pairing, often flanked by adenosines, indicates that thousands of human genes are microRNA targets. Cell *120*, 15-20.

Li, A.P., Kaminski, D.L., and Rasmussen, A. (1995). Substrates of human hepatic cytochrome P450 3A4. Toxicology *104*, 1-8.

Li, H., Xie, H., Liu, W., Hu, R., Huang, B., Tan, Y.F., Xu, K., Sheng, Z.F., Zhou, H.D., Wu, X.P., *et al.* (2009). A novel microRNA targeting HDAC5 regulates osteoblast differentiation in mice and contributes to primary osteoporosis in humans. J Clin Invest *119*, 3666-3677.

Li, M.P., Hu, Y.D., Hu, X.L., Zhang, Y.J., Yang, Y.L., Jiang, C., Tang, J., and Chen, X.P. (2016). MiRNAs and miRNA Polymorphisms Modify Drug Response. Int J Environ Res Public Health *13*.

Liang, G., Malmuthuge, N., Bao, H., Stothard, P., Griebel, P.J., and Guan le, L. (2016). Transcriptome analysis reveals regional and temporal differences in mucosal immune system development in the small intestine of neonatal calves. BMC Genomics *17*, 602.

Liang, Y., Li, S., and Chen, L. (2015). The physiological role of drug transporters. Protein Cell *6*, 334-350.

Liang, Z., Gao, Y., Shi, W., Zhai, D., Li, S., Jing, L., Guo, H., Liu, T., Wang, Y., and Du, Z. (2013). Expression and significance of microRNA-183 in hepatocellular carcinoma. TheScientificWorldJournal *2013*, 381874.

Liao, Y., Smyth, G.K., and Shi, W. (2014). featureCounts: an efficient general purpose program for assigning sequence reads to genomic features. Bioinformatics *30*, 923-930.
Liu, J. (2008). Control of protein synthesis and mRNA degradation by microRNAs. Current opinion in cell biology *20*, 214-221.

Liu, J., Zhao, R., Ye, Z., Frey, A.J., Schriver, E.R., Snyder, N.W., and Hebbring, S.J. (2017). Relationship of SULT1A1 copy number variation with estrogen metabolism and human health. J Steroid Biochem Mol Biol.

Lu, A.Y., and Coon, M.J. (1968). Role of hemoprotein P-450 in fatty acid omega-hydroxylation in a soluble enzyme system from liver microsomes. The Journal of biological chemistry *243*, 1331-1332.

Lu, A.Y., and Levin, W. (1972). Partial purification of cytochromes P-450 and P-448 from rat liver microsomes. Biochemical and biophysical research communications *46*, 1334-1339.

Marzolini, C., Telenti, A., Decosterd, L.A., Greub, G., Biollaz, J., and Buclin, T. (2001). Efavirenz plasma levels can predict treatment failure and central nervous system side effects in HIV-1-infected patients. AIDS *15*, 71-75.

McCarthy, D.J., Chen, Y., and Smyth, G.K. (2012). Differential expression analysis of multifactor RNA-Seq experiments with respect to biological variation. Nucleic Acids Res *40*, 4288-4297.

McCarver, D.G., and Hines, R.N. (2002). The ontogeny of human drug-metabolizing enzymes: phase II conjugation enzymes and regulatory mechanisms. The Journal of pharmacology and experimental therapeutics *300*, 361-366.

Michaud, V., Kreutz, Y., Skaar, T., Ogburn, E., Thong, N., Flockhart, D.A., and Desta, Z. (2014). Efavirenz-mediated induction of omeprazole metabolism is CYP2C19 genotype dependent. Pharmacogenomics J *14*, 151-159.

Michaud, V., Ogburn, E., Thong, N., Aregbe, A.O., Quigg, T.C., Flockhart, D.A., and Desta, Z. (2012). Induction of CYP2C19 and CYP3A activity following repeated administration of efavirenz in healthy volunteers. Clinical pharmacology and therapeutics *91*, 475-482.

Miller, R.P., Roberts, R.J., and Fischer, L.J. (1976). Acetaminophen elimination kinetics in neonates, children, and adults. Clinical pharmacology and therapeutics *19*, 284-294.

Mimura, S., Iwama, H., Kato, K., Nomura, K., Kobayashi, M., Yoneyama, H., Miyoshi, H., Tani, J., Morishita, A., Himoto, T.*, et al.* (2014). Profile of microRNAs associated with aging in rat liver. International journal of molecular medicine *34*, 1065-1072.

Miners, J.O., and Mackenzie, P.I. (1991). Drug glucuronidation in humans. Pharmacology & therapeutics *51*, 347-369.

Mooij, M.G., Schwarz, U.I., De Koning, B.A., Leeder, J.S., Gaedigk, R., Samsom, J.N., Spaans, E., Van Goudoever, J.B., Tibboel, D., Kim, R.B.*, et al.* (2014). Ontogeny of Human Hepatic and Intestinal Transporter Gene Expression During Childhood: Age Matters. Drug metabolism and disposition: the biological fate of chemicals.

Moore, L.B., Parks, D.J., Jones, S.A., Bledsoe, R.K., Consler, T.G., Stimmel, J.B., Goodwin, B., Liddle, C., Blanchard, S.G., Willson, T.M.*, et al.* (2000). Orphan nuclear receptors constitutive androstane receptor and pregnane X receptor share xenobiotic and steroid ligands. The Journal of biological chemistry *275*, 15122-15127.

Murakami, Y., Toyoda, H., Tanahashi, T., Tanaka, J., Kumada, T., Yoshioka, Y., Kosaka, N., Ochiya, T., and Taguchi, Y.H. (2012). Comprehensive miRNA expression analysis in peripheral blood can diagnose liver disease. PloS one *7*, e48366.

Nakajima, M., Komagata, S., Fujiki, Y., Kanada, Y., Ebi, H., Itoh, K., Mukai, H., Yokoi, T., and Minami, H. (2007). Genetic polymorphisms of CYP2B6 affect the pharmacokinetics/pharmacodynamics of cyclophosphamide in Japanese cancer patients. Pharmacogenet Genomics *17*, 431-445.

Nelson, D.R., Zeldin, D.C., Hoffman, S.M., Maltais, L.J., Wain, H.M., and Nebert, D.W. (2004). Comparison of cytochrome P450 (CYP) genes from the mouse and human genomes, including nomenclature recommendations for genes, pseudogenes and alternative-splice variants. Pharmacogenetics *14*, 1-18.

Ogburn, E.T., Jones, D.R., Masters, A.R., Xu, C., Guo, Y., and Desta, Z. (2010). Efavirenz primary and secondary metabolism in vitro and in vivo: identification of novel metabolic pathways and cytochrome P450 2A6 as the principal catalyst of efavirenz 7-hydroxylation. Drug metabolism and disposition: the biological fate of chemicals *38*, 1218-1229.

Okino, S.T., Pookot, D., Li, L.C., Zhao, H., Urakami, S., Shiina, H., Igawa, M., and Dahiya, R. (2006). Epigenetic inactivation of the dioxin-responsive cytochrome P4501A1 gene in human prostate cancer. Cancer Res *66*, 7420-7428.

Olsen, P.H., and Ambros, V. (1999). The lin-4 regulatory RNA controls developmental timing in Caenorhabditis elegans by blocking LIN-14 protein synthesis after the initiation of translation. Developmental biology *216*, 671-680.

Olsson, M., Gustafsson, O., Skogastierna, C., Tolf, A., Rietz, B.D., Morfin, R., Rane, A., and Ekstrom, L. (2007). Regulation and expression of human CYP7B1 in prostate: overexpression of CYP7B1 during progression of prostatic adenocarcinoma. Prostate *67*, 1439-1446.

Omura, T., and Sato, R. (1964a). The Carbon Monoxide-Binding Pigment of Liver Microsomes. I. Evidence for Its Hemoprotein Nature. The Journal of biological chemistry *239*, 2370-2378.

Omura, T., and Sato, R. (1964b). The Carbon Monoxide-Binding Pigment of Liver Microsomes. Ii. Solubilization, Purification, and Properties. The Journal of biological chemistry *239*, 2379-2385.

Organization, W.H. (2016). Consolidated guidelines on the use of antiretroviral drugs for treating and preventing HIV infection: recommendations for a public health approach.

Orom, U.A., Nielsen, F.C., and Lund, A.H. (2008). MicroRNA-10a binds the 5'UTR of ribosomal protein mRNAs and enhances their translation. Molecular cell *30*, 460-471.

Pan, Y.Z., Morris, M.E., and Yu, A.M. (2009). MicroRNA-328 negatively regulates the expression of breast cancer resistance protein (BCRP/ABCG2) in human cancer cells. Molecular pharmacology *75*, 1374-1379.

Paul, D., Standifer, K.M., Inturrisi, C.E., and Pasternak, G.W. (1989). Pharmacological characterization of morphine-6 beta-glucuronide, a very potent morphine metabolite. The Journal of pharmacology and experimental therapeutics *251*, 477-483.

Pearce, R.E., Gaedigk, R., Twist, G.P., Dai, H., Riffel, A.K., Leeder, J.S., and Gaedigk, A. (2016). Developmental Expression of CYP2B6: A Comprehensive Analysis of mRNA Expression, Protein Content and Bupropion Hydroxylase Activity and the Impact of Genetic Variation. Drug metabolism and disposition: the biological fate of chemicals *44*, 948-958.

Perez-Pinera, P., Ousterout, D.G., Brunger, J.M., Farin, A.M., Glass, K.A., Guilak, F., Crawford, G.E., Hartemink, A.J., and Gersbach, C.A. (2013). Synergistic and tunable human gene activation by combinations of synthetic transcription factors. Nat Methods *10*, 239-242.

Place, R.F., Li, L.C., Pookot, D., Noonan, E.J., and Dahiya, R. (2008). MicroRNA-373 induces expression of genes with complementary promoter sequences. Proceedings of the National Academy of Sciences of the United States of America *105*, 1608-1613.

Platt, A.R., Woodhall, R.W., and George, A.L., Jr. (2007). Improved DNA sequencing quality and efficiency using an optimized fast cycle sequencing protocol. BioTechniques *43*, 58, 60, 62.

Rae, J.M., Johnson, M.D., Lippman, M.E., and Flockhart, D.A. (2001). Rifampin is a selective, pleiotropic inducer of drug metabolism genes in human hepatocytes: studies with cDNA and oligonucleotide expression arrays. The Journal of pharmacology and experimental therapeutics *299*, 849-857.

Ramamoorthy, A., Li, L., Gaedigk, A., Bradford, L.D., Benson, E.A., Flockhart, D.A., and Skaar, T.C. (2012). In silico and in vitro identification of microRNAs that regulate hepatic nuclear factor 4alpha expression. Drug metabolism and disposition: the biological fate of chemicals *40*, 726-733.

Ramamoorthy, A., Liu, Y., Philips, S., Desta, Z., Lin, H., Goswami, C., Gaedigk, A., Li, L., Flockhart, D.A., and Skaar, T.C. (2013). Regulation of microRNA expression by rifampin in human hepatocytes. Drug metabolism and disposition: the biological fate of chemicals *41*, 1763-1768.

Rieger, J.K., Klein, K., Winter, S., and Zanger, U.M. (2013). Expression variability of absorption, distribution, metabolism, excretion-related microRNAs in human liver: influence of nongenetic factors and association with gene expression. Drug metabolism and disposition: the biological fate of chemicals *41*, 1752-1762.

Rieger, J.K., Reutter, S., Hofmann, U., Schwab, M., and Zanger, U.M. (2015). Inflammation-associated microRNA-130b down-regulates cytochrome P450 activities and directly targets CYP2C9. Drug metabolism and disposition: the biological fate of chemicals *43*, 884-888.

Robarge, J.D., Metzger, I.F., Lu, J., Thong, N., Skaar, T.C., Desta, Z., and Bies, R.R. (2017). Population Pharmacokinetic Modeling To Estimate the Contributions of Genetic and Nongenetic Factors to Efavirenz Disposition. Antimicrob Agents Chemother *61*.

Robinson, M.D., McCarthy, D.J., and Smyth, G.K. (2010). edgeR: a Bioconductor package for differential expression analysis of digital gene expression data. Bioinformatics *26*, 139-140.

Rowland, A., Miners, J.O., and Mackenzie, P.I. (2013). The UDP-glucuronosyltransferases: their role in drug metabolism and detoxification. Int J Biochem Cell Biol *45*, 1121-1132.

Rubin, K., Janefeldt, A., Andersson, L., Berke, Z., Grime, K., and Andersson, T.B. (2015). HepaRG cells as human-relevant in vitro model to study the effects of inflammatory stimuli on cytochrome P450 isoenzymes. Drug metabolism and disposition: the biological fate of chemicals *43*, 119-125.

Sage, D.P., Kulczar, C., Roth, W., Liu, W., and Knipp, G.T. (2014). Persistent pharmacokinetic challenges to pediatric drug development. Frontiers in genetics *5*, 281.

Salomon, C., Guanzon, D., Scholz-Romero, K., Longo, S., Correa, P., Illanes, S.E., and Rice, G.E. (2017). Placental exosomes as early biomarker of preeclampsia - Potential role of exosomal microRNAs across gestation. J Clin Endocrinol Metab.

Schirle, N.T., Sheu-Gruttadauria, J., and MacRae, I.J. (2014). Structural basis for microRNA targeting. Science *346*, 608-613.

Scott, G.K., Mattie, M.D., Berger, C.E., Benz, S.C., and Benz, C.C. (2006). Rapid alteration of microRNA levels by histone deacetylase inhibition. Cancer Res *66*, 1277-1281.

Selbach, M., Schwanhausser, B., Thierfelder, N., Fang, Z., Khanin, R., and Rajewsky, N. (2008). Widespread changes in protein synthesis induced by microRNAs. Nature *455*, 58-63.

Shi, X.B., Xue, L., Yang, J., Ma, A.H., Zhao, J., Xu, M., Tepper, C.G., Evans, C.P., Kung, H.J., and deVere White, R.W. (2007). An androgen-regulated miRNA suppresses Bak1 expression and induces androgen-independent growth of prostate cancer cells. Proceedings of the National Academy of Sciences of the United States of America *104*, 19983-19988.

Shi, Y.Y., and He, L. (2005). SHEsis, a powerful software platform for analyses of linkage disequilibrium, haplotype construction, and genetic association at polymorphism loci. Cell Res *15*, 97-98.

Sladek, F.M., Zhong, W.M., Lai, E., and Darnell, J.E., Jr. (1990). Liver-enriched transcription factor HNF-4 is a novel member of the steroid hormone receptor superfamily. Genes Dev *4*, 2353-2365.

Slaughter, R.L., and Edwards, D.J. (1995). Recent advances: the cytochrome P450 enzymes. Ann Pharmacother *29*, 619-624.

Snider, N.T., Sikora, M.J., Sridar, C., Feuerstein, T.J., Rae, J.M., and Hollenberg, P.F. (2008). The endocannabinoid anandamide is a substrate for the human polymorphic cytochrome P450 2D6. The Journal of pharmacology and experimental therapeutics *327*, 538-545.

Sonnier, M., and Cresteil, T. (1998). Delayed ontogenesis of CYP1A2 in the human liver. European journal of biochemistry / FEBS *251*, 893-898.

Spengler, R.M., Zhang, X., Cheng, C., McLendon, J.M., Skeie, J.M., Johnson, F.L., Davidson, B.L., and Boudreau, R.L. (2016). Elucidation of transcriptome-wide microRNA binding sites in human cardiac tissues by Ago2 HITS-CLIP. Nucleic acids research *44*, 7120-7131.

Stephens, M., and Donnelly, P. (2003). A comparison of bayesian methods for haplotype reconstruction from population genotype data. The American Journal of Human Genetics *73*, 1162-1169.

Stephens, M., Smith, N.J., and Donnelly, P. (2001). A new statistical method for haplotype reconstruction from population data. The American Journal of Human Genetics *68*, 978-989.

Swart, M., and Dandara, C. (2014). Genetic variation in the 3'-UTR of CYP1A2, CYP2B6, CYP2D6, CYP3A4, NR1I2, and UGT2B7: potential effects on regulation by microRNA and pharmacogenomics relevance. Frontiers in genetics *5*, 167.

Takagi, S., Nakajima, M., Mohri, T., and Yokoi, T. (2008). Post-transcriptional regulation of human pregnane X receptor by micro-RNA affects the expression of cytochrome P450 3A4. The Journal of biological chemistry *283*, 9674-9680.

Tao, Z.H., Wan, J.L., Zeng, L.Y., Xie, L., Sun, H.C., Qin, L.X., Wang, L., Zhou, J., Ren, Z.G., Li, Y.X.*, et al.* (2013). miR-612 suppresses the invasive-metastatic cascade in hepatocellular carcinoma. The Journal of experimental medicine *210*, 789-803.

Tirona, R.G., Lee, W., Leake, B.F., Lan, L.B., Cline, C.B., Lamba, V., Parviz, F., Duncan, S.A., Inoue, Y., Gonzalez, F.J.*, et al.* (2003). The orphan nuclear receptor HNF4alpha determines PXR- and CAR-mediated xenobiotic induction of CYP3A4. Nat Med *9*, 220-224.

To, K.K., Zhan, Z., Litman, T., and Bates, S.E. (2008). Regulation of ABCG2 expression at the 3' untranslated region of its mRNA through modulation of transcript stability and protein translation by a putative microRNA in the S1 colon cancer cell line. Molecular and cellular biology *28*, 5147-5161.

Todd, A.G., Lin, H., Ebert, A.D., Liu, Y., and Androphy, E.J. (2013). COPI transport complexes bind to specific RNAs in neuronal cells. Human molecular genetics *22*, 729-736.

Torres, L., Juarez, U., Garcia, L., Miranda-Rios, J., and Frias, S. (2015). External ear microRNA expression profiles during mouse development. Int J Dev Biol *59*, 497-503.

Trapnell, C., Pachter, L., and Salzberg, S.L. (2009). TopHat: discovering splice junctions with RNA-Seq. Bioinformatics *25*, 1105-1111.

Treluyer, J.M., Gueret, G., Cheron, G., Sonnier, M., and Cresteil, T. (1997). Developmental expression of CYP2C and CYP2C-dependent activities in the human liver: in-vivo/in-vitro correlation and inducibility. Pharmacogenetics *7*, 441-452.

Treluyer, J.M., Jacqz-Aigrain, E., Alvarez, F., and Cresteil, T. (1991). Expression of CYP2D6 in developing human liver. European journal of biochemistry / FEBS *202*, 583-588.

Tsuchiya, Y., Nakajima, M., Takagi, S., Taniya, T., and Yokoi, T. (2006). MicroRNA regulates the expression of human cytochrome P450 1B1. Cancer Res *66*, 9090-9098.

Twist, G.P., Gaedigk, R., Leeder, J.S., and Gaedigk, A. (2013). High-resolution melt analysis to detect sequence variations in highly homologous gene regions: application to CYP2B6. Pharmacogenomics *14*, 913-922.

Uehara, S., Uno, Y., Nakanishi, K., Ishii, S., Inoue, T., Sasaki, E., and Yamazaki, H. (2017). Marmoset Cytochrome P450 3A4 Ortholog Expressed in Liver and Small-Intestine Tissues Efficiently Metabolizes Midazolam, Alprazolam, Nifedipine, and Testosterone. Drug metabolism and disposition: the biological fate of chemicals *45*, 457-467.

Van Driest, S.L., and McGregor, T.L. (2013). Pharmacogenetics in clinical pediatrics: challenges and strategies. Personalized medicine *10*.

Vickers, K.C., Palmisano, B.T., Shoucri, B.M., Shamburek, R.D., and Remaley, A.T. (2011). MicroRNAs are transported in plasma and delivered to recipient cells by high-density lipoproteins. Nat Cell Biol *13*, 423-433.

Vieira, I., Sonnier, M., and Cresteil, T. (1996). Developmental expression of CYP2E1 in the human liver. Hypermethylation control of gene expression during the neonatal period. European journal of biochemistry / FEBS *238*, 476-483.

Vogel, F. (1959). Moderne probleme der humangenetik. Ergeb Inn Med U Kinderheilk *12*, 52-125.

Wang, H., Faucette, S., Sueyoshi, T., Moore, R., Ferguson, S., Negishi, M., and LeCluyse, E.L. (2003). A novel distal enhancer module regulated by pregnane X receptor/constitutive androstane receptor is essential for the maximal induction of CYP2B6 gene expression. The Journal of biological chemistry *278*, 14146-14152.

Wang, Y.M., Chai, S.C., Lin, W., Chai, X., Elias, A., Wu, J., Ong, S.S., Pondugula, S.R., Beard, J.A., Schuetz, E.G.*, et al.* (2015). Serine 350 of human pregnane X receptor is crucial for its heterodimerization with retinoid X receptor alpha and transactivation of target genes in vitro and in vivo. Biochem Pharmacol *96*, 357-368.

Ward, B.A., Gorski, J.C., Jones, D.R., Hall, S.D., Flockhart, D.A., and Desta, Z. (2003). The cytochrome P450 2B6 (CYP2B6) is the main catalyst of efavirenz primary and secondary metabolism: implication for HIV/AIDS therapy and utility of efavirenz as a substrate marker of CYP2B6 catalytic activity. The Journal of pharmacology and experimental therapeutics *306*, 287-300.

Waxman, D.J. (1999). P450 gene induction by structurally diverse xenochemicals: central role of nuclear receptors CAR, PXR, and PPAR. Arch Biochem Biophys *369*, 11-23.

Wei, P., Zhang, J., Dowhan, D.H., Han, Y., and Moore, D.D. (2002). Specific and overlapping functions of the nuclear hormone receptors CAR and PXR in xenobiotic response. Pharmacogenomics J *2*, 117-126.

Wilson, R.A., Deasy, W., Hayes, A., and Cooke, M.B. (2017). High fat diet and associated changes in the expression of micro-RNAs in tissue: Lessons learned from animal studies. Mol Nutr Food Res *61*.

Winter, J., Jung, S., Keller, S., Gregory, R.I., and Diederichs, S. (2009). Many roads to maturity: microRNA biogenesis pathways and their regulation. Nat Cell Biol *11*, 228-234.

Wirsing, A., Senkel, S., Klein-Hitpass, L., and Ryffel, G.U. (2011). A systematic analysis of the 3'UTR of HNF4A mRNA reveals an interplay of regulatory elements including miRNA target sites. PloS one *6*, e27438.

Xie, W., Ted Brown, W., and Denman, R.B. (2008). Translational regulation by non-protein-coding RNAs: different targets, common themes. Biochemical and biophysical research communications *373*, 462-466.

Xu, C., Quinney, S.K., Guo, Y., Hall, S.D., Li, L., and Desta, Z. (2013). CYP2B6 pharmacogenetics-based in vitro-in vivo extrapolation of efavirenz clearance by physiologically based pharmacokinetic modeling. Drug metabolism and disposition: the biological fate of chemicals *41*, 2004-2011.

Yang, J.S., Phillips, M.D., Betel, D., Mu, P., Ventura, A., Siepel, A.C., Chen, K.C., and Lai, E.C. (2011). Widespread regulatory activity of vertebrate microRNA* species. Rna *17*, 312-326.

Yekta, S., Shih, I.H., and Bartel, D.P. (2004). MicroRNA-directed cleavage of HOXB8 mRNA. Science *304*, 594-596.

Yu, D., Green, B., Tolleson, W.H., Jin, Y., Mei, N., Guo, Y., Deng, H., Pogribny, I., and Ning, B. (2015). MicroRNA hsa-miR-29a-3p modulates CYP2C19 in human liver cells. Biochem Pharmacol *98*, 215-223.

Yu, X., Liang, X., Xie, H., Kumar, S., Ravinder, N., Potter, J., de Mollerat du Jeu, X., and Chesnut, J.D. (2016). Improved delivery of Cas9 protein/gRNA complexes using lipofectamine CRISPRMAX. Biotechnol Lett *38*, 919-929.

Yuan, X., Ta, T.C., Lin, M., Evans, J.R., Dong, Y., Bolotin, E., Sherman, M.A., Forman, B.M., and Sladek, F.M. (2009). Identification of an endogenous ligand bound to a native orphan nuclear receptor. PloS one *4*, e5609.

Zeng, L., Chen, Y., Wang, Y., Yu, L.R., Knox, B., Chen, J., Shi, T., Chen, S., Ren, Z., Guo, L.*, et al.* (2017). MicroRNA hsa-miR-370-3p suppresses the expression and induction of CYP2D6 by facilitating mRNA degradation. Biochem Pharmacol.

Zhang, X., Azhar, G., Williams, E.D., Rogers, S.C., and Wei, J.Y. (2015). MicroRNA Clusters in the Adult Mouse Heart: Age-Associated Changes. Biomed Res Int *2015*, 732397.

CURRICULUM VITAE

KIMBERLY SHERRELLE BURGESS

EDUCATION

Indiana University Indianapolis, IN PhD. Pharmacology	 Graduation: Fall 2017 GPA: 3.9
Indiana University Indianapolis, IN Clinical Research Certificate	 Graduation: Spring 2017 GPA: 4.0
Fort Valley State University Fort Valley, GA B.S. Biology	Valedictorian Graduation: Fall 2011 GPA: 3.8

FUNDING

2016-2017	Ruth L. Kirschstein NRSA Individual Predoctoral Award
2013	Clinical Pharmacology Grant: ($5,000)
2013-2016	Southern Regional Education Board Doctoral Scholar
2012-2016	Adam W. Herbert Graduate Fellowship: $25,000/year

PATENT

Bobeck EA, **KS Burgess** and ME Cook, inventors. Peptide and method for reducing the phosphate requirement and excretion from farm animals. US 9,078,842 B2. 2015 July 14.

PUBLICATIONS

Burgess KS, IF Metzger, M Swart, J Ipe, J Lu, BT Gufford, N Thong, Z Desta, RE Pearce, R Gaedigk, A Gaedigk, Y Liu, TC Skaar. Variants in the CYP2B6 3'UTR alter in vitro and in vivo CYP2B6 activity: potential role of microRNAs. *Clin Pharmacol Ther.* 2017. Accepted.

Eadon MT, Hause RJ, Stark AL, Wheeler HE, **Burgess KS**, Benson EA, Jones RB, Cunningham PN, Bacallao RL, Dagher PC, Skaar TC, Dolan ME. Genetic variants contributing to colistin cytotoxicity: a population genomics approach identifies TGIF1 and HOXD10 in mediating renal cell toxicity. *Int J Mol Sci*. 2017 Mar; 18(3): 661.

Ipe J*, M Swart*, **KS Burgess*,** TC Skaar. High-throughput assays to assess the functional impact of genetic variants: a road towards genomic-driven medicine. *Clin Transl Sci*. 2017 Mar; 10(2):67-77. *Authors contributed equally.

Benson EA, **KS Burgess**, M Eadon, A Gaedigk, S Philips, M Segar, Y Liu, TC Skaar. Rifampin regulation of drug transporters and the role of microRNAs in human hepatocytes. *Front Pharmacol*. 2016 Apr 26;7.

Burgess KS, S Philips, EA Benson, R Gaedigk, A Gaedigk, Z Desta, MW Segar, Y Liu, TC Skaar. Age-related changes in microRNA expression and pharmacogenes in human liver. *Clin Pharmacol Ther.* 2015 Aug; 98(2):205-15.

Bobeck EA, **KS Burgess**, T Jarmes, ML Piccione, and ME Cook. Maternally-derived antibody to fibroblast growth factor-23 reduced dietary phosphate requirements in growing chicks. *Biochem Biophys Res Comm.* 2012; 420:666-670.

RESEARCH EXPERIENCE

2012-2017

PhD, Indiana University (IU)
Department of Pharmacology & Toxicology
Department of Medicine: Division of Clinical Pharmacology
Research Mentor: Todd Skaar, PhD

Project: *MicroRNA Regulation of Hepatic Drug Metabolism: Age-Related Changes in MicroRNA Expression and Genetic Variants in MicroRNA Target Sites*

Description: Pharmacogenetics has made great advancements in identifying genetic and copy number variants that affect drug metabolism and response and tailoring dosing accordingly, but variability still remains within groups after clinical factors and genetics has been considered. My dissertation research focused on developmental changes in microRNAs expressed in the liver that could contribute to this unaccounted variability by altering expression of clinically important adsorption, distribution, metabolism, and excretion genes, hence, drug disposition and response. These effects may be conveyed either directly on the genes or indirectly through upstream regulatory genes. Single nucleotide polymorphisms in the miRNA binding sites of these genes further contribute to the inter-individual variability in drug metabolism.

Techniques: real-time quantitative PCR, TaqMan gene expression, OpenArray, genotyping assays, cell culture, lipid-based transfections, RNA extraction, bacteria cloning and transformations, DNA isolation, RNA/cDNA synthesis, primer design, CRISPR/Cas9, protein purification, western blotting, luciferase assay, organic extraction, Graphpad Prism, JMP, statistical analyses using Graphpad Prism, JMP, Microsoft Excel, and R. Sequencing analysis using A Plasmid Editor, BioEdit, and Sequencher.

January-July 2012

Research Assistant, University of Alabama at Birmingham (UAB)
Clinical Pharmacology & Toxicology Department
Research Mentor: Jennifer King, PharmD

Project: *Evaluation of the Role of Metformin as a Chemopreventive Agent in Humans with Non-Small Cell Lung Cancer (NSCLC)*

Description: We were attempting to develop more preventative strategies for several drugs being studied for their abilities to prevent cancer. One such drug is metformin, a biguanide that is currently being used for the treatment of type 2 diabetes. In several retrospective studies, individuals that were taking normal doses of metformin were reported to have had decreased cancer incidence and mortality compared to those who were taking other diabetic drugs. The actual mechanisms of how metformin acts to reduce cancer incidence is currently unknown, but it is thought to act in two possible mechanisms. First, is to enter into the cell via a transporter system, such as the organic cation transporters and activate AMPK, which reduces mTOR signaling thereby causing an inhibition of protein synthesis and growth. The second method is to act in an extracellular manner and increase sensitivity to insulin, which can decrease insulin's circulation causing an inhibition of mTOR signaling.

Techniques*:* cell culture, real-time quantitative PCR

Summer 2011

Integrated Biological Sciences Summer Research Program, University of Wisconsin-Madison
Molecular & Environmental Toxicology, Animal Sciences Department
Research Mentors: Mark Cook, PhD, Elizabeth Bobeck, PhD

Project: *Neutralization of Fibroblast Growth Factor-23 Alters Phosphate Requirement of Growing Chicks*

Description: This project has been completed and the vaccine is currently being patented. We devised a commercially viable means of regulating FGF-23 via an antibody and investigated its use in an important agricultural species, chickens, as 8 billion are raised yearly in the United States. To determine the effectiveness of the anti-FGF-23 to reduce dietary supplemental needs of phosphate, feeding trials were conducted as the antibody was delivered by vaccinating the hen with passive transfer of antibody to the chick.

Techniques: animal husbandry, formulating animal diets, conjugating peptides, dry, fat-free bone ash test, plasma phosphate test, enzyme-linked immunosorbent assays

Summer 2010

Forensic Science Crime Research Experience for Undergraduates, UAB
Department of Justice Sciences (Forensic Science)
Research Mentor: Jason Linville, PhD

Project 1: *Assessing the Reproducibility of Real-Time Polymerase Chain Reaction on the Quantitation of DNA Recovered from Crime Scene*

Project 2: *Which Has More Touch DNA? Cell Phones vs. Drinking Straws*

Description: The first project focused on assessing the reproducibility of real-time PCR quantitation. When quantitating a sample multiple times, the same results are expected. Since variation does occur, experiments were conducted running multiple real-time PCR plates, varying the samples, standards, and days run to determine which conditions would produce the most precise results measured by calculating the standard deviation.

The second project was conducted to determine the better source for obtaining DNA, a cell phone or drinking straw. We expected cell phones to provide more DNA than straws because people generally touch their cell phones more on a regular basis compared to a drinking straw from a single use.

Techniques: organic extraction, real-time quantitative PCR, short tandem repeat measurements using an AmpFℓSTR® Identifiler® PCR Amplification Kit and 310 Genetic Analyzer

TEACHING EXPERIENCE

Summer 2016 — **Global Leadership Study Abroad Program: Stockholm, Sweden**
Advisors: NaShara Mitchell, MS, JD, Butler University
Cameron Beatty, PhD, Program Director, GLSA, Iowa State University

Taught two microteaching classes for 25 Iowa State undergraduates: Introduction to Epidemiology and Introduction to Clinical Trials.

2014-2015 — **National Organization for the Professional Advancement of Black Chemist and Chemical Engineers, Indianapolis Chapter Science Bowl Team Instructor/Volunteer**
Advisor: Paul Ardayfio, PhD, Clinical Research Scientist, Eli Lilly and Co.

Taught the biology and general science components in order to prepare a local team of four students for the national science bowl competition. Volunteered for the Indianapolis local science bowl competition.

2013-2016 — **NOBCChE College Prep Academy**
Advisor: Paul Ardayfio, PhD, Clinical Research Scientist, Eli Lilly and Co.

Mentored/taught Indianapolis high school students annually in a 20-week program covering various areas of science. Led the Crime Scene Investigator hands-on lab/lecture and cell culture techniques hands-on lab experience for 30 students.

2013-2016 — **Private Tutoring**

One-on-one tutor at the middle, high school and college levels in math, science, and literature courses.

2008-2011 **Academic Success Lab Tutor**
FVSU, Fort Valley, GA
One-on-one tutor for undergraduate students in biology, chemistry, algebra, pre-calculus, and literature courses.

SERVICE & LEADERSHIP

2016-Present **Mount Zion Academy Board of Directors, Member**
Decision making in all areas of the day care to ensure that the academy accomplishes its mission to provide academic success and development through a safe, nurturing environment by engaging students and parents in appropriate learning activities.

2016-2018 **American Society for Clinical Pharmacology and Therapeutics (ASCPT) Webinar Committee**
Solicits, shares, reviews and decides on webinar topics and proposals from ASCPT subgroups.

2015 **Hoosier Science and Engineering Fair High School Division Judge**
Serve as a judge for high school student's scientific poster session.

2013-2017 **IBMG Student Ambassador and Mentor**
Assist students during the interview weekend activities, participate in poster sessions and serve as a mentor for new students entering the program.

2013-Present **Big Brother Big Sister Chapter-Indianapolis**
Serve as a mentor and role model for my little sister.

2011-Present **Sigma Gamma Rho Sorority Incorporated**
Member, Alpha Sigma Graduate Chapter of Indiana (2013-Present)
Delta Pi Sigma Graduate Chapter of FVSU (2012)
Vice President, Zeta Pi Undergraduate Chapter of FVSU (2011)

A community service based organization whose goals are to enhance the quality of life within the community, public service, and leadership development.

2006-2016 **Pianist**
Mount Zion Baptist Church, Indianapolis, IN (2013-2016)
Green Grove Baptist Church, Elko, GA (2010-2012)
New Beginnings Church of Christ, Milledgeville, GA (2006-2009)

Play piano for church on Sunday, Wednesday, and/or special services.

PROFESSIONAL ASSOCIATIONS

2013-Present	American Society for Clinical Pharmacology and Therapeutics (ASCPT)
2011-2015	American Association for Cancer Research
2010-Present	Beta Kappa Chi Scientific Honor Society
2008-Present	Louis Stokes Alliance for Minority Participation (LSAMP)

INVITED PRESENTATIONS

LSAMP Meeting, Fort Valley State University
Fort Valley, GA, April 11, 2016
Presentation: My Academic Journey

Biology Colloquium, **Willamette University**
Salem, Oregon, April 4-5, 2016
Presentation: Age-related Changes in MicroRNA Expression Effect on Drug Metabolism in Human Liver

NOBCChE Meeting, IUPUI
Indianapolis, IN, February 9, 2015
Presentation: Getting Into and Through Graduate School

CONFERENCES

Great Lakes Drug Metabolism and Disposition Group (GLDMDG) Meeting (Student Abstract Presentation Winner)
Kalamazoo, MI, May 4-5, 2017
Oral & Poster Presentation: In Vitro and *In Vivo* Functional Testing of SNPs in the 3'UTR of *CYP2B6*

118th Annual Meeting ASCPT
Washington, DC, March 15-18, 2017
Oral & Poster Presentation: In Vitro and *In Vivo* Functional Testing of SNPs in the 3'UTR of *CYP2B6*
Poster Presentation: Association of UGT1A1*80 on Bilirubin Levels in Healthy Volunteers Treated with Efavirenz

117th Annual Meeting ASCPT
San Diego, CA, March 8-12, 2016
Poster Presentation: Use of Transcription Activator Like Effector-Transcription Factors (TALE-TFs) To Induce CYP1A2 Expression and Validate miRNA Predictions

22nd Annual Institute for Teaching and Mentoring
Arlington, VA, October 29-November 1, 2015

Indiana University Simon Cancer Center/Purdue University Center for Cancer Research Joint Scientific Retreat
West Lafayette, IN, May 2, 2015
Poster Presentation: Use of Transcription Activator Like Effector-Transcription Factors (TALE-TFs) As A New Technique to Induce CYP Gene Expression and Validate miRNA Predictions

116th Annual Meeting ASCPT (Travel Scholarship Recipient)
New Orleans, LA, March 3-7, 2015
Poster Presentation: Use of Transcription Activator Like Effector-Transcription Factors (TALE-TFs) As A New Technique to Induce CYP Gene Expression and Validate miRNA Predictions

21st Annual Institute for Teaching and Mentoring

Atlanta, GA, October 30-November 2, 2014

NOBCChE 41st Annual Conference New Orleans, LA, September 22-27th
IUPUI Exhibitor

Cancer Research Day
Indianapolis, IN, May 29, 2014
Poster Presentation: Effects of Developmental MicroRNA Regulation in Liver On Drug Disposition and Response

115th Annual Meeting ASCPT
Atlanta, GA, March 17-22, 2014

20th Annual Institute for Teaching and Mentoring
Arlington, VA, October 31-November 3, 2013

Annual Biomedical Research Conference for Minority Students
St. Louis, MO, November 9-12, 2011
Poster Presentation: Neutralization of FGF-23 Alters Phosphate Requirements of Growing Chicks

Society for Advancement of Hispanics/Chicanos and Native Americans in Science National Conference (Travel Scholarship Recipient)
San Jose, CA, October 27-30, 2011
Poster Presentation: Neutralization of FGF-23 Alters Phosphate Requirements of Growing Chicks

6th Annual Peach State LSAMP Fall Symposium & Research Conference
Savannah, GA, October 14-15, 2011
Oral Presentation: Assessing the Reproducibility of Real-Time Polymerase Chain Reaction on the Quantitation of DNA Recovered from Crime Scene

Committee on Institutional Cooperation/Summer Research Opportunity Program Summer Research Conference
Columbus, OH, July 15-17, 2011
Poster Presentation: Neutralization of FGF-23 Alters Phosphate Requirements of Growing Chicks

68th Joint Annual Meeting of Beta Kappa Chi Scientific Honor Society &National Institute of Science
Atlanta, GA, March 23-27, 2011
Oral Presentation: Assessing the Reproducibility of Real-Time Polymerase Chain
Reaction on the Quantitation of DNA Recovered from Crime Scene

Georgia Life Sciences Summit 2010
Atlanta, GA, October 28, 2010
Poster Presentation: Which Has More Touch DNA? Cell Phones vs. Drinking Straws

5th Annual Peach State LSAMP Fall Symposium & Research Conference
Athens, GA, September 24-25, 2010
Oral Presentation: Assessing the Reproducibility of Real-Time Polymerase Chain Reaction on the Quantitation of DNA Recovered from Crime Scene

HONORS/ AWARDS

IUSM

2017	GLDMDG Student Abstract Presentation Winner: $250
2017	ASCPT Presidential Trainee Award
2017	IUSM Travel Grant: $571
2017	Graduate-Professional Educational Travel Grant: $500
2017	ASCPT Dedicated Member: March 2017
2016	Premier 10 Award
2016	Elite 50 Award
2015	American Association of Pharmaceutical Sciences Drug Metabolism Newsletter Special Feature-Junior Scientist: December
2015	K.K. Chen Fellowship in Pharmacology & Toxicology: $1000
2015	Diversity Emissary Award: $300
2015	Elite 50 Award
2015	IUPUI Travel Fellowship Award: $1000
2015	Paradise Travel Award: $400
2015	Graduate-Professional Educational Travel Grant: $500
2015	ASCPT Jason Morrow Trainee Award (top trainee abstract)
2015	ASCPT Presidential Trainee Award: $750
2015	IUPUI EMBRACE Inaugural Magazine-Student Spotlight: January 2014 ASCPT New Member of the Month: April 2014

FVSU

2011	**Valedictorian**
2011	Summa Cum Laude
2011	Sigma Gamma Rho Sorority Highest GPA
2009	National Dean's List (3 years)
2009	Florine and Linda Early Health Sciences Departmental Award
	Scholarships/Grants,
2009	LSAMP Scholar (3 years)
2008	James H. Porter Merit Scholarship (2 years)
2008	FVSU Presidential Scholarship (4 years)
2008	Georgia's Helping Outstanding Pupils Educationally (HOPE) Scholarship (4 years)
2008	Kiwanis Club Scholarship (4 years)
2008	FVSU Women's Basketball Scholarship (2 years)
2008	Federal Smart Grant (2 years)
2008	Federal Academic Competitiveness Grant (2 years)
	Championship
2008-2009	Division II Southern Intercollegiate Athletic Conference Women's Basketball Championship